A METRIC INVESTIGATION OF THE CRANIAL BASE AND VERTEBRAE AMONG EXTANT AFRICAN HOMININAE: DISCRIMINATION ACROSS POSTURO-LOCOMOTORY COMPLEXES

By

David Alexander Lukaszek, M.A.

A Dissertation Submitted in Partial Fulfillment of the Requirements

for the Degree of

Doctor of Philosophy

in

Anthropology

University of Alaska Fairbanks, Alaska

May 2017

APPROVED:

Joel D Irish, Committee Chair
Kara Hoover, Committee Member
Brian Hemphill, Committee Member
Patrick Druckenmiller, Committee Member
Ben Potter, Chair
Department of Anthropology
Todd Sherman, Dean
College of Liberal Arts
Michael Castellini, *Dean of the Graduate School*

Abstract

Cranial base angle, vertebral dimensions, vertebral curvature, and locomotive behavior differ among *Homo*, *Pan*, and *Gorilla*; but many distinctions are obfuscated by dimensional and behavioral overlap among the genera and their fossil relatives. To address these issues, cranial and vertebral measurements (suites) were examined among *Homo*, *Gorilla*, and *Pan* as representative hominines for their posture and locomotion or positional-locomotory complexes. An additional analysis considered *Australopithecus afarensis* (A.L. 288-1 and A.L. 333) for comparative purposes. Using size-adjusted values with applied Bonferroni adjusted alpha levels, significant results for both the Kruskal-Wallis H-test and Mann-Whitney U-tests indicated statistically significant differences among species for cranial base angle ($p = 0.000$) and vertebral body dimensions with coronal and sagittal facet orientation ($p = 0.000 – 0.003$). Detected significance was present for thoracic and lumbar curvature ($p = 0.000$) and positional-locomotory complex ($p = 0.000$) among species, albeit only cranial base angle was significant for the *Pan-Gorilla* comparison. Moreover, *post hoc* Spearman's rho tests indicated significant results ($p = 0.000 – 0.009$) with strong positive and negative correlations throughout the column for each species. However, no pattern among vertebral measurements throughout the vertebral column was detected. Lastly, Multinomial Logistic Regression yielded a correct classification percentage with significant model fit ($p = 0.000$) of 86.4% for the cranial base, 82.8-97.0% for all subsequent vertebrae, and 80.3% for thoracic and lumbar curvature among species. Positional locomotory complexes were also significant ($p = 0.000$) and yielded a correct classification percentage of 82.2% among bipeds and the two modes of knuckle-walking practiced by *Pan* and *Gorilla* respectively. However, misclassifications between human and nonhuman primates for cranial base angle and calculated vertebral curvature suggest that these variables are not viable for assessing either genera or positional-locomotory complexes. Lastly, both *Australopithecus afarensis* specimens (A.L. 288-1 and A.L. 333) were incorrectly classified. The A.L. 288-1 specimen identified as *Homo* and the misclassification of A.L. 333 as *Pan* suggest either species or vertebra misidentification. Overall, the data indicate that both vertebral corpus dimensions and coronal and sagittal facet orientations differ significantly among hominine taxa and can distinguish species and their respective posturo-locomotory complex. As for the evolutionary implications, human bipedalism is distinct as related to cranial base angle and vertebral measurements; however

significant differences between *Pan* and *Gorilla* suggest homoplasy among measurements and denote parallelism for the emergence of knuckle-walking.

Dedication

To my parents, Edward A. and the late Barbara J. Lukaszek, for the sacrifices they made to help me achieve success.

Table of Contents Page

List of Figures Page

List of Tables Page

List of Appendices Page

Acknowledgements

I was privileged and very thankful to have been associated with many intellectuals – the best in their respective fields: Committee Chair, Dr. Joel D. Irish, for his guidance, patience, and encouragement to pursue this scientific line of inquiry, as well as his professional support in my academic development; my committee, Dr. Brian Hemphill, Dr. Kara C. Hoover, Dr. Ben A. Potter, and Dr. Pat Druckenmiller, for all their individual contributions; Dr. Yohannes Haile-Selassie and Lyman M. Jellema for access to the Hamann-Todd Collection at the Cleveland Museum of Natural History (CMNH); NextEngine, Inc.; Robert McNeel and Associates; Biotrax Laboratories, Inc.; Dr. H. James Birx, Canisius College, Professor of Anthropology; Dr. Randall Skelton, University of Montana, Professor of Anthropology; and Dr. John P. Holcomb, Cleveland State University, Professor and Department Chair of Statistics.

I would like to thank all of my colleagues in the Department of Anthropology, University of Alaska Fairbanks, for their support.

I am indebted to Ronald Kuwik, whose patronage provided the funding for the completion of this project.

Finally, I am grateful to the following people for their support throughout the years: Edward A. and the late Barbara Lukaszek; Edward J. and Patricia Lukaszek; Edmund Kuwik; the late Michael and the late Cecelia Kuwik; Ronald and Alexandra Stachowiak; the Ripley family; and the Ward family.

Chapter 1. Introduction

Cranial capacity and intellect are often stressed as critical distinctions between humans and other species (Falk et al. 2000; Holloway 1966; Ruff et al. 1997). While cranial capacity and neural reorganization are critical, human bipedalism also serves as a vital juncture for development and interaction within the cultural arena (Dombrowski et al. 2011; Mallau et al. 2007; McNeil et al. 1984; Miyakoshi et al. 2007). In this manner, any skeletal distinction between bipedal or quadrupedal species is an important point of contention for anthropologists regarding human evolutionary history and its implications of bipedalism on human culture. For example, the freeing of the hands for the simple act of using fire and intentional modification of material to create artistic expression were only possible with the aid of bipedalism. Although questions as to why ancestral hominins stood upright and what prompted the later development of culture are captivating, an understanding of the morphological and locomotive differences among Homininae (*Homo*, *Pan*, and *Gorilla*) with their respective extinct ancestral species gives the evolutionary history its contextual meaning. As such, this study sought to examine the metric differences in one part of the axial skeleton – specifically the cranial base and each sequential vertebra throughout the column with posture and locomotion in mind – to establish a connection between humans and their related extant African Homininae.

Differences exist in the dimensions and orientation of the cranial base and vertebrae among extant African Homininae. Subsequently, these distinctions also have an association with differences in posture and locomotion, e.g., bipedalism and quadrupedalism. Research into associations between the cranial base and vertebrae with locomotion are progressively adding to the understanding of the phenomenon, e.g., studies by Lieberman et al. (2000), Shapiro (1991), and Ward et al. (2010). However, a comprehensive understanding of the link between morphological configurations and both definitive postural and locomotive behaviors is understudied, problematic, or inconclusive. Both subtle and vast differences among taxa have potential implications for the emergence of human bipedalism.

Comparative primate anatomy and nonhuman primate behavior models are the bases for evolutionary inferences made about descent and locomotion. The reasons for this reliance are the human skeleton's possession of a mélange of morphological features shared among extant nonhuman primates and their related locomotory schemes (Bloch and Boyer 2002; Crompton et

al. 2008; Gebo 1989; Harcourt-Smith and Aiello 2004; Richmond et al. 2001; Sarmiento 1998; Senut 2006). These similarities and differences are not only depicted among extant species but also are evident in humankind's evolutionary past. Examining the evidence from the fossil record, habitual bipedalism – a distinguishing hallmark of *Homo sapiens* – long preceded other characteristics considered uniquely human. Although australopithecines are bipeds (McHenry and Coffing 2000; Ward 2007; Wood 2010), the discovery and analysis of *Orrorin tugenensis* and *Sahelanthropus tchandensis* tentatively dated the emergence of bipedalism at six to seven Ma (Brunet et al. 2005; Galik et al. 2004). Though the category of bipedalism covers an array of gaits, the range of locomotory behaviors among hominins is many, e.g., habitual or facultative bipeds (Aiello and Dean 2002; Fleagle 1998; McHenry 2002). Based on the selected traits among the array of morphological features and behavioral models, hominin classificatory schemes and theoretical models on the origin of bipedalism are far from conclusive (Crompton et al. 2008; Stokstad 2000; Tuttle 2008; Wolpoff 1983). Thus, human and nonhuman primates need quantitative analyses of individual skeletal elements as they relate to the complete and integrated structural unit.

1.1 Problem of interest

Quantifying osteological differences among extant taxa present unique problems when associating osteological features with either postural or locomotory behavior. Attempts to assess cranial and vertebral elements with posture and locomotion offer particular challenges: the degree of soft-tissue influences on vertebral column structure, variability in the range of motion, cranial and vertebral dimension overlap among taxa, and variability of posture and locomotive displays among species. While available landmarks or features limit osteological trait selection, defining primate locomotion has one distinct problem, namely, discriminating between the *potential* for a behavior and the *actual* behavior observed among species. Although the musculoskeletal configuration sets the potential for a particular form of locomotion, neither locomotion nor posture among primates is categorically exclusive. Posture and locomotion, mitigated by substrate or superstrate surfaces where an activity occurs, represent the static and dynamic repercussions of stable position and movement. Thus, a taxon's posturo-locomotory complex considers both posture and locomotion as one, encompassing the static and the dynamic and their interactions. As such, the positional-

locomotory complex for each species tacitly acknowledges potentiality factors, e.g., osteological diagnostic features as operating parameters within any expressed form of locomotion.

While multiple forms of locomotion and blending of morphological features are problematic, the selected variables for each taxon in this research seek to capture its positional-locomotory complex as indicated by subtle metric differences among species. This research addresses these issues in two ways. First, it considers each vertebra individually and within an integrated structural unit, combining posture and locomotion to be viewed as a positional-locomotory complex. This approach eliminated the extent of variation between static and dynamic movement within the column, e.g., the positional range of motion and structural stability within the column (Ahlborn 2004; Alexander 2003; Alfarno et al. 2004; Crompton et al. 2003; Granata and Wilson 2001; McGowan 1999). Second, the study employed 3-D laser scanning technology and engineering software to (1) determine morphological differences among *homininae* taxa; and to (2) classify taxa and their positional-locomotory complexes, based on the comprehensive view of the cranial base and vertebral column as a single unit. Comprehensive analyses in this study included *Homo sapiens*, *Gorilla gorilla*, and *Pan troglodytes*. Lastly, an analysis of hominin vertebrae from A.L. 288-1 and A.L. 333 determined the viability of this method for taxonomic and positional-locomotory complex classification.

The primary line of inquiry and assumptions had three specific aims: to investigate and identify key traits involved in cranial base angle, individual vertebrae, and spinal curvature in modern human and extant nonhuman primates; to use vertebralmetrics or measurement suites to determine differences and spinal curvature to identify the positional-locomotory complex; to provide potential insight into the vertebral similarities, with possibilities for identification of positional-locomotory complex in early hominins. These specific aims were the basis for five central research questions in this study.

1.2 Research questions

For a complete discussion, see Chapter 4, section 4.2.

The main point of inquiry was to determine, if possible, quantifiable differences in the cranial base and vertebrae among *Homo*, *Pan*, and *Gorilla* – and by extension, differences in the positional-

locomotory complex. Secondary to the main inquiry was an attempt to determine if the method was viable for assessing fossil hominins. Individual questions and related hypotheses follow:

First, are vertebrae sexually dimorphic within taxon? The size difference between males and females is striking among some primate species (Corruccini 1978; Fleagle 2000). While differences between males and females in *Pan* and *Gorilla* were almost certain from the onset of this study, the question aimed to determine if significant differences exist within the human species. Previous research by Marino (1995), Wescott (2000), and Bastir et al. (2014) provided additional insights into dimorphic differences than those depicted in pivotal research by Panjabi et al. (1991a; 1991b; and 1993a). The expectation in this study denoted additional differences from those previously explored by other researchers.

Second, can vertebralmetrics differentiate vertebrae among species? The question explores the quantifiable differences in vertebral measurements. Assumptions included differences in measurements between *Homo* to both *Pan* and *Gorilla* comparisons. Overlap in vertebral measurements among species was expected to be minimal. In fact, strong assumptions pointed to any measurement contributing to regional spinal curvature as the definitive variables used to distinguish both species and the positional-locomotory complex (see third and fourth questions).

In addition, can vertebralmetrics classify species? Given the vertebral measurement suite, this question aimed to single out which measurements were critical to distinguishing species at a high classification rate. Ultimately, the goal was to extract a few variables using this method for species identification of a single known or unknown vertebra.

Third, can cranial base angle and vertebral segment curvature differentiate among species? This question aimed to unite the cranium with its associated spinal curvatures, quantifying those osteological traits commonly referred to as flexed cranial base with an anteriorly-placed foramen magnum with S-shaped vertebral curvature for *Homo* and an elongated cranial base with a posteriorly-placed foramen magnum with a bow-like curvature for non-human primates. Given the assumptions regarding vertebral suite measurements as pivotal for curvature, the curvature for *Homo* will be different from either *Pan* or *Gorilla*. In addition, vertebral configuration without the presence of soft tissue determined regional curvature.

Fourth, can the cranial base angle and vertebral segment curvatures differentiate the positional-locomotory complex of a species? As in the previous question, the aim was to differentiate positional-locomotory complexes between the biped and both knuckle-walkers. Though obvious, e.g., the striking behavioral difference between a biped and quadruped, the same driving force of vertebral traits on curvature extends to positional-locomotory complex.

Furthermore, can cranial base angle and vertebral segment curvature classify positional-locomotory complex of a species? Given the vertebral measurement suite used to determine regional vertebral curvature, this question aimed to single out positional-locomotory complexes at a high classification rate. The assumption was that the positional-locomotory complex is distinct, as is the respective vertebral curvature, but differences between the two knuckle-walkers were not expected to vary.

Lastly, can the findings of this research help to distinguish fossil hominin vertebrae? The inclusion of this question relates to the emergence of bipedal characteristics of vertebrae from humankind's evolutionary past. Dispersed and often fragmented skeletal elements place paleontologists at a disadvantage. To circumvent some of these issues, traits selected within the vertebral suite considered these issues in determining their viability. Though prior analyses suggested bipedalism for hominins, in the case, *A. afarensis*, the hominin classification would be distinct due to variables used in this study. If not, *A. afarensis* would probably classify as *Homo*. If an additional method for classification were possible and available to paleontologists, an integrated approach to the vertebral column with other skeletal elements could provide additional insights.

1.3 Significance of the study

The significance of this study relative to previous research is four-fold due to its approach. First, the study explored and tested the viability for the orientation of the occipital condyles and foramen magnum (via reference plane) to the Frankfurt Horizon as a means for determining cranial base angle. Second, vertebral measurements encompass the primary measurements as they relate to both individual and regional structure. Central points determined the individual measurement points and angle construction after bone surface analysis, e.g., perpendicular surfaces for each skeletal element. Third, the approach used vertebral measurement suites to estimate regional vertebral curvature and rotation. Lastly, the study used both measurements and estimated curvature to

determine positional-locomotory complexes among species. Results (see Chapter 5) from this study confirm this approach and its significance.

1.4 Limitations and delimitations of the study

Limitations of this study do include sample size, bone condition, and line-of-sight issues during scanning. These limitations, specifically sample size and bone condition, influenced either the statistical tests used or skewed measurements. The latter issue has an impact on the results and subsequent interpretation. Although the limitations were beyond control, delimitating factors for both scanning and measurement procedures addressed scanning concerns, and to a degree, bone condition. Furthermore, eliminating skeletal elements with pathologies aided in alleviating any further limitations.

1.5 Organization

Seven main chapters followed by the appendices provide the organizational structure for this dissertation. Presented information covers background research, materials and methods, results, discussion, and summary and conclusions. Chapter 2 through 6 include additional discussion and summaries.

Chapter 2: Research Background: Extant primate and hominin locomotion

This chapter presents an exploration of locomotion and diagnostic skeletal features among extant nonhuman primates. Focus includes arboreal and terrestrial locomotion, with overlapping locomotive practices among primates. This chapter also includes a summary of fossil hominins with bipedal indicators and theoretical perspectives on the emergence of bipedalism.

Chapter 3: Research Background: Cranial Base and Vertebral Morphology

Previous research with particular attention to methodology is reviewed concerning both cranial base and vertebrae methods. Methodological differences between internal and external cranial base angle (CBA) analytical protocols are presented, including those methods used to determine head position. Additionally, exploration of previous studies includes cervical, thoracic, and lumbar vertebrae; sex estimation; and vertebral segment curvature.

Chapter 4: Material and Methods

The chapter describes in detail all the relevant materials and methods used in this study. It includes available specimens, questions, specific aims, testable hypotheses, and variables used. Detailed methods also include specific scanning procedures for both the cranium and vertebrae, with an outline of measurements using CAD software.

Chapter 5: Results

All reported significant results for Kruskal-Wallis, *post hoc* Mann-Whitney tests, Spearman's rho, and Multinomial Logistic Regression (MLR) are in this chapter. Additional *post hoc* tests results for their probative and explanatory value are also included.

Chapter 6: Discussion

Discussions of significant findings are at two levels – an individual and an integrated structural unit. Inferences regarding the vertebral measurement suites relate to individual and regional levels within the column. Furthermore, additional inferences about the cranial base, vertebral measurements, and curvature relate to the positional-locomotory complex.

Chapter 7: Summation and Conclusion

Research results and discussion chapters are synthesized into one theoretical construct based on the evidence relating to the specific aims and overarching question of this investigation. Subsequent ideas also present possibilities for future research.

Appendices

The appendices include information on biological materials and a documented list of significant results for PCA, Regression analysis, Kruskal-Wallis, *post hoc* Mann-Whitney, Spearman's rho, and Multinomial Logistic Regression (MLR).

Chapter 2. Background: Extant primate and hominin locomotion

Researchers differ in their assessment of taxonomic distinctions and phylogenic relationships among extant and fossil primates (Corruccini and McHenry 1980; Farber 2000; Freudenstein 2005; Rannala et al. 1998; Skelton et al. 1986; Wood and Lonergan 2008). The Order of Primates is divided into two Suborders: *Prosimian* and *Anthropoidea*. *Anthropoidea* is split into two Infraorders: *Platyrrhini* and *Catarrhini*. While *Platyrrhini* includes all New World monkeys, *Catarrhini* consists of two Superfamilies: *Cercopithecoidea* (Old World monkeys) and *Hominoidea*. *Hominoidea* is comprised of two Families: *Hylobatidae* (*Gibbon*) and *Hominidae*. *Hominidae* includes the Subfamily *Ponginae* (*Pongo*) and *Homininae*. Lastly, the Subfamily *Homininae* includes the Tribe *Panini* (*Gorilla* and *Pan*) and *Hominini* (*Homo*) taxa, albeit some researchers split *Pan* and *Gorilla* and place *Pan* with the *Homo* group. Estimates of the dates of evolutionary divergence among *Hominidae* includes *Hylobatidae* from *Hominidae* (12 – 15 Ma), *Ponginae* from *Homininae* (10 – 12 Ma), and *Panini* from the *Hominini* (4 – 7 Ma) Tribe (Fleagle 2013; Perelman et al. 2011; Purvis et al. 1995). As such, the term *hominine* includes the African apes and humans, whereas the term *Pongine* refers exclusively to *Pongo*. This classification would extend to all fossils deemed stem and crown ancestor respectively.

Morphological similarities are the basis for grouping taxa, using grade-based or clade-based classification. These features can either be homologous, e.g., similar in structures from a common ancestor, or homoplastic, e.g., the similar in function and not necessarily due to common ancestry (Wake 2003). While homologous features share a common ancestor that can be either synapomorphic (closely related) or symplesiomorphic (remotely related), homoplasy denotes either parallelism or convergence evolution (Hall 2007; Wake 2003). This distinction is critical for the evaluation of morphology and related behavioral indicators among taxa.

Modern *Homo sapiens* is unique among primates. Human characteristics include an enlarged brain, a complex social organization, a symbolic language, tool creation, and most importantly, the habitual use of a bipedal gait (Gibson et al. 1994; Stout 2011). Though humans are unique in many aspects, humans share many physical characteristics with nonhuman primates (Bloch and Boyer 2002; Richard 1985; Sarmiento 1998), particularly the great apes, and such homologous characteristics led many researchers to speculate on humankind's evolutionary descent and taxonomic relationship to extant nonhuman primate species.

Both physiological and morphological affinities among extant nonhuman primates are striking. In fact, some researchers stress the existence of more comparative similarities between the great apes and humankind than with any other primate taxa (Fleagle 1998; Groves 2001; Jenkins 1974; Oxnard 2000; Richard 1985). Charles Darwin observed such shared characteristics within an evolutionary framework and concluded humans differ only in degree and not in kind from the great apes (Darwin 1859; Darwin 1871); however, lesser apes and monkeys also share many of these characteristics. *Hylobatid*, *Ateline*, *Callithrichid*, and *Cercopithecoid* genera exhibit symplesiomorphic characteristics, such as external appearance, facial features, cranial structure, dentition, as well as neck, trunk, and limb composition (Ankel-Simons 2006; Bertram 2004; Crompton et al. 2010; Sarmiento 1998). This blending of primate skeletal morphology indicates the importance of osteological feature selection and locomotory models, but it can also obscure bipedal indicators as depicted in the theoretical explanations for the emergence of bipedalism.

Beyond the osteological similarities between human and nonhuman primates, locomotor inferences are primarily derived from primate behavior and their environmental settings. The geographic distribution of primates is limited to the tropical, temperate, subalpine and alpine biomes of South America, Central America, Africa, Madagascar, Asia, and the Oceania region (Fleagle 2013). As Table 2.1 illustrates, the most common biome to all primates is the rainforest, followed by seasonal forests and woodlands. The significance of this information in terms of evolutionary descent and the emergence of bipedalism are the multifaceted substrates which demonstrate a broad array of locomotory behaviors among members of a single family, the *Hominidae*, within the Order Primates.

Table 2.1. Primate biomes and mode of locomotion.

		Habitat								
Primate Family	Species (No.)	Rain Forest	Seasonal Forest	Woodland	Savanna	Semi-desert Scrub	Evergreen	Grassland	Elfinwood	Meadow
Cheirogaleiade	30	x	x	x						
Lemuridae	19	x	x	x						
Megaladapidae	22	x	x							
Indriidae	14	x	x	x						
Daubentoniidae	1	x								
Lorisidae	9	x	x	x						
Galagidae	19	x								
Tarsiidae	8	x								
Atelidae	24	x	x							
Cebidae	56	x	x	x						
Cercopithecidae	137	x	x	x	x	x	x	x	x	x
Hylobatidae	13	x	x							
Hominidae	6	x	x	x	x				x	x

Table 2.1. Primate biomes and modes of locomotion (cont.).

		Locomotion			
Primate Family	Species (No.)	Quadrupedal	Bipedal	Leaping	Brachiating/ Suspensory
Cheirogaleiade	30	X			X
Lemuridae	19	X			X
Megaladapidae	22				X
Indriidae	14	X			X
Daubentoniidae	1				X
Lorisidae	9	X			X
Galagidae	19			X	
Tarsiidae	8	X		X	
Atelidae	24				X
Cebidae	56	X			X
Cercopithecidae	137	X			X
Hylobatidae	13	X	X		
Hominidae	6	X	X		X

Compiled from Burton F. (1995), Fleagle, J. (1998), and Richard AE. (1985).

2.1 Primate locomotion

The primary mode of locomotion utilized by members within primate families is not species dependent. Activity, whether diurnal, nocturnal, or crepuscular, fosters competition within the arboreal or terrestrial niche of a particular environment or stratum. The habitual mode of locomotion for the majority of arboreal primates consists of various forms of arboreal quadrupedalism, often coupled with a modified form of branch bipedalism (Ankel-Simons 2006; Hunt et al. 1996). Suspension and brachiation, with vertical climbing and leaping, are the second and third most common habitual modes of locomotion, respectively (Ankel-Simons 2006; Fleagle 2000; Hunt et al. 1996). As previously depicted in Table 2, canopy stratification and exploitation of food resources do not always denote a primate's primary mode of locomotion. The arboreal primate remains similar to other primates within terms of multiple types of locomotion. Unlike arboreal primates, terrestrial primates are primarily quadrupedal; however, some species within the *Hylobatidae* and *Pongidae* exhibit arboreal and facultative short-term bipedalism (Bauer 1977; D'Aout et al. 2004; Gebo 1989; Robinson et al. 1972). Because species have multiple displays of locomotory behaviors, a certain locomotory assignment for each species is problematic. Thus, primates with their associated biome are not species-specific in terms of locomotory behaviors. Instead, locomotion tends to be multifaceted among primate species.

Previous researchers (Ankel-Simons 2006; Ashton 1981; Franz et al. 2005; Hunt et al. 1996; Hurov 1985) attempted to refine primate locomotion categorization based on observed behavior. These behaviors fall into four broad categories: brachiation (including suspensory behavior), quadrupedalism, leaping and climbing (arboreal locomotion), and bipedalism (refer to Table 2.1). Although gross categorization encompasses a broad range of motion, additional research by Hunt et al. (1996) reported distinctions within each of the standard four categories. Their re-categorization yielded a locomotory taxonomy consisting of 17 forms of locomotion (Table 2.2). Divisions within each mode of locomotion are dependent upon both the physical setting and placement of adjacent limbs during physical posture while initiating or sustaining locomotion. Additionally, Hunt et al. (1996) concluded hand and foot placement have nine different configurations during locomotion. These categories include palmigrade, plantigrade, digitigrade, knuckle-walk, fist-walk, grasp-walk, serpentine grasp-walk, schizodactyl grasp-walk, and clawed quadrupedalism. Distinctions among these configurations serve as an important factor when considering weight distribution in relation to a substrate.

Table 2.2. Definition of locomotion and hand placement.

Primate Forms of Locomotion
Quadrupedal walk
Tripedal walk
Bipedal walk
Bipedal hop
Quadrupedal run
Tripedal run
Bipedal run
Vertical climb
Torso-orthograde suspensory locomotion
Torso-pronograde suspensory locomotion
Bridge
Leap
Drop
Tail swing
Landing (leap, drop, and walk)
Tree sway
Ride
Scoot

Table 2.2. Definition of locomotion and hand placement (cont.).

Primate Forms of Locomotion
Hand and Foot Placement Definitions
Palmigrady – Contact using the volar area of the digits and palm
Plantigrade – A true heel strike
Digitigrady – Support contact via metacarpal heads and digits
Knuckle-walk – Support contact via intermediate phalanges (digits II-V)
Fist walk – Support contact via closed fist, similar to knuckle-walk
Grasp-walk – Support using the pollex and hallux with lateral digit alignment
Serpentine grasp-walk – Grasping without the hallux or pollex
Schizodactyl grasp-walk – Grasping which occurs between digit II and digit III
Clawed quadrupedalism – The utilization of claws for traction

Adapted from: Hunt K, Cant JGH, Gebo DL, Rose MD, Walker SE, and Youlatos D. 1996. Standardized description of primate locomotor and postural modes. Primates 37(4):363-387.

Among the various combinations, hand and foot placement is important among quadrupeds and serves to distinguish between two types of quadrupedalism: arboreal and terrestrial. Quadrupedal locomotion involves the torso held at a 45° angle to the substrate. Gait sequences observed include: (1) symmetrical with diagonal sequence, (2) asymmetrical with a simultaneous moment of forelimbs and hindlimbs, (3) tripedal bound with only one forelimb, (4) clutch, and (5) tri-axial bound. As noted, however, primates use various modes of locomotion and different combinations of hand placement within their overall locomotive repertoire (Ankel-Simons 2006; Ashton 1981; D'Aout et al. 2004; Jenkins 1972; Jenkins 1974). Variations within locomotory modes among primates suggest the consequence of the expansion of the primate brain and hemispheric specialization as depicted by gait sequence. Vilensky and Larson (1989) reported that a change to a diagonal-sequenced gait (forelimb follows the diagonal opposite) from a lateral-sequenced gait (forelimb follows the ipsilateral hindlimb) in many primates was the result of neurological changes. Since most nonhuman primates are capable of both diagonal and lateral sequences, some researches (Hunt et al. 1996; Hurov 1985; Kimura 1996; Pontzer et al. 2014; Zihlman 1992), suggest gait sequence and morphological differences among primates contribute to primary modes of locomotion, e.g., quadrupedalism with instances of bipedal gaits. Although a biomechanical rationale can associate diagonal-sequenced gait from a particular mode of locomotion, the ability to separate locomotory behaviors becomes problematic when based on observed behavior alone. For example, observed arboreal and terrestrial locomotion of chimpanzees have possible variations within their locomotive repertoire (Ankel-Simons 2006; Ashton 1981; Inman et al. 2006; Kimura

1985; Prost 1965). Nevertheless, despite these variations, each of the four traditional locomotory modes has distinct osteological characteristics.

2.2 Diagnostic locomotory features

Arboreal quadrupeds have distinct anatomically diagnostic features that include: forelimbs and hindlimbs of similar length (usually short), elliptically-shaped glenoid fossae, a broad humeral head with a moderately robust shaft, a medially-oriented medial epicondyle, a long olecranon process of the ulna, a broad hamate, a relatively high-angled femoral shaft, asymmetrically-sized femoral condyles and articulating surfaces of the tibial plateau, an asymmetrical tibiotalar (crural) joint, and a large hallux (Fleagle 1998; Fleagle 2000; Sarmiento 1998). In contrast to their arboreal counterparts, terrestrial quadrupeds exhibit limited anterior-posterior motion of the shoulder, a dorsal extension of the olecranon process, deep olecranon fossae, a short and posteriorly-oriented medial epicondyle, robust tarsals and metatarsals, and short and broad carpal bones (Fleagle 1998; Sarmiento 1998). Morphological variations with biomechanical repercussions are the cause of reported variations between these two types of quadrupedal locomotion. Primarily, the limitations placed on the range of motion influence weight distribution close to the center of mass (COM) and maintain balance control (Ahlborn 2004; Alexander 2003; Fleagle 1998; Harcourt-Smith 2007).

The diagnostic features for leapers, brachiators, and suspensory primates vary. Leaping primates have features that include deep femoral condyles, narrow tibiae, short femoral necks, slender fibulae, long calcanei and naviculars, and a long ischium (Fleagle 1998; Fleagle 2000; Sarmiento 1998). Brachiating and suspensory primates have narrow and dorsally-orientated scapulae, small and round glenoid fossae with a large humeral head, medially-oriented medial epicondyles, short olecranon processes, curved manual phalanges, broad and shallow femoral condyles, and a shallow patellar groove. The ulna of brachiating primates does not articulate with the proximal carpal elements (Fleagle 1998; Fleagle et al. 1981; Sarmiento 1998). Differences also can be seen in the relative length of the limbs between leapers and suspensory primates. Leaping primates have longer hindlimbs as compared to the forelimbs, whereas suspensory primates have longer forelimbs than hindlimbs (Fleagle 1998; Preuschoft 1990; Schultz 1953; Schultz 1961). Thus, joint orientation and configuration have biomechanical consequences for locomotory activities within an arboreal context.

Bipedalism likewise varies among human and nonhuman primates. Variations in bipedal gait displayed among nonhuman primates depend on not only morphological limitations but also upon the substrate (Ashton 1981; Badoux 1974; Crompton et al. 2010; D'Aout et al. 2004; Hildebrand 1967; Hirasaki et al. 2004). The consensus among researchers is that not all bipedal gaits are identical within the Primate Order. Subsequently, gait displays and osteological similarities obscure the issues regarding hominin gait when compared to modern *Homo* (Crompton et al. 2008; Crompton et al. 1998; Day 1985; Harcourt-Smith and Aiello 2004; Kidd and Oxnard 2005; McHenry 1986; Tuttle 1981; Tuttle et al. 1991).

Modern human bipedalism, defined as the constant cursorial utilization of the two lower limbs as a means of locomotion, is unique among primates. In their theoretical analysis of human bipedality, Inman et al. (2006) claim that the human gait encompasses pelvic rotation, transverse orientation, and knee flexion with lateral displacement amid leg, ankle, and foot rotation. With the COM located above the pelvis, both shoulder rotation and arm movement during forward motion aid in balance and maintain resonant frequency within the human gait. However, discrepancies among COM localities during locomotion, such as anterior or posterior placement in reference to the pelvis, indicate an inverted pendulum model with lateral displacements (Ahlborn 2004; Childress and Gard 2006; Stern et al. 2004). Both models were biomechanically inclusive and observable through weight distribution evident along the spinal column.

Weight distribution and COM among apes also differs from that observed during human locomotion. Raichlen et al. (2009) reported that the location of the COM in *Pan* was midway between the pelvis and shoulders, with 32–41% of the weight supported by the forelimbs. During locomotion, the position of COM and weight distribution occupied positions with respect to both forelimb and hindlimb placement (Hunt 1994). With differences in the positioning of COM, subtle differences have an association as depicted within morphology. For example, *Pan* and *Gorilla* exhibit different digit use during knuckle-walking. Variations and similarities within scaphoid, capitate, and hamate in terms of morphological and functional complexes denote the possibilities for homology or homoplasy for knuckle-walking (Kivell et al. 2009; Williams 2010). Overall, the placement of COM appears to vary among species due to body proportions and mass (Kimura 1996; Preuschoft 1990; Raichlen et al. 2009). This relative placement of COM, in conjunction with

morphological limitations, explains differences in posture and locomotion, as well as the awkward bipedalism exhibited by some nonhuman primates.

The extensive use of controlled systematic gaits and skeletal similarities among extant primates not only serves as a determining factor in primate locomotion (Ashton 1981; Bauer 1977; Davis et al. 2003; Fleagle 1998; Prost 1965; Vilensky and Larson 1989), but also acts as the starting point of theoretical conjecture regarding bipedalism in fossil hominins. For example, the presence of hominin bipedalism becomes apparent when juxtaposed only with extant primates. As modern human skeletal morphology reveals, shared ancestral traits within hominin taxa reflect possible modes of locomotion (Jenkins 1974; Oxnard 1973; Oxnard 2000). Also, evolutionary adaptations are not mutually exclusive to any one type of locomotion. The results yielded by such comparisons are twofold: (1) evolutionary descent is as depicted by morphology, and (2) inferred locomotor behavior based on physical limitations is indicated by morphology. These two intertwined implications are in the theoretical perspective on the origin of bipedalism, which stresses the morphological similarities of humankind's shared evolutionary past.

2.3 Bipedal indicators in fossil hominins

The discovery of fossil hominins in Africa, along with fossil primates in Europe and Asia, illustrates a blending of morphological features that suggest primate diversity despite shared evolutionary descent (McHenry 1982; McHenry 1994; McHenry and Coffing 2000; McHenry and Skelton 1985). The time frame for the emergence of a habitual bipedal gait in Africa becomes controversial when based on the available data and subsequent interpretation for taxonomic placement of these fossil specimens (Graybeal 1998; Hawkins 2000). Despite the limited number of fossil remains, morphological characteristics among fossil remains indicate obligate bipedalism. As such, the evidence suggests that modern humans, *Homo sapiens*, are not unique with regard to locomotion.

The African genera *Orrorin* and *Sahelanthropus* are the only two Miocene apes to possess the characteristic of bipedalism. If this interpretation is correct, bipedalism emerged earlier than the Pliocene epoch but also implied that the evolution of this trait originated in Africa.

Orrorin tugenensis

Orrorin tugenensis (6 -8.5 Ma) is a suggested bipedal hominin recovered at multiple sites (Aragai, Cheboit, Kapcheberek, and Kapsomin) in Kenya (Gibbons 2002; Pickford and Senut 2001; Senut 2007). Diagnostic post-cranial features include an anteriorly-convex curvature of the femoral diaphysis, the blend of the femoral tubercle into the greater trochanter, and the presence of an inter-trochanteric line which is absent in other Miocene apes (Pickford and Senut 2001). Furthermore, a medially-salient and well-developed lesser trochanter and an elongation of the femoral neck are closer in morphology as observed among australopithecines and humans (Pickford and Senut 2001). Additional femoral features depict a proximo-distally elongated gluteal tuberosity with a distal-leading crest, a mildly-cresting marked pectineal line with a spiral line below the lesser trochanter that joins the linea aspera, and a right-angled inter-trochanteric crest. The obturator groove originating from the trochanteric fossa to the inferior margin of the femoral neck indicates femoral hyper-extension with a developed but shallow hypo-trochanteric fossa (Senut et al. 2001). Lastly, the femoral neck is anteroposteriorly compressed, which along with the presence of an obturator externus groove, differs from both Miocene and modern apes (Pickford et al. 2002).

The fragmented femora, representative of several individual elements from differing localities, have several hominin features absent in hominoids. When comparing the diameter of the femoral head, shaft circumference, and femoral length of extant primates, *Orrorin* has an estimated femoral length range of 281 mm to 326 mm and an estimated stature of 1.1 m to 1.2 m and weight of 35 kg to 50 kg (Nakatsukasa et al. 2007). Similarly, the asymmetrical distribution of bone density in diaphyseal cross-section suggests weight distribution or loading patterns that reveal a degree of bipedalism (Galik et al. 2004).

Sahelanthropus tchadensis

Sahelanthropus tchadensis (6 – 7 Ma), a hominin recovered from Chad, also exhibits a blending of hominoid and hominin morphological characteristics based on dental, cranial, and mandibular fragments. Diagnostic anatomical features include a low cranial capacity (360 ml to 370 ml), a long and narrow basicranium, a thick and continuous supraorbital torus, marked post-orbital constriction, and small sagittal and large nuchal crests (Brunet et al. 2005). Additional features include a large mastoid process, small occipital condyles, a broad glenoid cavity with a large

glenoid process, small incisors, premolars with two roots, and molars with low and rounded cusps (Brunet et al. 2005; Brunet et al. 2002).

Although the cranium (TM 266) is partial and distorted, virtual cranial reconstruction by Zollikofer et al. (2005) depicts an orthognathic face, short premaxilla, a large foramen magnum which is greater in length than breadth and positioned more anteriorly, and a short basioccipital. The orientation of the foramen magnum suggests bipedalism due to the relative angle of the foramen magnum at a 95° angle to the orbital plane and the orientation of the nuchal plane at a 36° angle to the Frankfurt Horizontal (Zollikofer et al. 2005). When considering comparative results for morphological features among fossil apes – hominids, modern apes, and humans – those possessed by *Sahelanthropus* are closer to both *Australopithecus* and modern *Homo* than any other species. Because it exhibits morphological synapomorphines with other bipeds, bipedalism becomes its assumed form of locomotion (Guy et al. 2005). Nevertheless, trait selection and interpretation differ among researchers. For some, the distance of the anterior edge of the foramen magnum to the third molar and the angle of the nuchal plane could classify *Sahelanthropus* as a hominoid and semi-bipedal (Wolpoff et al. 2002). In short, trait selection and interpretation affect not only the assumed mode of locomotion that is presumed but also its very status as a hominin.

The emergence of australopithecines in Africa during the Pliocene epoch provides the best evidence for the appearance of bipedalism. The discovery of three genera – *Ardipithecus*, *Australopithecus*, and *Paranthropus* in present-day Chad, Ethiopia, Kenya, Tanzania, and South Africa – classify as bipedal (White et al. 1994).

Ardipithecus ramidus

Two species represent the genus *Ardipithecus*: *A. ramidus* (5.8 to 4.4 Ma) found at Arimis and *A. kadabba* (5.2 to 5.8 Ma) at Awash, both in Ethiopia. The species *A. ramidus*, first classified as *Australopithecus ramidus*, has cranial diagnostic features that include large non-elongated canines as well as a narrow and elongated lower first molar with a large protoconid and small metaconid (White et al. 1994). Further diagnostic features include a foramen magnum placed anterior to the carotid foramen, a hypoglossal canal placed anterior to the internal auditory meatus, a carotid foramen situated postero-medial to the tympanic angle, a small occipital condyle, and a blunt mastoid process (White et al. 1994). Post-cranial features include an elliptical humeral head,

a blunt olecranon process, an anterior trochlear notch, a large styloid process, and an extended lateral humeral epicondyle (White et al. 1994).

Ardipithecus kadabba

A. kadabba has diagnostic features similar to dental and humeral features exhibited in *A. ramidus* (see Haile-Selassie 2001), but recovered elements also include the hand and pedal phalanx and a partial clavicle. The distal half of the intermediate hand phalanx has minimal dorsal shaft curvature and a bilateral fossa on the palmer surface. The distal half of the proximal hand phalanx also has mild curvature. The proximal foot phalanx (left side, fourth digit) measures 31.9 mm in length, and the shaft exhibits a strong plantar curvature. The distal half of the shaft compresses dorso-ventrally, the proximal half medio-laterally. The clavicle features include a thick diaphyseal cortex and a medio-laterally elongated conoid tubercle (Haile-Selassie 2001).

Both *A. ramidus* and *A. kadabba* suggest biped possibility, marking the beginning of the hominin line based on the combined features of a short cranial base, an anteriorly-positioned foramen magnum, and a strong plantar curvature of the proximal foot phalanx (Harcourt-Smith 2007; McHenry 2002). The position of the foramen magnum as a sole indicator, however, may not denote speciation, even when considering the biserial correlation coefficient and discriminant analysis of the basion to bicarotid or basion to biporion measurements (Ahern 2005). If speciation is not possible as Ahern (2005) suspects, the elucidation of a specific locomotory repertoire becomes suspect and open to debate.

Although conclusions about *Ardipithecus*, as with *Orrorin* and *Sahelanthropus*, are controversial regarding habitual bipedalism, the acceptance of bipedal gait for the genus *Australopithecus* is without few reservations (Harcourt-Smith 2007). There are five species of *Australopithecus* located at sites in the southern, eastern, and central regions of Africa: *A. anamensis*, *A. afarensis*, *A. africanus*, *A. aethiopicus*, and *A. garhi* (Aiello and Dean 2002; Fleagle 1998; McHenry 2002). As a genus, *Australopithecus* represents the greatest distribution and variation of fossil hominins to date. General characteristics include a blending of human and ape-like features, such as small incisors and canines, large molars with thick enamel, pelvic morphology, femoral morphology, and ape-like body proportions (Fleagle 1998; McHenry 2002; McHenry and Coffing 2000).

Australopithecus anamensis

Australopithecus anamensis (4.2 to 3.9 Ma), recovered in Kenya and Ethiopia, represents a definitive form of bipedalism. Fragmentary elements exhibit the blending of ape and human characteristics with bipedal indicators (Leakey and Walker 2003). Specific anatomical features attributed to *A. anamensis* include parallel post-canine tooth rows, sexually dimorphic canines, narrow and shallow palates, and a strong receding symphyseal contour (Leakey and Walker 2003). Extensive pneumatization of the temporal bone, a small external auditory meatus, curved phalanx with flexor sheath ridges, and the absence of a facet on the capitate for the third metacarpal styloid process are also noted (Leakey and Walker 2003). Locomotive indicators consist of a tibial diaphysis oriented perpendicular to the talar joint surface and metaphyses that flare both proximally and distally – all indications of bipedal locomotion (Conroy 2005; Ward et al. 1999).

Australopithecus afarensis

Australopithecus afarensis (3.6 to 2.9 Ma), as exemplified by "Lucy" and the KSD-VP-1/1 specimens recovered at sites in Tanzania, Kenya, and Ethiopia, represents the greatest number of elemental indicators for bipedal locomotion. The diagnostic features for *Australopithecus afarensis* include large canines and upper central incisors, straight post-canine teeth, a long dental arcade, low cusps, thick enamel, a shallow palate, a pronounced temporonuchal crest, large mastoids, and ventrally-angulated occipital condyles (Fleagle et al. 1981; McHenry 2002). Post-cranially, *A. afarensis* presents the greatest blending of primitively-derived traits from previous hominins with added human-like characteristics (Haile-Selassie et al. 2010).

A. afarensis has upper limbs that possess weakly developed apical tufts on the distal phalanges, slender and curved proximal phalanges, a highly concavo-convex proximal surface of the first metacarpal, and large heads with no dorsal transverse ridges of the second through the fifth metacarpals (McHenry 1986). Further noted features indicate an elongated and rod-shaped pisiform, in addition to a capitate with a distally-placed trapezoid facet and prominent palmer break. The humerus has lateral cresting on the anterior trochlea and proximal orientation of the lateral epicondyle is also noted (Haile-Selassie et al. 2010). Distally, the humerus has a cranially-orientated medial epicondyle, a moderately developed supracondylar ridge, and a rounded olecranon fossa (Haile-Selassie et al. 2010). Further upper limb features include a long and narrow ulnae and incisura trochlearis, long and narrow columnar radii and tuberosities radii, and a large

proximal articulating surface of the radial head (Haile-Selassie et al. 2010; McHenry 1991). In reference to the axial skeleton, the scapula has a cranially-orientated glenoid (McHenry 1986).

The lower limbs are marked by long and curved proximal phalanges with a circumferential trochlea, a navicular with low dorsoplantar height, and a large right-angled cuboid facet. Also, a robust and triangular diaphysis of the first metatarsal, a calcaneus with a horizontal sustenaculum tali, a convergent hallux, and a lateral cuneiform with a plantar tuberosity are present (McHenry 1991). Additional lower limb features include a proximal femur with a short neck relative to femoral length, a high bicondylar angle, an elliptical lateral condyle, a posterior angle of the distal tibia, and a distal fibula with a deep peroneal groove (McHenry 1991). The placement of the iliac blade is posterior and includes robust anterior and posterior superior iliac spines, incorporating a sigmoid curve of the iliac crest, a thickened pubic symphysis (dorso-ventrally), and a short ischial shank (McHenry 1991; McHenry 2002).

A. afarensis presents an interesting problem in its morphological interpretation. Bipedalism is the result of multiple indicators, such as the presence of lumbar lordosis, a high bicondylar angle, short and wide iliac blades. Additional features include a prominent anterior inferior iliac spine, medio-lateral orientation of the talar surface (distal tibia), a trochlear surface of the talus, and a lateral plantar process of the calcaneus. The dorsal orientation of the proximal articulating facets on the proximal pedal phalanges suggests dorsiflexion, a necessary condition for bipedal walking, but falls outside the human range (Aiello and Dean 2002; Harcourt-Smith 2007). Paradoxically, relative to existing bipedal indicators, other aspects of post-cranial morphology denote arboreal diagnostic indicators in *A. afarensis*. Curved and long proximal phalanges with flexor ridges and a medial cuneiform similar to apes suggest hallucial opposability (Harcourt-Smith 2007). With a cranially-orientated glenoid fossa, the presence of a well-developed lateral trochlear crest of the distal humerus suggests that this feature prevents dislocation of the elbow joint during either climbing or suspension (Harcourt-Smith 2007).

Australopithecus africanus

Discovered in South Africa, *Australopithecus africanus* (3 to 2.4 Ma) shares many similar features with *A. afarensis*. Post-cranial elements are fragmentary but include a capitate, scapula, proximal humerus, distal femora, pelvic blade, an adolescent ischium, a fragmented piece of humeral shaft, vertebrae, left and right os coxae, incomplete sacrum, and a left proximal femur without the head

(McHenry 1986). *A. africanus* has wide and laterally flaring iliac blades coupled with small acetabular and iliosacral joints. Similar to *A. afarensis*, the bicondylar angle is high (Harcourt-Smith 2007).

Although *A. africanus* is considered bipedal, the discovery of "Little Foot" (Stw 573) suggests a difference in bipedal gait. As reported by Harcourt-Smith and Aiello (2004) and supported by Kidd and Oxnard (2005), results indicate that the talus is ape-like, the navicular appears as somewhat of a transition between ape and human, and a medial cuneiform resembles a human. When compared to *A. afarensis*, both the foot morphology and footprints point to a bipedal hominin with different bone morphology (Harcourt-Smith and Aiello 2004; Kidd and Oxnard 2005; Oliwenstein 1995).

Similarities in morphology extend beyond elements of the foot. Vertebral morphology and vertebral segment length, specifically in the lumbar region, exhibit many features, including lumbar lordosis and five lumbar vertebrae. Although questions remain regarding the classification of vertebrae, cranial shifting of the thoraco-lumbar border and the presence of the costo-transverse foramen with a rib that is not completely fused with the transverse process indicate the number of lumbar vertebrae (Haeusler et al. 2002). As indicated by McHenry (1986), *A. africanus* and *A. afarensis* share similar morphology in capitate, shoulder, pelvis, and femur features.

The capitate of *A. africanus* and *A. afarensis* is short, with a disto-lateral orientation of the second metacarpal facet (broad and single) and a dorsal orientation of the trapezoid facet. Their necks have constriction and the distal cuppings are shallow (McHenry 1986). Reported results for human, ape, and *Australopithecus* (AL 288-1, TM 1526 and AL 333-40) indicate that the capitate did not differ from that of *A. africanus* and *A. afarensis*; however, differences in capitate morphology, along with differences in the hamate and fifth metacarpal, suggest variations in grip and wrist extension (McHenry 1986).

A. africanus and A. afarensis also share similar shoulder morphology. As reported by McHenry (1986), results indicate that the angle between the glenoid fossae and the axillary borders of both species was approximately 119°. Additionally, both species have a narrow glenoid fossae, narrow humeral heads with medio-lateral orientation, and wide intertubercular sulci. However, *A. africanus* has a scapula with a greater glenoid fossa height and a humerus that has a head of larger diameter antero-posteriorly (McHenry 1986). When compared to modern humans,

similarities between traits shared by both australopithecine species and observed differences as compared to *Homo* traits cast doubt on the functional aspects of the shoulder.

McHenry (1986) reported that the pelvic morphology of *A. africanus* and *A. afarensis* is different from *Homo*. Small acetabulae, an anterior orientation of the iliac pillar, a small sacral surface, and high and broad iliac blades serve as distinguishing features for *Australopithecus*. Although the width and thickness of the ilium are similar to a degree, variations in the ischial and acetabular dimensions serve as possible indicators in the mechanical differences in bipedal locomotion. Morphological characteristics of the distal femur denote bipedalism for *A. africanus* and include the shape of the high shaft (oblique), patellar groove, and an ellipsoid-shaped epicondyle with the distal surface flattening out. Although these morphological characteristics are similar to *A. afarensis*, the antero-posterior width of the lateral condyle depicts greater notable differences (McHenry 1986). Nonetheless, any metric variations in post-cranial morphology within and among samples are due to differences in hominin size.

Paranthropus (Australopithecus)

Three species discovered at sites in South and East Africa – *P. aethiopicus, P. boisei,* and *P. robustus* – represent *Paranthropus*, formerly classified as *Australopithecus.* The general diagnostic anatomical features for these species include a robust mandible, small canines and incisors, large premolars and molars, a broader and "dished-out" face, and a greater degree of cranial base flexion (Fleagle 1998; McHenry 2002). These robust hominins, as suggested by the hardy appearance of their teeth as compared to those of *Australopithecus*, exhibit a degree of variability, but remain within many of the characteristics found among other species included within the genus *Australopithecus* (Wood and Richmond 2000).

Paranthropus aethiopicus (*P. aethiopicus*)

P. aethiopicus (2.7 to 2.3 Ma) consists of fragmentary fossil remains recovered from localities in Ethiopia and Kenya. Diagnostic features include a large flat face, a greater degree of prognathism than that observed in later species within this genus, and large nuchal and sagittal crests (Fleagle 1998; Strait et al. 2007; Tattersall 2000). No documented recovery of post-cranial elements associated with *P. aethiopicus* currently exists.

Paranthropus boisei (P. boisei)

The present-day sites Malawi, Tanzania, Kenya, and Ethiopia are locations for the hominin *P. boisei* (2.3 to 1.4 Ma). Post-cranial fragmentary elements attributed to this species include a clavicle, distal humeral shaft, fragmented proximal radius, and a proximal ulna and shaft fragments (Wood and Constantino 2007). Further excavation also recovered a distal femur, tibia (left and fragments of the right), distal fibula, and the right proximal third metatarsal (Grausz et al. 1988; Wood and Constantino 2007).

Due to the fragmentary nature of the recovered post-cranial elements, the exact form of locomotion cannot be determined; but the morphological similarities between recovered elements of *Paranthropus* and *Australopithecus*, especially the existence of a groove for *obturator externus*, suggest a degree of bipedalism. The limb proportions of *P. boisei* are larger than those of *A. afarensis* but smaller than the limbs of *Homo* in every category except the medio-lateral diameter of the femur taken at the lesser trochanter, e.g., 26.3 mm and 27 mm, respectively (Wood and Constantino 2007). However, an examination of proportion and size differentials led Grausz et al. (1988) to conclude that overall body proportions of *P. boisei* are very different from those of either *P. troglodytes* or *H. sapiens*, yet similar to the proportions of *A. afarensis*.

Paranthropus robustus (*P. robustus*)

P. robustus (2 to 1 Ma), recovered from sites in South Africa, has diagnostic anatomical features indicating bipedalism. The femoral features include the lack of lateral expansion of the great trochanter, the absence of a trochanteric line and femoral tubercle, and a deep trochanteric fossa with a groove for *obturator externus* (Day 1969; Wood and Richmond 2000). *P. robustus* and *Australopithecus* share similar bipedal gaits.

Australopithecus sediba

A. sediba (1.95 to 1.78 Ma), recovered from the Malapa Site in South Africa, consists of one juvenile holotype (MH1) and one adult paratype (MH2). Though each fossil specimen is incomplete with some fragmentary elements, MH1 consists of a partial cranium and mandible with post-cranial elements (Berger et al. 2010). Axial skeletal elements include twelve vertebrae and os coxae. Additionally, a right proximal femur, right clavicle, right humerus, a fragment of the left humeral proximal diaphysis, and a distal epiphysis of the right radius was also noted (Berger et al.

2010; Churchill et al. 2013; DeSilva et al. 2013; Williams et al. 2013). MH2 is limited to a partial mandible and post-cranial elements (Berger et al. 2010). Post-cranial elements include eleven vertebrae, right proximal femur, left proximal fibula, right distal tibia, talus, calcaneus, and a partial fifth metatarsal. Additionally, upper limb elements include a right clavicle, right humerus, right radius, as well as a partial left clavicle, left scapula, and left humerus (Berger 2012; Berger et al. 2010; Churchill et al. 2013; DeSilva et al. 2013; Williams et al. 2013).

The human-like configuration of the os coxae and a bicondylar angle that is approximately 9° suggests bipedal locomotion (Berger et al. 2010). The morphology of the calcaneus, the convex surface to the fourth metatarsal (midtarsal break), and an enlarged popliteal groove on the distal femur indicates hyperpronation (DeSilva et al. 2013; Williams et al. 2013).

Although the emergence of bipedalism appears to occur far earlier than previously estimated, the defining characteristics of *Homo* are beyond either an upright posture "to free the hands" or crossing the "Cerebral Rubicon." The discovery of elements attributed to *Homo habilis* (for example, OH 4, OH 6, OH 7, OH 8, OH 35, and OH 62), indicates particular changes in cranial capacity, limb proportions, a degree of sexual dimorphism, and cranio-dental features. These features are evolutionary links from the genus *Australopithecus* to early *Homo* in Africa (Leakey 1966; McHenry and Coffing 2000). Further morphological changes depicted in both *H. rudolfensis* and *H. erectus* are notable, but *H. habilis* is significant for two reasons: its association with the creation of tools; and, as with *H. rudolfensis*, the retention of some australopithecine morphological characteristics which denote obligate bipedalism.

A brief review of hominin characteristics further supports a bipedal trend amid blended human-ape morphological characteristics. Three key skeletal elements suggest sufficient bipedal indicators when compared to humans: cranial base flexion, the position of the foramen magnum, and pelvic and femoral morphology. To date, bipedalism emerged at least 6-7 Ma. Questions regarding the cause for the emergence of bipedalism and the debate surrounding its origin in an arboreal or terrestrial setting become an epistemological nightmare in any attempt to assess possible scenarios; yet, the context for the emergence of bipedalism is just as necessary to species identification as it is to definitive locomotion. Multiple analyses of marine oxygen isotopes, ice cores, sediments, loess sequences, pollen sequence, and stable isotopes can generate environmental insights (deMenocal 2004; deMenocal and Bloemendal 1995; Kingston 2007; Pickford 2006;

Wynn 2000). Ultimately, this combination of reconstructed environment, hominin fossil, and comparative extant primate morphology, yields multiple scenarios for the rise of bipedalism.

2.4 Theoretical explanations for the emergence of bipedalism

The diversity of primates within various biomes, and as a consequence, the different behaviors exhibited by primate species suggest they are a product of the environment acting as a natural selective force (Buss 1999; Corballis 1991; Corballis 1999; Wilson 1999). In a similar fashion, environmental conditions influenced the hominin condition. From reported results, the African hominin site at Lothagam (7.9 to 4.7 Ma) presented a mixture of open woodlands and grassy savannas. Other locations – Tugen Hills (5.0 to 2.5 Ma.), Aramis (4.4 Ma), Kanapoi (4.2 to 4.0 Ma), and Laetoli (3.8 to 3.5 Ma) – suggest the existence of woodlands and wooded savannas.

Fluctuations in aridity indicate a change from forests to grassy plains or a mosaic of open woodlands and savannas at both Hadar (3.3 to 3.0 Ma) and Omo-Turkana (4.0 to 2.5 Ma). Unlike other hominin African sites, environments at Sterkfontein (3.5 to 2.5 Ma) and Makapansgat (3.3 to 3.0 Ma) point to closed vegetation and a combination of woodland, forest, and savanna, respectively (Niemitz 2010; Potts 1998; Senut 2007). Various possible factors produced climatic changes in the Miocene, Pliocene, and Pleistocene epochs. Milankovitch cycling (orbital eccentricity, obliquity, and equinoctial timing), plate tectonics, and climatic events have accentuated the climatic effects during past glacial and interglacial periods. Environmentally traumatic events, e.g., the Messianian Salinity Crisis and Walker Circulation Pattern changes, also caused changes (Kingston 2007).

During these epochs, hominins adapted and migrated from tropical and subtropical forests to regions of open woodlands and grassy savannas (Haile-Selassie 2001; Pickford 2006). As a result, both speciation and extinction occurred rapidly, geologically speaking, due to the changes in environmental conditions. Together, seasonality and variability accounted for short-term and long-term cyclical environmental variations that influenced the tempo of early hominin adaptations (Niemitz 2010; Vrba 1995). With an increasingly arid climate and rapidly diminishing forests, an increase in savannas amid open woodland or grasslands coincided with the emergence of bipedalism in the late Miocene to early Pleistocene (Potts 1998). Yet, the appearance of early bipedalism from a quadrupedal ancestor was far from a complete adaptive advantage. As pointed out by Niemitz (2010), disadvantages of early bipedalism include slowness, a partially adapted

locomotive structure due to high COM, high energy consumption attributed to different joint configurations, and hydrostatic problems. Adaptive responses were the consequences of the changing environment, depicted through physiological regulation and expenditures.

Regulatory theory

One interpretation holds that bipedalism served as a regulatory mechanism in coping with the thermal stresses associated with an increasingly open and arid environment. The combination of an upright stance with the loss of body hair, water retention rate, and energy efficiency or metabolism reduced the amount of heat stress experienced. For example, an increase in diurnal water consumption between a naked biped and fully-haired biped at 30° C with the same metabolic expenditure (2.0 basal metabolic rate [BMR]) increases from 0.62 kg/12hr to 0.82 kg/12hr. This water consumption is lower in a biped than that of either a naked or fully-haired quadruped at the same temperature and metabolic rate: 1.16 kg/12hr and 1.1 kg/12hr, respectively (Amaral 1996; Wheeler 1991). As pointed out by Amaral (1996), hair loss and its associated thermal regulatory advantage were most beneficial when compared to fully-haired quadrupeds or bipeds with a lower thermal conduit. In this scenario, the benefit for bipedalism is dependent upon several factors: temperature, metabolism, degree of hair thickness or loss, and activity. However, one caveat remains. Causality between thermal regulation and bipedalism could not be linked to changes in morphology (Chaplin et al. 1994).

Energetic theory

The energetic theory considers two aspects: extant primate metabolic efficiency and mechanical efficiency (e.g., mass-specific cost of transport or COT). Kinematic studies on the differences between quadrupedal and bipedal locomotion are not conclusive as to which is more efficient. Some researchers (Rodman and McHenry 1980; Steudel 1996; Taylor and Rowntree 1973) claim that bipedalism is a more efficient form of locomotion, but the research of others (Aiello and Wells 2002; Okada 2006; Pontzer et al. 2014; Pontzer et al. 2009) found little difference in energy expenditure. To further confound the issue, research by Nakatsukasa et al. (2006) reported that Japanese macaques spent more energy during bipedal locomotion than during quadrupedal locomotion. Spider monkeys and lorises have lower energetic costs for bipedal walking in comparison to the higher energetic costs for quadrupedalism and brachiation. Consequently,

efficiency variations observed among human and nonhuman primates relate to species and substrate (Franz et al. 2005).

Variations in hominin skeletal morphology, particularly in *A. afarensis*, led some researchers to postulate the presence of an inefficient or awkward "Bent-Hip, Bent-Knee" (BHBK) gait (Crompton et al. 1998; Maus et al. 2010; Stern Jr and Susman 1983; Susman et al. 1984). Variation in energy expenditure differed among some primate species. These differences are the result of three fundamental variables: individual physiology, individual osteological conditions and parameters, and environmental setting (Ahlborn 2004; Nakatsukasa et al. 2006). Influencing factors include limb length, limb angle, body mass, and COM. Several researchers asserted that the energy needed to overcome joint resistance to produce movement in an awkward gait is greater than the energy required to achieve and maintain the resonant frequency during movement (Hayes et al. 1977; Hirasaki et al. 2004). Thus, resonant frequency to determine the energetics for bipedalism in a quadrupedal primate, whether forced or natural, becomes questionable. Asymmetry, the dominance of hindlimbs, and differing metabolic rates are problematic; however, these differences explain the variations in energy expenditure perceived within and among primates.

While adaptive response to a changing environment can quantify posture and locomotion via efficiency, morphological characteristics shared within lineages of evolutionary descent become a focus regarding origin and modes of locomotion. Based on nonhuman primate behavior, three prevalent models for the locomotory regime practiced by the last common ancestor shared among humans, chimpanzees, and gorillas include knuckle-walking, climbing, and brachiating theories.

Knuckle-walking

Proponents for the knuckle-walking theory focus on the morphological features of the shoulder, arm (forelimbs), wrist, and hand. Functional morphology becomes the critical factor in discriminating between African and Asian apes, hence the locomotory difference between knuckle-walkers and brachiators. However, shared morphology between knuckle-walkers and humans suggest that knuckle-walking is a generalized form of locomotion with roots deep within hominoid evolution (Begun 2004; Richmond et al. 2001). Research by Begun (2004) indicates that the human shoulder has similar proximal and distal humeral characteristics in addition to a comparable brachial index (length of forearm relative to the upper arm) and a strong lateral

trochlear keel with a deep zona conoidea (the area between the capitulum and the trochlea) to African apes.

The African ape and human wrist and hand share many features that are indicative of a knuckle-walking origin. The main morphological features include an early fusion of the *os centrale* or central portion of the scaphoid, the size and facet orientation of the scaphoid, and a dorsally-orientated scaphoid notch. Additionally cited features include a broad capitate and hamate with dorsal ridges, an enlarged trapezoid, a small triquetrum, and a palmer and proximal pisiform (Begun 2004; Richmond et al. 2001). The articulation of the scaphoid with the lunate, trapezium, trapezoid, and capitate – along with the articulation of the trapezoid with the capitate and the second metacarpal – have biomechanical implications for knuckle-walking (Begun 2004; Corruccini and McHenry 2001; Dainton and Macho 1999; Richmond et al. 2001). During knuckle-walking, hands and wrists experience compression and shear stress. The transfer of weight during locomotion in a rolling manner from the fourth digit to the second digit and sometimes to the fifth digit also places shear stress upon the carpals (Begun 2004; Matarazzo 2008; Richmond et al. 2001; Sarmiento 1998).

Although similarities in hand and wrist exist among knuckle-walkers, differences are observable among species when considering body size. Different growth trajectories in the lunate, triquetral, hamate, and capitate are evident between *Pan troglodytes* and *Gorilla gorilla* (Dainton and Macho 1999). These differences suggest a possible case of parallel evolution from a common quadrupedal ancestor (Begun 2004; McHenry and Temerin 1979; Stokstad 2000). Whereas humans share morphological similarities with knuckle-walkers, other researchers (Fleagle et al. 1981; Sarmiento 1998) point to shared osteological features with climbing and brachiating primates.

Brachiation and climbing

Climbing and brachiation theories suggest arboreal dwelling was a precursor to the emergence of human bipedalism due to morphological similarities. Proponents of the brachiation theory suggest bipedalism emerged from an arboreal ancestor who employed a combination of arm-hanging and arboreal branch bipedalism. These characteristics, which include long forelimbs, mobile shoulder and wrist joints, broad and coronally-orientated iliac blades, a laterally-facing scapula, long curved fingers, and highly developed pollices and halluces (Richmond et al. 2001; Senut 2006; Thorpe and Crompton 2006) provide some evidence in support of the brachiating theory.

The climbing (anti-pronograde) hypothesis for the origin of human bipedalism bases its theory upon both morphological characteristics and comparable biomechanical features. Richmond et al. (2001) cited the humeral shaft profile, scapula orientation, and the position of the vertebral column together with respect to the center of gravity. Although human hand and wrist morphology suggest an affinity with knuckle-walkers, an indication from hominin morphology implies an intermediate form of an arboreal existence with adaptive bipedal traits.

The climbing behavior of great apes, as with other primates, closely approximates human bipedalism more than any other mode of locomotion, including nonhuman primate bipedalism. Both kinematic and electromyographic studies of monkeys and apes illustrates limb patterns and muscle movement (e.g., *latissmus dorsi*, *caudal serratus anterior*, *deltoid*, *pectoralis major*, and *biceps brachii*) during climbing as similar to human locomotion (Fleagle et al. 1981; Gebo 1989; Isler 2005). However, it also should be noted that human kinematic similarities attributed to arboreal primates associate closely to terrestrial primate locomotion. Thus, the similarities and differences between human and various primates reflect the mosaic functional morphology of the human form and present a valid hypothesis.

While proponents of climbing, brachiating, and knuckle-walking hypotheses sought to ground their theories with appeals to functional morphology, other theories postulate different aspects. Theories include posture, display, food transport, and the aquatic ape (Hardy 1960; Hewes 1961; Jablonski and Chaplin 1993; Morgan 1997; Walter 2004; Wang and Crompton 2004; Wescott 1967a; Wescott 1967b). Other theories focus on reproduction and nascense (Gallup and Suarez 1983; Leutenegger 1981; Trevathan 1996). Together, these theories have no direct and/or quantifiable relationship to morphology per se, but possibly represent a co-emergence of traits and potential behaviors that are accidental to their related attributes.

2.5 Summary and conclusion

This second chapter explored both the variations in locomotion and common morphological similarities shared among extant primates. Such similarities not only reflect their common evolutionary descent but also quantify and describe differences among skeletal elements that serve as indicating factors for their locomotory diversification. However, the blending of human and nonhuman primate osteological features is not conclusive to only one type of locomotion. Locomotion among extant primates is two-fold: arboreal or terrestrial – with expressed variations

among brachiating, suspensory, quadrupedal, leaping, climbing, and bipedal behaviors (Bauer 1977; D'Aout et al. 2004; Fleagle 2000). These classes provide a generalized category for locomotion, gait rate and hand and foot placement, as well as limb sequence, presenting a basis for additional locomotive distinction (Gebo 1989; Hunt et al. 1996; Jenkins 1974; Vilensky and Larson 1989). Despite this distinction, a definite overlap of locomotive displays with shared morphological similarities, as opposed to diagnostics features among species, continues to be problematic. Finally, little distinction was made between normative posture and locomotion (Bauer 1977; D'Aout et al. 2004; Fleagle 2000; Gebo 1989; Hunt et al. 1996; Jenkins 1974; Vilensky and Larson 1989).

Amid the distinctly human characteristics, obligatory bipedalism is a distinct form of locomotion. Human bipedality differs from any facultative bipedalism exhibited by any extant nonhuman primate. Given a shared common ancestor among all primates within evolutionary history, indicators for habitual bipedalism are not recent. It emerged – perhaps multiple times – as an inherited characteristic (McHenry 1982; McHenry 1994; McHenry and Coffing 2000; McHenry and Skelton 1985). Previous research indicated bipedalism among hominins. *Orrorin tugenensis*, *Sahelanthropus tchandensis*, *Ardipithecus ramidus*, *Ardipithecus kadabba*, *Australopithecus anamensis*, *Australopithecus afarensis*, *Australopithecus sediba*, *Australopithecus africanus*, *Australopithecus aethiopicus*, *Australopithecus garhi*, *Paranthropus boisei*, and *Paranthropus robustus* are hominins which possess some *Homo* characteristics (Harcourt-Smith 2007; McHenry 1982; McHenry 1986; McHenry 1994; McHenry and Coffing 2000; McHenry and Skelton 1985; Senut et al. 2001; Senut 2007), but the exact gait of hominin bipedality remains inconclusive because of issues regarding blended morphology and multiple locomotive displays as exhibited among extant primates,.

Theories on the origins of habitual bipedalism vary according to the selective evidence used for interpretation. Common explanations include environment (Kingston 2007; Niemitz 2010; Potts 1998; Vrba 1995), thermal regulation (Wheeler 1991), and energetics (Pontzer et al. 2014; Rodman and McHenry 1980; Steudel 1996). Theories based on similarities among nonhuman primates include knuckle-walkers (Begun 2004; Richmond et al. 2001), brachiation (Richmond et al. 2001; Senut 2006; Thorpe and Crompton 2006), and climbers (Fleagle et al. 1981; Gebo 1989). Other theories include posture, display, food transport, and the aquatic ape (Hardy 1960; Hewes 1961;

Jablonski and Chaplin 1993; Morgan 1997; Walter 2004; Wang and Crompton 2004; Wescott 1967a; Wescott 1967b). Additional theories emphasize reproduction and nascense (Gallup and Suarez 1983; Leutenegger 1981; Trevathan 1996). Although these theories provide a varying degree of plausibility based on available evidence, the emergence of human bipedalism can be explained by the combination of several theories.

The review of locomotion and osteological indicators points to three problematic factors. First, posture and locomotion differ, and in many cases, overlap among taxon – thus, the necessity for a positional-locomotory complex is critical. Yet, it should be noted that perceived behavioral differences are biomechanically similar among certain skeletal elements, e.g., the vertebral column (Barr and Bear-Lehman 2001; Boszczyk et al. 2001; Boyd and Nigg 2007; Christiansen 2002). The second problem involves the blending of osteological characteristics as indicators. The last factor addresses the need for multiple indicators to determine fossil hominin status. The complexity of the posture and locomotion issue, along with the use of only osteological diagnostic indicators, demands a refinement between osteological traits and the use of the positional-locomotory complex as a standard for evaluation of taxa.

Chapter 3. Background: Cranial base and vertebral morphology

Primate anatomy divides the skeleton into two skeletal systems: axial and appendicular. The focus of this study is on the former, particularly the cranium and the vertebral column, exclusive of the sacral and coccygeal vertebrae. Cranial structure and orientation, particularly of the basicranium or cranial base, and the interlocking articulations between vertebrae present a unique systematic structure that yields similarities and differences among species. These morphological characteristics further the understanding of not only the form and function of integrated skeletal elements but also their implications for locomotor differences between orthograde and pronograde species.

3.1 Cranial base

Comparative analyses among human, nonhuman, and hominin crania focus on the morphological variations and orientation of cranial bones. Distinctly human characteristics include the expansion of the neurocranial vault with a reduction in prognathism and cranial base or basicranium flexion (Barbera et al. 2009; Fitzpatrick et al. 2006; Fleagle et al. 2010; Lieberman et al. 2000). Investigations of the cranial base, including flexion, are divided into two types: (1) measurements taken in the sagittal plane and (2) measurements taken in *norma basilaris* (Dean and Wood 1981; Lieberman and McCarthy 1999).

Cranial base landmarks and related sagittal plane methods used to determine cranial base angle (CBA) amid species vary among researchers. Commonly used reference points include the intersection of the postchordal and perchordal planes (Lieberman et al. 2008; Lieberman and McCarthy 1999; Lieberman et al. 2000; Ross and Henneberg 1995; Scott 1958; Strait 2001; Zuckerman 1955). Also, measurements depicting cranial integration (Neaux et al. 2013), the positioning of the foramen magnum, and orientation of the occipital condyles function to differentiate species (Ahern 2005; Dean and Wood 1981).

Sagittal plane and cranial base angle

Lieberman and McCarthy (1999) provide a comprehensive review and tests for correlations among different sagittal methods used to determine the cranial base angle for ontogenetic growth trajectories and pharyngeal dimensions not related to spinal curvature. Whereas different measurements under consideration employ different underlying assumptions (e.g., cranial

expansion, facial reduction, and cranial base angulation during ontogenetic growth), commonalities among angular measurements suggest common yet different developmental and integrational regimes in the cranium of members of different species.

In their research, Lieberman and McCarthy (1999) recorded the basion, sella, sphenoidal, anterior nasal spine, posterior nasal spine, planum spenoideum, and clivus measurements for *Homo sapiens* and *Pan troglodytes*. Additionally, cranial base angle measurements include determining the angle between the stella and foramen caecum planes, the stella and pre-sphenoid, clival and foramen caecum, clival and pre-sphenoid, and the external clival and hormoion planes.

Results by Lieberman and McCarthy (1999) indicated that *Homo* yielded significant differences for the stella and foramen caecum planes, as well as clival and pre-sphenoid landmarks across growth intervals. All internal cranial base angles denoted additional significant differences during the first 2.9 years of life. When growth trajectories were compared between members of the two species, *Pan* differed in terms of rapid postnatal extension as opposed to the flexion apparent in *Homo*. No differences between males and females at any age were reported for either species. Although not all measurements were linear, Lieberman and McCarthy (1999) also stated that strong correlations exist among the postchordal, sella, and clival planes. The external clival and hormoion plane angle, an external measurement associated only with *Homo*, had similar trajectories as reported in internal cranial base measurements with significant correlations between 0.25 and 0.49.

Lieberman and McCarthy (1999) concluded that internal cranial base angle measurements provide spatial relationships that involve the endocranial fossa and that the amount of flexion in *Homo* and extension in *Pan* differ only due to differences in the timing of growth trajectories, albeit at the same relative rate. Even though the external clival and hormoion plane angles have a similar trajectory in terms of internal measurements, angle differences reflect variation within cranial bone integration and orientation. Overall, Lieberman and McCarthy suggested that employment of a particular method to quantify cranial base angle depends on the type of study, the taxa under consideration, and the directed line of inquiry.

Norma Basilaris - Foramen magnum inclination

The position of the foramen magnum varies in size and position by species (Bilsborough and Rae 2007; Nevell and Wood 2008). Morphological landmarks are important to determine the relative positioning of the foramen magnum in relation to cranial base angle. As such, measurements sought to indicate that an anteriorly-positioned foramen magnum links with cranial base flexion in bipeds, whereas a posteriorly-placed foramen magnum is evident among nonhuman quadrupeds. Assessing the orientation of the foramen magnum becomes especially important when looking at foramen magnum orientation and cranial base angle in fossil hominins (Dean and Wood 1982; Dean and Wood 1981; Luboga and Wood 1990; Nevell and Wood 2008; Russo and Kirk 2013; Zuckerman 1955). Thus, two general approaches to the analysis of the basicranium include landmark-based metrics and the inclination of the foramen magnum.

In research by Dean and Wood (1981), basicranial investigations in *Homo sapiens*, *Gorilla gorilla*, *Pongo pygmaeus*, *Pan troglodytes*, *Australopithecus africanus*, and *Australopithecus boisei* considered the foramen magnum, bitympanic, bistylomastoid, bistyloid, bicarotid, biforamen ovale, bi-infratemporal fossa, a petrous portion of the temporal bone, and basioccipital length as potential discriminatory variables. Results indicate extant nonhuman primates have a greater mean distance between the bi-infratemporal line and the tympanic line than the distance found in *Homo*. These measurements depict the anterior orientation of the petrous temporal bone as it closes the distance between basioccipital and sphenoid. As such, the distance between the foramen magnum to the bi-infratemporal line is greater, and hence more anteriorly placed than observed among modern humans (Dean and Wood 1981). Lastly, the average angle between the joining carotid and the petrous temporal bone axis for all nonhuman primates was greater than the mean of that for *Homo*. Conversely, the angle between the parasagittal plane through the tympanic plate angle and tympanic to carotid averages were less than the angle averages of *Homo*.

Gracile and robust forms of australopithecines exhibit differences in these measurements. *Australopithecus africanus* had similar distances between the bi-infratemporal line and the tympanic line as seen with pongid. The robust australopithecine had temporal bones closer to the coronal plane as seen with humans. However, Dean and Wood (1981) observed that *Australopithecus boisei* exhibited an elongated tympanic plate resembling the elongation found in pongid. Though counterintuitive, positioning among the tympanic plate, carotid, and the anterior

petrous portion of the temporal bone relegates elongation/flexion as relative to the foramen magnum.

In contrast to nonhuman primates, Dean and Wood (1981) stated that *Homo* exhibits shortened petrous bones with the apex, indicating a separation between the basioccipital and sphenoid bones. Based on this separation and bone orientation to the coronal plane, the distance between the foramen magnum and the bi-infratemporal line is positioned more posteriorly (Dean and Wood 1981). Consequently, *Homo* lineal descent did not possess *Homo* traits exclusively, but a blending of characteristics. For example, species within the genus of *Australopithecus*, gracile or robust, have pongid elongation of the cranial base. Elongation is referenced by the bi-infratemporal line and the tympanic line, coupled with a *Homo*-like positioning of the foramen magnum. Similar results for *P. robustus* and *Homo erectus* depict this trend (Dean and Wood 1981).

In the research by Ahern (2005), the relative positioning of the foramen magnum on the occipital bone documented variation for *Homo sapiens*, *Pan troglodytes*, *A. aethieopecus*, *A. africanus*, *P. boisei*, and *H. egaster* species. Ahern's methodological approach includes basion, biporion chord, and bicarotid chord measurements. These measurements were contingent upon the anterior or posterior position of the biporion chord and the bicarotid chord relative to basion. Results indicated significant differences in mean values between *Homo* and *Pan* for both biporion chord and bicarotid chord variables. The ability to discriminate between species was questionable because both variables were influenced by the degree of overlap between *Pan* and *Homo*, even though both variables were significant within the model. Results indicate a greater degree of overlap among species, with 43% of *Pan* occupying positions within elliptical dispersal of *Homo*. Intriguingly, all of the fossil hominin individuals occupied positions outside the ellipses formed by both *Pan* and *Homo*. Lastly, discriminant function analysis reflects this overlap with misclassifications at 26.5% for *Pan* and 11.9% for *Homo*, with all fossil hominins misidentified as *Homo* (Ahern 2005).

From these results, Ahern (2005) concludes that employment of the biporion chord cannot serve as the sole criterion for distinguishing species, especially in the differentiation between hominin versus non-hominin primates. Univariate and bivariate tests indicated bicarotid chord would be a better option. As Ahern suggested, both biporion chord and bicarotid chord are two measurements that should be together.

External cranial base angle, as determined by the positioning of the foramen magnum, was explored by Luboga and Wood (1990). In their study, pooled subsets included *Homo sapiens*, *Pan troglodytes*, *Pan paniscus*, and representative samples from *A. boisei*, *A. africanus*, and *H. erectus*. Landmarks in relation to the Frankfurt Horizon considered the inclusion of the glabella, nasion, foramen caecum, sella, subnasale, alveolar, opisthocranion, opisthion, and basion. Linear measurements include opisthocranion to glabella, opisthocranion to subnasale, opisthocranion to foramen caecum, and opisthocranion to basion and three derived indices. Furthermore, defining the angle of the foramen magnum in ± values consisted of the line joining the orbital plane with the basion and the Frankfurt Horizontal. Positive values denote an anteriorly-placed foramen magnum while negative values identify a posteriorly-positioned foramen magnum.

Luboga and Wood (1990) found no significant differences in the three indices within subgroups of modern *Homo sapiens* or between modern human males and females. No differences between the two species of *Pan* were of reportable significance. Reported significant differences indicated allometry. *Homo* had only one isometric variable, opisthocranion to glabella, which indicated a larger cranium has a more posteriorly-placed foramen magnum. Between two species of *Pan*, each species is distinct: the position of the foramen magnum in *P. paniscus* was more posterior in position than its position in *P. troglodytes*.

Additionally, Luboga and Wood (1990) stated that foramen magnum inclination among members of the *Homo* sample differed from *Pan troglodytes* and *Pan paniscus*. Significant differences existed between the two species as the position of the foramen magnum was consistently located more anteriorly in *Pan paniscus* than in *Pan troglodytes*. In comparison, the relative position of the foramen magnum among fossil hominins varies within and among *P. boisei*, *A. africanus*, *H. erectus*, and *H. aff* species. Luboga and Wood (1990) concluded the evidence suggested that the orientation of the foramen magnum was invariant within the species *Homo*; however, significant differences existed between the two *Pan* species. When considering cranial size, only *Homo* and *Pan paniscus* were significant for allometry, as indicated by an anteriorly-placed foramen magnum. Based on these indicators, *A. africanus* represents a robust form of australopithecine.

As exemplified by these representative cases, the main approaches to cranial base angle have focused on both internal and external planes in reference to either the Frankfurt Horizon or the

Orbital Plane. Each case quantifies the relative positioning of specific cranial bones with such features as basicranium length or position of the foramen magnum. While Luboga and Wood (1990) quantified some differences among crania, little research was done to provide a quantifiable link between the cranial base with either posture or locomotion. Research by Strait and Ross (1999) addressed this issue and explored four possible angles or registration planes in relation to head and neck posture: line of gravity, the inclination of the orbital plane, neck inclination, inclination of the Frankfurt Horizontal, and neck/orbital plane angle.

Strait and Ross (1999) also compiled data on primate species encompassing quadrupeds, brachiators, suspenders, leapers, knuckle-walkers, and bipeds. According to Strait and Ross (1999), the results indicate that orbital inclination among species depicts clusters about a mean of 13.7°, which suggests that the orbits face anteriorly and somewhat inferiorly. In contrast, infraorbital porion to gravity measurement was bimodal, with infraorbital values inferior to porion. Neck inclination results indicated a separation between *Homo* and other primate species. Though overlaps exist, Strait and Ross (1999) reported that averages between knuckle-walkers differ by approximately 25°. Table 3.1 provides the comparative means for *Homo*, *Pan*, and *Gorilla* for these measurements.

Table 3.1. Reference plane averages for *Homo*, *Pan*, and *Gorilla*.

Species	Locomotion	Inclination Frankfurt Plane	Inclination Orbital Plane	Inclination Neck
Homo sapiens	Biped	93.2°	9.3°	17.9°
Pan troglodytes	Knuckle-walk	49.2°	23.4°	81.5°
Gorilla gorilla	Knuckle-walk	59.6°	18.4	56.4°

Compiled from Strait and Ross (1999).

Strait and Ross (1999) reported that results for correlation coefficients for clivus-presphenoid planes, orbital-axis orientation, the index of relative encephalization, and head-neck angle were significant among all extant species. As for all nonhuman primates, Strait and Ross (1999) reported similar results except for orbital-axis orientation and index of relative encephalization. Partial correlation results indicated that clivus-presphenoid planes were significantly correlated with the

index of relative encephalization. In addition to these correlations, head-neck angle also correlated with orbital-axis orientation.

In comparison to these conclusions for extant primates, Strait and Ross (1999) reported that head-posture results for *A. africanus*, *A. boisei*, and *H. habilis* consisted of the difference between the Frankfurt Horizon and orbital planes. As Strait and Ross (1999) speculated, if hominins held their heads within the proposed planes, differences would fall within the extant primate range based on orbital planes, but Frankfurt Horizon measurement would place the orbits more superiorly.

Strait and Ross (1999) conclude that head and neck posture is not a determinant of cranial base flexion. Instead, they propose that brain size has an influence on the amount of flexion. Moreover, although the Frankfurt Horizontal is used to determine the standard anatomical position of the cranium, Strait and Ross (1999) established the orbital plane as a better indicator of natural head posture across species.

Reference or registration planes, used to determine approximate head posture, also assume perceived positioning in relation to osteological landmarks. This view finds support as it relates to cranial base angle (Lieberman and McCarthy 1999; Luboga and Wood 1990) and foramen magnum orientation (Ahern 2005; Dean and Wood 1981) relative to the orbital plane direction (Strait and Ross 1999). A comprehensive review provided by Lieberman et al. (2000) illustrates these points; unfortunately, comparative research into the nature of multiple reference lines was absent.

Research by Barbera et al. (2009) addressed the absence of reference lines as they pertain to natural head position and corrected head position. They recorded nineteen angles and five linear measurements. Among the measurements, variables of particular interest include true horizon, true vertical, neutral horizontal axis, Frankfurt Horizon, Krogman-Walker line, P plane, posterior maxillary plane, mandibular plane, anterior tubercle-posterior tubercle, foramen magnum line, basion-opisthion, and odontoid process angle tangent (Barbera et al. 2009).

Results indicated significance for the true horizon to the foramen magnum line, foramen magnum line to the anterior tubercle, Krogman Walker line to the mandibular plane, basion to the Krogman Walker line, and anterior tubercle to the posterior tubercle. Random errors were greater than 10% for the neutral horizontal axis to the posterior maxillary plane and basion to Krogman Walker line,

and greater than 20 % for posterior maxillary plane and basion to odontoid process apex (Barbera et al. 2009).

Barbera et al. (2009) reported little difference in mean values for true horizon to the posterior maxillary plane and neutral horizontal axis-posterior maxillary plane. True horizon to the neutral horizontal axis, Frankfurt Horizon, Krogman Walker line, and P plane depicted similar findings. Also, strong correlations among these variables confirm the influence of the common plane, true horizon. Mandibular positioning had no influence on the results. These authors also suggest the use of neutral horizontal axis, Frankfurt Horizon, Krogman Walker line, and P plane as a correction factor to predict natural head position as opposed to other methods.

All of this previous research provides a background supporting the perspective that morphological features have more far-reaching consequences than linear measurements would indicate. Thus, the modularity and integration among individual bones reflect the results of these overall differences (Bruner 2007). The use of reference or registration planes, as related to linear and angular measurements, quantified both internal and external cranial base angles. These measurements denoted differences in cranial expansion, facial prognathism, and flexion or extension of the cranial base. Variations in significant results among the studies indicated that cranial base angles and reference planes play a major role in delineating species. Thus, neck angle and orbital angle quantified natural head position in terms of posture. Ultimately, this link denotes an orbital axis plane preference; however, measurements did not include the remaining axial skeletal system, e.g., vertebrae within the vertebral column.

3.2 Vertebrae

Classification of human vertebra consists of five main regions that constitute the vertebral column: seven cervical, twelve thoracic, five lumbar, five sacral, and five coccygeal or caudal (Degraff and Stuart 1986; Gray 1995). The number of vertebrae within the thoraco-lumbar region varies (± 1 to 2 vertebrae) among members of the *Hominoidea* (Aiello and Dean 2002; Ankel-Simons 2006; Danforth 1930; Dietrich and Kessel 1997; Williams and Russo 2015). Each vertebra, intraregional and interregional in placement, possesses morphological features or configurations that serve to integrate into an interlocking sequential series throughout the column (Panjabi et al. 1991a; Panjabi et al. 1993a; Panjabi et al. 1993b; Panjabi et al. 1991b; Rose 1975; Tan et al. 2004; Williams and

Russo 2015). Thus, both morphological configuration and vertebral formula reflect functional differences (Clauser 1980; Shapiro 1990; Shapiro 1991; Ward et al. 2010) within the column.

Beyond the pioneering research of Keith (1902, 1903), research by Schultz (1938, 1961) provided an analysis of vertebral number and length of each region based on the gross morphological definitions and essential functional aspects for regional vertebrae due to differences in the primary modes of locomotion of the species that possess them. Though cervical, sacral, and caudal/coccygeal vertebrae remain similar to traditional or clinical definitions, thoracic and lumbar regions were redefined as all vertebrae that bear ribs, and lumbar vertebrae are all vertebrae between the thorax and sacrum.

Vertebrae with blended characteristics are transitional vertebrae (Clauser 1980; Keith 1902; Keith 1903; Latimer and Ward 1993; Schultz 1961; Slijper 1946; Slijper 1947). The total percentage and the number of vertebrae per region vary among species and translate into an overall regional reduction among species. Table 3.2 depicts the differences in the number of vertebrae and length percentages among species.

Table 3.2. Number of vertebrae per region (Compiled).

Species	Cervical	Cervical length %	Thoracic	Thoracic Length %	Lumbar	Lumbar Length %	Sacral
H. sapiens	7	22.2	12	46.4	5	31.4	6
P. troglodytes	7	23.7	13	53.1	4	23.2	6
G. gorilla	7	23.4	13	49.2	4	27.4	5
P. pygmaeus	7	23.9	12	50.7	4	25.4	5
H. lar	7		13		5		4

Formula for most primates (not shown) – 7C:13T:6L or 7C:12T:7L.
Compiled from Williams and Russo (2015) and segment percentage of the presacral spine from Schultz (1938).

The number of thoraco-lumbar vertebrae is divided into two categories: the "short-backed" (Benton 1967; Jungers 1984; Keith 1903; Williams 2012) and "long backed" (Latimer and Ward 1993; McCollum et al. 2010; Ward 1993) models. They tacitly infer the addition or subtraction of

vertebra results in regional length, with differences reflecting the morphological configuration and their function. As pointed out by Williams and Russo (2015), differences in configuration are of particular importance at the thoraco-lumbar border, despite shared or mosaic vertebral morphology. Consequently, research of vertebral count and configuration denote differences between quadrupedal and bipedal forms of locomotion evident in extant primate species (Blue et al. 2006; Crompton et al. 2003; Crompton et al. 2008; Grausz et al. 1988; Haeusler et al. 2002; Harcourt-Smith and Aiello 2004; Jablonski and Chaplin 2004; Latimer and Ward 1993). Table 3.3 depicts traditional measurements used to capture morphological configuration among species. Excluding C1 and C2, which lack traditional corpora, the vertebra is split into the vertebral body and the vertebral arch.

Table 3.3. Common vertebral measurements.

Vertebral body	Measurements
Corpus Facet/demi-facet	Anterior height, posterior height, body width, surface area, volume
Vertebral arch	**Measurements**
Pedicle	Length, width, cross-section, angle
Lamina	Length, width, angle
Articular facet (superior/inferior)	Length, width, area, angles Distance
Transverse process	Width
Neural canal	Length, width, area
Spinous process	Length, angle
C2 - Dens	Length, angle

Compiled from Clauser 1980; Pal et al. 2001; Panjabi et al. 1991a, 1991b, 1993a, 1993b; Shapiro 1990; Ward et al. 2010.

Numerous researchers suggest that vertebral body dimensions provide insights into weight displacement since compression and vertebral wedging aid with the stability of spinal curvature (Biewener 1990; McGowan 1999; Oxnard 2000; Prakash et al. 2007). The orientation of the pedicle, transverse processes, and spinal process provides not only stability but also limits the range of potential movement. However, the interlocking articular facets (zygapophyses) are what allow for limited flexion, extension, rotation, and dorso-ventral and lateral movements (Bruno et

al. 2012; Granata and Bennett 2005; Scholten and Veldhuizen 1985; Williams and Russo 2015; Yamazaki et al. 1996).

3.3 Cervical vertebrae

Early research into the anatomy of cervical vertebrae indicated differences between C1 and C2 from the rest of the members of this spinal region (Gray 1995), as well as accepted variations in dimensions within *Homo* (Francis 1955a; Francis 1955b; Schultz 1961; Schultz 1931). As seen in Table 3.4, Francis (1955b) documented dimensional range for *Homo* and determined that centrum dimensions, vertebral height, and vertebral foramina show similar variations. As indicated by future research (Katz et al. 1975), Francis (1955b) concluded there were no significant differences between modern human populations and any differences between males and females were due to size.

Table 3.4. Cervical dimensions.

Vertebral Level	Corpus Anteroposterior Diameter (mm)	Corpus Lateral Diameter (mm)
C1	40-54	60-95
C2	44-64	43-64
C3	37-56	43-62
C4	34-56	44-64
C5	43.9-58	45-69
C6	40-64	46-73
C7	42-73	55-89

Adapted from Francis 1955b.

Although dimensional measurements reveal size variability, Francis (1955a) examined articular facet dimensions, facet angle, and facet angle to the sagittal plane. Results indicated a difference in the majority of vertebrae of less than five degrees in facet angle (left and right) for both superior and inferior articular facet measurements. Greater observed differences were seen in measurements from the facets to the sagittal plane (Table 3.5).

Table 3.5. Facet angle differences.

Element	Number of differences	Difference in degrees
C2	4 9	30 10
C4 upper	1	20
C5 upper/lower	3 1	10 15
C6 upper/lower	6,3/1	20,10/10

Adapted from Francis 1955a.

According to previous research (Whitney 1926), asymmetrical (tropism) differences among cervical facet dimensions among human populations and between the sexes reflect little variation. Francis (1955a) also concluded that variations in facet inclination were of greater importance than variations in the sagittal plane. However, as previously indicated in Table 3.5, differences observed at the C2-C3 juncture denote possible instability. Consequently, other than the omission of any congenital defect, facet dimensions and angles that maintain regional stability had minimal variations.

Further advances in technology allowed for greater in-depth analyses of vertebral configuration. The study by Panjabi et al. (1991a) uses three-dimensional measurements in reference to X, Y, and Z coordinates. Results obtained by Panjabi et al. (1991a) indicate a general increase in corporal dimensions until mid-region. The endplate tilt from the transverse plane was not significant between the superior and inferior centrum surface, with a constant posterior vertebral height. Pedicle dimensions reveal that corporal height is greater than corporal width, while pedicle inclination ranged from 8° below to 11° above the transverse plane. Pedicle inclination relative to the sagittal plane decreased from 40° to 29° at the anterior part of the vertebral corpus. Spinous process and transverse process lengths also noted slight decreases. Additionally, Panjabi et al. (1991a) reported significant test results that indicated differences throughout the cervical region. Recorded significant results include C6 and C7 in corporal dimensions; C2 in spinal canal dimensions; and C2, C6, and C7 in pedicle dimensions and angles.

Panjabi et al. (1991a) suggested that vertebral body dimensions exhibit progressive size differences due to weight distribution. However, C7 inferior endplate dimensions signaled a transition to the

upper thoracic region. Additional indicators identified in support of this conclusion were vertebral canal, uncovertebral joint area/inclination, and pedicular dimensions. Further investigation into facet orientation revealed that these angles to the transverse plane were less than the facet angles found in the sagittal plane and varied throughout the region with no change in orientation. Also, distance gradually increased, despite intra-regional variation (Panjabi et al. 1993b).

Using the methods of Panjabi et al. (1991a, 1993b), Tan et al. (2004) replicated the study using Chinese individuals for their study. Results yielded similar vertebral corpus dimensions. Since controversy among researchers concerning variability among world populations exists, the conclusion of Tan et al.'s 2004 study suggests consideration of the world's population before performing any analysis.

Previous research by Pal et al. (2001) also examined superior articular facet dimensions, the angle to the sagittal and transverse planes, and facet orientation. Results indicated variations in angular measurements, but no significant difference between the left and right sides of the sagittal or transverse planes. Facet dimensions and width-to-height ratios were the same for C3, C4, T2, and T3. Reported differences were at the C7/T1 juncture. Pal et al. suggested that the orientation of the facets, posteromedial versus posterolateral, reflects changes among vertebrae. Changes in orientation were sudden (37%) or gradual (63%). Reported angles and facet orientation (Table 3.6) differed from those obtained by Panjabi et al. (1993a) and indicated no significant differences in orientation.

Table 3.6. Facet orientation and movement.

Vertebral Level	Orientation	Movement
C2	NA	Fixed
C3/C4	Posteromedial	Resist rotation
C5/C6 (transition) C7-T3	Posterolaterally	Flexion, extension, rotation, lateral bending

Adapted from Pal et al. 2001.

As affirmed by Pal et al. (2001), four different functional zones encompass the cervical and upper thoracic regions of the spine. These include occipital condyle/C1 and C1/C2; C2/C3 and C3/C4; C4/C5 and C5/C6; and C6/C7 and T1/T2 joints. Additionally, the vertical orientation of the facets

in the transverse plane indicates reduced movement at C6/C7, C7/T1, and T1/T2 joints. The shifting of weight from the facets to the vertebral body via the pedicles provides the explanation for changes in facet orientation, including the presence of "butting" facets.

Recovery of hominin fossil cervical vertebrae is limited. Representative species include *A. afarensis* A.L. 333: elements 83 (C1), 101 (C2), and 106 (C5 or C6); and *A. sediba* MH1, consisting of elements UW88-71 (upper cervical), UW88-72 and UW88-73 (mid-cervical); and MH2, which includes UW88-93 (C3 or C4) and UW88-83 (C5 or C6) (Cook et al. 1983; Lovejoy et al. 1982; Williams et al. 2013). The few and fragmentary condition of the fossil elements severely restricts any extensive analyses.

Sex estimation using C1 and C2 vertebrae

Previous research pooled the sexes for intra-regional comparison. Only a few studies focus on the quantitative differences between the sexes. The study by Marino (1995) used metrical measurements to identify differences between human sexes. Using specimens from three osteological collections (Terry, Hamann-Todd, and 23PM5), results from separate multiple linear regression and discriminant analyses indicated differences between the sexes resulting in a high classification accuracy, e.g., Terry: 75-85%, Hamann-Todd: 60-77%, 23PM5: 70-85%. The use of different samples also indicated similar results (Marino 1995).

Wescott (2000) performed a similar study with C2 using samples from Terry and Hamann-Todd collections that utilized a battery of eight measurements. Results indicated that all variables contributed significantly for estimation of sex, which accounts for 67% of the total variation between males and females. The accuracy of the reported classification of males and females ranged from 81.7-83.4%. When males and females were pooled across osteological collections by population, misclassifications increased as stated by Wescott (2000), e.g., 89% correct for whites and 81% correct for blacks.

The ability to identify statistically significant differences in vertebrae between the sexes (Wescott 2000) has been confirmed by more recent research (Gomez-Olivencia et al. 2007). Differences in cortical and trabecular bone density, as well as the overall metrics, still supported Wescott's (2000) conclusions (Christensen et al. 2007; Cooper et al. 1992; Frobin et al. 2002; Gilsanz et al. 1994).

Regardless of approach, each researcher expressed caution in mixing samples of different human populations for sex estimations.

3.4 Thoracic vertebrae

Unlike the upper cervical vertebrae (C1 and C2), which are unique, the thoracic region consists of 12 ± 1 vertebrae (White 2000). Generalized features are consistent regarding the vertebral body and vertebral arch; however, as illustrated in Table 3.7, T1-T11 vary with the presence or absence of costal or demifacets (White 2000). Although rib articulation is not under consideration specifically, general metrical differences as previously depicted within the lower cervical region are noted.

Table 3.7. Thoracic whole and demifacets.

Vertebral level	Facet type/location
T1	Whole facet (superior) and demifacets (inferior)
T2 – T9	Demifacets on body (superior and inferior)
T10	Whole facets on body and transverse processes
T11	Whole facet on body (superior)

Adapted from White 2000.

Extensive research by Clauser (1980) examined metrical differences in the thoracic vertebrae among *H. sapiens*, *G. gorilla*, *P. troglodytes*, *P. pygmaeus*, *C. albigena*, *C. aethiops*, *C. ascanius*, *C. apella*, and *L. lagothricha*. Measurements included total height, total width, caudal centrum breadth, cranial centrum breadth, caudal centrum height, cranial centrum height. Additional physical measurements include left pedicle length, left pedicle width, neural spine height, neural spine breadth, neural spine length, neural spine angle, spinal canal height, spinal canal breadth, medial interfacetal width, lateral interfacetal width, left facet height, right facet height, and prezygapophysis angle.

The results obtained by Clauser (1980) for the vertebral body (corpus) dimensions distinguished between apes and monkeys within the hominoid classification, with two exceptions within the upper thoracic region. Monkeys showed little deviation from T1 to T13, exhibiting homogeneity,

whereas the thoracic vertebrae of the large-bodied apes depicted gradual increases in all dimensions.

Additionally, Clauser (1980) stated that the indical relationships among body measurements and centrum volume exhibit overlap among all species within the upper thoracic, but begin to deviate in the mid-thoracic region. Calculated moment of resistance (mm^3) was noted to indicate further differences. Regardless of size differences among extant nonhuman primates, the thoracic vertebrae of the great apes had lower mean momentary resistance values than those values observed among monkeys, which accounts for their type of mobility.

Pedicular dimensions and indices differ between monkeys and large-bodied apes as reported by Clauser, e.g., the pedicles of monkeys were smaller at each vertebral level. Clauser (1980) suggested that these differences reflect the position of the mortice joint and the distribution of weight along the vertebral column. This distinction between great apes and monkeys continues with the spinous process. Spinous process length differs between *Homo* and other hominoids, exhibiting the disparity between human and nonhuman primates. Facet and dimensions decreased from T1 to T8 in *Homo* and from T1 to T6/T7 in nonhuman primates. Regarding articulating facet dimensions, apes and monkeys share the same characteristics as revealed in vertebral body and arch measurements. After the last vertebral decrease, the trend depicts a general increase throughout the remaining thoracic region. Additionally, facet angle had similar means (greater than 90°) among all great apes and monkeys throughout the thoracic region, regardless of the open/closed orientation of the facets. This distribution of angles was similar to the results reported for facet dimensions as well. Clauser (1980) concludes that the size and shape of the vertebrae, including orientation, reflect differences in posture and mode of locomotion. The vertebral body, pedicle, facet, and spinous process provide thoracic stability, but flexion and extension also occur, in particularly among the diaphragmatic vertebrae.

Some support for Clauser's interpretation was provided in Panjabi et al.'s (1991b) three-dimensional analyses of the thoracic region. Their study yielded similar results using the same method and measurements depicted in Clauser's cervical study (1980); however, Panjabi et al. (1991b) included only modern humans in their study. Vertebral body dimensions were reported to increase gradually from T1-T12. Among individual measurements, upper and lower vertebral body areas, as well as length/depth and endplate angle (wedge), increased from cranial to caudal. Spinal

canal dimensions, specifically lateral width, could be divided into three distinct regions: a gradual increase from T1-T4, steady from T5-T7, and an increase from T8-T12. Pedicular dimensions were reported to increase from T1-T4, with a sudden drop at T4; an increase from T5-T8 with a sudden drop at T8; and an increase at T9 before leveling off from T10-T12. Pedicle angle exhibited greater dimensional variation from T1-T5, but calculated moments of inertia remained constant from T1-T8, with a sharp increase at T11. Other researchers (Tan et al. 2004) confirmed these results.

Observed contrary patterns by Panjabi et al. (1993b) were in the costalvertebral and costaltransverse – a sharp drop from T1 to T2 with a gradual increase to T6. T6 to T10 all have constant measurements, with sharp increases at T11. Spinal process dimensions exhibited a general increase from T1-T12. This pattern contrasts the transverse processes, resulting in variation which help to variation depict three distinct regions: a decrease from T1 to T4, consistency from T4 to T10, and further reduction from T11 to T12. When Panjabi et al. (1991b) analyzed trends amid significant vertebrae, they concluded that the thoracic spine encompasses three distinct regions based on both vertebral body and arch measurements. They include an upper zone (T1-T4), a middle zone or critical vascular zone for the spinal cord (T4-T9), and a lower zone (T10-T12). Articular facet dimensions and orientations further distinguish these zones (Panjabi et al. 1993b). Nonetheless, each of the three regions contributes to vertebral curvature and spinal stability.

In contrast, research by Latimer and Ward (1993) examined thoracic vertebrae among modern humans, *Pan troglodytes*, and KNM-WT-15000 (*H. egaster*). Comparative measurements included: vertebral wedging angle, interfacet distance, transverse body-to-distance ratio, inferior articular process length, facet angle, superior facet area, superior facet area-to-vertebral body ratio, and spinous process angle. The results indicated similar patterns to those in prior research.

As stated by Latimer and Ward (1993), modern humans exhibit a positive increase from T1-T6, indicating kyphosis; a decrease from T6-T10; and an increase from T11-T12. *Pan* had positive uniformity throughout the thoracic region (6.88°-5.58°). Examination of KNM-WT-15000 yielded trends that are more comparable to modern humans than to *Pan*, but two distinct regions at T1 and T7 were noted. Interfacet distance decreased steadily in *Homo* from T1-T6 and then increased to T12. Pan also exhibited parallel patterns.

Latimer and Ward (1993) indicated that the transverse body-to-distance ratio, inferior articular process length, facet angle, superior facet area, superior facet area-to-vertebral body ratio, and

spinous process angle were all distinctly different among the upper, mid, and lower thoracic region. In all cases, KNM-WT-15000 fell within or near the range of variation among modern humans. Latimer and Ward (1993) interpret their findings as an indication that the nature of thoracic kyphosis is similar to that of modern humans in KNM-WT-15000, although KNM-WT-15000 possessed vertebrae that were smaller and more varied in number within the thoraco-lumbar region. The similarities in hominins with thoracic kyphosis is the result of associated measurement suites – vertebral body shape, facet size and orientation, and spinous process dimensions – all related to bipedal locomotion.

Early fossil hominin thoracic vertebrae are more common than those of the cervical region. Recovered thoracic vertebrae include the following species: *A. afarensis* A.L. 288-1, elements am (T3 or T4), ae/ah (T6), af (T7), ag/aj (T8), ad (T10), ac (T11), and ai (T12); *A. afarensis* A.L 333, elements x12 (T10), 51 (T7, 8, or 9), and 81 (T2); *Paranthropus robustus*, SK 3981a (T12); *A. sediba*, MH1, elements UW88-11 (T2), UW88-96 (upper T), UW88-37 (mid T), UW88-69 (lower T), UW88-90 (lower T), and UW88-92 (lower T); *A. sediba*, MH2, UW88-188 (T3 or T4), UW88-189 (T4 or T5), UW88-190 (T5 or T6), UW88-191 (T6 or T7), UW88-114 (T10), UW88-43 (T11), and UW88-44 (T12) elements (Cook et al. 1983; Lovejoy et al. 1982; Sanders 1998; Williams et al. 2013).

Comparative metric assessment by Sanders (1998) included the following species: *A. afarensis*, *P. robustus*, *Homo sapiens*, *Pan trodylodytes*, *Gorilla gorilla*, *Pongo pygmaeus*, and *Hylobates lar*. Variables include ventral centrum length, dorsal centrum length, cranial centrum width, cranial centrum height, centrum shape index, and wedging index. In the exploration of both penultimate (T11 or T12) and last thoracic vertebrae (T12 or T13), the results obtained by Sanders (1998) for fossil hominin and nonhuman extant primate species are similar to results reported by Clauser (1980). Also, *A. afarensis* A.L. 288-1ac (T11) was reported to be smaller than the extant great apes considered in this analysis, but illustrated metrics similar to *A. africanus*. Furthermore, *P. robustus* SK 3981a had lower mean values for cranial centrum height and width, but mean values closer to *Gorilla* for ventral centrum length and closer to *Pan* for dorsal centrum length.

Serial positioning and species identification are problematic when considering incomplete vertebral columns. Research by Meyer et al. (2015) reconsidered the vertebral positioning for thoracic vertebral elements associated with A. afarensis A.L. 288-1. Comparative species include

Homo sapiens, *Pan trogylodytes*, *Gorilla gorilla*, *H. erectus*, *A. sediba*, *A. africanus*, and *A. afarensis*. Measurements include superior and inferior interfacet distance (minimum and maximum) and centrum dimensions. Results concur with Cook et al. (1983) for the following elements: ae/ah (T6), af (T7), ag/aj (T8), ad (T9), ac (T10), and ai (T11). Only the element am (T3 or T4) did not fall within the expected range for a single spinal column. This evidence suggests that the fossil element in question does not belong to *A. afarensis* A.L. 288-1, but to another species.

Sex estimation using the thoracic region

Previous research identified statistically significant sex-based differences between modern human males and females using C1 and C2 vertebrae (Marino 1995; Wescott 2000). The thoracic region, however, presents a unique situation. The morphological features indicate an interlocking series that result in kyphosis (Dietrich and Kessel 1997; Latimer and Ward 1993; Panjabi et al. 1984) and also provide the basis for rib articulation and rib cage configuration (Aiello and Dean 2002; Dansereau and Stokes 1988; Jellema et al. 1993; Watkins IV et al. 2005). Bastir et al. (2014) conducted 3-D analyses on thoracic vertebrae (T1-T10) to determine whether statistically significant differences exist between modern human males and females using vertebral size, costal facet, transverse process orientation, and spinous process dimensions and orientation. The results indicated that males were significantly larger than females and both sexes exhibited regional vector patterning (Table 3.8).

Table 3.8. Sex estimation reported by Bastir et al. 2014.

Units	% variance explained
Female (T1- T5)	63.7
Male (T1 –T5)	65.6
Female (T6-T10)	37.0
Male (T6-T10)	38.6

Adapted from Bastir et al. 2014.

Contributing factors, as stated by Bastir et al. (2014), for differences include the shape and orientation of the transverse processes, articulating facet orientation, foramen shape, the

orientation of the costal facets, and length and orientation of the spinous process. Differences between the sexes were necessary as compensation for weight displacement during pregnancy. Changes in the thoracic region allowed for greater thoraco-lumbar lordosis, which placed the developing fetus above the pelvis (Bastir et al. 2014).

3.5 Lumbar vertebrae

The lumbar region is distinctive among the three regions within the vertebral column. Lumbar vertebrae (5 ± 1 for *Homo* and 4 ± 1 for nonhuman primates) characteristics include a large vertebral body, prominent transverse processes, and a stout spinous process. Articulating facet orientation differs from previous vertebrae: superior articular facets are orientated medially, whereas inferior articular facets are orientated laterally (Bass 2005; Degraff and Stuart 1986; White 2000). When compared to extant primates, humans differ in both dimensional and morphological orientations that result in lordosis. The degree of lordosis exhibited by *Homo* denotes bipedal locomotion.

Clauser's (1980) research also documented variations and trends within the lumbar region. Results indicated a general increase in overall size from L1 to L5 for human and nonhuman primates. Also, centrum dimensions and indices continued the trend evident within the thoracic region, such as gradual increases with leveling towards the caudal end of the region. The greatest momentary resistance (cm^3) was reported at L4 for modern humans, whereas greatest momentary resistance within the lumbar region among the hominoids, specifically the great apes, occurs at L2/L3.

Pedicle dimensions were also found to differ between width and height among the great apes. Clauser (1980) noted that as pedicle length decreased from L1 to L4/L5, pedicle width experienced an associated increase caudally. Only monkeys exhibited stability among pedicle dimensions. Similar observable trends indicated differences in the spinous process among species. Facet and distance and prezygapophysis angle reported greater values than those of the thoracic vertebrae, whereas distance for the lumbar vertebrae among modern humans exhibits only a general increase caudally. The single dimensional difference between modern humans and all nonhuman primate lumbar vertebrae was the vertebral canal. Humans possess approximately 10 mm greater vertebral canal dimensions than any other nonhuman primate. Clauser (1980) suggests that the configuration and interlocking orientation of the lumbar vertebrae relate to the weight distribution detected

within the region. Differences were related directly to posture and locomotion, as illustrated in the differences among hominoids.

Panjabi et al. (1993a) provide some support for Clauser's interpretation with three-dimensional analysis of lumbar vertebrae. The results obtained by Panjabi et al. (1993a) reveal that vertebral body endplate dimensions (width-to-depth ratio) increased from L1 to L5. Upper end plates increased by only 12%, whereas the lower rose 21%. Spinal canal dimensions were reported to increase in lateral width (L1-L5). The distribution of depth was parabolic, with the smallest canal depth occurring at L3. Pedicle dimensions likewise exhibited parabolic distributions in width, height, and cross-sectional dimensions within the region. Angulation was reported to increase from L1 to L5. Facet dimensions, area, angulation, and interfacet distance also experience similar but larger increases than those observed in either the cervical or thoracic regions (Panjabi et al. 1993b).

Panjabi et al. (1993b) concluded that similar to the divisions within the thoracic region, three distinct zones delineate the lumbar region. These include the upper lumbar zone (L1, L2) characterized by a decrease in canal depth and pedicle height; a middle zone (L3) with a narrow spinal canal coupled with the greatest end plate areas and longest spinous processes; and a lower zone (L4-L5) with larger canal and pedicle sizes. The difference in morphology of L5 is due to the transition from the lumbar to the sacrum. As such, the role of the last vertebrae of the lower lumbar zone is similar to that of the lower thoracic region because both act as transitional elements from one region to the next.

Additional research by Latimer and Ward (1993) yielded similar results. Interfacet distance increased from L1 to L5 for modern humans, with parabolic distribution for *Pan*. Parabolic distribution with slight decreases reported transverse diameter-to-interfacet ratio, inferior process length, and orientation of the articular facet to the transverse plane. Spinous process and the articular facet area observed general increases. Reports of vertebral wedging indicated a positive value at L1, acting as a transitional zone, thereafter increasing caudally in a negative value to L5. Though negative values depicted lordosis, the gradual increase in lordosis did not correspond with a decrease in the changes in the vertebral area as indicated in previous research (Panjabi et al. 1993b). Whereas differences were apparent between modern humans and *Pan*, the lumbar region for hominin KNM-WT-15000 was similar to modern humans for vertebral wedging, interfacet distance, transverse-to-distance ratio, and the variable facet area-to-body to surface area ratio

(Latimer and Ward 1993). Slight variations among other hominins were dimorphic, ultimately attributing differences to size or body weight in relation to the number of vertebrae per region (Latimer and Ward 1993).

The study by Shapiro (1993) included a broader range of nonhuman primates, which included *Homo*, *Pan*, *Gorilla*, *Pongo*, *Hylobates*, *Ateles*, *Alouatta*, *Cebus*, Indri, *Propithecu*, *Varecia*, *Papio*, and *Cercopithecus*. Variables considered calculations for body surface area, pedicle area, and pedicle shape. Considering size and differences in the number of vertebral elements within the lumbar region of the spine, lumbar results indicated an increase in body area along the lumbar column with a decrease at L5 for hominoids. However, similar patterns were evident with hominin species, suggesting that increases in the direction of the lower lumbar region are not unique among primates and that these patterns are independent of either posture or locomotion. Body weight was significantly positively correlated with size for all species except platyrrhines.

In all species, pedicular area and shape along the column increased in a gradual fashion caudally, with a sharp increase nearing the last vertebra (Shapiro 1993). The increase in pedicular area and shape does not necessarily correlate with a decrease in vertebral area, e.g., the *Ateles* species. The discontinuity between corpus and pedicular dimensions was present in last lumbar and first sacral vertebrae (i.e., the lumbosacral junction). When Shapiro (1993) considered weight relative to pedicular area and shape, the relationship between pedicle area and body weight was not significant among platyrrhines. Pedicle shape was not significantly associated with body weight for any primate genera considered. Results for fossil hominin Sts 14 (*A. africanus*) placed the species within the *Homo* range for pedicle shape, but the length/body weight and the remaining calculations placed Sts 14 among hominoids, specifically the great apes.

Lumbar vertebrae are well-represented among early fossil hominins, especially given the number of vertebrae within the region. Species include: *A. afarensis*, A.L. 288-1, elements ak (L2), ar (L3 or L4); *A. afarensis*, A.L. 333 73 (L3); *A. africanus*, Sts-14, elements f (L1), e (L2), d (L3), c (L4), b (L5), and a (L6); *P. robustus*, elements SK 3981b (last lumbar) and SK 853 (lumbar vertebra). Lumbar vertebrae for *A. sediba* include MH1 elements UW88-92 (L1) and UW88-152 (L2); and MH2 lumbar UW88-127/153 (L4) and UW88-126/138 (L5) elements (Cook et al. 1983; Lovejoy et al. 1982; Meyer et al. 2015; Sanders 1998; Williams et al. 2013).

A comparative metric assessment by Sanders (1998) included: *A. afarensis*, *P. robustus*, modern *Homo sapiens*, *Pan trodylodytes*, *Gorilla gorilla*, *Pongo pygmaeus*, and *Hylobates lar*. Variables under consideration include ventral centrum length, dorsal centrum length, cranial centrum width, cranial centrum height, centrum shape index, and wedging index. The reported mean values for vertebral body dimensions, facet dimensions, and facet angles vary among species. At the same vertebral level, the body dimensions of *A. afarensis* were larger than those variables for *A. africanus*, but the body dimensions for *A. africanus* were smaller than those of *P. robustus*. Vertebral facet angle was reported to be larger in *A. africanus* than the facet angles of *A. afarensis* or *P. robustus*. Linear measurements were not incremental in light of serial positioning and comparative serial positioning, but variations were stated to be related to vertebral identification and functional role within the vertebral column, e.g., lumbar lordosis.

Meyer et al. (2015) provided additional insight as they reconsidered the vertebral positioning for the lumbar element assigned to *A. afarensis*, A.L. 288-1. Comparative species include modern *Homo sapiens*, *Pan trogylodytes*, *Gorilla gorilla*, *H. erectus*, *A. sediba*, *A. africanus*, and *A. afarensis*. Measurements include superior and inferior interfacet distance and centrum dimensions. The results differed from Cook et al. (1983), who designated element ab designated as L2 and element aa/ak/al as L3.

Though slight differences among researchers exist (Ankel 1972; Billmann et al. 2007; Davis 1955; Davis 1961; Ishii et al. 2006), the complexity of vertebral morphology is evident throughout the spinal column, as depicted in previous anthropological and medical studies. Furthermore, a consensus determined two specific factors in terms of vertebral morphology: the functional role of the vertebral body and the multiple integrated features of the vertebral arch.

The size and shape of the vertebral bodies throughout the column have an association with the compressive stresses related to weight distribution via soft tissue (see Appendix A for a review of biological materials). The distribution of weight in both extant primates tacitly suggests the result of direct weight placement and shifted weight displacement via the vertebral arch. The shift of the vertebral body primarily is primarily due to vertebral arch integration, specifically in the pedicle and both articulating facets where weight is both supported and redirected anteriorly. Furthermore, superior/inferior facet orientation, including corpal and transverse facets for rib articulation, has regional specificity with transitional vertebrae that serve to integrate regions, e.g., continuity via

zygapophyseal joints. Also, differences among vertebrae, intra-regionally and inter-regionally, limit movement. For this reason, vertebral architecture results in the overall design of the column as a whole.

3.6 Vertebral column and vertebral curvature

Previous researchers (Boszczyk et al. 2001; Dietrich and Kessel 1997; Frobin et al. 2002; Gangnet et al. 2003; Keller et al. 2005; Naderi et al. 2006; Naderi et al. 2007) investigated the concepts of weight distribution along the vertebral column with respect to the center of gravity, the vertebral body, pedicle, and articular facets. Studies of individual vertebrae or vertebral sequences, however, have not explored the column as an interlocking structural unit. Perceptions and theoretical foundations for viewing the structure in its entirety as a column are not new (Naderi et al. 2006; Naderi et al. 2007). Views of the spine as a column have changed from a conception of the spine as a single column (integration of the whole vertebrae) to a view of the spine as a two-column structure (vertebral body and vertebral arch). Additional speculations perceive the contact points among vertebrae as composing yet another columnar system. Conceptually from this perspective, "three" columns are now considered to be integrated.

Research by Louis (1985) examined and tested the three-column concept with morphological, biomechanical, and clinical cases from different sources. He found that the focus for spinal stability is along the vertical axis as related to the morphological configuration of the vertebrae. The atlas links the cranium to the column using two pillars via articulating facets. These pillars transition to the three pillars by way of the axis. The remaining vertebrae, C3 through L4, mirror C3, in that the vertebral body is one pillar on which the facets of the posterior arch contain the remaining two. In addition, L5 contains three pillars but accentuated vertebral wedging drastically changes the posterior pillar angles in line with the isthmic zones to the pelvis. Overall, the configuration between the body and the arch link the triangular apex anteriorly to the body and the isthmic angles posteriorly to the facets.

Contrary to expectation, Louis's study (1985) revealed that neither the transverse processes nor the spinous process contribute to spinal stability. Instead, unlike vertical stability, Louis claims that transverse stability is the result of bony stops and ligamentous brakes throughout the vertebral column. In this manner, flexion, extension, and rotation exhibit variation along a common opposing plane between anterior and posterior columns, e.g., cervical 45°, thoracic 60°, and

lumbar 90°. Weight distribution differs according to the orientation of the axis. Louis (1985) suggests that when the spine is held in the vertical position (i.e., orthogradic posture), the force of gravity, weight, and opposing muscular force produces a compressive force on the discs and shear on the posterior facets. When additional weight is added to the vertebral body, a shift from the compression of the discs and shearing of the facets to the opposite occur, causing compressive stress on the facets and shearing of the discs.

Louis's (1985) groundbreaking research employs an overall morphological framework with regard to vertebral articulations and weight distribution. Subsequent support for such a framework is available in an array of studies (Boszczyk et al. 2001; Dietrich and Kessel 1997; Frobin et al. 2002; Gangnet et al. 2003; Keller et al. 2005). In the study by Keller et al. (2005), the distribution of compressive forces within the intervertebral discs (IVD) was evenly located between anterior and posterior segments in C2-C6 (less than 10 kg), followed by a progressive increase in compressive loads ventrally from C7 to T9 (30 kg). The force is equal ventrally and dorsally. From T10 to S1, dorsal compression increases while ventral compression decreases, with a dip at the T12-L1 junction. Overall, the compressive forces at the IVD sections differ in degree but reflect spinal curvature by region.

In comparison, research by Gangnet et al. (2003) considered the distances in a sample of modern humans from the geometric center of the vertebral body to the acoustic meati, hip axis, gravity line, and both sagittal and ventral planes. Using radiographs, pressure platforms, and 3-D processing, the results indicated that the 3-D distance between the geometric center of the vertebra and the gravity line varies by anatomical position. In the sagittal plane, the distance to the gravity line increases cranially. Whereas L1 was closest to the gravity line, L4 lies most ventral and T7 furthest dorsal to this line. Ventral plane distance to the gravity line was steady after T4, indicating thoracic curvature. The lateralization of center of the vertebral body to the acoustic meati and hip axis, relative to individual vertebral elements, increased cranially, but ventral to the line of gravity. Additionally, the axis inclined caudally with slight ventral/dorsal variations. This three-dimensional description of the three-column concept attempts to create a visualization of the morphology and vertebral element placement within the column to illuminate spinal stability during posture and locomotion.

Overall, Gangnet et al. (2003) concluded that the gravity line was ventrally placed at T9, dorsally positioned at L4/L5, and transmitted to the pelvis. As for the location of vertebrae within both kyphotic and lordotic curvatures, the positioning of the gravity line relative to the vertebral geometric center exhibited variation, i.e., ventral (+) or dorsal (-) between the two planes. The results agree with IVD studies within the three-column conceptual framework. The dynamic relationship among force, vertebral body morphology, and spinal curvature also is supported by biomechanical and clinical research (Etnier 2001; Fazzalari et al. 2001; Goel and Clausen 1998; Kopperdahl et al. 2000; Legaye and Duval-Beaupere 2008; Liem et al. 2005; Silva et al. 1997; Smith et al. 1991). Vertebral body size, including the degree of wedging, pedicle morphology, and facet size/orientation, contribute to weight displacement along the column.

The exact placement of gravity needs further study in greater detail among extant nonhuman primates. However, general descriptive analyses suggest that the center of gravity among primates considered leapers and brachiators lie parallel to or near the center of the column. By contrast, quadrupedal primates, unlike other quadrupedal animals, have less pronounced spinal curvatures that are not parallel to the contact surface. Consequently, weight displacement was not depicted as perpendicular to the vertebral body but located as anteriorly in the lower thoracic (Ahlborn 2004; Preuschoft 1978; Preuschoft 1990; Preuschoft and Gunther 1994).

3.7 Summary and conclusion

The existence of posturo-locomotory complex indicators resides not in an individual vertebral trait, but in the mechanical combination of several vertebral traits. This is a perspective that is inferred but never directly stated by many researchers (Ahlborn 2004; Gal 1993; Lanyon 1990; Oxnard 2004; Preuschoft 1990). Morphology of the vertebral body, pedicle, superior and inferior articulating surface orientation – in conjunction with the cranial base – remains a morphological paradox. Cranial base and vertebral traits are distinct yet common to all extant primates, with displays of shared locomotive repertoire.

The cranial base and subsequent vertebrae present a unique problem for analysis due to integration. Approaches to the analysis of the cranial base include sagittal (Lieberman et al. 2008; Lieberman and McCarthy 1999; McCarthy 2001) and *norma basilaris* (Ahern 2005; Dean and Wood 1981; Lieberman and McCarthy 1999; Lieberman et al. 2000; Luboga and Wood 1990). In both cases, the approaches not only encompass morphological variation, but also include reference planes for

osteological landmark orientation (Barbera et al. 2009; Strait and Ross 1999). Conclusions suggest that sella, clival, and sphenoid orientation planes relate to cranial integration, whereas the orientation of the foramen magnum among the tympanic plate, carotid, petrous, and basion relates to external measurements (Ahern 2005; Dean and Wood 1981; Lieberman and McCarthy 1999; McCarthy 2001). Data suggest that the orbital axis, Frankfurt Horizontal, horizontal neutral axis, Krogman-Walker line, and P plane provide the best results to determine natural head position.

Vertebral analyses among the cervical, thoracic, and lumbar regions incorporate vertebral corpus dimensions, pedicle dimensions, and facet orientations. Distinctions throughout the column, with overlap among species, include a caudal increase in vertebral corpus size, canal dimensions, pedicle diameter, distance, and facet area/orientation to the sagittal, coronal, and transverse planes (Clauser 1980; Francis 1955a; Francis 1955b; Panjabi et al. 1991a; Panjabi et al. 1993a; Panjabi et al. 1993b; Panjabi et al. 1991b; Shapiro 1990; Shapiro and Simons 2002). Dimensional differences are limited to C1 (Marino 1995), C2 (Wescott 2000), and T1-T10 (Bastir et al. 2014) to determine sex estimation within the *Homo* species. Furthermore, intra-regional vertebral analyses indicated three distinct zones (upper, middle, and lower) within the thoracic (Panjabi et al. 1991b) and lumbar regions (Panjabi et al. 1993a). The differences found within the vertebral column, perceived as an integrated unit, provide the column with spinal stability during weight transmission (Keller et al. 2005; Louis 1985), in respect to COM (Gangnet et al. 2003). Although previous investigations into the cranial base and the vertebral column added to the scientific knowledge base, conflicting results with the introduction of new technology indicate understanding is far from complete.

Spinal stability is necessary for postured stance and locomotion in any animal, quadrupedal or bipedal. Louis (1985) suggested the concept of the three-column spine – the anterior and two posterior pillars providing both axial and transverse stability via articular orthogonal triangulation. In this manner, the plane of posterior articulations is opposite of the IVD: Cervical = 45°, Thoracic = 60°, and Lumbar = 90° (Louis 1985). Keller et al. (2005) also reported the distribution of compressive forces within the intervertebral discs spread evenly between the anterior and posterior areas in segments C2-C6. A progressive increase in compressive loads is placed anteriorly to T9, where the force is anteriorly and posteriorly equal. The distribution of compression varies at each level and produces an outline that is similar to spinal curvature.

The transmission of weight in respect to COM provided additional evidence of curvature and locomotion. According to Gangnet et al. (2003), body mass (GL) was anteriorly placed at T9, posteriorly placed at L4/L5, and transmitted to the pelvis. As for vertebrae within both kyphotic and lordotic curvatures, the GL to vertebral geometric center exhibited variation, e.g., anterior (+) or posterior (-) amid the two planes. Results agree with IVD studies within the three-column conceptual framework. The dynamic relationship among force, vertebral body morphology, and spinal curvature receive additional support by biomechanical and clinical research (Etnier 2001; Fazzalari et al. 2001; Goel and Clausen 1998; Kopperdahl et al. 2000; Legaye and Duval-Beaupere 2008; Liem et al. 2005; Silva et al. 1997; Smith et al. 1991). Corpus size, which includes the degree of wedging as well as pedicle and facet size/orientation, contributes to weight displacement along the vertebral column.

Considering the complicated issues regarding primate posture and locomotion (Chapter 2), the sequential morphological configuration of individual vertebra within the column must displace the weight during posture and locomotion. While greater variation can be seen in posture and locomotive behavior among genera and species, the biomechanical configuration of the vertebral column (including soft tissue), aided by equilibrium provided by natural head position, e.g., cranial base, sets the limit for potential movement. Excessive loading causes mechanical failure, and in the case "unnatural" gait, a disruption in resonant frequency results in an increase in energy expenditure.

Difficulties from previous research addressed in this research include: (1) select metric variables that have importance at an individual element level and as an integrated functional unit, (2) a measurement of the relationship between the cranial base and vertebral curvature, and (3) computation of the cranium and vertebral column to the positional-locomotory complex.

Chapter 4. Materials and methods

The overarching issue addressed by this research is whether the morphological features of the cranial base and vertebrae have the ability to differentiate among modern human, extant non-human hominines, and fossil hominin and their positional-locomotory complexes. The conceptual approach to answering this question considers the cranium and vertebral column as a single, integrated functional unit. Integrating multiple structures with observed locomotory behaviors takes into account two fundamental premises. First, the orientation of the basicranium is the most superior reference point for the vertebral column. During bouts of locomotion, basicranial orientation stabilizes and counterweights the column via the atlanto-occipital joint. Second, each vertebra within the column contributes to the overall regional curvature within that column by the posterior interlocking facets found at the vertebral arch. Vertebral morphology, though similar in appearance among elements within each region, reflects subtle changes from vertebra to vertebra due to the placement of individual elements within the column. Consequently, differences in posture and the stresses incurred during bouts of locomotion assumingly intensify the differences between bipeds and knuckle-walking species. These premises provided the basis for the selection of species and specific variables used in this research.

4.1 Materials

All specimens analyzed in this research are curated at the Cleveland Museum of Natural History (CMNH) in the Hamann-Todd Osteological Collection (H-TOC). Three extant species include *Homo sapiens*, *Pan troglodytes*, and *Gorilla gorilla*. Also, *Australopithecus afarensis* (A.L. 288-1, A.L. 333 x12, and A.L. 333 106) specimens were under consideration for comparative purposes. Table 4.1 provides the total sample size by individual and by the number of skeletal elements.

Table 4.1. Species and sample size.

Species	Female	Male	Total Sample	Total Elements
Homo	16	18	34	850
Pan	10	6	16	400
Gorilla	8	8	16	400
Total	**34**	**32**	**66**	**1650**
A.L. 288-1[1]			1	2
A.L. 333 x-12[1]			1	1
A.L. 333 106[1]			1	1
Grand Total	**34**	**32**	**69**	**1654**

[1] Denotes comparative vertebra.

4.2 Methods

Previous research successfully utilized scanning technology (Garvin and Ruff 2012; Kuzminsky and Gardiner 2012; Manzon et al. 2012; Sholts et al. 2011). Two separate NextEngine Desktop 3-D Scanners and ScanStudio software (HD Pro) created 3-D models for both cranial and vertebral elements. NextEngine uses MultiStripe Laser Triangulation to capture data points. Custom calibration for each scanner includes a camera and thermal management system to ensure consistency and optimal performance during the scanning process (Kim 2016).

Rhinoceros 5.0 engineering software was used to capture and record all individual and integrated measurements with 3-D models. Rhino 5.0 imports the 3D image (mesh) onto a plane and measures point-to-point calculations on the mesh (Associates 2016). All statistical analyses conducted in this research used SPSS v.22 software. Complete details for scanner and CAD software specifications are available at www.nextengine.com and www.rhino3d.com.

Scanning, model alignment, and model fusing

Checking measurement accuracy included scanning a skeletal element (L1 and L2) for measurement comparison. Vertebral corpus height and width measurements were taken via Rhino 5.0 software and compared to measurements using a digital caliper prior to fieldwork. Differences among measurements were negligible (± 0.002 - 0.003 mm).

A three-step process included scanning, processing, fusing, and measuring, establishing a detailed procedure for data collection to ensure accurate and replicable results and a means to avoid poor quality of images or inaccurate measurements.

Each cranium and vertebra were scanned, aligned, and fused with the settings depicted in Table 4.2. The settings considered the skeletal element size, camera foci, osteological feature resolution, and model integrity.

Table 4.2. Scanner, alignment, and fuse settings.

Scanning Settings[1]						
Element	Number of scans	Scanner-turntable distance	Divisions per 360°	Points per in^2	Range	
					Accuracy	Triangle Size
Cranium	3	17"	10	1.1k	0.015"	0.0300"
Vertebra	2	7.5"	8	10k	0.005"	0.0100"

Alignment and Fuse Settings[2]						
Element	Alignment			Fuse		
	Tolerance	Maximum Iterations	Sample Ratio	Deviation Tolerance	Pixel	Resolution Ratio
Cranium Vertebra	0.005"	10	1:1	0.025"	25	0.05

[1] Scan family consists of three individual 360° scans in monochrome.
[2] Scan family consists of three individual 360° scans aligned and fused into one 3D model.

For the cranium, three individual 360° scans (one scan family) were initiated to ensure complete data points of the cranium and to capture all complex morphological features. The scans include the positioning of the occipital, parietal, and frontal bone at 210° to the scanner. After completion, the scan family file was saved for processing. Except for the settings, vertebral scans followed the same procedure. Two individual 360° scans (one scan family) were initiated to ensure complete data points of the vertebra and to capture morphological features. The scans include the positioning of the superior vertebral centrum and inferior vertebral centrum at 210° to the scanner. Each family file was saved for processing.

Image processing was a four step procedure: (1) trimming, (2) aligning, (3) fusing, and (4) orienting. Proper trimming and aligning were necessary before any fusing or 3-D orientation. Each

scan within each scan family underwent trimming before alignment. Trimming is the removal of unwanted data from the scan, e.g., turntable or bone gripper. After trimming, the alignment process used three alignment-point placement pins for each scan within the scan family. Table 4.2 provides a record of those settings. The alignment of multiple scans created a single aligned model with multiple meshes. After alignment, fusing the individual scans resulted in one 3-D model. The fused skeletal element model was globally orientated in three dimensions (X, Y, and Z) by labeling the superior, inferior, anterior, and posterior views. Default settings assigned lateral views. Fused models were saved and exported as an .OBJ file.

Measurements

Each skeletal element (.OBJ file) was imported into Rhinoceros v.5.0 (64 bit). The orientation of each element underwent confirmation and was evaluated for measurement viability. Though scanning uses standard units of measurement, the CAD software processed the metric conversions. All measured distances are in millimeters (mm) and angles are recorded in degrees (°). Orientation differences in nomenclature between bipeds and quadrupeds were noted, e.g., superior (cephalic), inferior (caudal), anterior (ventral), and posterior (dorsal).

Cranial Variables

Cranial base angle (CBA) utilized two reference planes. One depicted the orientation of the Frankfurt Horizon (FH). The placement of the second plane on the basicranium depicted critical points below the occipital condyles and above opisthion and basion (Fig. 4.1).

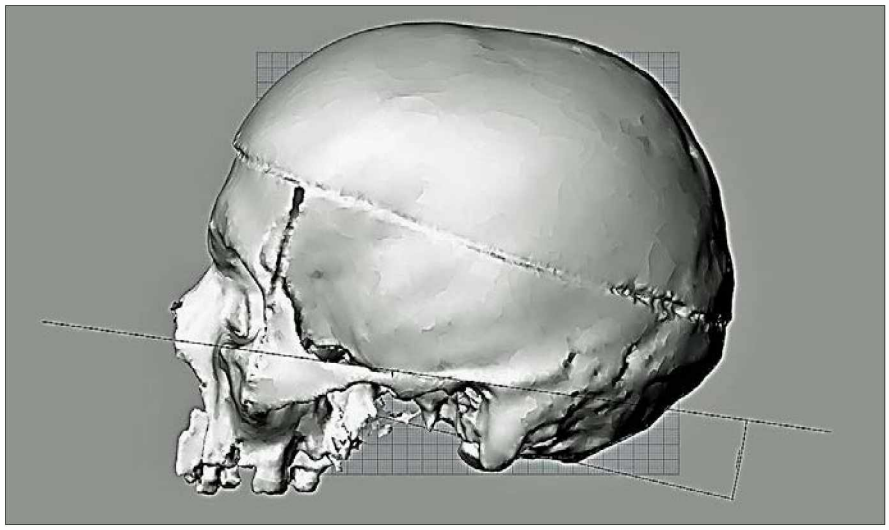

Figure 4.1. Cranial base angle. HTH 0288 depicted.
Scan**:** Cleveland Museum of Natural History Hamann-Todd Osteological Collection.

Using previous approaches (Ahern 2005; Dean and Wood 1981; Lieberman and McCarthy 1999), CBA in this research considers the orientation of *both* the foramen magnum and occipital condyles as it relates to the relative positioning of the foramen magnum on the cranial base to a standardized anatomical reference plane. The assumption and rationale take into account the foramen magnum position, as occipital condyles act as reference points for contact with C1 and C2 (atlanto-occipital joint) in determining the natural head position as it relates to spinal curvature.

Vertebrae

Vertebral orientation and measurements consist of three constructed reference planes perpendicular to the inferior surface of the vertebral body. The first two reference planes were placed at the vertebral body in the coronal and sagittal orientation. A third plane, parallel to the coronal, was placed at the arch. The orientation of the vertebra relative to the reference planes divides the vertebra into quadrants within a 3-D space. Measurements were taken after orientation confirmation.

Articular angle measurements (C3-L5)

After ascertaining the total facet breadth, surface lines for both superior and inferior articular facets were positioned midline through each facet, according to the orientation. These surface lines were used to measure facet angles (Fig. 4.2) relative to the reference planes for left and right sides. Variables are as follows: superior facet angle (SFAL and SFAR), superior facet projected angle (SFPAL and SFPAR), inferior facet angle (IFAL and IFAR), and inferior facet projected angle (IFPAL and IFPAR).

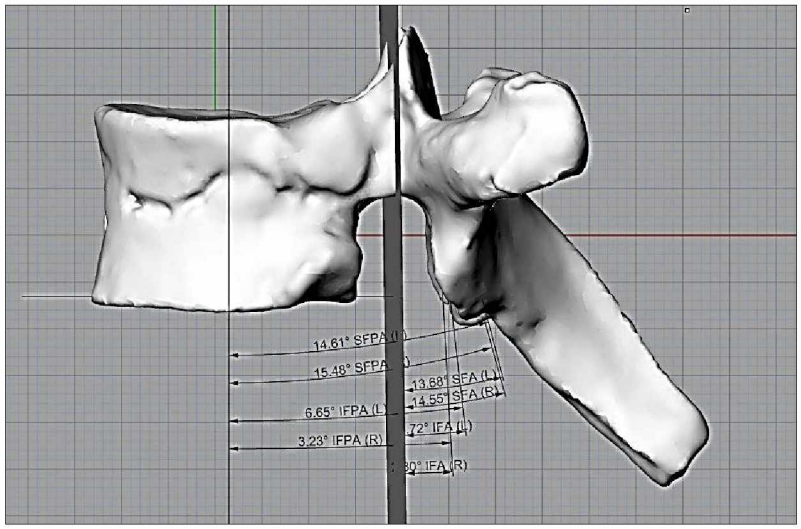

Figure 4.2. Facet angles. HTH 0288 depicted.
Scan**:** Cleveland Museum of Natural History Hamann-Todd Osteological Collection.

As noted in Figure 4.2, the differences in the angle "pull draw," as illustrated by all superior and inferior lines, do not affect the angled measurement. As such, the depicted pull draw is for illustrative purposes only.

The assumptions and rationale for the SFA/SFPA and IFA/IFPA variables considered facet angles as an integral and distinct mechanism for both interlocking vertebrae and spinal curvature. Previous research (Pal et al. 2001; Panjabi et al. 1991a; Panjabi et al. 1993a; Panjabi et al. 1993b; Panjabi et al. 1991b) using similar measurements indicated possible value. Similar approaches were used for C1 and C2. Calculated averages eliminated sporadic variation beyond lateral

dominance. The assumption was that these averages presented a better image of the three-pillar concept of the spine.

Measurements differ for C1 and C2 due to vertebral morphology. C1 superior and inferior facet angles consisted of surface lines across each articular facet and a posteriorly-placed plane at a 90° angle to the vertebral body placement. Surface lines across each articular facet and posteriorly placed plane at a 90° angle to the vertebral body (Fig. 4.3) yielded both superior and inferior facet angles for C2. Variable designations are the same as previously depicted.

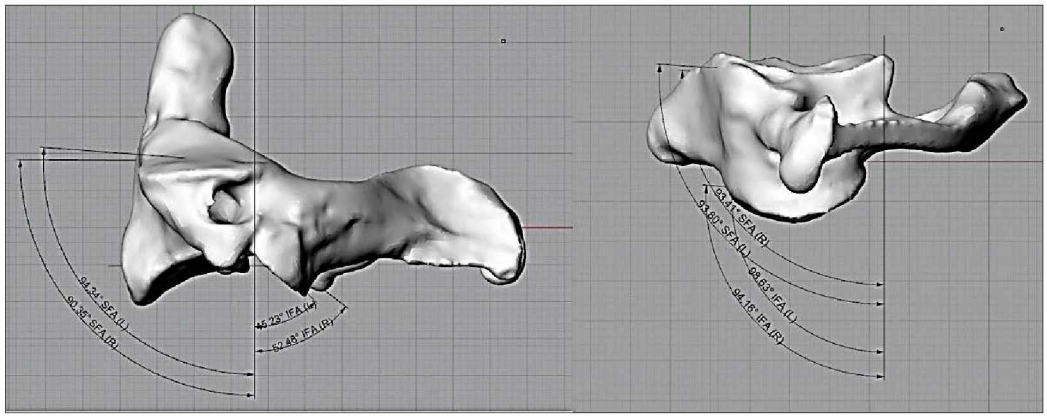

Figure 4.3. C1 and C2 facet angles**.** HTH 0288 depicted.
Scan**:** Cleveland Museum of Natural History Hamann-Todd Osteological Collection.

Vertebro-articular angle (C1-L5)

A second articular facet reference line was placed at 90° to the first reference plane for all vertebro-articular measurements (Fig. 4.4). Lateral measurements ran point-to-point from the articular facet line to the sagittal plane. The variables include a superior vertebro-articular angle (SVAPAL and SVAPAR) and an inferior vertebro-articular angle (IVAPAL and IVAPAR).

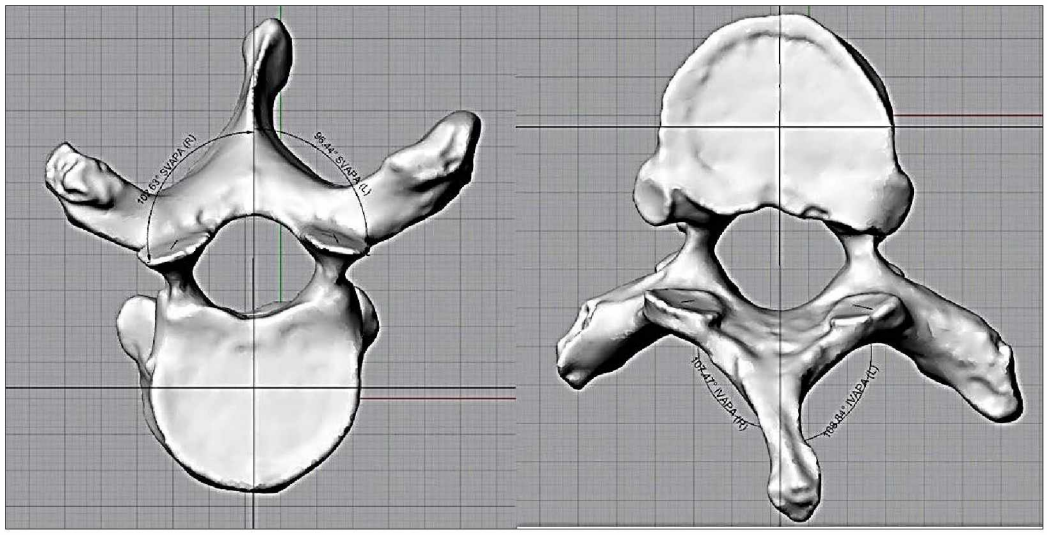

Figure 4.4. Vertebro-articular angle (superior and inferior). HTH 0288 depicted.
Scan**:** Cleveland Museum of Natural History Hamann-Todd Osteological Collection.

Based on previous research (Clauser 1980; Gommery 2006; Pal et al. 2001; Panjabi et al. 1991a; Panjabi et al. 1993b; Ward et al. 2010), the vertebro-articular measurement considered individual variation within each region and the presence of a mortice joint at key transitional vertebrae. Lateral dominance and tropism are distinct possibilities, but the variable average was used to circumvent positional variation not attributed to lateral dominance.

Interfacet Distance (C3-L5)

Superior distance (SFID) and inferior distance (IIFD) measurements (mm) were taken at the midpoint or center of each facet after facet height and width were documented with a reference line (Fig. 4.5).

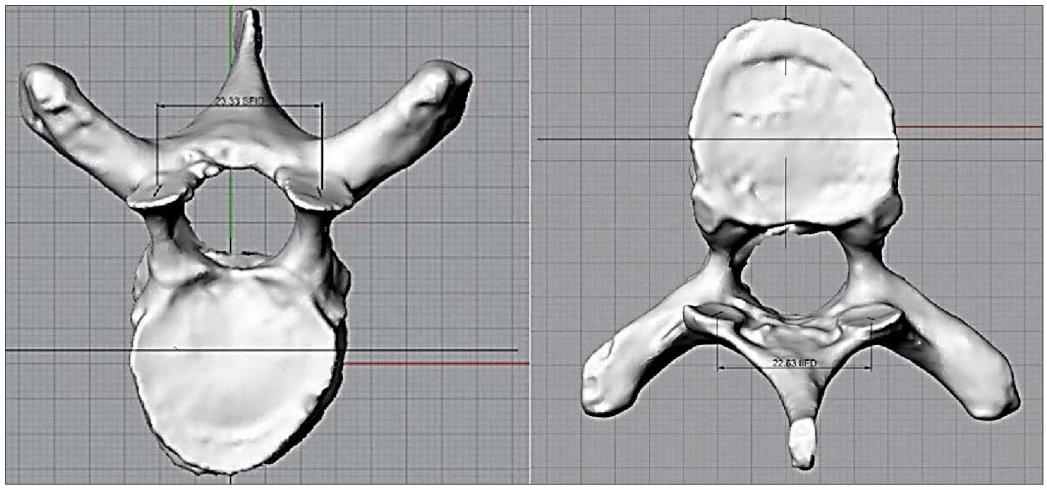

Figure 4.5. Interfacet Distance. HTH 0288 depicted.
Scan: Cleveland Museum of Natural History Hamann-Todd Osteological Collection.

In addition to the SVAPA, IVAPA, SFA, and IVA, the primary assumption regarding interfacet distance involves vertebral column stability variables. Unlike previous research (Clauser 1980; Pal et al. 2001; Panjabi et al. 1993b), the center of the articular facet was supposedly more stable and less prone to lateral variations. Further assumptions include the location for weight distribution which passes through adjacent vertebral facets (SFA and IFA) and is more centrally located.

Vertebral body height (C3-L5)

Vertebral body posterior height (VBPH) and vertebral body anterior height (VBAH) were taken at the anterior and posterior points along the sagittal plane, respectively (Fig. 4.6).

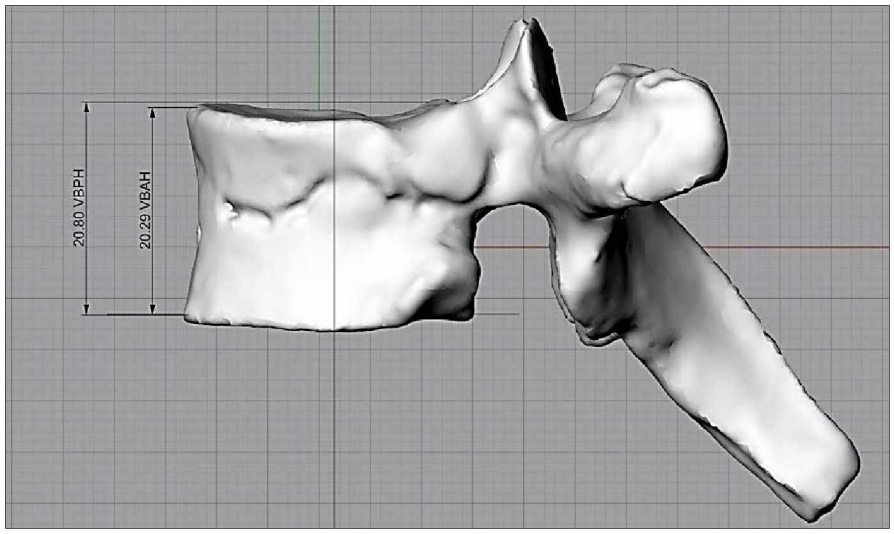

Figure 4.6. Vertebral body height (anterior and posterior). HTH 0288 depicted.
Scan**:** Cleveland Museum of Natural History Hamann-Todd Osteological Collection.

Previous research indicated differences in vertebral body height (Clauser 1980; Francis 1955a; Francis 1955b; Panjabi et al. 1991a; Panjabi et al. 1993a; Panjabi et al. 1993b; Panjabi et al. 1991b; Shapiro 1990; Shapiro and Simons 2002). The assumption and rationale for VBHA and VBAH were directly related to the degree of vertebral wedging per vertebra. Greater differences between the anterior and posterior indicate not only wedging, but also curvature per region. The definition of curvature in this research is the summed regional curvature created by adjacent vertebrae in the absence of soft tissue.

Pedicle angle

A reference plane was placed transversely through the pedicle (Fig. 4.7). Pedicle inclination to the coronal plane (PICP) refers to the measurement taken from the pedicle reference plane to the superiorly-orientated coronal plane.

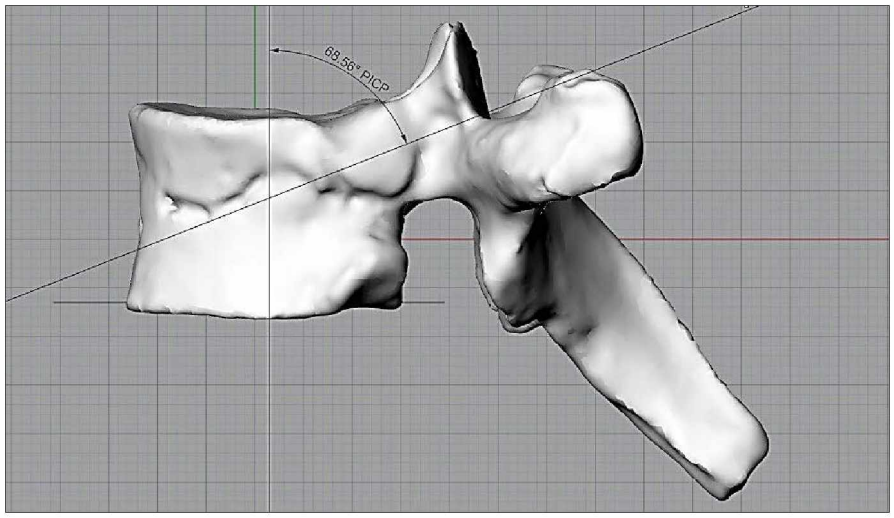

Figure 4.7. Pedicle inclination. HTH 0288 depicted.
Scan**:** Cleveland Museum of Natural History Hamann-Todd Osteological Collection.

According to previous research (Panjabi et al. 1991a; Panjabi et al. 1993a; Panjabi et al. 1991b), the pedicle acts as a bridge between the vertebral arch and body. Variation within and among vertebral regions are assumed to transfer weight from the arch to the body, illustrating the three-pillar concept. The variable PICP is not the same as that defined in previous research. PICP in this research is oriented to weight distribution.

Adjacent Body Angle (C3–L5 only)

Importing two adjacent vertebra models determined adjacent body angle (CPBA). Starting with C3, the adjacent superior vertebra was positioned to where the articular facets were conjoined (Fig. 4.8). The meshes were not fused, and the space between surfaces was 2 mm ± 1 mm. The adjacent body angle measured (superior) the angle from both coronal reference planes.

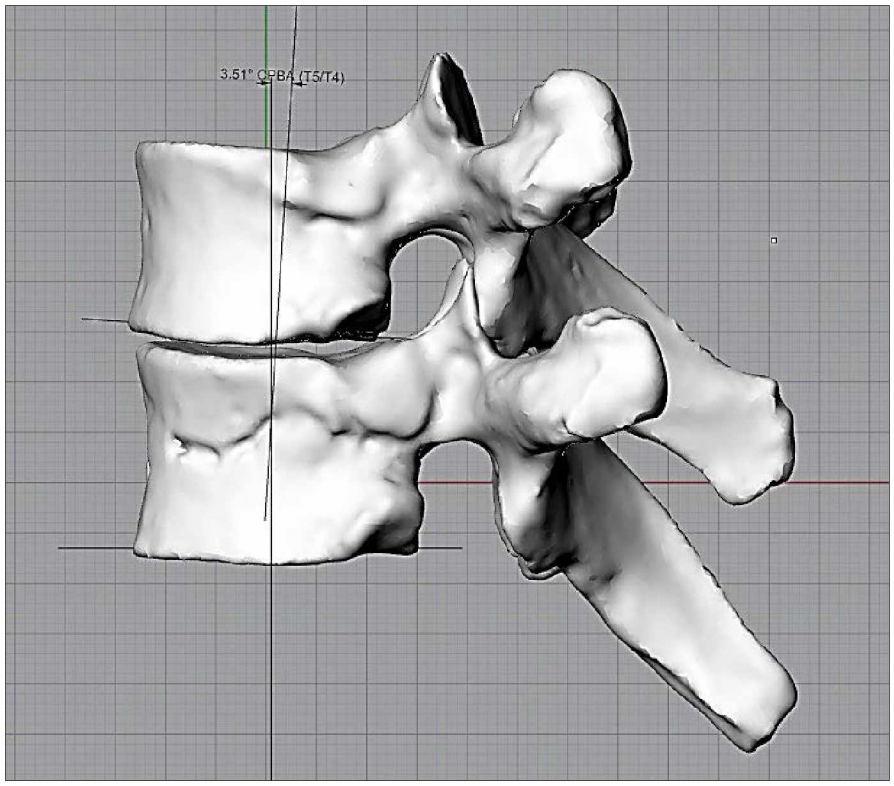

Figure 4.8. Adjacent body angle. HTH 0288 depicted.
Scan**:** Cleveland Museum of Natural History Hamann-Todd Osteological Collection.

The assumption and rationale for the CPBA measurement directly involve the individual vertebra's contribution to total regional spinal curvature due to the combination of the orientation of the SFA, IFA, SVAPA, IVAPA, VBPH, and VBAH variables. In reality, this regional curvature is a proxy curvature because it lacks soft tissue from the calculations. Table 4.3 provides the record of calculated measurements and categorical variables, as well as physical measurements.

Table 4.3. Calculated and categorical variables.

Calculated Variables
SFA – Superior facet angle average
IFA – Inferior facet angle average
SVAPA - Superior vertebro-articular process angle average

Table 4.3. Calculated and categorical variables (cont.).

Calculated Variables
IVAPA – Inferior vertebro-articular process angle average
Area – Computed vertebral area (mm^2)
RT – Vertebra Rotation (SVAPA-IVAPA)
TCC – Total cervical pseudo-curvature (sum of regional CPBA)
TTC – Total thoracic pseudo-curvature (sum of regional CPBA)
TLC – Total lumbar pseudo-curvature (sum of regional CPBA)
TCR – Total cervical rotation (sum of RT)
RTCR – Regional cervical total rotation (1st SVAPA – last IVAPA)
TTR- Total thoracic rotation (sum of RT)
RTTR – Regional thoracic total rotation (1st SVAPA – last IVAPA)
TLR – Total lumbar rotation (sum of RT)
RLTR – Regional lumbar total rotation (1st SVAPA – last IVAPA)
Categorical
Species- *Homo sapiens, Pan troglodytes, Gorilla gorilla, Australopithecus africanus*
Sex – Male or female
Locomotion – $Bipedal_H$ (HB), $knuckle\text{-}walk_G$ (KG), and $knuckle\text{-}walk_P$ (KP)

The overall rationale for the variables mentioned above is threefold: (1) to test the assumption that quadrant divisions yield more information for each skeletal element and the column as a whole; (2) to test the assumption about the integrated nature of each variable found with each vertebra; and (3) to test the assumption that elimination of soft tissue, e.g., vertebral disc and facet joints from the analyses, does not affect column integration adversely.

Elemental suites consist of sets of measurements broken into elemental units. Construction of suites at the elemental level reflects the difference in the number of measurements taken from the cranium, C1, C2, and the remaining vertebrae. Measurement suites include the cranium, C1, C2, C3–L5, curvature, and rotational variables.

Statistical analyses

Initial data evaluation revealed a non-normal distribution for many of the variables considered. Logarithmic transformations proved ineffective. Consequently, this investigation used nonparametric tests throughout.

In recognition of multiple nonparametric tests, each appropriate test used the Bonferroni correction. Implementing a correction factor reduces the possibility of Type I errors; however, a large number of tests or measurements, in this case, can increase the likelihood of Type II errors (Field 2009). To address the correction, each skeletal element with its number of measurements was designated a suite. The simplified correction factor for each suite was calculated as:

Eq. 1. $p = \frac{\alpha}{n}$ (Costigan 2005; Leroy 2011) or defined as:

$$p = \frac{.05}{number\ of\ measurements} .$$

Table 4.4 denotes the new α levels based on the Bonferroni correction. The listed correction was applied to all appropriate tests.

Table 4.4. Anatomical suite and adjusted $\boldsymbol{\alpha}$ levels.

Suite	Number of Measurements	Bonferroni Correction
Cranium	1	0.05
C1	5	0.01 (0.005)
C2	6	0.008 (0.004)
C3 – L5[1]	14	0.004 (0.001)
Curvature	3	0.017 (0.008)
Rotational	6	0.008 (0.004)

[1] Each vertebra contains suite measurements

Intra-observer error

Determining replicability is an important criterion for protocol validity. After collection of the initial set measurements, an additional 20 random samples from the 66 complete samples were re-measured and checked for significant differences. The appropriate nonparametric test for comparing paired non-normally distributed data (original and replicate) is the Wilcoxon signed-rank test. This test consists of subtracting one score from the other. Both negative (T-) and positive (T+) summed values are ranked. The test statistic is the smaller of the two values. Using mean ($\overline{T}$) and the standard error (SE_T), z scores can be determined with exact significance values (Field 2009). The Wilcoxon ranked-sign test was used to test the hypothesis:

H_0 = the median of the differenced paired value is 0 vs. H_A= the median of the differenced paired value is not 0.

Symmetry or lateral dominance

Lateral dominance, defined as one side – left or right – as greater for all measurements throughout that region, can skew results and their interpretations. Explanations for asymmetry can fall into one of two categories or both: naturally occurring (e.g., variation due to tropism or pathology) or measurement error. Natural variation could result in sporadic vertebral or regional lateral dominance. Whereas measurement error could produce dominance with a few vertebrae, it is highly unlikely that all individually imported images would provide the same results. While the expectation of asymmetry among the vertebro-articular process angle variables throughout the vertebral column was minimal, differences in facet angle variables are not. Regarding superior and inferior orientations of these measurements, the expectation of adjacent variables was to reflect or complement the differences between variables. The dominant lateral variable will be used for further analysis only if all variables exhibit the same lateral dominance, left or right, throughout a specific vertebral region. The Wilcoxon signed-rank test was conducted with all lateral measurements among *Homo*, *Gorilla*, and *Pan* to determine whether:

H_0 = the median value between left and right is 0 vs. H_A= the median value between left and right is not 0.

Allometry or isometry

Differences in geometric size and shape that can influence measurements are commonly referred to as allometry or isometry. The definition of isometry is "the principle that body form of one organism can be made identical to another by simply multiplying all linear dimensions by a single scaling factor" (Sylvester and Kramer 2008). Allometry, defined as any changes in shape with size, encompasses various definitions of "common characteristics in relation to absolute magnitude," e.g., evolutionary, ontogenetic, and intraspecific, which include individual and race allomorphoses (Gould 1966). Statistical description of allometry is "described in terms of allometric slope (b), based on the equation, $Y = aX^b$, where Y and X are indices of trait size and body size" (Bonduriansky 2007). Thus, isometry occurs when $b = 1$, negative allometry is when $b < 1$, and positive allometry is when $b > 1$ (Bonduriansky 2007; Lleonart et al. 2000; Sylvester et al. 2008).

Accounting for absolute size is important for comparative studies. Although including or excluding size from the analysis can be controversial (Bonduriansky 2007; Gould 1966), implementing various methods can determine whether to remove or take into account the influence of size via scaling (Darroch and Mosimann 1985; Jungers et al. 1995; Mosimann 1970; Mosimann and James 1979; Sylvester et al. 2008). Data screening for allometry uses principal component analysis (PCA) with log data to determine the contributions of the variables for the first component. Reducing the dimensions (vectors) of the data set into discrete principal components based on eigenvectors and eigenvalues found within an orthogonal-shaped variance-covariance matrix determines the contributions of variables (Cook 2007; Wold et al. 1987). The contribution of each predictor within a component is a ratio between the squared factored score of the observation and the eigenvalue of the component. If the maximum sum value is one, component loadings in excess of |0.05| contribute significantly to the component (Abdi and Williams 2010; Field 2009). The first or leading component is often disregarded, as depicted within regression, as a method to reduce variables without losing valuable information (Cook 2007; Darroch and Mosimann 1985).

Although various methods can be utilized to check for allometry (Jungers et al. 1995; Mosimann 1970; Mosimann and James 1979), this research used the geometric mean (GM) and size-adjusted values, as outlined by Darroch and Mosimann (1985). The calculation of the geometric mean is "the n^{th} root of the products of all n variables" (Jungers et al. 1995, p.144). Size-adjusted variables

were defined as Variable/GM (Darroch and Mosimann 1985; Jungers et al. 1995). Using linear regression, each variable regressed against the geometric mean. Allometry is apparent when the intercept (constant) is significant ($p < 0.05$) from zero (Darroch and Mosimann 1985; Jungers et al. 1995). The hypothesis for allometry was simply:

H_0: intercept = 0 vs. H_A: intercept ≠ 0.

Two separate tests were done to test for allometry between males and females within each species and among taxa. If allometry is present, remaining tests will use only sized-adjusted variables.

Main research questions

The primary line of inquiry, along with its underlying assumptions, has three specific aims: first, to investigate and identify key traits of the cranial base angle, individual vertebrae, and spinal curvature in modern human and extant nonhuman primates. Second, to use vertebralmetrics and spinal curvature to identify positional-locomotory complexes; and lastly, to provide potential insight into the vertebral similarities and possibilities for the identification of the positional-locomotory complexes in early hominins. Based on the overarching question and specific aims, five questions and their associated hypotheses include:

First, are vertebrae sexually dimorphic within taxon?

Sex estimation among skeletal elements is possible (Bass 2005; White 2000), yet a standardized method to determine sex from vertebrae remains elusive (Gilsanz et al. 1994; Marino 1995; Panjabi et al. 1991a; Panjabi et al. 1993a; Panjabi et al. 1991b; Wescott 2000). The Mann-Whitney U-test used the entire vertebral suites for *Homo*, *Pan*, and *Gorilla*. Mann-Whitney ranks the scores within the two groups, determines the sum for each group, and calculates the statistic:

Eq. 2. $U = n_1 n_2 + \frac{n_1 (n_{1+1})}{2} - R_1$ (Field 2009)

Whereas n_1 and n_2 are sample sizes from Group 1 and Group 2 respectively, and R_1 is the sum of ranks for Group 1.

The Mann-Whitney also tested the following hypothesis:

H_0: there are no differences in measurements between males and females within species vs. H_A: there are differences in the distribution of measurements between males and females within species.

Second, can vertebralmetrics differentiate vertebrae among species? If so, can vertebralmetrics classify species?

When comparing vertebrae across species, the observed differences are often striking to the naked eye and these differences can be documented. A Kruskal-Wallis H-test determined whether metric differences between species are statistically significant. Similar to the Mann-Whitney test, which is appropriate for two groups, the Kruskal-Wallis test uses ranked and summed ranked scores to assess the differences among groups when the number of groups is greater than two.

The test statistic (H) calculation is:

Eq. 3. $H=\frac{12}{N\,(N+1)}\sum_{i=1}^{k}\frac{R_i^2}{n_i}-3\,(N+1)$ (Field 2009).

Wherein R_i is the sum rank of each group, N is the total sample size, n_i is the sample size of a particular group, and the calculated degrees of freedom are $(k-1)$ (Field 2009).

The hypothesis to test for differences among species is:

H_0: there are no differences in the distribution of measurements across the three species vs. H_A: there are significant quantifiable differences across species.

If a significant difference was identifiable by a Kruskal-Wallis H-test across all three taxa, a *post hoc* Mann-Whitney U-test determined which of the pair-wise differences among *Homo*/*Pan*, *Homo*/*Gorilla*, and *Pan*/*Gorilla* are driving the overall difference.

The hypothesis to test between species comparison is:

H_0: there are no differences in the distribution of measurements between species vs. H_A: there are significant quantifiable differences between species.

To resolve the question as to whether vertebralmetrics can classify species, multinomial logistic regression (MLR) with Main effect/Forward stepwise methods determined the accuracy of skeletal element's classification and the likelihood of the variables within the model. MLR is a form of Logistic Regression (LR) with more than two levels/categories, one of which is the base or reference level. Unlike canonical variate analysis, the parametric equivalent to MLR, this test does not assume linearity between variables, normal distribution, and homoscedasticity, which makes the statistical test appropriate in regard to the non-normal distribution of the data for many of the variables under consideration (El-Habil 2012; Goeman and Cessie 2006). However, the assumptions that variables are independent and the independent variables are linear to the logit of the dependent variable must be met.

The derived calculations used in MLR are from Logit Analysis (LA). For a variable Y with two measurements and explanatory variable x, the probability is calculated as:

Eq. 4. $\pi(x) = p(Y = 1|X = x) = 1 - p(Y = 0|X = x)$ (El-Habil 2012).

The logit uses this probability:

Eq. 5. $\text{Logit}[\pi(x)] = \log\left[\frac{\pi(x)}{1-\pi(x)}\right] = \alpha + \beta x$, and odds $= \frac{\pi(x)}{1-\pi(x)}$ (El-Habil 2012).

Considering n independent observations, p explanatory variables, and k categories (number of categories), MLR calculates the probability that an observation falls into j^{th} category as:

Eq. 6. $$\text{Log}(\pi_j\ (x_i)) = \frac{\exp\ (\alpha_{0i}+\beta_{1j}\ x_{1j}+\beta_{2j}x_{2j}+\ ..+\ \beta_{pj}\ x_{pj}\ )}{1+\sum_{j=1}^{k-1}\exp(\alpha_{0i}+\beta_{1j}\ x_{1i}+\beta_{2j}\ x_{2i}+..+\beta_{pj}\ x_{pj})}$$

Where j = 1, 2 ... (k-1) and i = 1, 2... n. (El-Habil 2012).

To address the issue of whether metric variables have the ability to correctly assign the vertebra by taxon with a reasonable degree of accuracy, MLR with stepwise method tested the hypotheses phrased as:

H_0: species classification with a reasonable rate of accuracy using metrics is possible vs. H_A: species classification with a reasonable rate of accuracy using metrics is not possible.

Additionally, MLR validation test (50 test average) used random subsets of the original dataset (*Homo* = 26, *Pan* = 11, and *Gorilla* = 11). The averages were recorded.

Third, can cranial base angle and vertebral segment curvature differentiate among species?

Cranial base angle and vertebral segment curvature, together or separately, provide a unique database for distinguishing differences among species. Whereas differences are apparent between human and nonhuman primate basicrania, assessing vertebral curvature via vertebral morphology alone has not been fully explored. Using the variables CBA, TCC, TTC, and TLC, MLR tested whether the total of these regional variables can distinguish among the individuals of the three species. The hypothesis to test species classification based on cranial base angle and segment curvature is:

H_0: cranial base angulation and spinal curvature are not unique among species vs. H_A: cranial base angulation and spinal curvature are unique and can discriminate between modern humans and nonhuman hominoid taxa.

Additionally, MLR validation test (50 test average) used random subsets of the original dataset (*Homo* = 26, *Pan* = 11, and *Gorilla* = 11). The averages were recorded.

Fourth, can the cranial base angle and vertebral segment curvatures differentiate the positional-locomotory complex of a species? If so, can cranial base angle and vertebral segment curvature classify the positional-locomotory complex of a species?

Locomotory behavior is difficult to ascertain for some skeletal elements. A group of skeletal traits might be good indicators of locomotive behavior, e.g., vertebral wedging for bipedalism. However, it may fail to distinguish various forms of quadrupedal locomotion (Ahlborn 2004; Badoux 1968; Badoux 1974; Biewener 1990; Christiansen 2002) or to differentiate between the two forms of knuckle-walking practiced by *Pan* and *Gorilla* (Doran 1997; Matarazzo 2008; Richmond 2006).

No known previous study attempted to quantify cranial base angle and curvature together as a single unit as indicators of locomotory behavior. The variables considered include CBA, TCC, TTC, and TLC, whereas the categorical assignment is $Biped_H$ for *Homo*, $Knuckle\text{-}walk_P$ for *Pan*, and $Knuckle\text{-}walk_G$ for *Gorilla*.

As with question two, a Kruskal-Wallis H-test determined whether a significant difference exists across all three genera, and for those variables yielding statistically significant H-values, *post hoc* Mann-Whitney U-tests determined which pair-wise contrasts are significant. The hypothesis to test for a species' positional-locomotory complex based on cranial base angle and segment curvature is:

H_0: cranial base angle and spinal curvature cannot differentiate taxa with their associated positional-locomotory complex vs. H_A: base angle and curvature can differentiate between taxa and their associated positional-locomotory complex.

To address the second part of this question, MLR determined classification for the following hypothesis:

H_0: cranial base angle and spinal curvature cannot classify taxa with their associated locomotory repertoire vs. H_A: base angle and curvature can classify taxa and their associated positional-locomotory complex.

Additionally, MLR validation test (50 test average) used random subsets of the original dataset (*Homo* = 26, *Pan* = 11, and *Gorilla* = 11). The averages were recorded.

Lastly, can the findings of this research help to distinguish fossil hominin vertebrae?

When evaluating fossil hominins, previous research by Gommery (2000, 2006) on cervical body dimensions and superior vertebro-articular process angles place the australopithecine *A. afarensis*, AL 333-106 between those of modern humans and extant nonhuman primates. Articular facet angles in *P. robustus*, SK 854 and *A. afarensis*, AL 333-101 yielded similar results. Gommery (2000, 2006) gave no consideration to the inter-vertebral relationships among body dimensions and facet angles, yet some indications noted by articular facet angles suggested an angulated shift to subsequent caudal vertebral bodies (Manfreda et al. 2006). The selected variables in this study

sought to provide some quantifiable answers. The hypothesis to test differentiation among species is:

H_0: hominin vertebrae cannot be classified using metrics vs. H_A: hominin vertebrae can be classified using vertebralmetrics.

The hypotheses and answers to the questions that provided the framework for this research used a data collection process. Included are detailed processes for scanning and measuring skeletal elements, as outlined in Section 4.3.

4.3 Data collection

Data collection took place at the Cleveland Museum of Natural History (CMNH) from May 21, 2014 to July 28, 2014. Table 4.5 depicts all specimens used in this study. Two separate NextEngine Desktop 3-D Scanners and ScanStudio software (HD Pro) were used to create 3-D models for both cranial and vertebral elements as outlined in the Method section 4.2. The total number of scans encompassed by the present study included approximately 3,684 individual scans for extant species and 19 scans for fossil hominins. Total scan time was 432.75 hours. All designated raw files were then saved for image processing. Image run-processing took place from July 27, 2014 to August 20, 2014. Every final model was processed and checked and rechecked for misalignment and fusing errors. The total number of processed scans were 1,909, with a total processing time of approximately 281.5 hours.

Table 4.5. Specimens used in this study.

Species	Specimen number
Homo sapiens (HTH)	0260, 0269, 0306, 0437, 0454, 0476, 0514, 0536, 0603, 0604, 0690, 0774, 1049, 1119, 1494, 2125, 0087, 0088, 0130, 0244, 0267, 0275, 0288, 0308, 0328, 0361, 0375, 0380, 0386, 0392, 0462, 0628, 0889, 1848
Gorilla gorilla (HTB)	1422, 1756, 1764, 1798, 1851, 1856, 1932, 1997, 1430, 1787, 1795, 1797, 1859, 1954, 2025, 2029
Pan troglodytes (HTB)	1434, 1731, 1737, 1741, 1755, 1775, 1843, 1880, 2771, 1056, 1708, 1722, 2027, 3537, 3552
A. afarensis	A.L. 288-1, A.L. 333 X-12, A.L. 333 106

Measurements took place from September 19, 2014 to February 12, 2015. Each skeletal element (.OBJ file) was imported into Rhinoceros v.5.0 (64 bit). The orientation of each skeletal element was rechecked and evaluated for measurement viability. Measurements, as outlined in the Method section 4.2, were taken and recorded. Each extant species sample required 599 measurements and a total of 39,534 measurements for the complete data set. Categorical and variable averages were calculated and recorded. The total measurement time was 1159.60 hours.

4.4 Summary and conclusion

To address questions regarding the viability of cranial base and vertebral morphology to serve as indicators for species and mode of locomotion, testable hypotheses with specific variables were selected to assess assumptions and maximize exploratory efforts. Using specimens housed at the Cleveland Museum of Natural History in the Hamann-Todd Osteological Collection (H-TOC), scans for viable crania and all vertebrae include 34 *Homo sapiens*, 16 *Pan troglodytes*, and 16 *Gorilla gorilla*. For comparative purposes, this study included additional vertebral scans for *Australopithecus africanus* (A.L. 288-1, A.L. 333 x12, and A.L. 333 106).

The scanning procedure conceived for this research addressed and circumvented issues such as bone condition, line-of-sight issues, and quality/accuracy of the 3-D image. In addition to scanning, specific details expressed instituted methods for each measurement. The variables used in this study reflected an integrated approach based on biomechanical principles and the availability of new technology. Implementing planes and reference lines allowed for the division of skeletal elements into four quadrants, with reference to the X, Y, and Z axes. Quadrants and reference planes provide two important controls: (1) a standardized orientation and (2) an assessment of symmetrical issues in relation to orientation. SPSS v.22 imported all measurements for statistical analyses.

Chapter 5. Results

During initial data evaluation, Shapiro-Wilk's tests revealed that many of the variables had non-normal distributions. Logarithmic transformations proved ineffective. While reducing the number of non-normally distributed variables, data transformations did not resolve the normality issue completely. Consequently, this investigation used nonparametric tests. Except where noted, all tests used the Bonferroni correction factor for adjusted alpha levels (refer to Table 4.4).

5.1 Intra-observer error

Results indicated *no* significant difference between the first and second set of measurements (Appendix B, Table B-1). Without statistically significant results, the null hypothesis could not be rejected. No difference between the two sets of measurements was detected.

5.2 Allometry and isometry

Results (Appendix C, Table C-1) within PCA's first component indicated differences among influential variables throughout the vertebral column. The most common variables that contributed to the first component among all vertebrae included: VBPH and VBAH, SFID, IIFD, and Area. Using the variables that were significant contributions within the PCA's first component, linear regression was used to check for allometric influence among variables.

As indicated in Appendix D (Tables D-1 – D-4), two separate test results for allometry exhibited significance for at least one measurement among all vertebrae between males and females within and among species. Consequently, the null was rejected. Allometry was present throughout the vertebral column between males and females within each species and among taxa, albeit not consistently with all variables for each vertebra. In fact, excluding C1, C2, C7, T13, and L4, approximately 80% of the variables were significant. An interesting result was the significance for Area, among which only C1, C7, T11, L1, L2, and L3 were significant. The remaining tests used only size-adjusted values.

5.3 Symmetry or lateral dominance

Results indicated significant differences between left and right measurements among species. Not all species exhibited differences in each vertebral region.

Homo

Within the cervical region (Table 5.1), significant differences in facet angles were greater in number than those values of vertebro-articular process angles (SVAPA and IVAPA). All median values for the right were greater than those of the left.

Table 5.1. Significant lateral differences in the cervical region (*Homo*).

Species: *Homo sapiens*							
Level	Variable Left	Mdn	Variable Right	Mdn	z	r	p value[1]
C2	SFA	95.99	SFA	97.92	-3.411[b]	-0.584	0.001
C2	IFA	42.37	IFA	46.21	-3.069[b]	-0.526	0.002
C2	SVAPA	16.35	SVAPA	18.28	-2.966[b]	-0.508	0.003

[1] Bonferroni Correction: C2, $p < 0.008$.
[a] Based on negative ranks.
[b] Based on positive ranks.

The thoracic region exhibited significant differences. As illustrated in Table 5.2, the observed differences were limited to the inferior articulating facet angle. The right-side median value was greater than left median value. Based on the statistical evidence, the *Homo* sample indicated asymmetry.

Table 5.2. Significant lateral differences in the thoracic region (*Homo*).

Species: *Homo sapiens*							
Level	Variable Left	Mdn	Variable Right	Mdn	z	r	p value[1]
T3	IFA	5.92	IFA	7.94	-2.907[b]	-0.498	0.004

[1] Bonferroni Correction: C3 – L5, $p < 0.004$.
[a] Based on negative ranks.
[b] Based on positive ranks.

Pan

For *Pan,* as depicted in Table 5.3, the cervical region displayed the greatest stability among taxa; that is, there were fewer significant differences. Only the vertebro-articular process angle (IVAPA) had significant differences between left and right. No differences in facet angles, superior or inferior, were found.

Table 5.3. Significant lateral differences in cervical region (*Pan*).

Species: *Pan troglodytes*							
Level	Variable Left	Mdn	Variable Right	Mdn	z	r	p value[1]
C2	IVAPA	16.13	IVAPA	22.80	-3.516[b]	-0.879	0.000

[1] Bonferroni Correction: C2, $p < 0.008$.
[a] Based on negative ranks.
[b] Based on positive ranks.

The thoracic region continued to demonstrate significant departures from symmetry (Table 5.4). The majority of the superior facet angles were located either above or below the mid-thoracic region, and the vertebro-articular process angles were found among adjacent vertebrae. Median differences between left and right variables varied among vertebrae without any discernible pattern. The right side had a greater median value than the median value of the left, except for T2 SVAPA, and T3 SVAPA. Based on the statistical evidence, the *Pan* sample depicted asymmetry.

Table 5.4. Significant lateral differences in the thoracic region (*Pan*).

Species: *Pan troglodytes*							
Level	Variable Left	Mdn	Variable Right	Mdn	z	r	p value[1]
T2	SVAPA	109.12	SVAPA	104.02	-2.844[a]	-0.711	0.004
T3	SVAPA	106.95	SVAPA	104.74	-2.017[a]	-0.504	0.004
T8	SFA	17.79	SFA	19.07	-2.844[b]	-0.711	0.004

[1] Bonferroni Correction: C3 – L5, $p < 0.004$.
[a] Based on negative ranks.
[b] Based on positive ranks.

Gorilla

Gorilla exhibited the greatest number of significant differences in every vertebral region. The results from the cervical region, as provided in Table 5.5, indicated differences only for the vertebro-articular process angle variables. Except for C3 SVAPA and C5 SVAPA, the median was greater on the right side than on the left for the remaining variables.

Table 5.5. Significant lateral differences in cervical region (*Gorilla*).

Species *Gorilla gorilla*							
Level	Variable Left	Mdn	Variable Right	Mdn	z	r	p value[1]
C2	IVAPA	22.91	IVAPA	26.68	-2.741[a]	-0.685	0.006
C3	SVAPA	72.28	SVAPA	64.33	-3.309[b]	-0.827	0.001
C5	SVAPA	82.96	SVAPA	77.78	-2.896[b]	-0.724	0.004
C5	IVAPA	68.39	IVAPA	74.77	-2.856[a]	-0.714	0.004

[1] Bonferroni Correction: C2, $p < 0.008$; C3 – L5, $p < 0.004$.
[a] Based on negative ranks.
[b] Based on positive ranks.

In the lumbar region, the only statistically significant differences between sides in *Gorilla* occur for the inferior articular facet angle variables at L2 and L4 (Table 5.6). Median values of the significant variables favored the right side. Statistical evidence indicated asymmetry was present in the in the *Gorilla* sample.

Table 5.6. Significant lateral differences in lumbar region (*Gorilla*).

Species: *Gorilla gorilla*							
Level	Variable Left	Mdn	Variable Right	Mdn	z	r	p value[1]
L2	IFA	10.79	IFA	14.55	-2.947	-0.736	0.003
L2	IFPA	12.24	IFPA	15.67	-2.947	-0.736	0.003
L4	IFPA	10.98	IFPA	14.51	-3.233	-0.808	0.001

[1] Bonferroni Correction: C3 – L5, $p < 0.004$.
[a] Based on negative ranks.
[b] Based on positive ranks.

Symmetrical observations applied to all taxa

The null hypothesis was rejected due to the presence of significant differences between left and right measurements among taxa. Asymmetry is present within the vertebral column, yet variable differences indicating asymmetry were not the same within or among regions that span across taxa.

Main results

In recognition of multiple nonparametric tests, Bonferroni correction was included. Implementing a correction factor reduces the possibility of Type I errors; however, a significant number of tests or measurements, in this case, can increase the likelihood of Type II errors (Field 2009). To address the correction, each skeletal element with its number of measurements is designated as a suite (refer to Table 4.3 for details).

5.4 Sexual dimorphism

Question 1. Are vertebrae sexually dimorphic within taxon?

As described in detail below, the Mann-Whitney U test results indicated significant differences between males and females for each taxon analyzed.

Homo

Among elements of the cervical region (Appendix E, Table E-1), only the Areas for C1, C4, and C7 proved to be statistically different between males and females. In each case, males possessed larger values than those of females.

Statistically significant differences between males and females in the thoracic region were limited to T1 through T7. In addition to the common variable Area, only T2 and T5 indicated statistically significant differences between the two sexes for variables measured inferiorly – that is, IIFD, IFA, and IFPA. Males possessed larger values than those values for females in this region. But for T2 IFA and T2 IFPA, the situation is reversed as females now possessed larger values than those of males. Variables among elements of the mid-to-lower thoracic region did not yield statistically significant differences between the sexes. Results for the lumbar region indicated that only one variable, L1 Area, as statistically significant between the two sexes, and males possessed larger values as those of females. Overall, results suggest that *Homo* showed no discernible pattern among vertebrae within and among vertebral regions with regard to sexual dimorphism.

Pan

Pan had the least number of differences between males and females when compared to other species. Results indicated statistical significance was limited to the cervical region (Table 5.7). Interestingly, only two variables at three vertebral levels – C1 SFA, C5 and C6 Area – were significant. Males in this region were larger than females in size, but females had a greater median for C1 SFA than males. Results indicated an almost complete absence of statistically significant differences between members of the two sexes with regard to the size of vertebrae.

Table 5.7. Significant differences between males and females in the cervical region (*Pan*).

Species: *Pan troglodytes*							
Level	Variable	Male Mdn	Female Mdn	U	z	r	p value[1]
C1	SFA	92.62	93.16	22.00	-0.868	-0.219	0.002
C5	Area	3559.41	2930.16	3.00	-2.929	-0.732	0.003
C6	Area	4220.08	3582.66	2.00	-3.037	-0.840	0.002

[1] Bonferroni Correction: C1, $p < 0.01$; C3 – L5, $p < 0.004$.

Gorilla

Gorilla showed the greatest number of differences between the sexes throughout the vertebral column. Results for the cervical region (Appendix E, Table E-2) yield statistically significant differences between males and females throughout the cervical region from C1 to C7 for VBPH, VBAH, SFID, IIFD, PICP, CPBA, and Area variables. Although the variables Area and vertebral body heights were universally and statistically significant across the cervical elements, statistical significance among the remaining variables was limited to the lower cervical region. In all statistically significant cases, males possessed larger values than those values of females.

The thoracic region of *Gorilla* yielded statistically significant results for each vertebra as well. As expected, males possessed larger values than females for all variables that yielded a statistically significant difference between the sexes. Statistically significant variables common to all vertebrae include VBPH, VBAH, and Area. Only IIFD and SFID were unique, e.g., limited to the upper thoracic region (T1 for the former, T4 for the latter).

Lastly, results for the *Gorilla* lumbar region indicated statistically significant differences between members of the two sexes for the Area variable across all elements within the region. In all cases, males possessed larger values than those values of females.

Gorilla exhibited the greatest number of differences between the sexes in comparison to *Homo* and *Pan*. Every result revealed significant differences within and throughout vertebral regions. VBPH and VBAH were constant in the thoracic-lumbar regions.

Based on the above results, the null hypothesis was rejected. Statistically significant differences do exist between males and females within and across taxa.

5.5 Taxon delineation

Question 2: Can vertebralmetrics differentiate vertebrae among species? If so, can vertebralmetrics classify species?

Kruskal-Wallis results

The results for the Kruskal-Wallis H-test indicated significant differences among variables. In the cervical region (Appendix F, Table F-1), every vertebra exhibited significant differences for at least two or more variables. Interestingly, CPBA, PICP, and Area yielded statistically significant difference only among the lower cervical vertebrae.

Similar trends were present within the thoracic region. SFA, SFPA, IFA, IFPA, SVAPA, IVAPA, VBPH, VBAH, SFID, and IIFD were consistently significant statistically. Unlike the cervical region, Area was statistically significant throughout the thoracic segments. Variables PICP and CPBA were sporadically statistically significant, and such differences occurred in both the upper (T1-T7) and lower (T10-T12) thoracic regions. Only vertebrae T6–T10 had additional statistically significant variables and these included VBDPH, VBVAH, SFID, and IIFD.

For *Pan* and *Gorilla*, T13 exhibited a reduction in the number of statistically significant variables. Remarkably, all metric differences were significant with only two angle measurements: IVAPA and CPBA. None of the articulating facet angles were significantly different statistically across taxa.

The lumbar region continued the pattern of differences across taxa previously described for the cervical and thoracic regions. While SFA, SFPA, IFA, IFPA, SVAPA, IVAPA, and Area were

apparent, both PICP and CPBA were evident throughout the columns among *Homo*, *Pan*, and *Gorilla*, except for L1.

In light of the statistical evidence, the null hypothesis indicating no differences in the distribution of measurements across taxa was rejected. Statistically, significant quantifiable differences were noticeable throughout the spinal columns across taxa. Every vertebra within each region indicated at least three significant variables which were related to distance or area. No vertebra, however, indicated significance for all variables. Except for C1 and C2, the number of significant variables varies among regions without any detectable pattern. *Post hoc* tests determined which pair-wise contrasts yield the significant differences across members of the three taxa considered.

Post hoc Mann-Whitney U-tests

Mann-Whitney U-tests assessed pair-wise differences among *Homo*, *Pan*, and *Gorilla*. The contrasts include *Homo-Gorilla*, *Homo–Pan*, and *Pan–Gorilla*. All statistically significant results incorporate the Bonferroni correction factor for multiple comparisons.

Homo-Gorilla

Significant results were present throughout the vertebral column. In the cervical region (Appendix G, Table G-1), SFID and/or IIFD, SVAPA and/or IVAPA, and Area were common to all or in part to all vertebrae. VBDPH and/or VBVAH statistically were significant in the lower cervical region. SFA and/or IFA and SFPA and/or IFPA variables were inconsistent and limited to the end of the cervical region.

The median value for the statistically significant variables for these taxa indicated *Homo* was larger than *Gorilla* for more than half of the variables within its column. Among the variables where the median for *Gorilla* was larger, only the Area was consistent after C1 throughout the column when it was compared to humans.

Regarding the thoracic region, variables SFID and/or IIFD as well as SVAPA and/or IVAPA were common within the region, except for Area. Additionally, SFA and/or IFA and SFPA and/or IFPA variables were more common within the thoracic vertebrae than within the cervical region. The variable Area was not significant at any vertebral level.

The median value for *Homo* continued to be greater than the median value for *Gorilla* for many variables. Within the respective columns, only T2 and T3 variables exhibited complete *Homo* dominance in values. The remaining 29 variables with greater values were present among T1, T4, T7, T8, T9, T10, and T12 vertebrae. *Gorilla* had greater values for T6 and T11. The thoracic region exhibited VBPH and VBAH for T4, T7, T8, T9, T10, and T12. In all instances, *Homo* had greater median values than the median values possessed by *Gorilla*.

Results for the lumbar region indicated SFID and/or IIFD, SVAPA and/or IVAPA, SFA and/or IFA, and SFPA and/or IFPA variables were significant. CPBA was significant only after L1. Similar to the thoracic region, Area was not significant at any level.

The comparative median values shifted from the previous vertebral regions. Median values were greater for *Gorilla* than the median values for *Homo,* except for L1 RT, L3 CPBA, L4 IVAPA, L4 IIFD, and L4 CPBA.

Homo – Pan

Statistically significant differences for the contrast between *Homo* and *Pan* can be observed throughout the cervical region (Appendix G, Table G-2). Results indicated statistical significance among vertebrae SFID and/or IIFD, SVAPA and/or IVAPA, SFA and/or IFA, and SFPA and/or IFPA variables. Unlike the contrast between *Homo* and *Gorilla*, Area is significant at each vertebral level within the cervical region for *Homo-Pan*. Among the significant variables, the median value for *Homo* was greater than the median values for *Pan* in 30 variables throughout the cervical region. Patterns for median values of variables for *Homo* tend to increase from C3 to C7.

Results for the contrast between *Homo* and *Pan* for variables within the thoracic region indicated statistically significant differences among vertebrae for SFID and/or IIFD, SVAPA and/or IVAPA, SFA and/or IFA, and SFPA and/or IFPA variables. Except for C1, Area also was statistically significant throughout the thoracic region. The median values for *Homo* were greater than median values for *Pan* in 48 variables throughout the region. Only T1 yielded uniformly greater median values for *Homo* relative to *Pan*'s median values. In no instance were vertebrae suites exclusive to *Pan*.

Results obtained among variables of the lumbar region yielded statistically significant values among vertebrae for SFID and/or IIFD, SVAPA and/or IVAPA, SFA and/or IFA, and SFPA and/or IFPA variables. The variable Area was significant for all lumbar vertebrae.

The median values for *Homo* were greater than the median values for *Pan* in 12 variables throughout the lumbar region. Common throughout the region, the median value for *Homo* was greater than the median value for *Pan* in Area. With the exception of L3, the median values for all variables for *Homo* were greater than the median values for *Pan*. In no case were vertebrae suites exclusive to *Pan*.

Pan - Gorilla

Although both *Pan* and *Gorilla* are knuckle-walkers, statistically significant differences between members of these two taxa were found throughout their vertebral columns (Appendix G, Table G-3). The contrast between *Pan* and *Gorilla* shows similar trends among the variables. These trends were also observable in the contrast between *Homo* and *Gorilla* and between *Homo* and *Pan*. Results for the cervical region yielded statistically significant differences among the vertebrae for SFID and/or IIFD, SVAPA and/or IVAPA, SFA and/or IFA, and SFPA and/or IFPA variables. The variable Area was significant at each vertebral level.

The median for statistically significant variables indicated that *Gorilla* had greater median values than those of *Pan*, except in nine variables: C1 IFA, C4 SFA, C4 SFPA, C5 IVAPA, C5 PICP, C6 IVAPA, C6 PICP, C7 SVAPA, and C7 IVAPA. *Gorilla* was the only taxon illustrating significantly larger values for all variables at C2 and C3.

Thoracic region results indicated statistical significance among vertebrae for SFID and/or IIFD, SVAPA and/or IVAPA, SFA and/or IFA, SFPA and/or IFPA, and Area. CPBA was significant for T9, T10, and T13. *Gorilla* had greater median values than those of *Pan*, except for 17 dispersed variables at T1, T2, T5–T10, and T13. *Gorilla* was the only taxon possessing significantly larger median values for all variables at T2-T4, T11, and T12.

Among the three regions, the lumbar region had the fewest statistically significant variables in contrast between *Gorilla* and *Pan*. Results revealed statistical significance among vertebrae for IIFD, VBPH and/or VBAH, IFA, and Area. Greater median values for *Gorilla* were present across

all variables, except for two – L1 IFA and L3 IFA. In addition, *Gorilla* had greater median values than those of *Pan* for all variables assessed for L2 and L4.

In summary, *post hoc* Mann-Whitney U-tests indicated that *Homo* possesses median values that are greater than the median values for *Gorilla*. Whereas Area was greater with *Gorilla* throughout, SFID, IIFD, SFA, SFPA, IFA, IFPA, SVAPA, and IVAPA were distinctive but inconsistent variables. *Homo* and *Pan* had similar trends.

5.6 Taxon classification

Based on the results obtained during this research, taxa exhibit significant differences, but the question remains as to whether these vertebral measurements can be used for accurate classification of individual members of these taxa to the correct taxon. Preliminary analysis focused on possible logit problems and/or multicollinearity issues. Although multicollinearity was present in several models, negation of the problem was due to the focus on main effects rather than the effects of interaction among variables. Also, omitted variables reduced predictor blending, i.e., the inability to distinguish variables due to multicollinearity. In all instances, the tests did not indicate error codes for Hessian Matrix, quasi-complete separation, or calculation overflow.

Results for each test, C1–L4 (Appendix H, Tables H1 – H-30), indicated acceptable classification (20% above probability and predicted) with significant model fit. Variables that contribute significantly to each model varied by region. Even though no single variable was significant throughout the models, Area was present in 10 of the 24 models. Table 5.8 provide individual model and validation classification results.

As Table 5.8 indicates, the average cervical vertebrae classification rate of 88.78% and validation rate of 85.8% indicated suitability for classifying cervical vertebrae. While statistically significant variables were present in both MLR and previous Mann-Whitney U-tests among taxa, the cervical region had more misclassifications regarding the number of vertebrae than either the thoracic or lumbar regions. Out of the 51 misclassifications, only nine were between *Pan* and *Gorilla*.

Table 5.8. Species model and validation classification (cervical region).

Element	Model[1]		Validation[2]		Variables
	Overall Classification %	Number of Misidentifications	Classification %	Number of Misidentifications	
C1	92.2	5	90.1	228	Area, SVAPA, IFA
C2	82.8	11	84.4	362	IFA, SVAPA, RT
C3	84.1	10	83.9	369	IFA, SVAPA, IVAPA, CPBA
C5	84.4	10	71.9	582	IVAPA, RT
C6	96.9	2	95.9	95	SFID, SVAPA, IVAPA, IIFD
C7	91.9	5	89.9	163	IVAPA, Area

1 Model, p = 0.000.
2 Validation: Bonferroni Correction, p = 0.000.

With the fewest number of misclassifications between the two taxa, data suggest distinct differences within the cervical region between the two knuckle-walking species. The contrast between *Homo* and *Pan* yielded five misclassifications, while the contrast between *Homo* and *Gorilla* yielded 17 misclassifications (five cases with *Pan* and 17 with *Gorilla*). The total number of *Pan-Homo* and *Gorilla-Homo* misidentification was 25, eight and 17, respectively. This trend was also present with the validation results as seen in Table 5.9.

Table 5.9. Incorrect classification for the cervical region (validation).

	Homo sapiens	*Gorilla gorilla*	Total	Percent of total Misclassification
C5 *Pan troglodytes*	421	80	501	86.0
C7 *Pan troglodytes*	62	0	62	38.0

The average thoracic accurate classification rate of 90% to 91% and validation rate of 86.0% indicated the acceptability for classifying thoracic vertebrae (Table 5.10). The significant variables included in the model and validation test were not consistent throughout the thoracic region.

Common variables include vertebral body dimensions, e.g., anterior and posterior vertebral body height and articular facet orientation. The majority of the significant variables were limited to vertebral arch measurements.

Table 5.10. Species model and validation classification (thoracic region).

Element	Model[1]		Validation[2]		Variables
	Overall Classification %	Number of Misidentifications	Classification %	Number of Misidentifications	
T1	89.4	7	88.5	277	IFPA, SVAPA, SFID
T2	79.4	13	82.9	389	IVAPA, IIFD
T3	95.2	3	91.7	201	Area, IIFD, IVAPA, SFPA
T4	90.6	6	89.3	252	SVAPA, IIFD, RT
T5	80.3	13	58.6	991	IFA, VBPH, SFA
T6	96.9	2	90.1	233	Area, SFPA, VBPH, SVAPA, PICP, IFA
T7	98.5	1	91.4	203	Area, IFA, VBPH, PICP
T8	91.9	5	86.3	302	Area, IFA, CPBA
T9	90.8	4	86.8	304	SVAPA, IFA, VBPH
T10	91.8	5	85.5	295	IFPA, VBAH, VBPH, CPBA
T11	97.0	2	94.0	142	VBPH, PICP, Area
T12	87.9	8	82.6	415	IVAPA, SFID
T13	93.3	2	92.3	204	IVAPA, VBAH

[1] Model, p = 0.000.
[2] Validation: Bonferroni Correction, p = 0.000.

T2 and T5 had the greatest number of misclassifications out of 72 instances of misidentification from thoracic elements. Incorrect classifications for the validation mirrored the model. Tables 5.11 depict the number of errors and the percent of total misclassifications for the thoracic.

Table 5.11. Incorrect classification for the thoracic region (*Pan*).

Observed	*Homo sapiens*	*Gorilla gorilla*	Total	Percent of total Misclassification
T1 *Pan troglodytes*	11	0	11	3.9
T5 *Pan troglodytes*	197	32	229	23.1

The classifications among *Pan*, *Gorilla*, and *Homo* constituted the majority of errors, indicating the similarities between *Pan* and *Gorilla* and an overlap with *Homo* at T1, T2, T4, T5, T6, T9, and T10. The total number of *Homo* misclassifications confirms the overlap – including those misclassifications within the validation results. In Table 5.12, misclassifications for *Gorilla* included T12, in addition to the concurrent misclassifications of thoracic vertebrae in the original MLR model.

Table 5.12. Incorrect classification for the thoracic region (*Gorilla*).

Observed	*Homo sapiens*	*Pan troglodytes*	Total	Percent of total Misclassification
T5 *Gorilla gorilla*	20	0	20	2.0
T8 *Gorilla gorilla*	7	3	10	3.3
T12 *Gorilla gorilla*	18	4	22	5.3

The average lumbar region accurate classification rate of 91.5% and validation rate of 88.9% indicated the acceptability for classifying lumbar vertebrae (Table 5.13). The significant variables included in the model and validation test were not consistent throughout the thoracic region. Common variables include vertebral body dimensions, e.g., vertebral body height and articular facet orientation. Except the Area variable, the majority of the significant variables were limited to vertebral arch measurements.

Table 5.13. Species model and validation classification (lumbar region).

Element	Model[1]		Validation[2]		Variables
	Overall Classification %	Number of Misidentifications	Classification %	Numbers of misidentifications	
L1	88.7	7	79.3	364	IVAPA, VBAH
L2	97.0	2	94.8	121	Area, IIFD, IVAPA
L3	95.4	3	86.0	331	IIFD, SVAPA, VBPH, SFID, Area
L4	86.7	8	95.5	453	IFPA, IVAPA, Area, RT

[1] Model, p = 0.000; [2] Validation: Bonferroni Correction, p = 0.000.

The total number of misclassifications in the lumbar region includes *Pan* and *Gorilla*, *Gorilla* and *Pan* (Table 5.14 and 5.15). Both nonhuman primates and *Homo* comprised the majority of errors, indicating the similarities between *Pan* and *Gorilla* and an overlap with *Homo* at L1, L3, and L4.

Table 5.14. Incorrect classification for the lumbar region (*Pan*).

Observed	*Homo sapiens*	*Gorilla gorilla*	Total	Percent of total Misclassification
L1 *Pan troglodytes*	17	68	85	23.3

As depicted in Table 5.15, *Homo* misclassifications failed to confirm complete overlap due to an additional misclassification between *Pan* and *Gorilla*, e.g., *Pan* L2, *Pan L3*, *Pan* L4, and *Gorilla* L4. Misclassification percentages between *Pan* and *Gorilla* varied at the vertebral level. Such variations were similar to those found within the cervical and thoracic region.

Table 5.15. Incorrect classification for the lumbar region (*Gorilla*).

Observed	*Homo sapiens*	*Pan troglodytes*	Total	Percent of total Misclassification
L3 *Gorilla gorilla*	9	2	11	3.3
L4 *Gorilla gorilla*	1	3	4	0.008

Based upon the statistical significance of each model and the rate of correct classifications overall presented in this research, the data suggest that vertebralmetrics can distinguish species. Therefore, the null was rejected.

The overall classification results for each MLR test indicated a substantial classification rate that includes any test in which the final classification is 20% greater than predicted or by chance. Among taxa, only two cases fell below 50%: *Gorilla* T2 at 46% and *Gorilla* T5 at 43.8%; nevertheless, the percentages of correct classification exceeded the predicted percentage from chance alone. The validation test results were similar to the model. All correct percentages were well above those predicted and within 25% or less than those of the original MLR model.

The number of individual vertebrae misclassified by taxon throughout the vertebral column varied by region. No single taxon was more at risk for misclassification; however, in many instances, *Homo* and *Gorilla* had a tendency to misclassify as each other. Misclassifications with *Pan* or an even misclassification among all taxa were noted. Lastly, no discernible pattern among variables that contributed to each model throughout each region was detected, especially with the misclassified cases.

Because of numerous inconsistencies of significant variables for each vertebra throughout the regions, the percentage of misclassifications suggests influencing factors among variables. Further inquiry for *Homo*, *Pan*, and *Gorilla* used Spearman's correlation coefficient (Spearman's rho), a bivariate nonparametric method to determine correlations between two variables when the data is not normally distributed (Field 2009).

5.7 Spearman's rho correlation coefficient results

The results indicated that both positive and negative correlations were significant among vertebral variables for all taxa (Appendix I, Tables I-1 – I-3). However, significance and strength of correlations for each variable differed throughout the vertebral column within and among taxa.

Homo

Among *Homo* cervical vertebrae, moderate to strong positive correlations (0.549-0.787) among VBAH, VBPH, and Area were present from C3 through C7. Moderate to strong positive correlations (0.572-0.648) also were evident among SFID, IIFD, and Area from C4 through C7. Also, positive correlations were present amid VBPH, VBAH, SFID, and IIFD variables. In relation to vertebral body dimensions, the correlation between corpus dimensions to IFA was positive. The PICP variable had a negative correlation at C3 and positive correlation at C6. No correlations between SVAPA and IVAPA variables were present at any vertebral level.

Correlations among VBPH, VBAH, and Area variables in the thoracic region differ from the cervical region. Moderate to strong positive correlations (0.585-0.766) for both VBPH and VBAH with Area were at T1-T6, T8, and T10 levels. T7 exhibited positive correlation for VBPH and negative for VBAH. Only VBPH positively correlated with Area. Correlations among SFID, IIFD, and Area variables were positive at T1 and T4-T11. In relation to body dimensions, facet angles (SFA/SFPA and IFA/IFPA) had low to strong negative correlations (-0.343 to -0.667) with either VBPH or VBAH at T1 and T5-T9. Negative and positive correlations between body and angle variables with PICP were at T2, T4-T6, T9-T11 levels. Low to moderate positive correlations, however, were apparent only at T9 and T11 (0.389-0.439). Correlation between both SVAPA and IVAPA with other variables was evident at T4, T5, and T9-T12. All correlations were negative except at T5 and T10, which were positive.

The human lumbar region exhibited moderate positive correlation (0.471-0.508) with vertebral body height, specifically VBPH with the variable Area at L1-L4. Similarly, only IIFD depicts positive correlation with Area at L4 and L5 level. The relationship among VBPH and facet angles depicts a significant negative correlation. Finally, no significant correlation exists between SVAPA and IVAPA or SVAPA and IVAPA among other variables.

Gorilla

Results for the *Gorilla* sample depicted strong correlations (0.766-0.926) among VBPH, VBAH, and Area, but were limited to C3-C7. Among SFID, IIFD, and Area, positive correlations (0.635-0.900) were discovered at C3-C7. Moderate correlations (0.524-0.568) among facet angles with other variables indicated that only C7 and SFA/SFPA with VBPH/VBAH had a positive correlation. Amid the angled and body measurements, PICP had a negative correlation at C4-C7. Similar to the *Homo* sample, no significant correlation was present between SVAPA and IVAPA at any cervical level.

The thoracic region depicted some uniformity among VBPH, VBAH, and Area. Strong positive correlations (0.773-0.971) were observable throughout the thoracic region. Similar positive trends among SFID, IIFD, and Area variables were present, except for T13. Additionally, PICP had significant negative correlations at T2-T4 and T11-T13. Only T8 had a positive correlation. In regards to comparing SVAPA and IVAPA with other variables, a mixture of positive and negative correlations was at T5 and T12 levels.

Lastly, the lumbar region displayed trends similar to those in the thoracic region. L1-L4 exhibited strong positive correlation (0.778-0.929) among VBPH, VBAH, and Area. Additional positive correlations were observable for SFID, IIFD, and Area variables from L1 to L3. Although positive correlations exist between vertebral body height and facet width, PICP has a negative correlation with the above variables at the same vertebral levels.

Pan

Moderate-to-strong correlations (0.529-0.779) among VBPH, VBAH, and Area were present within the cervical region. Detectable positive correlations among these variables were at C3-C7 levels. Unlike the previous samples, the only positive correlations among SFID, IIFD, and Area were at C4 and C7, with a lack of significance in either SFA/SFPA or IFA/IFPA variables. With regards to PICP, negative correlations were observable at C3 and C6 with IIFD and VBPH variables, respectively. No significant correlations were evident between SVAPA and IVAPA variables.

The thoracic region continues positive correlation among VBPH, VBAH, and Area variables. Moderate-to-strong correlations (0.508-0.770) were observable at T2-T12. Both VBPH and

VBAH variables were correlated at the T3-T11 levels. Whereas correlations among SFID, IIFD, and Area exhibit moderate-to-strong positive correlations (0.518-0.767) from T2-T12, alternating positive and negative correlations between SFID and Area and IIFD and Area were observable at T7-T11. Correlations among variables with PICP depict a positive correlation at the T2, T7, T12, and T13. Lastly, the variables SVAPA and IVAPA exhibited significant positive correlations at T4 and T13. The only negative correlation was at T8.

Finally, strong positive correlations (0.664-0.785) were present in *Pan's* lumbar region. Among VBPH, VBAH, and Area variables, only VBPH depicts a positive correlation at the L1-L3 levels. SFID, IIFD, and Area also exhibited a positive correlation from L1-L4. In relation to the above significant variables, negative correlations with PICP were observed at L1, L3, and L4. Only positive correlation between PICP and VBAH was at the L2 level. Facet orientation to the SVAPA and IVAPA variables demonstrated a positive correlation among the above variables at all levels.

The differences in the correlation among variables across taxa align with the variables identified as useful for classification (refer to Tables 5.8, 5.10, and 5.13). However, common positive correlations were evident among VBPH, VBAH, SFID, IIFD, and Area variables. Since "Area" is the area of the entire vertebra, the positive and negative correlations exhibited variability among SVAPA, IVAPA, SFA, SFPA, IFA, IFPA, CPBA, PICP, and RT variables.

Overall, the statistical evidence from both the MLR and Spearman's rho identified both predictors within each MLR model (Table 5.16). The statistically significant positive and negative correlations for each variable differs from vertebra to vertebra. Variable similarities or convergence that result in misclassification of cases for each taxon was parallel to the differences in the strength of both positive and negative correlations across taxa.

Table 5.16. Significant correlations and MLR predictors.

Pillars	*Homo*	*Gorilla*	*Pan*
Anterior VBPH to VBAH	C3-C7, T1-T12, L1-L5	C3-C7, T1-T13, L1-L4	C4, T3-T6, T7*, T8-T13
Anterior/Posterior VBAH to VBPH SFID to IIFD	C3-C5, C6-C7*, T1*, T7	C3-C7, T1-T6, T7*, T8*, T9-T12 L1*, L2*, L3*	C7*, T7*, T8*, T10*, T12*, T13*
Anterior/Posterior Area to SVAPA, IVAPA	C4, T3, T11	T5, T9, T11-T12	C7, L3

Table 5.16. Significant correlations and MLR predictors (cont.).

Pillars	*Homo*	*Gorilla*	*Pan*
Intermediate PICP and/or CPBA	C3, C6, C7, T2, T4-T12, L1, L3-L5	C4-C7, T2-T8, T10-T13, L1-L4	C3-C7, T1-T2, T6-T7, T9-T13, L1-L4
Intermediate Area to SFA, SFPA, IFA, IFPA	C4, C6, T2, T4-T6, T8, T11	C2, T7-T8, T10-T11	T1, T13, L2-L3
Posterior SFID to IIFD	C3, C6, C7, T1*, T2, T3, T5 - T12*, L2*, L3, L4*, L5	C3-C4, C5*, C6-C7, T1-T6, T8-T12, L1-L3	C3-C6, T1-T12, T13*, L1-L4
Rotational only SVAPA to IVAPA	T4, T5, T9, T10, T11, T12	T1, T5, T12, L1-L3	T4, T8, T13, L1-L4

* Indicates only one variable among the anterior, posterior, or paired variables. Variables in bold indicate MLR predictors for C3–L5.

5.8 Classification of taxon by cranial base angle and segment curvature

Question 3: Can cranial base angle and vertebral segment curvature differentiate between species?

The results indicated that only cranial base angle (CBA), total thoracic curvature (TTC), and total lumbar curvature (TLC) provide significant contributions to the success rate of the MLR model. Correct classifications based on CBA at 86.4%, with validation at 85.9%, suggest a divergence between *Pan* and *Gorilla*. Misclassifications also were detected in *Pan*, but the total number of misclassifications for *Pan* was split unevenly between *Homo* and *Gorilla* (Appendix J, Table J-1), e.g., two instances of misclassification between *Homo* and *Pan*.

The results for spinal curvature followed similar patterns. Both TTC and TLC variables yielded a model classification of 80.3%, with a validation classification of 82.2%. *Homo* was misclassified as *Pan* twice (Appendix J, Table J-2). *Pan* continued to be misclassified, with a split classification between *Homo* and *Gorilla*. All *Gorilla* misclassifications for curvature were designated erroneously as *Pan*. The variables TTC and TLC indicated differences among taxa. Excluding the two instances with a *Homo–Pan* overlap, the nine misclassifications between *Pan* and *Gorilla* indicated a greater degree of similarity.

Based on the significance of the MRL model and the overall rate of classification accuracy, the null hypothesis was rejected. Statistical evidence indicated that the angle of the cranial base and the nature of spinal curvature aid in differentiating among members of these three taxa.

A *post hoc* Spearman's rho was conducted using CBA, TCC, TTC, and TLC variables to link CBA with spinal curvature. Results indicated that no significant correlation between CBA and each segment curvature exists for *Homo* and *Gorilla*. *Pan* had the only significant positive correlation between CBA and TLC: $r_s = .51$, $p = 0.041$.

5.9 Identification of taxa by positional-locomotory complex

Question 4: Can the cranial base angle and vertebral segment curvatures differentiate the positional-locomotory complex of a species? If so, can cranial base angle and vertebral segment curvature classify positional-locomotory complex of a species?

As seen in Table 5.17, Kruskal-Wallis H-tests indicated significant differences across positional-locomotory complex for the CBA, TTC, and TLC. The results indicated that statistically significant differences occur between positional-locomotory complexes and the cranial base angle, thoracic curvature, and lumbar curvature.

Table 5.17. Significant variables for the positional-locomotory complex.

Locomotion: $Biped_H$, $Knuckle\text{-}walk_G$, and $Knuckle\text{-}walk_P$		
Variable	H(2)	p value[1]
CBA	51.100	0.000
TTC	29.693	0.000
TLC	43.767	0.000

[1] Bonferroni Correction: $p < 0.017$.

Therefore, the null hypothesis was rejected. As such, the positional-locomotory complex can delineate taxa by cranial base angle and curvature. However, only thoracic and lumbar curvatures proved to be statistically significant. Two *post hoc* tests were undertaken to determine these differences and if classification was possible.

Post hoc Mann-Whitney U-tests

Overall, results indicated that statistically significant differences occur by positional-locomotory complex and the cranial base angle, thoracic curvature, and lumbar curvature for each taxon. However, differences in curvature were limited to biped and both knuckle-walkers.

$Biped_H$--Knuckle-$walk_P$

As depicted in Table 5.18, results indicated CBA, TTC, and TLC differs significantly between the positional-locomotory complex possessed by modern *Homo* and the positional-locomotory complex possessed by *Pan*. In both cases, the median values for Knuckle-$walk_P$ are greater than those values for $Biped_H$. $Biped_H$ had lesser median values for CBA and TTC and greater median values for TLC than the median values for Knuckle-$walk_P$.

Table 5.18. Significant variables between $Biped_H$ and Knuckle-$walk_P$.

Locomotion: $Biped_H$ (HB) and Knuckle-$walk_P$ (KP)						
Variable	HB Mdn	KP Mdn	U	z	r	p value[1]
CBA	8.01	18.45	13.00	-5.387	-0.761	0.000
TTC	36.40	51.89	47.00	-4.679	-0.661	0.000
TLC	28.19	16.78	40.00	-4.825	-0.682	0.000

[1] Bonferroni Correction: $p < 0.017$.

$Biped_H$–Knuckle-$walk_G$ results indicated CBA, TTC, and TLC were significant across locomotory categories (Table 5.19). Except for TLC, the median values for Knuckle-$walk_G$ were greater than the median values for $Biped_H$.

Table 5.19. Significant variables between $Biped_H$ and Knuckle-$walk_G$.

Locomotion: $Biped_H$ (HB) and Knuckle-$walk_G$ (GK)						
Variable	HB Mdn	GK Mdn	U	z	r	p value[1]
CBA	8.01	29.90	0.00	-5.657	-0.800	0.00
TTC	36.40	44.30	86.00	-3.869	-0.547	0.00
TLC	28.19	12.81	2.00	-5.616	-0.794	0.00

[1] Bonferroni Correction: $p < 0.017$.

Knuckle-$walk_G$ and Knuckle-$walk_P$

As depicted in Table 5.20, the results for Knuckle-$walk_G$ and Knuckle-$walk_P$ indicated that the only statistically significant variable across these two positional-locomotory complexes was CBA. The median values were greater for Knuckle-$walk_G$ than those values for Knuckle-$walk_P$.

Table 5.20. Significant variable between Knuckle-walk$_G$ and Knuckle-walk$_P$.

Locomotion: Knuckle-walk$_G$ (GK) and Knuckle-walk$_P$ (PK)						
Variable	PK Mdn	GK Mdn	U	z	r	p value[1]
CBA	18.45	29.90	17.00	-4.183	-0.739	0.00

[1] Bonferroni Correction: $p < 0.017$.

Overall, the results indicated statistically significant differences across the positional-locomotory complexes Biped$_H$, Knuckle-walk$_G$ and Knuckle-walk$_P$ for CBA, TTC, and TLC variables. However, these differences were observed only between Biped$_H$ and the knuckle-walkers.

The last *post hoc* Mann-Whitney U-tests considered total cervical rotation (TCR), regional cervical total rotation (RTCR), total thoracic rotation (TTR), regional thoracic total rotation (RTTR), total lumbar rotation (TLR), and regional lumbar total rotation (RLTR) variables. The results for Biped$_H$ and Knuckle-walk$_P$, as detailed in Table 5.21, indicated statistically significant differences in the rotation limit within the thoracic and lumbar regions. The median values for Biped$_H$ were greater for TTR but lesser in RTTR and RLTR than the median values for Knuckle-walk$_P$.

Table 5.21. Significant rotational variables between Biped$_H$ and Knuckle-walk$_P$.

Locomotion: Biped$_H$ (HB) and Knuckle-walk$_p$ (PK)						
Variable	HB Mdn	PK Mdn	U	z	r	p value[1]
TTR	176.64	150.55	123.00	-3.099	-0.483	0.000
RTTR	72.89	50.53	46.00	-4.700	-0.661	0.000
RTLR	9.11	28.09	45.00	-4.722	-0.667	0.000

[1] Bonferroni Correction: $p < 0.008$.

In contrast, the results for Biped$_H$ and Knuckle-walk$_G$ yield more statistically significant differences (Table 5.22). Of rotational limits – RTCR, RTTR, and RTLR and two total limits — TTR and TLR were statistically significant. Except for RTLR, Biped$_H$ had greater median values.

Table 5.22. Significant rotational variables between $Biped_H$ and $Knuckle\text{-}walk_G$.

Locomotion: $Biped_H$ (HB) and $Knuckle\text{-}walk_G$ (GK)						
Variable	HB Mdn	GK Med	U	z	r	p value[1]
RTCR	83.40	54.27	120.00	-5.532	-0.782	0.000
TTR	174.64	124.83	49.00	-4.683	-0.655	0.000
RTTR	72.89	10.49	0.00	-5.657	-0.800	0.000
TLR	82.23	52.85	98.00	-3.619	-0.511	0.000
RTLR	9.11	34.70	60.00	-4.409	-0.623	0.000

[1] Bonferroni Correction: $p < 0.008$.

The final results (Table 5.23) between $Knuckle\text{-}walk_G$ and $Knuckle\text{-}walk_P$ yield statistically significant differences for RTCR and RTTR. In each case, $Knuckle\text{-}walk_G$ had greater median values than the median values of $Knuckle\text{-}walk_P$.

Table 5.23. Significant rotational variables between $Knuckle\text{-}walk_G$ and $Knuckle\text{-}walk_P$.

Locomotion: $Knuckle\text{-}walk_G$ (GK) and $Knuckle\text{-}walk_P$ (PK)						
Variable	GK Mdn	PK Mdn	U	z	r	p value[1]
RTCR	76.27	54.27	2.00	-4.664	-0.796	0.000
RTTR	50.53	10.49	17.00	-4.183	-0.717	0.000

[1] Bonferroni Correction: $p < 0.008$.

5.10 Classification of taxa by positional-locomotory complex

MLR results (Appendix K, Tables K-1 – K-2) indicated a highly accurate rate of correct classification by positional-locomotory complex across the three taxa. Classification rate of 80.3% and model fit, with a high validation test classification of 87.3%, depicted similar results as previously explored with CBA and curvature for speciation. For example, $Knuckle\text{-}walk_P$ continued to be misclassified, with misclassifications split between $Biped_H$ and $Knuckle\text{-}walk_G$. Even the patterning of misclassification with the CBA was the same. Consequently, it appears that differentiation of taxa based upon the positional-locomotory complex was shown to be viable with a reasonable rate of accuracy using CBA, TTC, and TLC. Therefore, the null was rejected.

A *post hoc* MLR test used individual CPBA variables in each vertebral region (Appendix K, Tables K-3 – K-5). The results obtained for variables of the cervical region indicated a 70% accurate

classification rate with a validation classification of 60.9% by category of the positional-locomotory complex for C3 and C7. The rate of correct classification for variables of the thoracic region was 86.3%, with validation test at 94.1%. T2, T4, T7, and T10 vertebrae were statistically significant for the CPBA variable. Using CPBA, the rate of correct classification increased by 6% over the previously employed TTC variables. Lastly, the lumbar region yielded a 70.9% correct classification rate and a validated classification rate of 61.4% by primary mode of locomotion category, with L2 and L3 serving as influential elements. A 9.3% decrease was observable when compared to the previous MLR. Overall, delineation of taxa by positional-locomotory complex using regional CPBAs indicated influential vertebrae within spinal regions.

5.11 Fossil hominin classification

Question 5: Can the findings of this research help to distinguish fossil hominin vertebrae?

For exploratory purposes, MLR results indicated significant model fit for all tests with a good overall classification (Appendix L, Tables L-1 – L-6). Each fossil hominin vertebra, however, was misclassified. The results for A.L. 288-1 indicated classification for element AH designated as *Homo* for T6 with an 80.3% classification rate. The classification for element AK was designated as *Homo* for L3 at a classification rate of 73.1% and as *Pan* for L2 at 66.7%. Furthermore, A.L. 333 x-12, designated as T10, was categorized as *Gorilla*, with a higher overall classification rate of 76.2% based on IFPA and SFA variables. Similar to the lumbar designation as observed for A.L. 288-1, A.L. 333 106 has two possible designations – C5 or C6. The results for both tests classified the fossil element as *Pan*, but the overall classification rates differ: C5 was classified at 92.4% as compared to the classification of C6 at 78.5%.

Chapter 6. Discussion

Contributions from previous research relating to the morphology of the cranial base proved to be significant (Ahern 2005; Barbera et al. 2009; Dean and Wood 1981; Lieberman et al. 2000; Luboga and Wood 1990; Strait 2001). Studies concerning cervical, thoracic, and lumbar vertebrae illustrate the multi-faceted approach to quantifying differences and similarities within and across taxa (Clauser 1980; Pal and Routal 1986; Panjabi et al. 1991a; Panjabi et al. 1993b; Shapiro 1990). Differences and similarities within species relate directly to sex estimation that is beyond allometric influence (Bastir et al. 2014; Gomez-Olivencia et al. 2007; Marino 1995; Wescott 2000). This discussion chapter consists a brief summary, significance, and interpretation for each of the research questions. Additionally, a comprehensive interpretation explores possible explanations as they relate to the overarching research question.

6.1 Initial evaluation, allometry, and symmetry or lateral dominance

Initial assessment of the data set revealed non-normal distributions and various degrees of skewing among variables throughout the vertebral column. Log transformations were attempted to normalize the distribution, but the data set remained non-normally distributed. Though speculative when compared to previous research, the non-normal distribution was due to measurement sensitivity and the degree of tropism exhibited among vertebrae.

Three preliminary tests checked for observer error and allometry before conducting the main tests. First, there was no indication of observer error. Results indicated *no* significant difference between the first and second set of measurements (Appendix B, Table B-1). Taking into considerations the standardized method for cranial and vertebral orientation coordinates (X, Y, and Z) with related reference planes, nonsignificant differences between measurements were not surprising.

In so far as addressing size differences within and among taxa, significant variables checked for allometry as outlined by Darroch and Mosimann (1985). Principal component analysis (PCA) results indicated a significant contribution of the variables to the first component for each vertebra (Appendix C, Table C-1). When regressed against the geometric mean, results indicated inconsistency in variable significance throughout the vertebral column, e.g., facet angle, vertebro-facet angle, vertebral body height, interfacet distance, pedicle inclination, and adjacent body angle (Appendix D, Tables D-1 – D-4).

The amount of allometry found throughout the vertebral column is not surprising in itself. Considering the differences in body size within and among species, the interpretation of significant differences is the result of structural adaptations necessary for weight distribution. This scenario is plausible but fails to account for the inconsistency of significant variables – unless an intervening variable exists that exerted some influence.

Symmetry or lateral dominance

Lateral dominance or tropism, as indicated by Wilcoxon signed-rank tests that yielded statistically significant results within each vertebral region, was noted due to the number of vertebrae depicting greater median values between the left and the right; however, no one taxon exhibited statistically significant differences for each variable limited to one side. Also, not every vertebra throughout the vertebral column exhibited differences between sides.

Differences in facet orientation across taxa regarding tropism (Francis 1955a; Pal et al. 2001; Panjabi et al. 1993b) and joint configuration (Clauser 1980; Pal et al. 2001) were documented previously. The addition of facet angle variables to the coronal plane yielded statistically significant results in this study that were similar to the outcomes of prior research using other measurements (Francis 1955a; Masharawi et al. 2004; Pal et al. 2001; Panjabi et al. 1993b). Statistically significant differences are not surprising, but the distribution of these variables throughout the spinal regions across taxa becomes a point of interest, e.g., the presence of tropism and/or mortice joints (Davis 1955; Davis 1961). Results across taxa indicated not only sporadic significance throughout each region but also inconsistency for superior/inferior facet orientation to either the coronal or sagittal planes at any given vertebral level. These inconsistencies were observable among statistically significant variables with distributions of greater median values between left and right measurements. Although no correlations between the lateral differences with any other variables were present, it is possible that the inconsistency is related to adjacent vertebral body angle, total regional curvature, and rotational variables. If this possibility is correct, it would be consistent with previous medical research that included soft tissue (Drerup 1984; Kouwenhoven et al. 2006; Kozanek et al. 2009; Lee et al. 2004; Masharawi et al. 2004; Yazici et al. 2001).

6.2 Sexual dimorphism

Question 1: Are vertebrae sexually dimorphic within a taxon?

Sexual dimorphism is apparent among the taxa chosen for this study. The results from the Mann-Whitney U-tests indicated that all taxa exhibited differences between males and females. The null was rejected. In the modern *Homo* sample, differences were observable at C1, C4, C7, T1-T7, and L1 levels. The common statistically significant variable was Area. The *Pan* sample exhibited statistically significant differences only within the cervical region – namely, C1 and C6. When compared to *Homo* and *Pan*, *Gorilla* depicted the greatest number of differences between males and females among the three taxa. Each taxa had vertebra that exhibited at least one variable which was statistically significant difference, with Area as the most common variable.

The inconsistency among significant variables for allometry was puzzling. This bewilderment extends to the inconsistencies found throughout the column. The sporadic distribution of significant variables, such as Area, SFID, IIFD, VBPH, and VBAH follows no discernible pattern within or across taxa. Unlike of the variables employed in previous studies (Bastir et al. 2014; Marino 1995; Wescott 2000), vertebrae that are considered good estimators of sex in this research (Table 6.1) include the same vertebral levels as reported by Marino (1995) and over 50% of the same levels as reported by Bastir et al. (2014). This agreement with C1, T1-T5, and T6-T7 justifies the conclusion that estimation of sex via metric variation in vertebrae is possible with humans and can be extended to nonhuman primates as well.

Table 6.1. Significant differences between males and females (Spp. /sex).

Species	Vertebral level differences (M/F)
Homo	C1, C4, C7, T1, T2, T3, T4, T5, T6, T7, and L1
Pan	C1 and C6
Gorilla	C1-C7, T1-T3, and L1-L4 (ALL vertebrae)

The conclusion, however, warrants a second look at the evidence. Two issues cast doubt on such claims. First, significant differences at the vertebral level between two quadrupedal species raise

suspicions, e.g., dimorphism observed in *Gorilla* but limited in *Pan*. The results are counterintuitive to observed differences in size between males and females within each taxon.

Second, the variables Area, SFID, IIFD, VBPH, and VBAH are commonly greater in males than in females, with only two significant facet measurements – T2 IFA and IFPA for humans – that indicated a greater median value for females. The lack of facet orientation contradicts previous research (Bastir et al. 2014; Marino 1995; Wescott 2000) and those differences attributed to weight distribution and curvature accommodations for female pregnancy (Bastir et al. 2014). Although the exact relationship between lumbar curvature and pelvic orientation for the developing fetus is unknown, if the above assertions were true, the number of significant facet angle measurements, including vertebral body variables, would be present throughout the vertebral column or key junctures in human females.

The data suggest that inconsistent differences among vertebral levels might primarily be related to body mass, as depicted in previous research (Bastir et al. 2014; Marino 1995; Wescott 2000). The addition of facet variables would provide more compelling evidence than just the variables Area, VBPH, VBAH, SFID, and IIFD, or any combination of those variables as demonstrated within this research in almost every case among taxa. Furthermore, distribution of statistically significant vertebral dimensions within the vertebral column would also bolster this claim of sex estimation.

Despite what seems to be counterintuitive results, the results are important in two ways. First, it shows that differences do exist beyond mere observable size. Variables that include articular facet orientation and vertebral body height with overall vertebral area supports this view. Second, the evidence points to the possibility that the combination of several variables used in a mathematical formula, which takes into account the complex interrelationships among vertebrae, would serve to distinguish between males and females. Unfortunately, the results of this study are far from conclusive because of the caveats stated regarding the variables or a variable acting as a contributing factor to a definitive method for sex estimation.

6.3 Vertebralmetrics as means for delineation and classification

Question 2: Can vertebralmetrics differentiate vertebrae among species? If so, can vertebralmetrics classify species?

Results for the Kruskal-Wallis H-test indicated significant differences across taxa throughout the vertebral column (Appendix F, Table F-1). Consequently, the null hypothesis was rejected. The distribution of statistically significant variables was present throughout the vertebral column without any discernible pattern. *Post hoc* Mann-Whitney U-tests (Appendix G, Tables G-1 – G-3) determined which pair-wise contrasts drive the collection's statistically significant differences across taxa identified by the Kruskal-Wallis H-tests. The results obtained for the contrast between modern *Homo* and *Gorilla* identified statistically significant differences for each vertebra. The contrast between modern *Homo* and *Pan* yielded similar trends. Each vertebra had similar variables that resulted in statistically significant differences across the two taxa throughout the vertebral column, except for the thoracic region, which contained more significant vertebral body variables in its lower region. Lastly, results obtained for the contrast between *Pan* and *Gorilla* yielded statistically significant differences for each vertebra within the vertebral column. Common variables in each region included facet angle, vertebro-articular angle, interfacet distance, and vertebral area.

Complete or partial combinations among vertebral Area, VBPH, VBAH, SFID, IIFD variables were common among paired taxon contrasts. Unlike the previously discussed issues with sex estimation, differences also encompassed various superior and inferior articular facet orientation variables. Previous research studies (Clauser 1980; Latimer and Ward 1993; Pal et al. 2001; Panjabi et al. 1991a; Panjabi et al. 1993a; Panjabi et al. 1993b; Panjabi et al. 1991b; Shapiro 1991; Ward et al. 2010) have identified the differences. However, the inclusion of averaged facet orientation to both the coronal and sagittal planes in this study becomes a critical point in the comparison of paired species that is absent in previous research.

Interpretation of the pair-wise contrasts suggests that two distinct phenomena exist within vertebral morphology. First, vertebral area, SFID, and IIFD represent two parts of the first phenomenon. The data suggest two distinct vertebral columns: vertebral body/arch (Area) and interfacet distance. If true, as suggested by previous research (Etnier 2001; Goel and Clausen 1998; Legaye and Duval-Beaupere 2008; Louis 1985), the regional weight distribution "flows" from contact points with anterior/posterior weight displacement placed upon the vertebral body. The second phenomenon regards facet orientations and quadrant approach to quantify vertebral angle and limits on vertebral rotation. Medical research seems to support this scenario (Drerup 1984;

Kouwenhoven et al. 2006; Kozanek et al. 2009; Lee et al. 2004; Masharawi et al. 2004; Yazici et al. 2001).

As indicated in Chapter 3, the mechanical limits regarding curvature and rotation are tacitly acknowledged by previous researchers (Adams et al. 1996; Bogduk and Mercer 2000; Duan et al. 2001; Gangnet et al. 2003; Vrtovec et al. 2009). Pedicle and facet orientation reflects the interconnection between curvature and rotation (Drerup 1984; Kouwenhoven et al. 2006; Kozanek et al. 2009; Lee et al. 2004; Masharawi et al. 2004; Yazici et al. 2001). Further confirmation extends into areas of other research (Adams et al. 1996; Andriacchi et al. 1974; Bogduk and Mercer 2000; Duan et al. 2001; Gangnet et al. 2003; Vrtovec et al. 2009). However, extending an evaluation of curvature and rotation to both human and nonhuman primates in this study acknowledges the need for caution. Based on the perspective above, this research extends variation in facet orientation (primary) and pedicle orientation that contribute to the amount of regional curvature and rotational range in terms of restriction or less restriction among taxon.

In Table 6.2, inferences pointing to these phenomena coincide with significant paired differences. Incremental regional breakpoints (indicated by vertebral Area with VBPH and VBAH variables) and restrictiveness (indicated by vertebral arch/facet orientation) can explain these differences, which suggest limits in rotation throughout each region.

Table 6.2. Regional breakpoints and restrictions.

Paired comparison	Regional breakpoints	Regional Restriction (RT)
Homo - Gorilla	T7 – T12	T12, L1
Homo - Pan	C4 – C7, T8 – T12, L1 – L3	T3, T4, T12, L1, L4
Pan – Gorilla	C4 – C7, L2, and L4	NA
Single Species	Regional breakpoints	Regional Restriction (RT)
Homo	C5, T3, L4	C5/C6, T3, T8, T10, L4
Gorilla	C7, T6, L4	C7, T4, T8, T11, L2
Pan	C7/T1, L4	C6, T6, T9, T11

Single taxon and pair-wise comparisons illustrate differences with strong significant correlations among other variables not deemed relevant to both, in either breakpoint and/or rotation. Median values and the number of median values depicted *Homo* as less restrictive in the cervical, thoracic,

and the lower lumbar regions than those same regions of either *Gorilla* or *Pan*. The two knuckle-walkers, *Gorilla* and *Pan*, suggest a distinction among vertebrae, with less restriction for *Pan* than for *Gorilla*. Collectively, the data indicated that variables Area, VBPH, and VBAH do not indirectly dominate other variables. Finally, the two variables selected to capture a vertebra's contribution to curvature (CPBA) and the bridge between pillars (PICP) among facet orientation did not play an influential role among pair-wise contrasts. This conclusion is also consistent with vertebral classification.

Classification results for the MLR model and validation test results (Appendix H, Tables H-1 – H-24) indicated that classification by taxon was possible. Each model fit depicted the data correctly and was statistically significant. The rate of correct classification was sufficiently high (88.7% for cervical, 90% for thoracic, and 91.5% for lumbar) and statistically significant for each vertebra throughout the vertebral column. In fact, the correct classification average for the entire column is 90.0%. Additionally, results from a *post hoc* Spearman's rho indicated significant differences in correlation between variables across taxa that aligned themselves with those variables identified as useful for classification purposes (Table 5.16). The variables contributing to each model fit were not consistent regionally. The result indicated the main contributing factors such as Area, VBPH, and VBAH with facet orientation. Examples are SFPA (T6), IFA (C1-C3 and T5–T7), IFPA (C4, T1, T10, and L4), PICP (C4, T6–T7, and T11), and CPBA (C3, T8, and T10).

Interpreting variables and overall classification rates require caution. Evidence for *Homo*, *Gorilla*, and *Pan* suggests the following scenario for each region: (1) the cervical region holds facet orientation of primary importance over vertebral body dimension. C1, C4, and C7 also consider body dimension, e.g., theoretical regional breakpoints. Furthermore, variables SVAPA and/or IVAPA at each vertebral level indicate the probable degree of rotation. (2) The thoracic region continues facet orientation as a primary and dominant variable that indicates rotational movement upon and angled to the tilted posterior axis. Vertebral body dimensions, specifically the combination with Area at T3, T6-T8, and T11 depict breakpoints or semi-breakpoints within the region. (3) Lastly, the lumbar region continues the primacy of facet orientation with significant breakpoints found at L2-L4.

These scenarios, which considered significant variables to determine classification, appear random when paralleled to the results from contrasts between paired taxa, especially the results involving

the greater median values. The question here becomes what can account for the various combinations of vertebral body dimensions and facet-orientation characteristics for each of the three species. Beyond the caveat regarding predictors as stated in Chapter 5, plausible explanations to reconcile test results are limited. Only two cogent explanations reside in the significant correlation coefficients among variables at each vertebral level.

First, these strong significant correlations, i.e. Spearman's rho, create a web of correlations directly or indirectly among taxa via common variables. For all species, the majority of the positive correlations are among VBPH, VBAH, SFID, IIFD, and Area variables. The link of facet orientation to the significant correlation with either VBPH or VBAH to SVAPA or IVAPA variables is interesting. Additionally, SFA, SFPA, IFA, and IFPA had a significant correlation among variables via SFID and/or IIFD. No tentative pattern of positive or negative correlations among variables in relation to vertebral level was detected. In fact, some variables were not significant at various levels, e.g., *Homo* PICP at C4, C5, C7, T1, T3, T7, T12, L3, and L4. Differences in variable correlations, both positive and negative among species, can account for the presence/absence of variables without regional patterning. Additionally, differences among paired correlations would also account for some of the misclassifications.

The second plausible explanation is less complicated and more mundane. Variations among variable significance and the lack of distinct patterns are a result of differences in vertebral regional length per vertebral count, as dictated by facet orientation (Clauser 1980; Schultz 1938; Schultz 1961; Schultz and Straus 1945; Williams and Russo 2015). This scenario would be highly plausible, but initially calculated averages for laterally-paired variables negated the orientation differences that were used to determine the regional length and intra-regional differences among primate species.

The distribution of the SVAPA variable supports the first scenario and illustrates the posterior-pillars concept. It is very likely that the average between lateral measurements circumvented the issues regarding tropism and facet orientation, while simultaneously preserving the interconnected functionality among vertebral regions. Though vertebrae share some similarities, each vertebra is unique regarding its placement in the column. The relationship between vertebral positioning and morphology assumes a biomechanical functionality among traits.

Reported test results and their interpretation confirm some of the assumptions about the integrated nature of each vertebral variable found amid adjacent vertebrae. Significant variables vary at different vertebral levels within and among taxa. Stemming from the data and its subsequent interpretation, two important factors emerge from this study. First, noted significant variables are at each vertebral level. Uncovering the differences, even though there is a lack of uniformity, suggests that articular facet orientation serves as an influencing factor in determining taxa. It is a partial glimpse into the complete picture. Second, the significant differences between *Pan* and *Gorilla* for each vertebra throughout the vertebral column (with a 94.4% average correct classification) suggest that knuckle-walking was a homoplastic feature and very likely a product of parallel evolution. Essentially, knuckle-walking is not the same between the two species, but two types of knuckle-walking developed independently in both *Pan* and *Gorilla* sometime after the *Pan-Gorilla* split that occurred approximately 17 Ma (Ho et al. 2005).

Vertebralmetrics as a method for both vertebral identification and speciation regarding theory and statistical evidence seems viable, but unfortunately, it is not conclusive. The lack of conclusiveness is due to (1) erratic distribution of significant variables within and among vertebral regions; (2) the inability to assess variable interaction due to linearity issues; and (3) the limited scope of this research, e.g., not addressing intra-regional classification. Reported significant results with their interpretations suggest a starting point and provide evidence that points to an abstract and unifying principle for determining vertebral placement, speciation, and perhaps sex estimation.

Whereas assessment of individual vertebrae provides interesting results and interpretation, addressing the cranial base and vertebral curvature would provide a useful and needed quantifiable link between the cranium and the spinal column. Moreover, determining differences among segment curvatures, as depicted by an arc or a bow, would assist in understanding the inter-regional relationships among curvatures.

6.4 Cranial base angle and segment curvature

Question 3: Can cranial base angle and vertebral segment curvature differentiate among species?

Results from the MLR model indicated a high classification rate overall (86.4%), with significant model fit for CBA and accurate classification rate for curvature (80.3%). MLR validation test results were similar to the model, 85.9%, and 82.2% respectively. Additionally, a *post hoc* Spearman's rho determined the correlation between CBA and TCC, TTC, and TLC. Results

indicated no significant correlation between CBA and each segment curvature for *Homo* and *Gorilla*. *Pan* was the only species that depicted a significant positive correlation between CBA and TLC: $r_s = .51$, $p < 0.05$.

Significant results for CBA indicated that the constructed plane, which takes into account the inclination of the foramen magnum and occipital condyle orientation, can discriminate when measured to the Frankfurt Horizon. Measurement and results for the CBA differ from those published in previous research (Ahern 2005; Barbera et al. 2009; Dean and Wood 1981; Lieberman and McCarthy 1999; Luboga and Wood 1990; Strait 2001; Strait and Ross 1999). The evidence suggests that the external plane measurement, with an 86.4% correct classification rate, has the potential for correctly defining the CBA. However, any misclassifications between extant human and nonhuman primates are points of concern. While misclassifications between *Pan* and *Gorilla* are understandable, i.e., both have a posteriorly placed foramen magnum, misclassifications between *Homo* and *Pan* in the present study suggests that a different approach to measurement is needed – specifically choosing a different registration or reference plane.

This need for a different registration or reference plane is evident when comparing external CBA from this study (*Homo* = 8.83°, *Pan* = 1.19°, and *Gorilla* = 1.68°) with the results of Strait and Ross (1999) or Luboga and Wood (1990). Only the results for *Homo* in this study are similar to those provided by other researchers, specifically the 8.2° in reference to the orbital inclination plane as reported by Strait and Ross (1999), or the 9.3° in reference to the inclination of the Frankfurt Horizon as reported by Luboga and Wood (1990). Such similarities between CBA in this study with either orbital inclination plane or the Frankfurt Horizon in the latter study stress the uniqueness in quantifying the position of the foramen magnum by the inclination of the occipital bone. Differences among reported results from this study, including those from the Spearman's rho and other published results, illustrate the need to provide additional inquiry into a more accurate method to quantify CBA.

Regarding curvature, interpretations of the evidence support the paradigm offered by the three-column concept. Each articular facet acts as one column, which combines into an interlocking mechanism and transitional means between adjacent vertebrae. Previous research indicates this possibility (Dietrich and Kessel 1997; Gangnet et al. 2003; Louis 1985). Lateral variations found among facet orientations to both coronal and sagittal planes suggest that the two posterior vertebral

"pillars" – superior and inferior – act independently, but function as a single unit. The distribution of compression, shear, and strain among the vertebral discs that vary at each vertebral level (Adams et al. 1996; Frobin et al. 2002; Humzah and Soames 1988; Keller et al. 2005) are prime examples. Furthermore, evidence within vertebral microstructure supports the claim that applied forces are spread within the spinal column (Bouvier 1985; Briggs et al. 2004; Cowin 1986; Legrand et al. 2000; Linden et al. 2001; Panjabi et al. 2001; Prakash et al. 2007). Consequently, in this author's opinion, inconsistent lateral variations are interpreted as an individual compensatory mechanism that ensures spinal stability for each species' positional-locomotory complex.

Previous research (Adams et al. 1996; Butler et al. 1990; Goto et al. 2002; Pal and Routal 1991) tacitly supports lateral facet orientations as a fluid structural shift from two pillars to one vertebral column. Thus, using the averages as a representative value for the two-to-one posterior column concept is justified. Additionally, slight pathologies and transitional junctures as depicted in previous research eliminated the problem regarding tropism (Adams et al. 1996; Butler et al. 1990; Goto et al. 2002; Pal and Routal 1991). Essentially, lateral averages take into account the lateral variations while focusing on the rotational-curvature orientation. This interpretation would be consistent with medical diagnoses involving soft tissue (Drerup 1984; Kouwenhoven et al. 2006; Kozanek et al. 2009; Lee et al. 2004; Masharawi et al. 2004; Yazici et al. 2001).

The regional curvature presented here is a sum total of CPBA variables for each region. Thus, the method used to calculate curvature for this study differs from other methods used in a clinical setting (Vrtovec et al. 2009). For example, the established approximate range for normal human spinal curvature within a clinical setting is 43° for the cervical region, 20-40° for the thoracic region, and 30-50° for the lumbar region (Boyle et al. 2002; Harrison et al. 1996; Norkin and White 2009c; Singer et al. 1990; Vrtovec et al. 2009). In contrast, the reported averages as indicated in this study differed and placed cervical curvature at 19.25°, thoracic curvature at 37.57°, and lumbar curvature at 28.96°. Figure 6.1 illustrates the difference between facet articulations as they relate to adjacent vertebral body angle (CBPA) in this study and other methods. The differences between clinical range and the results from this study suggest two possible explanations: (1) soft tissue has a greater influence on overall curvature, independent from vertebral orientation, and/or (2) the smallest amount of deviation due to soft tissue among vertebrae

has an accumulative amplifying effect on overall curvature. Explanations for the differences are probably due to the latter.

Curvature, as depicted in Figure 6.1, differs not only in methodology, but also the quantifiable differences in rotation. The approximate range for normal human spinal rotation within a clinical setting is 49-80° for cervical region, 45-50° for the thoracic region, and 42-46° for the lumbar region (Norkin and White 2009a; Norkin and White 2009b). Comparatively, the results indicated the total cervical rotation at 71.82°, thoracic rotation at 182.02°, and lumbar rotation at 86.40°.

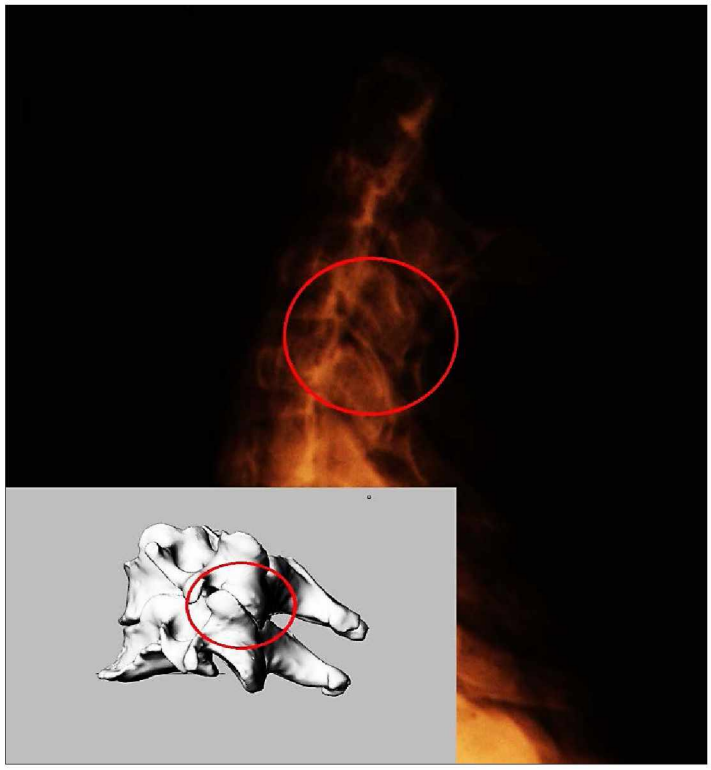

Figure 6.1. Facet articulation with and without soft tissue.
X-Ray Photo and scan**:** Cleveland Museum of Natural History
Hamann-Todd Osteological Collection.

As with the case of vertebral curvature, differences between clinical range and the results from this study suggests three possible explanations. First, soft tissue has a greater influence on overall rotation that is independent of vertebral facet orientation. Second, the smallest degree of deviation due to soft tissue among vertebrae has a cumulative amplifying effect on regional rotation. And

lastly, a combination of the two reasons results in variable degrees of tropism. It is very likely that a combination of these factors, perhaps with contributions from an unknown factor or factors, is responsible for the difference depicted within this research, e.g., the thoracic region.

Results from this study indicated that only TTC and TLC were significant, with an overall classification rate (80.3%). Variable significance and misclassifications have possible explanations regarding adjacent body angle and related correlations (positive and negative) among vertebral variables. Interpretation allows for two statements regarding curvature. First, the cervical region is too generalized among species to depict significant weight distribution with current variables. This generalization of the cervical region is counterintuitive because of the weight (mass) of the head for the *Gorilla*. Secondly, both the thoracic and lumbar regions are distinct for *Homo*, e.g., the amount of kyphosis and lordosis in *Homo* as compared to that found in both nonhuman hominoids. The evidence suggested that TTC and TLC infer these differences in COM are related to vertebral morphology. Curvature related to COM would explain both the omission of TCC from the model and the misclassification rate between *Pan* and *Gorilla* samples. However, explanations for the misclassifications between *Pan* and *Homo* are not readily apparent: either some pathology, e.g., results from degenerative disc diesease, influenced the orientation of the facets to the coronal plane or curvature compensation with soft tissue would better separate the members of the two taxa.

While classification of species via CBA, TTC, and TLC provides an interesting and important scenario, linking the cranium via segment curvatures or among curvatures remains elusive. The results reported for Spearman's rho (see Appendix I, Tables I-1 – I-3) indicated no significant correlation between the cranium and each segment curvature or among regions for both *Homo* and *Gorilla*. Only *Pan* had a significant negative correlation between CBA and TLC. In fact, negative correlations also were noted between cervical and thoracic pseudo-curvature. The lack of significant correlation between CBA and all three regions is perplexing, especially within the cervical region. For example, when considering CBA and C1 variables, no significant correlations exist among any variables with CBA. The lack of correlation between CBA and C1 SFA, which parallel each other, defies explanation. The best explanation is that the CBA variable is incorrect in its depiction by the current variable definition. Calculations for the CBA measurement needs to be more comprehensive. Currently, the head remains decapitated from the column.

6.5 Cranial base angle and segment curvature by positional-locomotory complex

Question 4: Can the cranial base angle and vertebral segment curvatures differentiate the positional-locomotory complex of a species? If so, can cranial base angle and vertebral segment curvature classify positional-locomotory complex of a species?

Three categories of positional-locomotory complexes were under consideration: $Biped_H$, $Knuckle\text{-}walk_G$, and $Knuckle\text{-}walk_P$. Results from Kruskal-Wallis H-tests indicated statistically significant difference by category of locomotion for CBA, TTC, and TLC variables. The *post hoc* Mann-Whitney U-tests identified statistically significant differences between $Biped_H$ and both knuckle-walkers – $Knuckle\text{-}walk_G$ and $Knuckle\text{-}walk_P$. In comparison, the only significant variable between the two knuckle-walkers was CBA. Similar results were observable with all rotational limits, i.e. TTR, RTTR, and RLTR. MLR results confirm the outcomes obtained by the Kruskal-Wallis H-tests. Overall classification by primary mode of locomotion was 86.4% for CBA and 80.3% for curvature. Both models were significant for model fit. MLR validation results indicated similar percentages, 87.3% and 82.2% respectively. Results differ for regional CPBA variables. The results indicated high correct classification rates with significant model fit. For the cervical region (70.7%), C3 and C7 contributed to the model. Elements T2, T4, T7, and T10 were significant for the thoracic region (86.3%) and L2 and L3 for the lumbar region (70.9%). However, validation test results were lower than the original MLR model: cervical region (60.9%), thoracic (94%), and lumbar (61.4%).

Cranial base angle and spinal curvature (Chapter 3) are often referred to when distinguishing modes of locomotion (Chapter 2). Inferences themselves are tenuous due to the overlapping of morphological traits and variations in posture and locomotion among nonhuman primates, thus assuming the positional-locomotory complex for the latter. Interpretation of the evidence assumes the distinction regarding the placement of COM amid CBA, TCC, TTC, and TLC variables as they pertain to positional-locomotory complexes, e.g., $Biped_H$, $Knuckle\text{-}walk_G$, and $Knuckle\text{-}walk_P$.

Results from both the Kruskal-Wallis H-tests and *post hoc* Mann-Whitney U-tests indicated significant differences between paired taxa, based on previously acknowledged observations of locomotion. Interpretation mirrors the observations presented in the discussion of vertebralmetrics as a means for delineation and classification. CBA, TTC, and TLC variables were significantly different between $Biped_H$ and both $Knuckle\text{-}walk_G$ and $Knuckle\text{-}walk_P$. Only CBA was significant

between Knuckle-walk$_G$ and Knuckle-walk$_P$. The inclusion of these variables will provide contrast for the rotational variables TCR, RTCR, TTR, RTTR, TLR, and RLTR.

Reported results indicated that TTR, RTTR, and RLTR were significant between Biped$_H$ and Knuckle-walk$_P$. Similar significance was observable with the addition of RTCR and LTR variables. Only RTCR and RTTR were significant between Knuckle-walk$_G$ and Knuckle-walk$_P$. The differences among regional rotational variables involving the regional total, e.g., TCR, TTR, and LTR, have been established. The difference between the first vertebral SVAPA and the last vertebral IVAPA assumes rotational movement during locomotion. Results also depicted that Biped$_H$ had greater medians in all variables except RTLR. In the case of RTLR, both Knuckle-walk$_G$ and Knuckle-walk$_P$ had greater medians than those of Biped$_H$. Greater median values suggest that bipeds have less restriction than either knuckle-walker. Knuckle-walk$_P$, however, has less restriction than Knuckle-walk$_G$ due to morphological restrictions as previously noted.

The total results for CBA, TTC, TLC, RTCR, TTR, RTTR, LTR, and RLTR are interpreted in relation to head position and weight displacement with rotational limits of the vertebral column. For example, the degree of flexion and extension (TTC and TLC) with rotation (RTCR, TTR, RTTR, LTR, and RLTR) is evident in the bipedal range of motion with COM located above the pelvis. Greater limitations infer that stiff-backed knuckle-walkers differ with an anteriorly-placed COM.

Classification results from the MLR model and validation test suggested CBA can delineate positional-locomotory complex with a reasonably high degree of accuracy. Similar to the discussion regarding classification via vertebralmetrics among species, results between Knuckle-walk$_G$ and Knuckle-walk$_P$ continue misclassification and mirror previous results from this research. The number of misclassifications, however, was similar, but the percent correct differed, e.g., Knuckle-walk$_G$ (81.3%) and Knuckle-walk$_P$ (68.8%). Misclassification percentages in this study suggest that a different approach to quantifying CBA measurements may yield better results.

Also, results indicated that only TTC and TLC were significant, with an overall classification rate of 80.3% for separating samples based on positional-locomotory complex. Explanations for variable significance and misclassifications are due to adjacent body angle and related positive and negative correlations among vertebral variables with reference to COM. Classification based on pseudo-curvature, namely the estimated curvature without soft tissue, may give vertebral region

identification clarity for locomotion; but intra-regional analyses of regional CPBA variables depicted more accurate results, indicating greater delineation for the positional-locomotory complex (Appendix K, Tables K-3 – K-5). However, absolute certainty is not possible. The lack of certainty is due to the effect of soft tissue on overall curvature, independent from vertebral orientation and/or the smallest amount of deviation. Soft tissue has a sum amplifying effect on overall curvature.

The *post hoc* MLR and validation results indicated classification with significance for the positional-locomotory complex is possible for the cervical (C3 and C7), thoracic (T2, T4, T7, and T10), and the lumbar (L2 and L3) regions; but, it is the presence of rotational variables which increases the likelihood for positional-locomotory classification. However, the likelihood is doubtful due to this influence of soft on overall rotation (independent from vertebral facet orientation), the sum amplifying of small deviations in regional rotation, and variable degrees of tropism among vertebrae. Nevertheless, this presents an interesting perspective when considering the established range of both vertebral curvature and rotation found in the human species. Unfortunately, in-depth studies into curvature and rotation among extant nonhuman primates are lacking. Consequently, an evaluation of results is not possible at this time.

Despite this obstacle, evidence suggests that the location of significant CPBA variables are within or near regional breakpoints (Table 6.2). Regarding the positional-locomotory complex, C3, C7, T2, T4, T7, T10, L2, and L3 act as transitional points for regional curvature that would ultimately displace weight in relation to COM. This explanation, however, is more relevant to bipeds than to knuckle-walkers, due to curvature characteristics.

6.6 Fossil hominins

Question 5: Can the findings of this research help to distinguish fossil hominin vertebrae?

An MLR considered each vertebra from A.L. 288-1 (AH and AK) and A.L. 333 (x-12 and 106) specimens for classification. All results depicted an overall high classification rating and significant model fit; however, the classification of all fossil samples was incorrect. Results for A.L. 288-1 AH (T6) classified the fossil vertebra as *Homo* (80.3%). The element AK, identified as either L2 or L3, was tested twice. Classification results for L2 (73.1%) classified the element as *Pan*. L3 classification (66.7%) placed the element within the *Homo* category. Results for A.L. 333

(x-12 and 106) differ from A.L. 288-1. The x-12 element (T10) classification (76.2%) was considered to be *Gorilla*. Element 106, previously determined to be C5 or C6, depicted no difference between correct classification and misclassification. C5 (92.4%) classification, as well as C6 (78.5%) classification, assigned the element to *Pan*.

Although fossil hominins are not the focus of this study, classification results for A.L. 288-1 (AH and AK) indicated good classification with significant model fit. In the case with element AH, previously determined as T6, the classification for the sample, as *Homo* with IFA and IVAPA variables was incorrect. Element AK differs in respect to previously determined vertebral placement as L2 or L3. Analysis for L2 classifies the element as *Pan* with an IVAPA variable. L3 classifies the element as *Homo* with PICP and IFA variables. Similar misclassifications were observable for specimen A.L. 333 x-12, which was assumed to be T10 and therefore classified as *Gorilla*. A.L. 333 106, assumed to be either C5 or C6, was identified as *Pan*.

Fossil hominin results and interpretation have a few caveats: (1) an insufficient number of hominin samples necessary for powerful statistical analyses; (2) previous element identification; and (3) incomplete vertebral columns for inter-regional and intra-regional analyses. Interpretation for A. L. 288-1 results suggest that element AH (T6) is *Homo*-like, based on inferior facet variables. Also, the element AK is most likely L3, since it is more *Homo*-like than the *Pan*-like L2, which contains PICP and IFA variables. Results and interpretation of this study would be in agreement with previous research (Cook et al. 1983; McHenry and Temerin 1979; Meyer et al. 2015), but based on different approaches.

The fact that those elements for either A.L. 333 x–12 or A.L. 333 106 would have *Gorilla/Pan* features, respectively, is highly improbable. Interpretation for A.L. 333 x–12 and A.L. 333 106 vertebral elements suggests three possible scenarios: (1) different species, (2) incorrect identification for vertebral positioning due to the lack of complete vertebral columns, and (3) fossil condition. Incorrect vertebral identification and fossil condition are the most probable explanations for the results, so in order to infer locomotion, a larger sample size needs to be examined or additional fossil vertebrae (Chapter 2) of the same species need to be available.

6.7 Results and interpretation: An integrated synthesis

Individual test results (Chapter 5) and their respective interpretations presented in this section generate some knowledge; however, interpretation of the combined results may give a glimpse into the abstract nature of and greater insights into the vertebral column. Each vertebra is considered to be a single component within a series of regional vertebrae and the vertebral column as a whole. The attributes of each vertebra must reflect subtle differences in morphology to provide individual vertebral integrity and regional stability for weight distribution within the two-three-pillar concept. Spinal stability is essential within each positional-locomotory complex. Results from this research (Chapter 5) indicated that the variables SFA, SFPA, IFA, IFPA, SVAPA, IVAPA, SFID, IIFD, PICP, CPBA, and Area contribute to distinguishing vertebrae across the three primary taxa considered. Additional variables RT, RTCR, TTR, RTTR, TLR, RTLR, TTC, and TLC give further discernment. Figure 6.2 illustrates significant variables and their correlations within the pillar concept. It is critical to note the importance regarding articular facet angles, vertebro-articular facet angles, and vertebral body height within the column concept. Statistically significant differences among species indicate not only metrics, but also differences in positional-locomotory complexes.

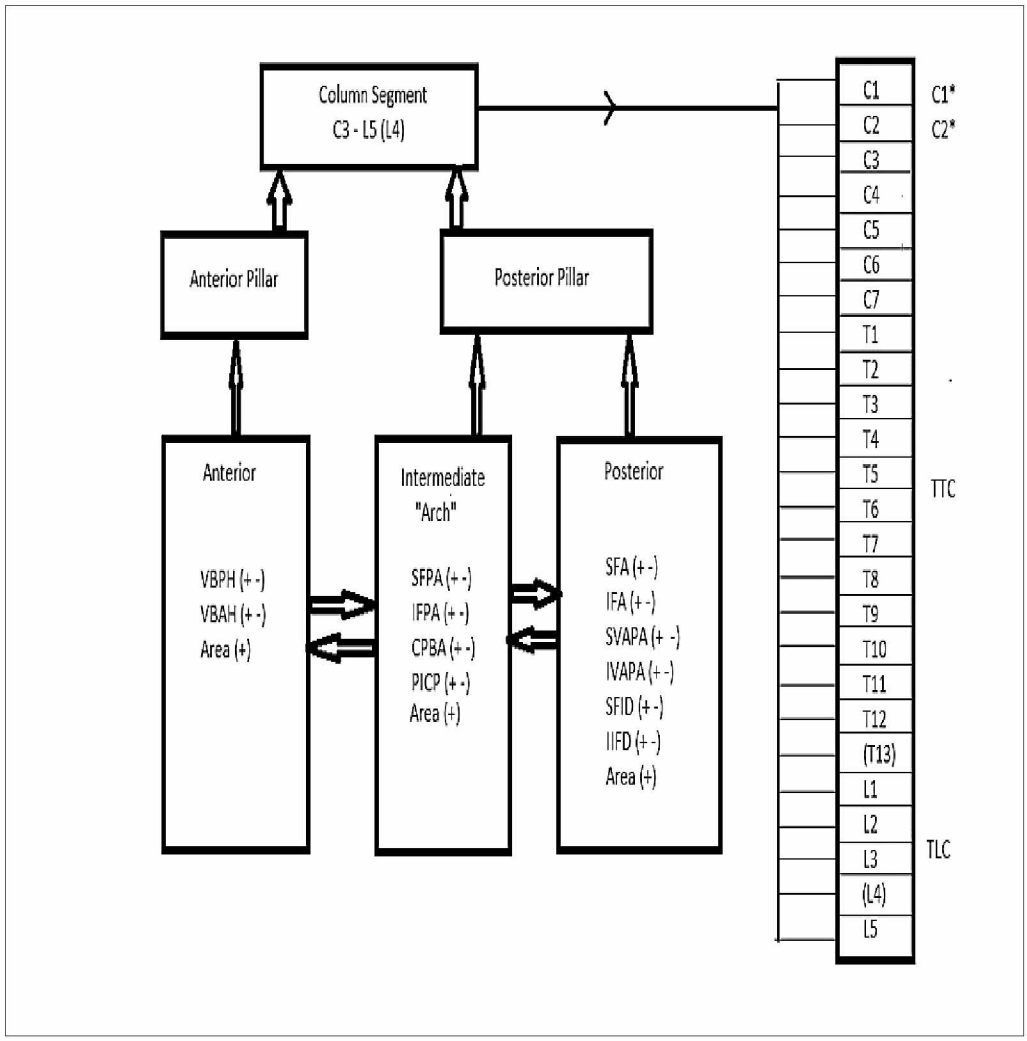

Figure 6.2. Variable integration, segment to vertebral column.
* Denotes cranium to column transitional zone

For each vertebra, the anterior (corpus) is assumed to be one pillar. The posterior (facets) converge from the two pillars to a single pillar via the "intermediate" or connective arch. Just as vertebral height is specifically related to the corpus, facet angles are related to the arch. This intermediate arch links them together by projected angles, pedicle angle, and projected facet angle as they relate to the coronal plane of the vertebral body. Furthermore, vertebral area unites and is common to all three pillars. Lastly, synchronicity among VBAH, VBPH, SFID, and IIFD indicates stability among the pillars.

As the vertebral corpus (pillar) increases sequentially in size caudally toward the sacrum, corpus height also increases with lateral interfacet distance (pillars) caudally, as indicated by the variable

Area. Simultaneously, the orientation of the facets to the coronal and sagittal planes changes their direction per vertebral element. Whereas facet angle, SFA, and IFA anchor adjacent vertebrae within curvature, the simultaneous anchoring at the vertebro-articular angles, e.g., SVAPA and IVAPA, sets one point to accentuate rotation via adjacent vertebrae. This intermediate arch variable, primarily the pedicle, also incorporates SFPA, IFPA, and CPBA variables that transcend only the pedicle. The combination of the posterior arch and this intermediate arch gives the vertebra or segment its place within the vertebral column (Fig. 6.2). Any differences between the angles located at the arch versus those angles measured at the corpus captures arch distortion in reference to pedicle angle and adjacent body angle. This observation is important due to the relationship of weight distribution to COM for both bipeds and knuckle-walkers. This distribution of significant variables among ventral (corpus), intermediate (pedicle and projected facet), and dorsal (facet) depicts the three-pillar concept. Clearly, differences exist among all taxa, not only in distribution, but also between negative and positive correlations (Appendix I, Tables I-1 – I-3).

Furthermore, when comparing regional breakpoints to restriction (Table 6.2), vertebral segments match or fall near those variables considered "intermediate" between pillars for *Homo*, *Gorilla*, and *Pan*. The comparison of breakpoints to overall general patterns presents noticeable overall differences between *Gorilla* and *Pan*. This pattern is an important indication for homoplasy found between the two species.

Distinctions are apparent in the results themselves and as depicted within the pillar concept. Statistical differences exist between the individual pair-wise comparisons in greater median values among all paired taxa. A further distinction in differences is observable within the context related to significant correlations at the level of individual vertebral element. These positive and negative correlations for SFA, SFPA, IFA, and IFPA variables differ among taxa as they relate to the anterior or ventral pillar (corpus) and the intermediate categories. No discernible pattern exists among negative and positive correlations, but speculation is that another structure will compensate for the structural failing of another. All regional vertebrae and calculated summed variables interact as one segment that provides regional curvature and rotational restriction in reference to the positional-locomotory complex. The differences between the positional-locomotory complex and vertebral curvature among taxa are evident. Some possible commonalities can link these

aspects together. In Figure 6.3, the exploratory variables used in this study within the three pillar concept depict this possibility.

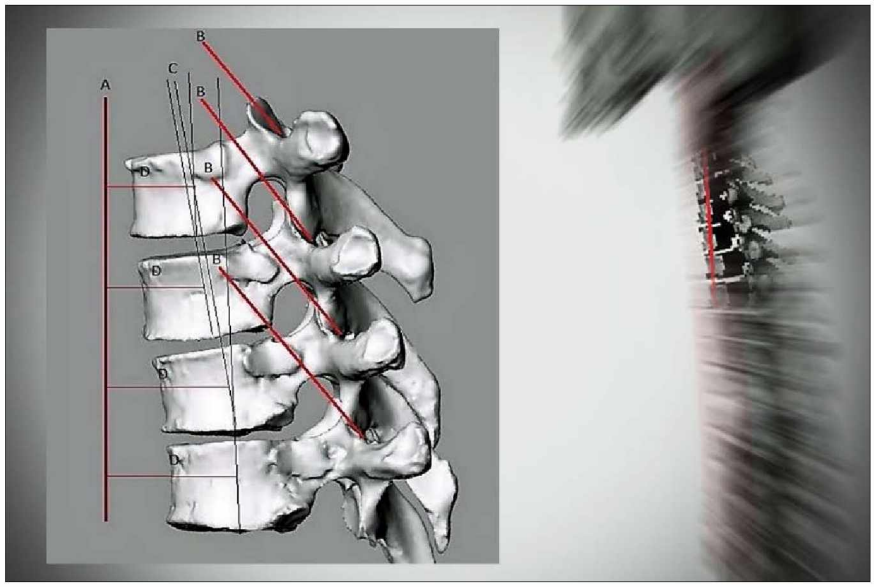

Figure 6.3. Curvature as related to the center of mass (COM) in *Homo*.
Scan**:** Cleveland Museum of Natural History Hamann-Todd Osteological Collection. Legend: (A) Center of mass (COM) from the cranial base; (B) superior facet angle and projected angle – SFA and SFPA; (C) adjacent body angle (CPBA); and (D) distance between the center of the vertebral body and COM.

As depicted in Figure 6.3, the superior facet angle and projected angle, adjacent vertebral body angle, and vertebro-articular angle would be comparable among *Homo*, *Pan*, and *Gorilla* when considering the distance to the center of mass. However, exhibited differences in the distance between the center of the vertebral body and the center of mass outside the vertebra (COM) would differ due to the position of the column to the substrate, e.g., bipedal and quadrupedal. Any similarities between facet angle and adjacent body angle among taxa would yield similar distance measurements from the center of each vertebra to the center of mass. Speculation points that this variation would explain the inconsistent vertebral variables that are significant. This view has additional support. Since vertebral rotation has an influence on spinal curvature (including curvature on rotation) as depicted by previous researchers (Kouwenhoven et al. 2006; Kozanek et al. 2009; Lee et al. 2004), speculation emerges that the amount of rotational restriction, as indicated

by vertebro-articular angle (SVAPA and IVAPA variables) would have limits. These limits include (1) facet and vertebral body angle, (2) the distance of COM, and (3) reinforcement by soft tissue. This scenario would explain not only similarities and differences in this research but also explain previous results as they pertain to the cranium and vertebral column (Clauser 1980; Legaye and Duval-Beaupere 2008; Lieberman et al. 2000; Pal et al. 2001; Shapiro 1990). This scenario would also extend to locomotion (Ahlborn 2004; Childress and Gard 2006; Kimura 1996; Raichlen et al. 2009; Stern et al. 2004).

At this point, identification of individual vertebra within all regions, with possible inference to pseudo-curvature and related locomotory gait, is far from conclusive. The significant differences, misclassifications, and inconsistent correlations reported in this study, within the contextual framework, are a starting point to a universal mathematical principle to determine individual vertebra and its related segment curvature. Nevertheless, interpretation of the evidence gives some credence to the hypothesis that taxon can be determined by morphological variations of the cranial base and cervical, thoracic, and lumbar vertebrae, as depicted within the samples used in this research.

6.8 Implications for the emergence of bipedalism

Based on physical evidence and some speculation, the discovery of fossil hominins in Africa suggested that the blending of morphological features depicts a mosaic of primate features within evolutionary descent (McHenry 1982; McHenry 1994; McHenry and Coffing 2000; McHenry and Skelton 1985) with morphological characteristics that indicate habitual or obligate bipedalism. As suggested by the evidence, *Homo sapiens* is not unique when it comes to bipedal locomotion. Common explanations include environment (Kingston 2007; Niemitz 2010; Potts 1998; Vrba 1995), thermal regulation (Wheeler 1991), and energetics (Pontzer et al. 2014; Rodman and McHenry 1980; Steudel 1996). Theories based on similarities among nonhuman primates include knuckle-walkers (Begun 2004; Richmond et al. 2001), brachiation (Richmond et al. 2001; Senut 2006; Thorpe and Crompton 2006), and climbers (Fleagle et al. 1981; Gebo 1989). Other theories include posture, display, food transport, and the aquatic ape (Hardy 1960; Hewes 1961; Jablonski and Chaplin 1993; Morgan 1997; Walter 2004; Wang and Crompton 2004; Wescott 1967a; Wescott 1967b). Additional theories emphasize reproduction and nascense (Gallup and Suarez 1983; Leutenegger 1981; Trevathan 1996).

Whereas the above explanations encompass a wide range of evidence, the results of this study do not conform to any particular explanation. If commonalities exist that would indicate descent, the expectation is that one set or perhaps two common measurements would be apparent in one or many species through time. This expectation regarding common measurements is certainly not the case, as the results of this research indicate. Currently, the evidence limits interpretation to the blending of nonhuman primate osteological features exhibited by the human species with distinguished cranial base flexion and vertebral curvature. Thus, the consideration of several theories would explain that the emergence of human bipedalism is very likely and that other attributes associated with remaining theories are accidental.

Chapter 7. Summary and conclusion

Determining whether the morphology of the cranial base and vertebrae can differentiate between taxa and their attendant primary mode of locomotion was the main objective of this research. The approach to answering this overarching research question considered the cranium and each subsequent vertebra within the vertebral column as a single integrated functional unit among three primary taxa: *Homo*, *Gorilla*, and *Pan*. Three specific aims were necessary to achieve the answer to this research question.

An investigation to identify key traits of the cranial base, individual vertebrae, and spinal curvature in human and extant nonhuman primates accomplished the first specific aim. The second aim investigated the use of variables to identify the positional-locomotory complex. The final aim applied fossil hominins to the same criteria used in the study of *Homo*, *Pan*, and *Gorilla* to determine speciation. The results presented in Chapter 5 indicated that cranial base, vertebrae, and subsequent curvature could indeed differentiate between the primary taxa considered in this research. Objectives and specific aims led to specific answers posed in research question.

The first specific aim investigated and identified key traits of the cranial base angle, individual vertebrae, and spinal curvature in human and extant nonhuman hominines. The overall rationale for the variables included three assumptions: (1) quadrant divisions yield more information per variable for each skeletal element and the vertebral column as a whole; (2) an integrated nature of each variable may be found within each vertebra; and (3) the elimination of soft tissue, e.g., vertebral disc and facet joints, from the analyses does not affect vertebral column integration adversely. In light of these criteria, two related questions explored the expression of sexual dimorphism in the vertebrae with the three taxa and considered the use of vertebralmetrics to correctly classify taxa with an acceptably high rate of accuracy among members of the three taxa.

The differences among vertebrae results allowed for sex estimation within taxa. Results from the Mann-Whitney U-tests, using size-adjusted variables, indicated that all taxa exhibited differences between males and females. Consequently, the null hypothesis was rejected. Statistically significant differences were identified between males and females among all taxa. However, the lack of regional or cross-regional continuity among variables, excluding area, indicates that no common variable trend served to estimate sex across the three taxa.

Pooled samples circumvent this trend of no common variable for sex estimation, which then provided observable differences between and among species. Results for Kruskal-Wallis H-tests indicated statistically significant differences across taxa throughout the vertebral column. Consequently, the null hypothesis was rejected. The distribution of significant variables was observable throughout the column without any discernible pattern. *Post hoc* Mann-Whitney U-tests determined exact differences among taxa. Results for the contrasts between *Homo* and *Gorilla* identified statistically significant differences at each vertebra. The pair-wise contrast between *Homo* and *Pan* yielded similar results. Every vertebra had similar significant variables throughout the vertebral column except for the thoracic region. The thoracic region contained more vertebral body variables toward the lower end of its region. Lastly, the pair-wise contrast between *Pan* and *Gorilla* yielded statistically significant variables for each vertebra within the vertebral column.

Furthermore, results from multinomial logistic regression (MLR) indicated correct classification. Each model fit correctly depicted the data and was significant. Thus, the null was rejected. Classification rate was sufficient for each vertebra throughout the vertebral column (Appendix H, Tables H-1 – H-30). Differences within variable significance throughout the vertebral column were explained by the *post hoc* Spearman's rho results which indicated significant correlative differences between variables across taxa. These differences aligned with classification variables.

The test results pertaining to vertebral variables, cranial base angle, and curvature also provided a means for differentiating individuals of different taxa. The results obtained with MLR indicated an overall high correct classification rate (86.4%) with significant model fit for CBA. Curvature, with an 80.3% correct classification rate, had similar significance and model fit with the TTC and TLC regions. Additionally, results for *post hoc* Spearman's rho indicated no significant correlation between CBA and each segment curvature for *Homo* and *Gorilla*. *Pan* was the only species that indicates a significant positive correlation between CBA and TLC variables. With these results, the documentation of key traits of the cranial base angle, individual vertebra, and curvature achieved the first goal and specific aim.

The second specific aim – to investigate the use of variables to identify the positional-locomotory complex – was phrased as the question whether the cranial base and vertebral curvature can delineate and classify the positional-locomotory complex of a species.

Kruskal-Wallis H-tests indicated a statistically significant difference across taxa with associated positional-locomotory complexes among CBA, TTC, and TLC variables. Thus, the null hypothesis was rejected. Differences existed among all three taxa. Additional *post hoc* Mann-Whitney U-tests identified statistically significant differences between $Biped_H$ and both knuckle-walkers – $Knuckle\text{-}walk_G$ and $Knuckle\text{-}walk_P$. MLR results confirmed the Kruskal-Wallis tests. Overall, correct classification by locomotory category was 86.4% for CBA and 80.3% for curvature with TTC and TLC variables. Both models were significant for model fit.

In addition, two additional *post hoc* tests yielded further support using different variables. Mann-Whitney U-test results indicated that TTR, RTTR, and RLTR were significant between $Biped_H$ and $Knuckle\text{-}walk_P$. Similar statistical significance was observable between these two locomotory categories with the addition of RTCR and LTR variables. Only RTCR and RTTR were statistically significant between the two forms of knuckle-walking ($Knuckle\text{-}walk_G$, $Knuckle\text{-}walk_P$). Furthermore, the MLR results for CPBA variables depicted a high correct classification rate with significant model fit for cervical (70.7%), thoracic (86.3%), and lumbar (70.9%) regions. These results were consistent with previous results, except for the cervical region. Additional *post hoc* tests confirmed the assumptions regarding the integrated nature of vertebrae throughout the vertebral column. These results led to achieving the second goal and specific aim.

The third specific aim sought to provide potential insight into the vertebral similarities found in early hominins and the evolution of bipedality. Classification results for A.L. 288-1 (AH and AK) indicated good classification with significant model fit. In the case with element AH, previously determined as T6, the classification of the sample as *Homo* with IFA and IVAPA variables was incorrect. Element AK differs in respect to previously determined vertebral placement as L2 or L3. Analysis for L2 classifies the element as *Pan* with an IVAPA variable, and L3 classifies the element as *Homo* with PICP and IFA variables. Similar misclassifications were observable for specimen A.L. 333 x-12, assumed to be T10 and therefore classified as *Gorilla*. A.L. 333 106, assumed to be either C5 or C6, was identified as *Pan*.

Interpretation of the evidence reflected the assumption that each vertebra is a single component embedded within a series of regional vertebrae and part of a vertebral column as a whole. Each vertebra must reflect subtle morphological differences to provide individual vertebral integrity and regional stability for weight distribution, both essential for posture and locomotion. Key variables

SFA, SFPA, IFA, IFPA, SVAPA, IVAPA, SFID, IIFD, PICP, CPBA, and Area contribute to distinguishing vertebrae across taxa. Additional variables RT, RTCR, TTR, RTTR, TLR, RTLR, TTC, and TLC provide additional discernment among significant variables and correlations within the pillar concept. The evidence obtained and the interpretation of that evidence is not without limitations. For example, statistical differences regarding greater median values among all possible pair-wise contrasts between taxa also differ within the context related to statistically significant correlations at the vertebral level. Positive and negative correlations for SFA, SFPA, IFA, and IFPA variables differ among taxa in relation to the ventral pillar (corpus) and the intermediate categories with no discernible pattern. All variables acting as one segment within the pillar context (Fig. 6.2), together with the calculated summed variables TTC, TLC, TTR, RTTR, TLR, and RLTR, provide regional curvature and rotational restriction as those variables pertain to the positional-locomotory complex. These observations achieved the final aim and goal.

The interpretation of the significant results for all tests satisfied the specific aims and goals, providing an answer to the overarching research question. In addition to this achievement, the methods used in this study indicated some potential usefulness for paleontological applications. Prior evidence for human evolutionary descent with the emergence of paralleled forms of bipedal gait is acceptable when compared to both the morphology and the positional-locomotory complex of extant nonhuman primates. Different focal points and interpretations among the blended morphological traits between humans and extant nonhuman primates lead to theoretical obfuscation for the origins of bipedality (Chapter 2). In the examination of the pillar concept (Chapter 6) in relation to COM for posture and locomotion, the evidence collected for this study, with the stated caveats, indicates agreement with a common knuckle-walking ancestor. However, even though everything indicates agreement with human and extant nonhuman primates, the scarcity and condition of fossil vertebral elements at this point should not be the sole source for information regarding speciation and the positional-locomotory complex. Perhaps the significant differences, misclassifications, and inconsistent correlations reported in this study, within the context of the pillar concept, will serve as a starting point to a mathematical formula to determine the unique position of an individual vertebra, its contribution to segment curvature, and its relevance to speciation and the positional-locomotory complex.

Though inconclusive, this research ascertained the following: (1) differences in vertebral measurements occur between males and females among species, (2) differences in vertebral measurements occur among species and provide a basis for classification, and (3) differences exist among cranial base angle, total thoracic curvature, and total lumbar curvature among taxon. These differences include references to the positional-locomotory complex for each taxon. However, the number of misclassifications indicated these variables were poor predictors for either classification. Overall, the data suggest that both vertebral corpus dimensions and coronal and sagittal facet orientation differ significantly among hominine taxa and the positional-locomotory complexes. Inferences from the data conclude that the complex integration among the cranium and vertebrae indicates an unknown variable is influencing the number of significant variables for each skeletal element as related to their respective taxa and positional-locomotory complex.

7.1 Final observations and future research

For the biological anthropologist, morphology and its implications for evolutionary descent face epistemological problems, as illustrated in other branches of science (Dougherty 2009; Feyerabend 1981; McKelvey 2002; Moore and Sanders 2006). Perception is critical - more so when considering an integration of objects, e.g., vertebrae, or when examining elements that are fragmented. Differences in perception and comprehension are exemplified in trait selection, measurements, and subsequent result interpretation as depicted by various researchers (Ahern 2005; Barbera et al. 2009; Clauser 1980; Dean and Wood 1981; Lieberman and McCarthy 1999; Luboga and Wood 1990; Oxnard 1998; Panjabi et al. 1991a; Panjabi et al. 1993a; Panjabi et al. 1991b; Strait and Ross 1999). In this aspect, this research is not different. What does distinguish this research is the unique perspective revealed by utilizing scanning technology and CAD software, which allows for measurements that are not possible using other traditional methods. Consequently, results and interpretation (Chapters 5 and 6) described the phenomena of the cranial base, cervical vertebrae, thoracic vertebrae, and lumbar vertebrae in terms of a structural framework, providing important preliminary answers that demonstrate merit.

Important key measurements revealed in this research involve the discriminatory power of the articular facet orientation. This revelation is evident due to high MLR classification results. The primacy of these measurements is above interfacet distance, vertebral body height measurements,

and in most cases – overall vertebral area. These important key measurements contribute to the overall importance of the study.

The overall importance of this study is three-fold. First, the cranial base angle, as indicated by the orientation of the foramen magnum to the Frankfurt Horizon, is significant but inconsistent and suggests the lack of landmarks in determining cranial base orientation. It is important to note the contributing factors in determining the orientation of the foramen magnum for future research. Using the foramen magnum orientation alone is a poor proxy to distinguish anterior from posterior placement on the occipital bone.

Second, vertebral variables are significant between males and females and significant among taxa. The diversity of significant variables at the vertebral and regional level are greater than previously reported by past research. In terms of dimorphism, differences are not size orientated. Despite differences within species, differences among species present thought-provoking results. Although *Homo* differs vastly from either *Pan* or *Gorilla*, it is important to note the differences between *Pan* and *Gorilla*. Such differences found within each vertebral measurement suite throughout the vertebral column suggest homoplastic features that resulted in the evolution of two forms of knuckle-walking. Significant results from this study and results from previous researchers (Begun 2004; Kivell et al. 2009; Richmond et al. 2001) support this conclusion.

Lastly, curvature and rotation depicted significant difference among taxa for their positional-locomotory complexes. The importance resides in not only the ability to distinguish but also the measurement and calculation of variables in the absence of soft tissue. The approach, which was successful to varying degrees, depicted the vertebral column within three-dimensional space via measurements of the articulating facet orientation in six directions individually and four directions regionally.

Contributing to the importance of this research, the practical merit and value as illustrated were due to several factors. First is the ability to positively assess variables for discriminatory value. Differences in measurements are beyond size measurement alone. Variations were found among facet angles and distance. Second, these differences, which allow for the ability to identify patterns, suggest uniqueness within and among species. Lastly, results indicate the capacity to reject medically-accepted homogeneity of vertebral measurements and spinal curvature. Additionally, the ability to quantify previously-assumed relationships between cranial flexion and spinal

curvature and determine a distinction between curvature and positional-locomotory complex has added value.

Future research

Future research should continue to include a comprehensive approach to the study of both the cranial base and the complete vertebral column. Beyond the need for an ever-growing sample size that would increase statistical power and simultaneously reduce the possibility of Type I or Type II errors, medical-grade equipment would prove beneficial. The use of advanced computerized tomography (CT) or computerized axial tomography (CAT) scans would allow the incorporation of soft tissue and perhaps provide more accurate skeletal integrated measurements (Gilsanz et al. 1994; Glocker et al. 2012; Göçen et al. 1999; Ho et al. 1993). Future research, following the approach established in this study, may shed greater insight on the cranial base, vertebral column, and vertebral curvature. Possible inquiries are as follows:

Cranium

Refinement in the quantification of the cranial base angle is necessary. Evidence suggests two alternative approaches. In addition to the retained cranial base plane and Frankfort Horizon, a vertical plane placed at the apex of basion could depict differences in the coronal plane. This reference plane was not under consideration in this research. The second approach would be to retain the occipital base plane and to use the average from the Frankfurt Horizon and Krogman-Walker planes (Barbera et al. 2009), with a vertical plane based at the apex of the basion. The additional planes will create alternative angles, in which one value (a true CBA) might negate the anterior or posterior placement of the foramen magnum and provide a better assessment of the cranium and C1 articulation.

Vertebrae

In addition to the vertebral measurements suggested within this study, additional variables should include vertebral canal dimensions, as well as the calculation of vertebral canal area and vertebral body area, which can be used to compute the complete vertebral area ratio. The suggestion that the added variables will provide additional discriminative power both within and among vertebra is alluded to by previous researchers (Clauser 1980; Latimer and Ward 1993; Panjabi et al. 1991a; Panjabi et al. 1993a; Panjabi et al. 1991b; Rose 1975; Shapiro 1993). However, the combination

of several variables used in a mathematical formula, which takes into account the complex interrelationships among vertebrae, would serve both to distinguish among taxa as well as to differentiate between males and females within a species. Quantifying and reducing variables to a single mathematical value remains a plausible possibility.

Curvature

As suggested by results obtained in this study (Chapter 5), quantification of regional spinal curvature through the use of CPBA variables should expand to include morphological analyses with and without the presence of soft tissue. It is possible that such an explorative approach will yield a patterned difference or a ratio that might provide a critical link and a better method to determine approximate curvature than vertebral morphology alone, e.g., a corrected CPBA value that considers IVD, superior/inferior articular joints, and rib articulations. Furthermore, as indicated by previous research (Adams et al. 1986; Adams et al. 1996; Fazzalari et al. 2001; Keller et al. 2005), the inclusion of additional variables that capture the distribution of weight within the IVD discs per individual may also prove to be informative. Theoretically, the numerical value would bridge the gap between the presence and absence of soft tissue.

Cranial base, vertebrae, and spinal curvature

Within an integrated and synthetic analytical framework, speculation includes that the CBA, individual vertebrae, and curvature values yield greater discrimination within and among taxa. In addition to greater classification accuracies, correlations among elements ought to be greater than those reported in this study. Furthermore, future research can be expanded to include skeletal elements outside the vertebral column. Progressive analyses should include the sacrum, orientation and dimensions of the iliac blades, and acetabulum, femoral neck, and tibial plateau angles.

Relevancy for anthropology and related disciplines

The importance of this research for anthropology resides in the ability to distinguish vertebrae within and among species. Consequently, this method's ability has profound implications for determining evolutionary descent (in conjunction with other methods), positional-locomotory complexes, and to an extent – cultural influences, e.g., behavior influencing vertebral curvature. Furthermore, benefits from this research can extend to anatomy, biology, biomechanics, forensics, medicine, and osteology.

In conclusion, this research endeavor explored morphological distinctions among the cranial base, cervical vertebrae, thoracic vertebrae, and lumbar vertebrae among primate taxa as possible indicators to elucidate skeletal differences associated with different primary modes of posturo-locomotory practiced by extant primates. Through the exploration of the morphology of the cranial base and vertebral column, variables were created to illustrate both skeletal element structure and its subsequent integration. Whereas some variables were similar to those employed by previous researchers (Chapter 4.3), other calculated variables provided additional insight. Inferences drawn from the statistical evidence suggest that the selected variables within this research are more viable than those used in previous studies. Differences between this and previous research regarding significant results are not contradictory or contrary; rather, its difference in perspective gives a glimpse into individual phenomena and their unforeseen implications as a whole. Thus, the direction of future research should be toward the goal of a comprehensive and integrated approach.

References

Abdi H, and Williams LJ. 2010. Principal component analysis. Wiley Interdisciplinary Reviews: Computational Statistics 2(4):433-459.

Adams M, Dolan P, and Hutton W. 1986. The stages of disc degeneration as revealed by discograms. J Bone Joint Surg (Br) 68(1):36-41.

Adams M, McNally D, and Dolan P. 1996. 'Stress' distributions inside intervertebral discs. J Bone Joint Surg (Br) 78B (6):965-972.

Ahern JC. 2005. Foramen magnum position variation in Pan troglodytes, Plio-Pleistocene hominids, and recent Homo sapiens: implications for recognizing the earliest hominids. American Journal of Physical Anthropology 127:267-276.

Ahlborn BK. 2004. Zoological physics: quantitative models of body design, action, and physical limitations of animals. New York: Springer.

Aiello L, and Dean C. 2002. An introduction to human evolutionary anatomy. New York: Academic Press.

Aiello L, and Wells J. 2002. Energetics and the evolution of the genus Homo. Annual Review of Anthropology 31:323-338.

Alexander RM. 2003. Principles of animal locomotion. New Jersey: Princeton University Press.

Alfarno ME, Bolnick DI, and Wainwright PC. 2004. Evolutionary dynamics of complex biomechanical systems: an example using the four-bar mechanism. Evolution 58(3):495-503.

Amaral L. 1996. Loss of body hair, bipedality and thermoregulation. Comments on recent papers in the Journal of Human Evolution. Journal of Human Evolution 30:357-366.

Andriacchi T, Schultz AH, Belytschko T, and Galante J. 1974. A model for studies of the mechanical interactions between the human spine and rib cage. Journal of Biomechanics 7:497-507.

Ankel-Simons F. 2006. Primate anatomy: an introduction. Burlington, MA, USA: Academic Press.

Ankel F. 1972. Vertebral morphology of fossil and extant primates. The functional and evolutionary biology of primates. Chicago: Aldine Atherton. p 223-240.

Ashton EH. 1981. Primate locomotion: some problems in analysis and interpretation. Philosophical Transactions of the Royal Society of London, Series B, Biological Sciences 292(1057):77-87.

Associates RM. 2016. Rhinoceros 5.0. 5.0 ed. p Rhinoceros.

Badoux DM. 1968. Some notes on the curvature of the vertebral column in vertebrates with special reference to mammals. Acta morph neerl-scand 7:29-40.

Badoux DM. 1974. Introduction to biomechanical principles in primate locomotion and structure. In: F J, editor. Primate locomotion. New York: Academic Press.

Barbera AL, Sampson WJ, and Townsend GC. 2009. An evaluation of head position and craniofacial reference line variation. Homo 60:1-28.

Barr A, and Bear-Lehman J. 2001. Biomechanics of the wrist and hand. In: Nordin M, and Frankel V, editors. Basic biomechanics of the musculoskeletal system. Baltimore: Lippincott Williams & Wilkins. p 358-389.

Bass W. 2005. Human Osteology: a laboratory and field manual. Columbia: Missouri Archaeological Society.

Bastir M, Higuero A, Ríos L, and García Martínez D. 2014. Three-dimensional analysis of sexual dimorphism in human thoracic vertebrae: implications for the respiratory system and spine morphology. American Journal of Physical Anthropology 155(4):513-521.

Bauer HR. 1977. Chimpanzee bipedal locomotion in the Gombe National Park, East Africa. Primates 18(4):913-921.

Begun D. 2004. Knuckle-walking and the origin of human bipedalism. In: Meldrum D, and Hilton C, editors. From biped to strider: the emergence of modern human walking, running, and resource transport. New York: Kluwer Academic/Plenum Publishers. p 9-33.

Benjamin M, and Evans EJ. 1990. Research review: fibrocartilage. J Anat 171:1-15.

Benton R. 1967. Morphological evidence for adaptations within the epaxial region of primates. In: F vdH, editor. The baboon medical research. Austin: University of Texas Press. p 201-216.

Berger LR. 2012. Australopithecus sediba and the earliest origins of the genus Homo. Journal of Anthropological Sciences 90:117-131.

Berger LR, de Ruiter DJ, Churchill SE, Schmid P, Carlson KJ, Dirks PHGM, and Kibii JM. 2010. Australopithecus Sediba: a new species of Homo-Like australopith from South Africa. Science 328(5975):195-204.

Bertram JEA. 2004. New perspectives on brachiation mechanics. Yearbook of Physical Anthropology S39:100-117.

Biewener AA. 1990. Biomechanics of mammalian terrestrial locomotion. Science, New Series 250(4984):1097-1103.

Billmann F, Le Minor J-M, and Steinwachs M. 2007. Bipartition of the superior articular facets of the first cervical vertebra (atlas or C1): a human variant probably specific among primates. Annals of Anatomy 189:79-85.

Bilsborough A, and Rae T. 2007. Hominid cranial diversity and adaptation. In: W H, and I T, editors. Handbook of paleoanthropology. Berlin: Springer. p 1031-1105.

Bloch J, and Boyer D. 2002. Grasping primate origins. Science, New Series 298(5598):1606-1610.

Blue K, McCrossin M, and Benefit B. 2006. Terrestriality in Middle Miocene context: Victoriapithecus from Maboko, Kenya. Human origins and environmental backgrounds. New York: Springer. p 45-58.

Bogduk N, and Mercer S. 2000. Biomechanics of the cervical spine. I. Normal kinematics. Clinical Biomechanics 15:633-648.

Bonduriansky R. 2007. Sexual selection and allometry: a critical reappraisal of the evidence and ideas. Evolution 61(4):838-849.

Boszczyk B, Boszczyk A, and Putz R. 2001. Comparative and functional anatomy of the mammalian lumbar spine. The Anatomical Record 264:157-168.

Bouvier M. 1985. Application of in vivo bone strain measurement techniques to problems of skeletal adaptations. Yearbook of Physical Anthropology 28:237-248.

Boyd SK, and Nigg B. 2007. Bone. In: Nigg B, and Herzog W, editors. Biomechanics of the musculo-skeletal system. England: John Wiley & Sons Ltd. p 65-95.

Boyle JJ, Milne N, and Singer KP. 2002. Influence of age on cervicothoracic spinal curvature: an ex vivo radiographic survey. Clinical Biomechanics 17(5):361-367.

Briggs A, Greig A, Wark J, Fazzalari N, and Bennell K. 2004. A review of anatomical and mechanical factors affecting vertebral body integrity. International Journal of Medical Sciences 1:170-180.

Bruner E. 2007. Cranial shape and size variation in human evolution: structural and functional perspectives. Child's Nervous System 23(12):1357-1365.

Brunet M, Guy F, Pilbeam D, Lieberman D, Likius A, Taisso Mackaye H, Ponce de Leon M, Zollikofer C, and Vignaud P. 2005. New material of the earliest hominid from the Upper Miocene of Chad. Nature 434:752-755.

Brunet M, Guy F, Pilbeam D, Taisso Mackaye H, Likius A, Ahounta D, Beauvilain A, Blondel C, Bocherens H, Boisserie J-R et al. 2002. A new hominid from the Upper Miocene of Chad, Central Africa. Nature 418:145-151.

Bruno AG, Anderson DE, D'Agostino J, and Bouxsein ML. 2012. The effect of thoracic kyphosis and sagittal plane alignment on vertebral compressive loading. Journal of Bone and Mineral Research 27(10):2144-2151.

Buss D. 1999. Evolutionary Psychology: The new science of the mind. Needham Heights: Allyn & Bacon.

Burton F. 1995. The multimedia guide to the non-human primates. Ontario Prentice Hall.

Butler D, Trafimow J, Andersson G, McNeill T, and Huckman M. 1990. Discs degenerate before facets. Spine 15(2):111-113.

Chaplin G, Jablonski NG, and Cable NT. 1994. Physiology, thermoregulation and bipedalism. Journal of Human Evolution 27(6):497-510.

Childress D, and Gard S. 2006. Commentaries on the six determinants of gait. In: Rose J, and Gamble JG, editors. Human walking. New York: Lippincott Williams and Wilkins. p 19-21.

Christensen DM, Eastlack RK, Lynch JJ, Yaszemski MJ, and Currier BL. 2007. C1 anatomy and dimensions relative to lateral mass screw replacement. Spine 32(8):844-848.

Christiansen P. 2002. Locomotion in terrestrial mammals: the influence of body mass, limb length and bone proportions on speed. Zoological Journal of the Linnean Society 136:685-714.

Churchill SE, Holliday TW, Carlson KJ, Jashashvili T, Macias ME, Mathews S, Sparling TL, Schmid P, De Ruiter DJ, and Berger LR. 2013. The upper limb of Australopithecus sediba. Science 340(6129):1233477.

Clauser DA. 1980. Functional and comparative anatomy of the primate spinal column: some locomotor and postural adaptations. Milwaukee: University of Wisconsin.

Conroy GC. 2005. Reconstructing human origins. New York: WW Norton.

Cook D. 2007. Fisher lecture: dimension reduction in Regression. Statistical Science 22(1):1-26.

Cook DC, Buikstra JE, DeRousseau CJ, and Johanson DC. 1983. Vertebral pathology in the Afar australopithecines. American Journal of Physical Anthropology 60:83-101.

Cooper RG, Hollis S, and Jayson M. 1992. Gender variations of human spinal and paraspinal structure. Clinical Biomechanics 7:120-124.

Corballis M. 1991. The Lopsided Ape: Evolution of the generative mind. New York: Oxford University Press.

Corballis M. 1999. Phylogeny from apes to humans. In: Corballis, and Lea, editors. The Descent of Mind: Psychological Perspectives on Hominid Evolution. New York: Oxford University Press.

Corruccini RS. 1978. Primate skeletal allometry and hominid evolution. Evolution 32(4):752-758.

Corruccini RS, and McHenry H. 1980. Cladometric analysis of Pliocene hominids. Journal of Human Evolution 9:209-221.

Corruccini RS, and McHenry HM. 2001. Knuckle-walking hominid ancestors. Journal of Human Evolution 40(6):507-511.

Costigan T. 2005. Bonferroni inequalities and intervals. Encyclopedia of Biostatistics: John Wiley & Sons, Ltd.

Cotton JR, Zioupos P, Winwood K, and Taylor M. 2003. Analysis of creep strain during tensile fatigue of cortical bone. Journal of Biomechanics 36:943-949.

Cowin SC. 1986. Wolff's law of trabecular architecture at remodeling equilibrium. Journal of Biomechanical Engineering 108:83-88.

Cowin SC. 1989a. Mechanical materials. In: Cowin SC, editor. Bone Mechanics. Boca Raton: CRC Press. p 15-42.

Cowin SC. 1989b. The mechanical properties of cancellous bone. In: Cowin SC, editor. Bone Mechanics. Boca Raton: CRC Press. p 129-157.

Crompton R, Thorpe S, Weijie W, Yu L, Payne RC, Savage R, Carey T, Aerts P, Van Elsacker L, Hofstetter A et al. 2003. The biomechanical evolution of erect bipedality. In: Franzen J, Kohler M, and Moya-Sola S, editors. Walking Upright. Bad, Homburg v.d. H: CFS. p 135-146.

Crompton R, Vereecke E, and Thorpe S. 2008. Locomotion and posture from the common hominoid ancestor to fully modern hominins, with special reference to the last common panin/hominin ancestor. Journal of Anatomy 212:501-543.

Crompton R, Yu L, Weijie W, Gunther M, and Savage R. 1998. The mechanical effectiveness of erect and "bent-hip, bent-knee" bipedal walking in Australopithecus afarensis. Journal of Human Evolution 35:55-74.

Crompton RH, Sellers WI, and Thorpe SK. 2010. Arboreality, terrestriality and bipedalism. Philosophical Transactions of the Royal Society of London B: Biological Sciences 365(1556):3301-3314.

D'Aout KD, Vereecke E, Schoonaert K, De Clercq D, Elsacker L, and Aerts P. 2004. Locomotion in bonobos (*Pan paniscus*): differences and similarities between bipedal and quadrapedal terrestrial walking, and a comparison with other locomotor modes. Journal of Anatomy 204:353-361.

Dainton M, and Macho G. 1999. Did knuckle-walking evolve twice? Journal of Human Evolution 36:171-194.

Danforth CH. 1930. Numerical variation and homologies in vertebrae. American Journal of Physical Anthropology 14(3):463-481.

Dansereau J, and Stokes IA. 1988. Measurements of the three-dimensional shape of the rib cage. Journal of Biomechanics 21(11):893-901.

Darroch J, and Mosimann J. 1985. Canonical and principal components of shape. Biometrika 72(2):241-252.

Darwin C. 1859. On the origin of species. London: Murray.

Darwin C. 1871. The descent of man. London: John Murray.

Davis PR. 1955. The thoraco-lumbar mortice joint. Journal of Anatomy 89:370-377.

Davis PR. 1961. The thoraco-lumbar mortice joint in West Africans. Journal of Anatomy 95:589-593.

Davis RB, DeLuca PA, and Ounpuu S. 2003. Analysis of Gait. In: Schneck DJ, and Bronzino JD, editors. Biomechanics: principles and applications. Boca Raton: CRC Press. p 131-139.

Day M. 1969. Femoral fragment of a robust Australopithecine from Olduvai Gorge, Tanzania. Nature 221:230-233.

Day M. 1985. Hominid locomotion- From Taung to the Laetoli footprint. Hominid evolution: past, present and future: proceedings of the Taung Diamond Jubilee International Symposium, Johannesburg, and Mmabatho, Southern Africa, 27th January-4th February 1985. New York: Liss. p 115-127.

Dean M, and Wood B. 1982. Basial anatomy of Plio-Pleistocene hominids from East and South Africa. American Journal of Physical Anthropology 59:157-174.

Dean MC, and Wood BA. 1981. Metrical analysis of the basicranium of extant hominoids and Australopithecus. American Journal of Physical Anthropology 54:63-71.

Degraff K, and Stuart F. 1986. Concepts of human anatomy and physiology. Iowa: Wm. Brown Publishers.

deMenocal PB. 2004. African climate change and faunal evolution during the Pliocene–Pleistocene. Earth and Planetary Science Letters 220(1-2):3-24.

deMenocal PB, and Bloemendal J. 1995. Plio-Pleistocene climatic variability in subtropical Africa and the paleoenvironment of hominid evolution: a combined data-model approach. Paleoclimate and evolution with emphasis on human origins. New Haven: Yale University Press. p 262-288.

deSilva JM, Holt KG, Churchill SE, Carlson KJ, Walker CS, Zipfel B, and Berger LR. 2013. The lower limb and mechanics of walking in Australopithecus sediba. Science 340(6129):1232999.

Dietrich S, and Kessel M. 1997. The vertebral column. In: Thorogood P, editor. Embryos, Genes, and Birth Defects. New York: J. Wiley. p 281-302.

Dombrowski SC, Gischlar KL, Mrazik M, and Greer III FW. 2011. Feral Children. Assessing and treating low incidence/high severity psychological disorders of childhood: Springer. p 81-93.

Doran D. 1997. Ontogeny of locomotion in mountain gorillas and chimpanzees. Journal of Human Evolution 32:323-344.

Dougherty ER. 2009. Translational science: epistemology and the investigative process. Current Genomics 10(2):102-109.

Drerup B. 1984. Principles of measurement of vertebral rotation from frontal projections of the pedicles. Journal of Biomechanics 17(12):923-935.

Duan Y, Seeman E, and Turner C. 2001. The biomechanical basis of vertebral body fragility in men and women. Journal of Bone and Mineral Research 16(12):2276-2283.

El-Habil AM. 2012. An application on multinomial logistic regression model. Pakistan Journal of Statistics & Operation Research 8(2):271-291.

Etnier S. 2001. Flexural and torsional stiffness in multi-jointed biological means. Biol Bull 200:1-8.

Falk D, Redmond JC, Guyer J, Conroy C, Recheis W, Weber GW, and Seidler H. 2000. Early hominid brain evolution: a new look at old endocasts. Journal of Human Evolution 38(5):695-717.

Farber P. 2000. Finding order in nature: the naturalist tradition from Linnaeus to E.O. Wilson. Baltimore: John Hopkins University Press.

Fazzalari N, Manthey B, and Parkkinson I. 2001. Intervertebral disc disorganization and its relationship to age-adjusted vertebral body morphology and vertebral bone architecture. The Anatomical Record 262:331-339.

Feyerabend P. 1981. Realism, rationalism, and scientific method. New York: Cambridge University Press

Field A. 2009. Discovering Statistics Using SPSS. Thousand Oaks: SAGE.

Fitzpatrick RC, Butler JE, and Day B. 2006. Resolving head rotation for human bipedalism. Current Biology 16:1509-1514.

Fleagle J. 1998. Primate adaptation and evolution. NY: Academic Press.

Fleagle J. 2000. The century of the past: one hundred years in the study of primate evolution. Evolutionary Anthropology: Issues, News, and Reviews 9(2):87-100.

Fleagle J, Gilbert C, and Baden A. 2010. Primate cranial diversity. American Journal of Physical Anthropology 142:565-578.

Fleagle J, Stern J, Jungers W, and Susman R. 1981. Climbing: A biomechanical link with brachiation and with bipedalism. Symp Zool Soc London 48:359-375.

Fleagle JG. 2013. Primate adaptation and evolution: Academic Press.

Francis C. 1955a. Variations in the articular facets of the cervical vertebrae. The Anatomical Record 122(4):589-602.

Francis CC. 1955b. Dimensions of the cervical vertebrae. The Anatomical Record 122(4):603-609.

Frankel V, and Nordin M. 2001. Biomechanics of bone. In: Nordin M, and Frankel V, editors. Basic biomechanics of the musculoskeletal system. Baltimore: Lippinscott Williams & Wilkins. p 27-58.

Franz T, Demes B, and Carlson K. 2005. Gait mechanics of lemurid primates on terrestrial and arboreal substrates. Journal of Human Evolution 48:199-217.

Freudenstein JV. 2005. Characters, states, and homology. Systematic Biology 54(6):965-973.

Friedman A. 2006. Important determinants of bone strength. Journal of Clinical Rheumatology 12(2):70-77.

Frobin W, Leivseth G, Biggemann M, and Brinckmann P. 2002. Vertebral height, disc height, posteroanterior displacement and dens-atlas gap in the cervical spine: precision measurements protocol and normal data. Clinical Biomechanics 17:423-431.

Gal JM. 1993. Mammalian spinal biomechanics. Journal of Experimental Biology 174:247-280.

Galik K, Senut B, Pickford M, Gommery D, Treil J, Kuperavage AJ, and Eckhardt RB. 2004. External and internal morphology of the BAR 1002'00 Orrorin tugenensis femur. Science 305(5689):1250-1253.

Gallup GG, and Suarez SD. 1983. Optimal reproductive strategies for bipedalism. Journal of Human Evolution 12:193-196.

Gangnet N, Pomero V, Dumas R, Skalli W, and Vital J. 2003. Variability of the spine and pelvis location with respect to the gravity line: a three-dimensional steroradiographic study using force platform. Surgical and Radiologic Anatomy 25:424-433.

Garvin H, and Ruff C. 2012. Sexual dimorphism in skeletal browridges and chin morphologies determined using a new qantitative method. American Journal of Physical Anthropology 147(4):661-670.

Gebo DL. 1989. Locomotor and phylogenetic considerations in anthropoid evolution. Journal of Human Evolution 18:201-233.

Gibbons A. 2002. In search of the first hominids. Science, New Series 295(5558):1214-1219.

Gibson KR, Gibson KR, and Ingold T. 1994. Tools, language and cognition in human evolution: Cambridge University Press.

Gilsanz V, Boechat MI, Gilsanz R, Loro ML, Roe TF, and Goodman WG. 1994. Gender differences in vertebral sizes in adults: biomechanical implications. Radiology 190:678-682.

Glocker B, Feulner J, Criminisi A, Haynor DR, and Konukoglu E. 2012. Automatic localization and identification of vertebrae in arbitrary field-of-view CT scans. Medical image computing and computer-assisted intervention–MICCAI 2012: Springer. p 590-598.

Göçen S, Havitçioğlu H, and Alici E. 1999. A new method to measure vertebral rotation from CT scans. European Spine Journal 8(4):261-265.

Goel V, and Clausen J. 1998. Prediction of load-sharing among spinal components of the C5-C6 motion segment using the finite element approach. Spine 23(6):684-691.

Goeman JJ, and Cessie Sl. 2006. A Goodness-of-Fit Test for Multinomial Logistic Regression. Biometrics 62(4):980-985.

Gomez-Olivencia A, Carretero JM, Arsuaga JL, Rodriguez-Garcia L, Garcia-Gonzalez R, and Martinez I. 2007. Metric and morphological study of the upper cervical spine from the Sima de los Huesos site (Sierra de Atapuerca, Burgos, Spain). Journal of Human Evolution 53:6-25.

Gommery D. 2000. Superior cervical vertebrae of a Miocene hominoid and a Pilo-Pleistocene hominid from South Africa. Palaeont Afr 36:139-145.

Gommery D. 2006. Evolution of the vertebral column in Miocene hominoids and Plio-Pleistocene hominids. In: Ishida H, Tuttle R, Pickford M, Ogihara N, and Nakatsukasa M, editors. Human origins and environmental backgrounds. Berlin: Springer.

Goto K, Tajima N, Chosa E, Totoribe K, Kuroki H, Arizumi Y, and Arai T. 2002. Mechanical analysis of the lumbar vertebrae in a three-dimensional finite element method model in which intradiscal pressure in the nucleus pulposus was used to establish the model. Journal of Orthopaedic Science 7(2):243-246.

Gould SJ. 1966. Allometry and size in ontogeny and phylogeny. Biological Reviews 41:587-640.

Granata KP, and Bennett B. 2005. Low-back biomechanics and static stability during isometric pushing. Human Factors 47(3):536-549.

Granata KP, and Wilson SE. 2001. Trunk posture and spinal stability. Clinical Biomechanics 16:650-659.

Grausz H, Leakey R, Walker A, and Ward C. 1988. Associated cranial and postcranial bones of Australopithecus boisei. In: Grine F, editor. Evolutionary history of 'robust' australopithecines. New York: Aldine de Grugter. p 127-132.

Gray H. 1995. Anatomy: descriptive and surgical. New York: Barnes and Nobel.

Graybeal A. 1998. Is it better to add taxa or characters to a difficult phylogenetic problem? Systematic Biology 48:9-17.

Groves C. 2001. Primate Taxonomy. Washington: Smithsonian.

Guy F, Liberman D, Pilbeam D, Ponce De Leon M, Likius A, Mackaye H, Vignaud P, Zollikofer C, and Brunet M. 2005. Morphological affinities of Sahelanthropus tchadensis (Late Miocene hominid form Chad). Proceedings of the National Academy of Sciences of the United States of America 102(52):18836-18841.

Haeusler M, Martelli S, and Boeni T. 2002. Vertebrae numbers of early hominid lumbar spine. Journal of Human Evolution 43:621-643.

Haile-Selassie Y. 2001. Late Miocene hominids from the Middle Awash, Ethiopia. Nature 412:178-181.

Haile-Selassie Y, Latimer BM, Alene M, Deino AL, Gibert L, Melillo SM, Saylor BZ, Scott GR, and Lovejoy CO. 2010. An early Australopithecus afarensis postcranium from Woranso-Mille, Ethiopia. Proceedings of the National Academy of Sciences of the United States of America 107(27):12121-12126.

Hall BK. 2007. Homoplasy and homology: Dichotomy or continuum? Journal of Human Evolution 52(5):473-479.

Harcourt-Smith WEH. 2007. The origins of bipedal locomotion. Handbook of paleoanthropology. Berlin: Springer. p 1483-1518.

Harcourt-Smith WEH, and Aiello D. 2004. Fossils, feet, and the evolution of human bipedal locomotion. Journal of Anatomy 204:403-416.

Hardy A. 1960. Was man more aquatic in the past? The New Scientist 7:642-645.

Harrison DD, Janik TJ, Troyanovich SJ, and Holland B. 1996. Comparisons of lordotic cervical spine curvatures to a theoretical ideal model of the static sagittal cervical spine. Spine 21(6):667-675.

Hawkins JA. 2000. A survey of primary homology assessment: different workers perceive and define characters in different ways. In: Scotland RW, and Pennington RT, editors. Homology and systematics: coding characters for phylogenetic analysis. London: Taylor and Francis. p 22-53.

Hayes KC, Winter DA, and Norman RW. 1977. Energetics of bipedal locomotion. Yearbook of Physical Anthropology 20:481-490.

Herzog W. 2007a. Muscle. In: Nigg B, and Herzog W, editors. Biomechanics of the musculo-skeletal system. London: John Wiley & Sons Ltd. p 169-225.

Herzog W. 2007b. Tendons/Aponeurosis. In: Nigg B, and Herzog W, editors. Biomechanics of the musculo-skeletal system. London: John Wiley & Sons Ltd. p 146-168.

Herzog W, and Federico S. 2007. Articular Cartilage. In: Nigg B, and Herzog W, editors. Biomechanics of the musculo-skeletal system. London: John Whiley & Sons Ltd. p 95-122.

Hewes GW. 1961. Food transport and the origins of bipedalism. American Anthropologist, New Series 63(4):687-710.

Hildebrand M. 1967. Systematic gaits of primates. American Journal of Physical Anthropology 26:119-130.

Hirasaki E, Ogihara N, Hamada Y, Kumakura H, and Nakatsukasa M. 2004. Do highly trained monkeys walk like humans? a kinematic study of bipedal locomotion in bipedally trained Japanese macaques. Journal of Human Evolution 46:739-750.

Ho EK, Upadhyay S, FL Chan D, Hsu L, and Leong J. 1993. New methods of measuring vertebral rotation from computed tomographic scans: an intraobserver and interobserver study on girls with scoliosis. Spine 18(9):1173-1177.

Ho SY, Phillips MJ, Cooper A, and Drummond AJ. 2005. Time dependency of molecular rate estimates and systematic overestimation of recent divergence times. Molecular Biology and Evolution 22(7):1561-1568.

Holloway RL. 1966. Cranial capacity, neural reorganization, and hominid evolution: a search for more suitable parameters. American Anthropologist 68(1):103-121.

Humzah MD, and Soames RW. 1988. Human intervertebral disc: structure and function. The Anatomical Record 220:337-356.

Hunt K. 1994. The evolution of human bipedality: ecology and functional morphology. Journal of Human Evolution 26:183-202.

Hunt K, Cant JGH, Gebo DL, Rose MD, Walker SE, and Youlatos D. 1996. Standardized description of primate locomotor and postural modes. Primates 37(4):363-387.

Hurov J. 1985. Monkey locomotion during gait transition: how do interlimb time intervals, step sequences, and kinematics change? American Journal of Physical Anthropology 66:417-427.

Inman V, Ralston H, and Todd F. 2006. Human Locomotion. In: Rose J, and Gamble JG, editors. Human Walking. New York: Lippincott Williams and Wilkens. p 1-18.

Ishii T, Mukai Y, Hosono N, Sakaura H, Fujii R, Nakajima Y, Tamura S, Iwasaki M, Yoshikawa H, and Sugamoto K. 2006. Kinematics of the Cervical Spine in lateral bending. Spine 31(2):155-160.

Isler K. 2005. 3D-kinematics of vertical climbing in hominoids. American Journal of Physical Anthropology 126(1):66-81.

Jablonski N, and Chaplin G. 2004. Becoming bipedal: how do theories of bipedalization stand up to anatomical scrutiny? In: Anapol, German, and Jablonski, editors. Shaping primate evolution: form, function, and behavior. New York: Cambridge University Press. p 281-296.

Jablonski NG, and Chaplin G. 1993. Origin of habitual terrestrial bipedalism in the ancestor of Hominidae. Journal of Human Evolution 24:259-280.

Jellema LM, Latimer B, and Walker A. 1993. The rib cage. Cambridge, MA: Harvard University Press. p 294-325

Jenkins F. 1972. Chimpanzee bipedalism: cineradiographic analysis and implications of the evolution of gait. Science 178:877-879.

Jenkins F. 1974. Primate locomotion. New York: Academic Press.

Jungers W. 1984. Aspects of size and scaling in primate biology with special reference to the locomotor skeleton. Yearbook of Physical Anthropology 27:73-97.

Jungers W, Falsetti A, and Wall C. 1995. Shape, relative size, and size-adjustments in morphometrics. Yearbook of Physical Anthropology(38):137-161.

Katz P, Reynolds H, Foust D, and Baum J. 1975. Mid-sagittal dimensions of cervical vertebral bodies. American Journal of Physical Anthropology 43:319-326.

Keith A. 1902. The extent to which the posterior segments of the body have been transmuted and suppressed in the evolution of man and allied primates. Journal of Anatomy and Physiology 37(Pt 1):18.

Keith A. 1903. The extent to which the posterior segments of the body have been transmuted and suppressed in the evolution of man and allied primates. Journal of Anatomy and Physiology 37:18-40.

Keller T, Colloca C, Harrison DE, Harrison DD, and Janik T. 2005. Influence of spine morphology on intervertebral disc loads and stresses in asymptomatic adults: implications for the ideal spine. The Spine Journal 5:297-309.

Kidd R, and Oxnard CE. 2005. Little foot and big thoughts- a re-evaluation of the Stw 573 foot from Sterkfontein, South Africa. Homo 55:189-212.

Kim M. 2016. Scanner Accuracy. In: Lukaszek DA, editor.

Kimura T. 1985. Bipedal and quadrupedal walking of primates. In: Kondo S, editor. Primate morphophysiology, locomotor analyses, and human bipedalism. Tokyo: University of Tokyo Press. p 81-104.

Kimura T. 1996. Center of gravity of the body during ontogeny of primate bipedal walking. Folia Primatologica 66(1-4):126-136.

Kingston JD. 2007. Shifting adaptive landscapes: progress and challenges in reconstructing early hominid environments. Yearbook of Physical Anthropology 50:20-58.

Kivell TL, Schmitt D, and Walker A. 2009. Independent evolution of knuckle-walking in African apes shows that humans did not evolve from a knuckle-walking ancestor. Proceedings of the National Academy of Sciences of the United States of America 106(34):14241-14246.

Kopperdahl D, Pearlman J, and Keaveny TM. 2000. Biomechanical consequences of an isolated overload on the human vertebral body. Journal of Orthopaedic Research 18:685-690.

Kouwenhoven J-WM, Vincken KL, Bartels LW, and Castelein RM. 2006. Analysis of preexistent vertebral rotation in the normal spine. Spine 31(13):1467-1472.

Kozanek M, Wang S, Passias PG, Xia Q, Li G, Bono CM, Wood KB, and Li G. 2009. Range of motion and orientation of the lumbar facet joints in vivo. Spine 34(19):E689-E696.

Kuzminsky S, and Gardiner M. 2012. Three dimensional laser scanning: potential uses for museum conservation and scientific research. Journal of Archaeological Science 39:2744-2751.

Lanyon LE. 1990. The relationship between functional loading and bone architecture. Primate life history and evolution. London: Wiley-Liss. p 269-284.

Latimer B, and Ward C. 1993. The thoracic and lumbar vertebrae. In: Walker A, and Leakey R, editors. Nariokotome Homo Erectus Skeleton Cambridge: Harvard University Press. p 266-293.

Leakey LSB. 1966. Homo habilis, Homo erectus and the Australopithecines. Nature 209(5030):1279-1281.

Leakey M, and Walker A. 2003. Early hominid fossils from Africa. Scientific American Special Edition 13(2):14-19.

Lee S-M, Suk S-I, and Chung E-R. 2004. Direct vertebral rotation: a new technique of three-dimensional deformity correction with segmental pedicle screw fixation in adolescent idiopathic scoliosis. Spine 29(3):343-349.

Legaye J, and Duval-Beaupere G. 2008. Gravitational forces and sagittal shape of the spine. International Orthopaedics 32(6):809-816.

Legrand E, Chappard D, Pascaretti C, Duquenne M, Krebs S, Rohmer V, Basle M, and Audran M. 2000. Trabecular bone microarchitecture, bone minderal density, and vertebral fractures in male osteoporosis. Journal of Bone and Mineral Research 15(1):13-19.

Leroy G. 2011. Conducting multiple comparisons. Designing User Studies in Informatics: Springer London. p 125-130.

Leutenegger W. 1981. Encephalization and obstetrics in primates with particular reference to human evolution. In: Armstrong E, and Falk D, editors. Primate brain evolution: methods and concepts. New York: Plenum. p 85-92.

Lieber RL. 1993. Skeletal muscle mechanics: implications for rehabilitation. Physical Therapy 73(12):844-856.

Lieberman DE, Hallgrímsson B, Wei L, Parsons TE, and Jamniczky HA. 2008. Spatial packing, cranial base angulation, and craniofacial shape variation in the mammalian skull: testing a new model using mice. Journal of Anatomy 212(6):720-735.

Lieberman DE, and McCarthy RC. 1999. The ontogeny of cranial base angulation in humans and chimpanzees and its implications for reconstructing pharyngeal dimensions. Journal of Human Evolution 36(5):487-517.

Lieberman DE, Ross C, and Ravosa M. 2000. The primate cranial base: ontogeny, function, and integration. Yearbook of Physical Anthropology 43:117-169.

Liem K, Singh MD, and Kecskemethy A. 2005. Analysis of vertebral motion with computer simulation using elementary contact pairs. PAMM 5:207-208.

Linden JCvd, Birkenhager-Frenkel DH, Verhaar JAN, and Weinans H. 2001. Trabecular bone's mechanical properties are affected by its non-uniform mineral distribution. Journal of Biomechanics 34:1573-1580.

Lleonart J, Salat J, and Torres G. 2000. Removing allometric effects of body size in morphological analysis. Journal of Theoretical Biology 205:85.93.

Lorenz T, and Campello M. 2001. Biomechanics of skeletal muscle. In: Nordin M, and Frankel V, editors. Basic biomechanics of the musculoskeletal system. Baltimore: Lippincott Williams & Wilkins. p 149-174.

Louis R. 1985. Spinal stability as defined by the three-column spine concept. Anatomical Clin 7:33-42.

Lovejoy CO, Johanson DC, and Coppens Y. 1982. Elements of the axial skeleton recovered from the Hadar formation: 1974-1977 collections. American Journal of Physical Anthropology 57:631-635.

Luboga SA, and Wood BA. 1990. Position and orientation of the foramen magnum in higher primates. American Journal of Physical Anthropology 81(1):67-76.

Mallau S, Bollini G, Jouve J-L, and Assaiante C. 2007. Locomotor skills and balance strategies in adolescents idiopathic scoliosis. Spine 32(1):E14-E22.

Manfreda E, Mitteroceker P, Bookstein F, and Schaefer K. 2006. Functional morphology of the first cervical vertebra in humans and nonhuman primates. The Anatomical Record 289B:184-194.

Manzon VS, Hohenstein UT, and Gualdi-Russo E. 2012. Injuries on a skull from Ancient Bronze Age (Ballabio, Lecco, Italy): a natural or an anthropic origin? Journal of Archaeological Science 39:3428-3455.

Marino E. 1995. Sex estimating using the first cervical vertebra. American Journal of Physical Anthropology 97:127-133.

Masharawi Y, Rothschild B, Dar G, Peleg S, Robinson D, Been E, and Hershkovitz I. 2004. Facet orientation in the thoracolumbar spine: three-dimensional anatomic and biomechanical analysis. Spine 29(16):1755-1763.

Matarazzo S. 2008. Knuckle-walking signal in the manual digits of Pan and Gorilla. American Journal of Physical Anthropology 135(1):27-33.

Maus H-M, Lipfert S, Gross M, Rummel J, and Seyfarth A. 2010. Upright human gait did not provide a major mechanical challenge for our ancestors. Nature Communications 1:70.

McCarthy RC. 2001. Anthropoid cranial base architecture and scaling relationships. Journal of Human Evolution 40:41-66.

McCollum M, Rosenman B, and Suwa G. 2010. The vertebral formula of the last common ancestor of the African apes and humans. J Exp Zool Part B 314B:123-134.

McGowan C. 1999. A practical guide to vertebrate mechanics. Cambridge Cambridge University Press.

McHenry H. 1982. The pattern of human evolution: studies on bipedalism, mastication, and encephalization. Annual Review of Anthropology 11:151-173.

McHenry H. 1986. The first bipeds: a comparison of the A. afarensis and A. africanus postcranium and implications for the evolution of bipedalism. Journal of Human Evolution 15:177-191.

McHenry H. 1991. First steps? Analysis of the postcranium of early hominids. Origine(s) de la bipedie chez les hominideds. Paris: CNRS. p 133-141.

McHenry H. 1994. Tempo and mode in human evolution. Proceedings of the National Academy of Sciences of the United States of America 91:6780-6786.

McHenry H. 2002. Introduction to the fossil record of human ancestry. In: Hartwig W, editor. The Primate fossil record. New York: Cambridge University Press. p 401-405.

McHenry H, and Coffing K. 2000. Australopithecus to Homo: transformations in body and mind. Annual Review of Anthropology 29:125-146.

McHenry H, and Skelton R. 1985. Is Australopithecus africanus ancestral to Homo? In: Tobias P, editor. Hominid evolution: past, present and future. New York: Alan Liss.

McHenry H, and Temerin A. 1979. The evolution of hominid bipedalism: evidence from the fossil record. Yearbook of Physical Anthropology 22:105-131.

McKelvey B. 2002. Model-centered organization science epistemology. Companion to Organizations:752-780.

McNally D, Adams M, and Goodship A. 1993. Can intervertebral disc prolapse be predicted by disc mechanics. Spine 18(11):1525-1530.

McNeil MC, Polloway EA, and Smith JD. 1984. Feral and isolated children: historical review and analysis. Education and training of the mentally retarded:70-79.

Meyer MR, Williams SA, Smith MP, and Sawyer GJ. 2015. Lucy's back: Reassessment of fossils associated with the AL 288-1 vertebral column. Journal of Human Evolution 85:174-180.

Miyakoshi N, Hongo M, Maekawa S, Ishikawa Y, Shimada Y, and Itoi E. 2007. Back extensor strength and lumbar spinal mobility are predictors of quality of life in patients with postmenopausal osteoporosis. Osteoporosis International 18(10):1397-1403.

Moore HL, and Sanders T. 2006. Anthropology and epistemology. Anthropology in theory: issues in epistemology:1-21.

Morgan E. 1997. The aquatic ape theory: the most credible theory of human evolution. London: Souvenir Press

Mosimann J. 1970. Allometry: size and shape variables with characterizations of lognormal and generalized Gamma distributions. Journal of the American Statistical Association 65(330):930-945.

Mosimann J, and James F. 1979. New statistical method for allometry with applications to Florida Red-Winged Blackbirds. Evolution 33(1):444-459.

Moskovich R. 2001. Biomechanics of the cervical spine. In: Nordin M, and Frankel V, editors. Basic biomechanics of the musculoskeletal system. Baltimore: Lippincott Williams & Wilkins. p 286-317.

Mow V, and Hung C. 2001. Biomechanics of articular cartilage. In: Nordin M, and Frankel V, editors. Basic biomechanics of the musculoskeletal system. Baltimore: Lippincott Williams & Wilkins. p 61-100.

Naderi S, Andalkar N, and Benzel E. 2006. History of spine biomechanics: Part I - the Pre-Greco-Roman, Greco-Roman, and medieval roots of spine biomechanics. Neurosurgery 60(2):382-391.

Naderi S, Andalkar N, and Benzel E. 2007. History of spine biomechanics: Part II - from the Renaissance to the 20th Century. Neurosurgery 60(2):392-404.

Nakatsukasa M, Hirasaki E, and Ogihara N. 2006. Locomotor energetics in non-human primates: a review of recent studies on bipedal performing macaques. In: Nakatsukasa, Hirasaki, and Ogihara N, editors. Human origins and environmental backgrounds. Berlin: Springer. p 157-166.

Nakatsukasa M, Pickford M, Egi N, and Senut B. 2007. Femur length, body mass, and stature estimates of Orrorin tugenensis, a 6 Ma hominid from Kenya. Primates 48:171-178.

Neaux D, Guy F, Gilissen E, Coudyzer W, and Ducrocq S. 2013. Covariation between midline cranial base, lateral basicranium, and face in modern humans and chimpanzees: a 3D geometric morphometric analysis. The Anatomical Record 296(4):568-579.

Nevell L, and Wood B. 2008. Cranial base evolution within the hominin clade. Journal of Anatomy 212:445-468.

Niemitz C. 2010. The evolution of the upright posture and gait—a review and a new synthesis. Naturwissenschaften 97(3):241-263.

Nigg B. 2007a. Measuring techniques. In: Nigg B, and Herzog W, editors. Biomechanics of the musculo-skeletal system. Chichester: John Wiley & Sons. p 293-310.

Nigg B, and Herzog W. 2007. Biological Materials. In: Nigg B, and Herzog W, editors. Biomechanics of the musculo-skeletal system. England: John Wiley & Sons Ltd. p 49-64.

Nigg BM. 2007b. Internal properties of the human or animal body. In: Nigg BM, and Herzog W, editors. Biomechanics of the musculo-skeletal system. England: John Wiley and Sons LTD. p 453-475.

Nordin M, Lorenz T, and Campello M. 2001. Biomechanics of tendons and ligaments. In: Nordin M, and Frankel V, editors. Basic biomechanics of the musculoskeletal system. Baltimore: Lippincott Williams & Wilkins. p 102-125.

Norkin C, and White D. 2009a. The cervical spine. Measurement of Joint Motion: A Guide to goniometry. Philadelphia: F. A. Davis Company. p 319-363.

Norkin C, and White D. 2009b. The thoracic and lumbar spine. Measurement of Joint Motion: A Guide to Goniometry. Philadelphia: F. A. Davis Company. p 365-407.

Norkin CC, and White DJ. 2009c. Measurement of Joint Motion. Philadelphia: F. A. Davis Company.

Okada M. 2006. The prehominid locomotion reflected: energetics, muscles, and generalized bipeds. In: Pickford, Tuttle, Ogihara N, Nakatsukasa, and Hirasaki, editors. Human origins and environmental backgrounds. Berlin: Springer. p 225-233.

Oliwenstein L. 1995. New foot steps into walking debate. Science 269:476-477.

Oxnard C. 1973. Functional inferences from morphometrics: problems posed by uniqueness and diversity among primates. Systematic Zoology 22(4):409-424.

Oxnard C. 1998. The information content of morphometric data in primates: function, development, and evolution. In: O'Higgins P, editor. Primate locomotion: recent advances. New York: Plenum Press. p 255-275.

Oxnard C. 2000. Morphometrics of the primate skeleton and the functional and developmental underpinnings of species diversity. In: O'Higgins P, editor. Development, growth, and evolution. London: Academic Press. p 235-264.

Oxnard C. 2004. Design, level, interface, and complexity: morphometric interpretation revisited. In: Anapol, German, and Jablonski, editors. Shaping primate evolution: form, function, and behavior. New York: Cambridge University Press. p 391-414.

Pal G, Routal R, and Saggu S. 2001. The orientation of the articular facets of the zygapophyseal joints at the cervical and upper thoracic region. Journal of Anatomy 198(04):431-441.

Pal GP, and Routal RV. 1986. A study of weight transmission through the cervical and upper thoracic regions of the vertebral column in man. Journal of Anatomy 148:245-261.

Pal GP, and Routal RV. 1991. Relationship between the articular surface area of a bone and the magnitude of stress passing through it. The Anatomical Record 230:570-574.

Panjabi M, Chen NC, Shin EK, and Wang J. 2001. The cortical shell architecture of the human Cervical Vertebral bodies. Spine 26(22):2478-2484.

Panjabi M, Krag MH, Dimnet JC, Walter SD, and Brand R. 1984. Thoracic spine centers of rotation in the sagittal plane. Journal of Orthopaedic Research 1:387-394.

Panjabi MM, Duranceau J, Goel V, Oxland T, and Takata K. 1991a. Cervical human vertebrae- quantitative three dimensional anatomy of the middle and lower regions. Spine 16(861-869).

Panjabi MM, Goel V, Oxland T, Takata K, Duranceau J, and Krag M. 1993a. Human lumbar vertebrae- quantitative three dimensional anatomy. Spine 17:299-306.

Panjabi MM, Oxland T, Takata K, Goel V, Duranceau J, and Krag M. 1993b. Articular facets of the human spine- quantitative three dimensional anatomy. Spine 18:1298-1310.

Panjabi MM, Takata K, Goel V, Federico D, Oxland T, Duranceau J, and Krag M. 1991b. Thoracic human vertebrae- quantitative three dimensional anatomy. Spine 16:888-901.

Perelman P, Johnson WE, Roos C, Seuánez HN, Horvath JE, Moreira MA, Kessing B, Pontius J, Roelke M, and Rumpler Y. 2011. A molecular phylogeny of living primates. PLoS Genet 7(3):e1001342.

Pickford M. 2006. Paleoenvironments, paleoecology, adaptations, and the origins of bipedalism in Hominidae. In: Pickford, Tuttle, Ogihara N, Nakatsukasa, and Hirasaki, editors. Human origin and environmental background. Berlin: Springer. p 175-198.

Pickford M, and Senut B. 2001. "Millennium Ancestor", a 6-million-year-old bipedal hominid from Kenya. South African Journal of Science 97:22.

Pickford M, Senut B, Gommery D, and Treil J. 2002. Bipedalism in Orrorin tugenesis revealed by its femora. Comptes Rendus Paleovol 1(4):191-255.

Pontzer H, Raichlen DA, and Rodman PS. 2014. Bipedal and quadrupedal locomotion in chimpanzees. Journal of Human Evolution 66:64-82.

Pontzer H, Raichlen DA, and Sockol MD. 2009. The metabolic cost of walking in humans, chimpanzees, and early hominins. Journal of Human Evolution 56(1):43-54.

Potts R. 1998. Environmental hypotheses of hominid evolution. Yearbook of Physical Anthropology 41:93-136.

Prakash LV, Prabhu VV, Saralaya VV, Pai MM, Ranade AV, Singh G, and Madhyastha S. 2007. Vertebral body integrity: a review of various anatomical factors involved in the lumbar region. Osteoporos Int 18:891-903.

Preuschoft H. 1978. Recent results concerning the biomechanics of man's acquisition of bipedality. In: Chivers DJ, and Joysey KA, editors. Recent advances in primatology. New York: Academic Press. p 435-458.

Preuschoft H. 1990. Gravity in primates and its relation to body shape and locomotion. Gravity, posture, and locomotion in primates. Firenze: Editrice II Sedicesimo. p 109-127.

Preuschoft H, and Gunther M. 1994. Biomechanics and body shape in primates compared with horses. Zeitschrift fur Morphologie und Anthropologie 80(1):149-165.

Prost JH. 1965. A definitional system for the classification of primate locomotion. American Anthropologist, New Series 67(5):1198-1214.

Purvis A, Nee S, and Harvey PH. 1995. Macroevolutionary inferences from primate phylogeny. Proceedings of the Royal Society of London B: Biological Sciences 260(1359):329-333.

Raichlen DA, Pontzer H, Shapiro LJ, and Sockol MD. 2009. Understanding hindlimb weight support in chimpanzees with implications for the evolution of primate locomotion. American Journal of Physical Anthropology 138(4):395-402.

Rannala BJ, Huelsenbeck JP, Yang Z, and Nielsen R. 1998. Taxon sampling and the accuracy of large phylogenies Systematic Biology 47:702-710.

Richard AE. 1985. Primates in nature. New York: W.H. Freeman and Company.

Richmond B, Begun D, and Strait DS. 2001. Origin of human bipedalism: the knuckle-walking hypothesis revisited. Yearbook of Physical Anthropology 44:70-105.

Richmond BG. 2006. Functional morphology of the midcarpal joint in knuckle-walkers and terrestrial quadrupeds. Human origins and environmental backgrounds. Berlin: Springer. p 105-122.

Robinson JT, Freedman L, and Sigmon BA. 1972. Some aspects of pongid and hominid bipedality. Journal of Human Evolution 1:361-369.

Rodman P, and McHenry H. 1980. Bioenergetics and the origin of hominid bipedality. American Journal of Physical Anthropology 52:103-106.

Rose MD. 1975. Functional proportions of primate lumbar vertebral bodies. Journal of Human Evolution 4:21-38.

Ross C, and Henneberg MJ. 1995. Basicranial flexion, relative brain size, and facial kyphosis in Homo sapiens and some fossil hominids. American Journal of Physical Anthropology 98:575-593.

Ruff CB, Trinkaus E, and Holliday TW. 1997. Body mass and encephalization in Pleistocene Homo. Nature 387:173-176

Ruimerman R, Hilbers P, van RB, and Huiskes R. 2005. A theoretical framework for strain-related trabecular bone maintenance and adaptation. Journal of Biomechanics 38:931-941.

Russo GA, and Kirk EC. 2013. Foramen magnum position in bipedal mammals. Journal of Human Evolution 65(5):656-670.

Sanders WJ. 1998. Comparative morphometric study of the australopithecine vertebral series Stw-H8/H41. Journal of Human Evolution 34:249-302.

Sarmiento EE. 1998. Generalized quadrupeds, committed bipeds, and the shift to open habitats: an evolutionary model of hominid divergence. New York: The American Museum of Natural History.

Scholten P, and Veldhuizen A. 1985. The influence of spinal geometry on the coupling between lateral bending and axial rotation. Engin Med 14:167-171.

Schultz A. 1953. The relative thickness of the long bones and the vertebrae in primates. American Journal of Physical Anthropology 11(3):277-311.

Schultz AH. 1938. The relative length of the regions of the spinal column in old world primates. American Journal of Physical Anthropology 24(1):1-22.

Schultz AH. 1961. Vertebral column and thorax. Primatologia 4:1-66.

Schultz AH, and Straus WL. 1945. The numbers of vertebrae in primates. Proceedings of the American Philosophical Society 89(4):601-626.

Schultz A. 1931. Man as primate. The Scientific Monthly 33(5):385-412.

Scott HJ. 1958. The cranial base. American Journal of Physical Anthropology 16(3):219-348.

Senut B. 2006. Arboreal origin of bipedalism. Human origins and environmental backgrounds. Berlin: Springer. p 199-208.

Senut B. 2007. The earliest putative hominids. In: Henke W, and Tattersall I, editors. Handbook of paleoanthropology. Berlin: Springer. p 1519-1538.

Senut B, Pickford M, Gommery D, Mein P, Cheboi K, and Coppens Y. 2001. First hominid from the Miocene (Lukeino Formation, Kenya). CR Academy of Sciences, Paris Earth and Planetary Sciences(332):137-144.

Shapiro LJ. 1990. Vertebral morphology in Hominoidea. American Journal of Physical Anthropology 81:294.

Shapiro LJ. 1991. Functional morphology of the primate spine with special reference to orthograde posture and bipedal locomotion. Stony Brook: State University of New York.

Shapiro LJ, and Simons CVM. 2002. Functional aspects if strepsirrhine lumbar vertebral bodies and spinous processes. Journal of Human Evolution 42:753-783.

Shapiro L. 1993. Functional Morphology of the vertebral column in primates. In: Gebo DL, editor. Postcranial adaptation in nonhuman primates. Illinois: Northern Illinois University Press. p 121-149.

Sholts SB, Flores L, Walker PL, and Warmlander SKTS. 2011. Comparison of coordinate measurements precision of different landmark types on human crania using a 3D laser scanner and 3D digitiser: Implications for applications of digital morphometrics. International Journal of Osteoarchaeology 21(5):535-543.

Silva MJ, Keaveny TM, and Hayes WC. 1997. Load sharing between the shell and centrum in the lumbar vertebral body. Spine 22(2):140-150.

Singer K, Jones T, and Breidahl P. 1990. A comparison of radiographic and computer-assisted measurements of thoracic and thoracolumbar sagittal curvature. Skeletal Radiology 19(1):21-26.

Skelton R, McHenry H, and Drawhorn G. 1986. Phylogenetic analysis of early hominids. Current Anthropology 27(1):21-43.

Slijper E. 1946. Comparative biologic-anatomic investigations on the vertebral column and spinal musculature of mammals. Verhandelingen der koninklijke Nederlansche Akademie von Wetenschappen, afd. Natuurkunae Tweede 42(5).

Slijper E. 1947. Observations on the vertebral column of the domestic animals. The British Veterinary Journal 103(11):376.

Smith JT, and Fernie GR. 1991. Functional biomechanics of the spine. Spine 16(10):1197-1203.

Sobelman OS, Gibeling JC, Stover SM, Hazelwood SJ, Yeh OC, Shelton DR, and Martin RB. 2004. Do microcracks decrease or increase fatigue resistance in cortical bone? Journal of Biomechanics 37:1295-1303.

Stern J, Demes B, and Kerrigan C. 2004. Modeling human walking as an inverted pendulum of varying length. In: Anapol, German, and Jablonski, editors. Shaping primate evolution: form, function, and behavior. New York: Cambridge University Press. p 297-333.

Stern Jr JT, and Susman RL. 1983. The locomotor anatomy of Australopithecus afarensis. American Journal of Physical Anthropology 60(3):279-317.

Steudel K. 1996. Morphology, bipedal gait, and the energetics of hominid locomotion. American Journal of Physical Anthropology 99:345-355.

Stokstad E. 2000. Hominid ancestors may have knuckle walked. Science, New Series 5461:2131-2132.

Stout D. 2011. Stone toolmaking and the evolution of human culture and cognition. Philosophical Transactions of the Royal Society of London B: Biological Sciences 366(1567):1050-1059.

Strait D, Grine FE, and Fleagle JG. 2007. 15 Analyzing hominid phylogeny. Handbook of paleoanthropology: Springer. p 1781-1806.

Strait DS. 2001. Integration, phylogeny, and the hominid cranial base. American Journal of Physical Anthropology 114:273-297.

Strait DS, and Ross C. 1999. Kinematic data on primate head and nect posture: implications for the evolution of basicranial flexion, and an evaluation of registration planes used in paleoanthropology. American Journal of Physical Anthropology(108):205-222.

Susman RL, Stern Jr J, and Jungers WL. 1984. Arboreality and bipedality in the Hadar hominids. Folia Primatologica 43(2-3):113-156.

Sylvester A, and Kramer P. 2008. Brief communication: stand or shuffle: When does it make energetic sense. American Journal of Physical Anthropology 135:484-488.

Sylvester AD, Kramer PA, and Jungers W. 2008. Modern humans are not (quite) isometric. American Journal of Physical Anthropology 137:371-383.

Tan SH, Teo EC, and Chua HC. 2004. Quantitative three-dimensional anatomy of cervical, thoracic and lumbar vertebrae of Chinese Singaporeans. European Spine Journal 13(2):137-146.

Tattersall I. 2000. Once we were not alone. Scientific American 282(1):56-62.

Taylor C, and Rowntree VJ. 1973. Running on two or four legs: which consumes more energy? Science, New Series 179(4069):186-187.

Taylor D, O'Reilly PO, Vallet L, and Lee TC. 2003. The fatigue strength of compact bone in torsion. Journal of Biomechanics 36:1103-1109.

Thornton GM, Frank CB, and Shrive NG. 2007. Ligament. In: Nigg B, and Herzog W, editors. Biomechanics of the musculo-skeletal system. London: John Wiley & Sons Ltd. p 123-145.

Thorpe S, and Crompton R. 2006. Orangutan positional behavior and the nature of arboreal locomotion in Hominoidea. American Journal of Physical Anthropology 131:384-401.

Trevathan WR. 1996. The evolution of bipedalism and assisted birth. Medical Anthropology Quarterly, New Series 10(2):287-290.

Tuttle R. 2008. Footprint clues in hominid evolution and forensics: lessons and limitations. Ichnos 15:158-165.

Tuttle RH. 1981. Evolution of hominid bipedalism and prehensile capabilities. Philosophical Transactions of the Royal Society of London, Series B, Biological Sciences 292(1057):89-94.

Tuttle RH, Webb D, and Tuttle NI. 1991. Laetoli footprint trails and the evolution of hominid bipedalism. Origines(s) de la bipedie chez les hominides. Paris: CNRS. p 187-198.

Vilensky J, and Larson SG. 1989. Primate locomotion: utilization and control of systematic gaits. Annual Review of Anthropology 18:17-35.

Vrba E. 1995. On the connection between Paleoclimate and evolution. In: Vrba E, Denton G, Partridge T, and Burckle L, editors. Paleoclimate and evolution, with emphasis on human origins. New Haven: Yale University Press. p 24-45.

Vrtovec T, Pernus F, and Likar B. 2009. A review of methods for quantitative evaluation of spinal curvature. Eur Spine J 18:593-607.

Wake DB. 2003. Homology and homoplasy. Keywords and Concepts in Evolutionary Developmental Biology:191-201.

Walter M. 2004. Defense of bipedalism. Human Evolution 19(1):19-44.

Wang J, and Crompton R. 2004. The role of load-carrying in the evolution of modern body proportions. Journal of Anatomy 204:417-430.

Ward C. 1993. Torso morphology and locomotion in *Proconsul nyanzae*. American Journal of Physical Anthropology 92:291-328.

Ward C, Leakey M, and Walker A. 1999. The hominid species Australopithecus anamensis. Evolutionary Anthropology 7(6):197-205.

Ward C. 2007. Postcranial and locomotor adaptations of hominoids. In: W H, and I T, editors. Handbook of Paleoanthropology. Berlin: Springer. p 1011-1030.

Ward C, Mays S, Child S, and Latimer B. 2010. Lumbar vertebral morphology and Isthmic Spondylolysis in a British Medieval Population. American Journal of Physical Anthropology 141:273-280.

Watkins IV R, Watkins III R, Williams L, Ahlbrand S, Garcia R, Karamanian A, Sharp L, Vo C, and Hedman T. 2005. Stability provided by the sternum and rib cage in the thoracic spine. Spine 30(11):1283-1286.

Wescott D. 2000. Sex variation in the second cervical vertebra. Journal of Forensic Sciences 45(2):462-466.

Wescott R. 1967a. The exhibitionistic origin of bipedalism. Man, New Series 2(4):630.

Wescott R. 1967b. Hominid uprightness and primate display. American Anthropologist, New Series 69(6):738.

Wheeler PE. 1991. The influence of bipedalism on the energy and water budgets of early hominids. Journal of Human Evolution 21(2):117-136.

White TD. 2000. Human osteology. New York: Academic Press.

White TD, Suwa G, and Asfaw B. 1994. Australopithecus ramidus, a new species of early hominid from Aramis, Ethiopia. Nature 371(22):306-312.

Whitney C. 1926. Asymmetry of vertebral articular processes and facets. American Journal of Physical Anthropology 9(4):451-455.

Whyne C, Hu S, Klisch S, and Lotz J. 1998. Effect of the pedicle and posterior arch on vertebral body strength predictions in finite element modeling. Spine 23(8):899-907.

Williams S. 2012. Variations in anthropoid vertebral formulae: implications for homology and homoplasy in hominoid evolution. J Exp Zool Part B 318:134-147.

Williams SA. 2010. Morphological integration and the evolution of knuckle-walking. Journal of Human Evolution 58:432-440.

Williams SA, Ostrofsky KR, Frater N, Churchill SE, Schmid P, and Berger LR. 2013. The vertebral column of Australopithecus sediba. Science 340(6129):1232996.

Williams SA, and Russo GA. 2015. Evolution of the hominoid vertebral column: the long and the short of it. Evolutionary Anthropology: Issues, News, and Reviews 24(1):15-32.

Wilson E. 1999. The diversity of life. New York: W. W. Norton & Company.

Wold S, Esbensen K, and Geladi P. 1987. Principle component analysis. Chemometrics and Intelligent Laboratory Systems 2:35-52.

Wolpoff M. 1983. Lucy's lower limbs: long enough for Lucy to be fully bipedal? Nature 304:59-61.

Wolpoff M, Senut B, Pickford M, and Hawks J. 2002. Sahelanthropus or 'Sahelpithecus'? Nature 419:581-582.

Wood B, and Constantino P. 2007. Paranthropus boisei: fifty years of evidence and analysis. Yearbook of Physical Anthropology 50:106-132.

Wood B, and Lonergan N. 2008. The hominin fossil record: taxa, grades, and clades. Journal of Anatomy 212:354-376.

Wood B, and Richmond B. 2000. Human evolution: taxonomy and paleobiology. Journal of Anatomy 196:19-60.

Wood B. 2010. Reconstructing human evolution: Achievements, challenges, and opportunities. Proceedings of the National Academy of Sciences of the United States of America 107:8902-8909.

Wynn JG. 2000. Paleosols, stable carbon isotopes, and paleoenvironmental interpretation of Kanapoi, Northern Kenya. Journal of Human Evolution 39(4):411-432.

Yamazaki N, Hase K, Ogihara N, and Hayamizu N. 1996. Biomechanical analysis of the development of human bipedal walking by a neuro-musuclo-skeletal model. Folia Primatologica 66(1-4):253-271.

Yazici M, Acaroglu ER, Alanay A, Deviren V, Cila A, and Surat A. 2001. Measurement of vertebral rotation in standing versus supine position in adolescent idiopathic scoliosis. Journal of Pediatric Orthopaedics 21(2):252-256.

Zihlman AL. 1992. Locomotion as a life history character: the contribution of anatomy. Journal of Human Evolution 22(4–5):315-325.

Zollikofer C, Ponce de Leon M, Liberman D, Guy F, Pilbeam D, Likius A, Mackaye H, Vignaud P, and Michel B. 2005. Virtual cranial reconstruction of Sahelanthropus tchadensis. Nature 434:755-759.

Zuckerman S. 1955. Age changes in the basicranial axis of the human skull. American Journal of Physical Anthropology 13(3):521-539.

Appendices A - G

Appendix A. Biological materials

Comparative primate morphology continues to be the subject of various comparative analyses to explain traits with an underlying reference to the evolution of human bipedal locomotion (Boszczyk et al. 2001; Davis et al. 2003; Harcourt-Smith and Aiello 2004; Jablonski and Chaplin 2004). As a structural unit, factors such as mass, density, applied internal and external forces, moments of inertia, velocity, and center of gravity (COM) influences locomotion (Nigg 2007a; Nigg 2007b). Biological materials such as bone, cartilage, tendons, and muscle gross morphology exert important influences on locomotion. Since soft tissue is not the main focus of this research, this review is limited to those materials that act as influencing factors.

Cortical and trabecular bone

Cortical bone is biphasic. Phase 1 refers to the mineral content (inorganic); Phase 2 refers to collagen (organic) and ground substance (Frankel and Nordin 2001). Inorganic material accounts for 60 to 70% of cortical bone composition, water for 5-8%, and organic material for the remaining percentage. The combination of calcium and phosphate in the form of hydroxyapatite crystals attach to collagen fibers held together by organic and inorganic material matrices. The direction of these collagen fibers is regionally dependent and has different mechanical responses to force (Cowin 1989a; Frankel and Nordin 2001). In comparison, trabecular bone consists a varying orientation of struts and rods which create multiple spaces for bone marrow (Cowin 1989b; Nigg and Herzog 2007). Trabecular tissue or individual trabecula consists of interstitial bone with a less mineralized surface that is not homogeneous with variation in strut orientation (Cowin 1989b; Frankel and Nordin 2001; Friedman 2006; Ruimerman et al. 2005).

Cortical and trabecular bone are anisotropic, e.g., they differ in mechanical properties dependent on the load placement on different axes. Stress or strain placed upon the surface of the bone will elicit a primary response and a secondary tissue response (Cotton et al. 2003; Frankel and Nordin 2001; Sobelman et al. 2004; Taylor et al. 2003). Cortical bone's biomechanical response to stress, strain, compression, and tension varies according to the surface area, the directional loading on different axes, and the density of the tissue. For example, cortical bone with an apparent density of 1.85 g/cc can withstand stress nearing 180 Mpa, with a yield and fracture point roughly 2% of the applied stress (Frankel and Nordin 2001). Trabecular bone differs in its mechanical response.

The density of trabecular tissue and the spatial arrangement among the individual trabecula show an apparent density of 0.030 g/cc to 0.90 g/cc that lessens the strength in both tension and compression, with a yield of 48 Mpa to 10 Mpa (Frankel and Nordin 2001).

Hyaline and fibrocartilage

Hyaline cartilage contains a heterogeneous matrix with fine collagen fibers that provide flexible support and protection (Degraff and Stuart 1986). Articular cartilage functions to transmit force to joints with minimal stress concentrations by providing a gliding surface between skeletal elements (Herzog and Federico 2007). According to Mow and Hung (2001), four structural zones exist: the superficial zone, the middle or transitional zone, the deep or radial zone, and the calcified zone. The superficial zone, the thinnest layer which is approximately $2\mu m$ in thickness, contains one layer of randomly-aligned collagen fibers in a wavelike pattern with a second, deeper, parallel layer. In the middle or transitional zone, collagen fibers are greater in diameter and randomly orientated. The deep or radial zone contains the largest diameter of collage fibers, which are perpendicular to the subchondral bone and the remaining cartilage surface. The calcified zone is the mechanical "transition" zone that separates the cartilage layer above from the subchondrial bone located below. This zone contains hydroxyapatite and collagen fibers that orientate and anchor the cartilage to the underlying bone (Mow and Hung 2001).

Fibrocartilage tissue differs from hyaline cartilage. Structurally, the chondrocytes are either irregular in distribution or align in longitudinal rows. The types and ratio of collagen depend upon the site. Similar to hyaline cartilage, collagen fiber patterns vary according to location (Benjamin and Evans 1990). For example, intervertebral discs (IVD) consist of three distinct tissues: nucleus pulposus (NP), annual fibrosis (AF), and hyaline cartilage endplates. Glycosaminoglycan, collagen, and a saline-like fluid combined with a gel-like substance compose the nucleus pulposus (Humzah and Soames 1988). Unlike the nucleus pulposus, the annual fibrosis consists of lamellae (200 to 400 μm in width) with orientated fibers greater than 60° to the transverse plane (Adams et al. 1996; Humzah and Soames 1988; Mow and Hung 2001). Intervertebral discs can sustain a greater amount of compressive stress, nearing 2.5 MPa, without compromising structural integrity. Within the intervertebral disc, the annulus fibrosis experiences a greater amount of stress (maximum 2.5 MPa) than stress at the nucleus populous (approximately 2.0 MPa). Differences in

stress between these two tissue vary from each other by .5 MPa to 1.2 MPa (Adams et al. 1986; Adams et al. 1996; McNally et al. 1993).

The biomechanical properties also differ due to the variation in collagen and collagen orientation, the distribution of chondrocytes, and the differences within the cartilaginous layers. Essentially, cartilage is anisotropic and inhomogeneous which is adept for compression, but can fail during excessive tensile and shear stress (Cowin 1989a; Herzog and Federico 2007; Nigg and Herzog 2007).

Ligaments

Ligaments bind bones to form a joint that guide movement and maintain joint congruency (Thornton et al. 2007). The structure of a ligament consists of a group of fiber bundles, with some organized into fascicles and fibroblasts surrounded by an epiligament. The fibril structure (collagen midsubstance) is an aggregation of tropocollagen (1.5 nm in diameter) grouped into microfibril (3.5 nm in diameter), microfibrils grouped into a subfibril (10-20 nm in diameter), and subfribrils grouped into a fibril (50-500 nm in diameter). This ending fiber structure encompasses all previous structures (50-300 nm in diameter). Structurally, individual fibers within the epiligament are crimped, and the length among crimps varies within the ligament at various locations (Thornton et al. 2007). For example, the ligament-to-bone insertion point has four distinct zones: Zone 1, a normal ligament midsubstance where collagen bundles have a parallel orientation; Zone 2, a non-mineralized fibrocartilage where collagen bundles are surrounded by a rows of cells; Zone 3, a layer of calcified fibrocartilage; and Zone 4, a blending of ligament and bone collagen (Thornton et al. 2007).

Ligament composition includes fibroblasts or fibrocytes (20%) within a matrix (80%). Collagen fibers vary in diameter (10 to 1500 nm) and direction within the matrix and also provide protection against stress creep (Thornton et al. 2007). When a force (load) is applied, the force causes a deformation of the ligament. This deformation, primarily in the form of an elongation (strain), is directly related to the amount of force versus tissue composition (Nordin et al. 2001). For example, while applying force (load) to the surface of the bone, ligament tissue – which forms the fulcrum between bones – acts as lever arms. Lower stress yield of ligaments limits the amount of mechanical force produced by the lever system, e.g., via joints. If an applied force exceeds the

mechanical perimeter of the ligament, the yield-to-failure point prevents any mechanical damage (Nordin et al. 2001; Thornton et al. 2007).

Tendons

Tendons are fibrous tissues connecting muscle to bone. Tendon junctions include three categories: muscle-to-tendon (aponeurosis) or myotendinous junction, tendon proper, and the bone-to-tendon or osteotendinious junction. Although the physical configuration of tendons will vary according to the placement and orientation found on the body, tendons are very similar to ligaments. The basic structure includes tropocollagen grouped into microfibrils; microfibrils grouped into subfibrils; subfibrils grouped into fiber (heterogeneous in diameter), which result in fascicles and endotendon. The endotendons contains these bundles along with fibroblasts, blood vessels, lymphatic vessels, and nerves. In addition to these groupings, an outer layer has two parts – an inner epitenon and an outermost layer of paratenon or tendon sheath (Herzog 2007b). The orientation these structures provides both additional binding support and allows the fibers to slide against each other during joint movement (Herzog 2007b).

Tendons, normally "loaded" in tension, exhibit high tensile stiffness nearing 1.6 Gpa and strength approximately at 140 Mpa (Herzog 2007b). Currently, no clear-cut mechanical parameters for tendons exist, except for the load-to-failure limit. Apart from the load-to-failure limit, variations within zone content and the contact surface area of the bone suggest that elastic strain energy, load, and cycle rate influence and limit the amount of force (Herzog 2007b).

Muscle

Muscle classification includes two categories: non-striated or striated (Herzog 2007a). Muscles have various configurations, and the arrangement of muscle fibers can be parallel fibered, fusiform, or pennate. Whereas parallel fiber and fusiform fibers are both parallel along the length of the muscle, the remaining pennate fibers (unipennate, bipennate, and multipennate) are directional and angled at the tendons (Degraff and Stuart 1986; Herzog 2007a). The individual structure of muscle is similar, but differs from those found in either ligament or tendon. An individual muscle fiber (cell) is a group of parallel myofibrils surrounded by a sarcolemma (a plasma membrane) and an endomysium (fibrous sheathing). The final layer, the perimysium, consists of fascia and the epimusium (Degraff and Stuart 1986; Herzog 2007a). The length of a

muscle fiber varies within muscle groups but often can reach 30 cm in length and 10 to 100 μm in diameter (Degraff and Stuart 1986).

The pattern of myofibrils, which gives the muscle its striated pattern, includes sarcomere (unit) segmentation-marked transitional line known as "Z" lines. Each sarcomere composition includes alternating horizontal cross-bands of thick and thin filaments of protein. The thin filaments, known as "I" bands (6 nm in thickness), comprise of two randomly-patterned chains of actin globules, tropomyosin, and troponin (Herzog 2007a).

The thick filaments within the sarcomere or "A" bands (12 nm in thickness) include myosin molecules with a "tail and globular head" of meromyosin (ATPase enzymes) orientated in the opposite direction. The meromyosin allows for the binding of actin and promotes hydrolysis for muscle contraction. When attached to a thin filament made of actin, cross-bridging occurs at 14.3 nm in the axial direction and 60° in the radial direction (Degraff and Stuart 1986; Herzog 2007a). In addition to these filaments, an elastic horizontal filament develops tension during sarcomere stretching, as elastic horizontal filaments aid in contraction (Lorenz and Campello 2001).

Biomechanically, muscular contraction is achieved by the myosin "cross-bridges" in the actin and myosin filament junctions. The contact of the myosin bridge with the actin filament causes a release of ATP from the ATPase of the globular head of myosin. This process causes the thin filaments, "I" bands, to pull toward and over the center of the thicker filaments, the "A" bands. While the "A" bands remain at the same length, a reduction in distance occurs between the "Z" lines and "I" bands; thus, the shortening of the myofibrils would induce movement from insertion to the origin point of the muscle to the bone (Degraff and Stuart 1986). The amount of force upon the surface of the bone from muscle contraction has several influencing factors. Sarcomere length and tension (stored energy), load, velocity, time, and heat are factors which have a cyclical relationship (Lorenz and Campello 2001). The amount of force will vary according to the length of the muscle fibers. According to Lieber (1993), short fibers with larger cross-sections produce larger muscle force, approximately 100 N, with a length of approximately 14 cm. Longer fibers with smaller cross-sections have about half the force, 50 N, with a length of approximately 20 cm (Lieber 1993).

Relevancy

As reviewed in Section 3.6, the three-column spine concept considers the vertebral body and posterior pillars (articular processes) as columns that provide both axial and transverse stability (Louis 1985). In this view, the anterior column includes the anterior longitudinal ligament, the anterior annulus fibrosis, and the anterior half of the vertebral body. The middle column includes the posterior longitudinal ligament, the posterior half of the annulus fibrosis, and the posterior half of the vertebral body. The posterior column includes the vertebral arch as well as interspinous and supraspinous ligaments, all reinforced by muscle (Moskovich 2001). As in the three-column concept, the configuration of the superior and inferior articulation facets, as it relates to spinal curvature, influences lordotic and kyphotic curvatures in addition to the amount of stress and shear experienced throughout the column (Smith et al. 1991).

Several studies depict curvature and weight distribution in humans (Boszczyk et al. 2001; Dietrich and Kessel 1997; Frobin et al. 2002; Gangnet et al. 2003; Keller et al. 2005). The compressive forces at the intervertebral discs is distributed evenly between the anterior and posterior segments at C2-C6 (less than 10 kg), with a progressive increase anteriorly in compressive loads to T9 (30 kg). From T10 to S1, posterior force increases while anterior force decreases, with a dip at the T12-L1 junction. As substantiated by IVD studies, compressive forces at the IVD differ, but these forces are what outline spinal curvature (Keller et al. 2005). Additionally, the vertebral arch increases stiffness in the transverse plane (60 Mpa) as it simultaneously decreases the posterior displacement of the vertebral body (Whyne et al. 1998).

As reported by Panjabi et al. (1991a, 1993a, and 1993b), the distribution of compressive forces aligns with variations in the surface areas at both the superior and inferior articulating facets. The articulating surface area remains constant in the cervical region (approximately 100 mm^2). The cervical/thoracic junction depicts an increase in area in the superior articular facets, with a decrease in the inferior articular facets between C6-T9 (approximately 90 to 110 mm^2), and a steady increase from T10 to L5 (from 110 to 200 mm^2). As indicated by Panjabi et al. (1993b), the sagittal angle of the superior-articular facets decreases from 116° at C2 to 80° at C7, remains a steady 70-75° at T2-T12, and decreases from 137° at L1 to 118° at L5. Facets to the transverse plane depict a decrease from 35° at C2 to 75° at T4, remain a steady 75 to 76° at T5-T12, with a slight increase to 80° in the lumbar region (Panjabi et al. 1993b). The articular surface area and the sagittal angle

at T9 and L3 also coincide with the center of gravity (COM) as anterior to T9 (28 mm) in the thoracic region and L3 (26 mm) in the lumbar region (Legaye and Duval-Beaupere 2008). The anterior vertebral height of L4 and L5 directs the force to the femoral head via the pelvic girdle. Additional research by Garnet and colleagues (2003) support this conclusion (Legaye and Duval-Beaupere 2008) in regard to weight distribution throughout the column.

Appendix B: Wilcoxon signed-rank test results for intra-observer error

Table B-1. Non-significant differences between measurements.

Level	Variable	N	Mean	z	r	p value[1]
Cranium	CBA	19	17.521	-0.825[a]	-0.189	0.409
C1	SFAR	19	90.392	-0.746[b]	-0.171	0.456
C1	SFAL	19	92.821	-0.440[b]	-0.100	0.660
C1	SFA	19	91.630	-0.880[b]	-0.100	0.379
C1	IFAR	19	98.083	-1.476[b]	-0.338	0.140
C1	IFAL	19	97.761	-0.777[b]	-0.178	0.437
C1	IFA	19	98.847	-1.089[b]	-0.249	0.276
C1	SVAPAR	19	26.630	-0.880[b]	-0.201	0.201
C1	SVAPAL	19	27.820	-0.089[b]	-0.020	0.929
C1	SVAPA	19	26.959	-0.597[b]	-0.136	0.551
C1	IVAPAR	19	24.210	-0.345[b]	-0.079	0.730
C1	IVAPAL	19	25.961	0.000[c]	0.000	1.000
C1	IVAPA	19	25.082	-0.129[b]	-0.029	0.897
C1	Area	19	4509.824	-1.604[a]	-0.367	0.109
C2	SFAR	19	101.052	-1.867[b]	-0.428	0.062
C2	SFAL	19	99.669	-0.220[a]	-0.050	0.826
C2	SFA	19	100.274	-0.543[b]	-0.124	0.587
C2	IFAR	19	47.459	-0.220[b]	-0.050	0.826
C2	IFAL	19	43.854	-1.018[a]	-0.233	0.309
C2	IFA	19	45.505	-1.018[a]	-0.233	0.308
C2	SVAPAR	19	16.581	-0.188[a]	-0.043	0.851
C2	SVAPAL	19	15.276	-1.170[a]	-0.229	0.242
C2	SVAPA	19	15.966	-0.754[a]	-0.172	0.451
C2	IVAPAR	19	27.8058	-0.251[b]	-0.057	0.802
C2	IVAPAL	19	25.618	-0.028[a]	-0.006	0.977
C2	IVAPA	19	26.698	-0.256[a]	-0.058	0.798
C2	Area	19	4883.293	0.000[c]	0.000	1.000
C2	RT	19	12.246	-1.303[c]	-0.298	0.192
C3	SFAR	19	31.514	-0.196[a]	-0.044	0.844
C3	SFAL	19	31.318	-0.938[b]	-0.215	0.348
C3	SFA	19	31.308	-0.044[a]	-0.010	0.965
C3	SFPAR	19	32.242	-0.267[a]	-0.061	0.790
C3	SFPAL	19	32.047	-0.227[b]	-0.052	0.820
C3	SFPA	19	32.141	-0.330[a]	-0.075	0.741
C3	IFAR	19	38.029	0.000[c]	0.000	1.000
C3	IFAL	19	38.207	-0.625[a]	-0.143	0.532

[1] Bonferroni Correction: CBA, $p < 0.05$; C1, $p < 0.01$; C2, $p < 0.008$; C3 – L5, $p < 0.004$.
[a] Based on negative ranks.
[b] Based on positive ranks.
[c] The sum negative ranks equals the sum of positive ranks.

Table B-1. Non-significant differences between measurements (cont.).

Level	Variable	N	Mean	z	r	p value[1]
C3	IFA	19	38.637	-0.052[b]	-0.011	0.959
C3	IFPAR	19	39.151	-0.945[a]	-0.216	0.345
C3	IFPAL	19	38.939	-0.597[a]	-0.136	0.551
C3	IFPA	19	39.042	-0.427[a]	-0.097	0.097
C3	SVAPAR	19	69.512	-0.155[a]	-0.035	0.877
C3	SVAPAL	19	73.515	-1.915[b]	-0.439	0.056
C3	SVAPA	19	71.120	-0.980[b]	-0.224	0.327
C3	IVAPAR	19	85.985	-1.569[b]	-0.359	0.117
C3	IVAPAL	19	90.940	-0.776[b]	-0.178	0.438
C3	IVAPA	19	88.267	-1.188[b]	-0.272	0.235
C3	VBPH	19	12.592	-1.450[b]	-0.332	0.147
C3	VBAH	19	12.183	-0.805[b]	-0.184	0.421
C3	SFID	19	37.731	-1.512[a]	-0.346	0.131
C3	IIFD	19	35.333	-1.638[a]	-0.375	0.101
C3	PICP	19	101.047	-1.642[b]	-0.376	0.101
C3	CPBA	19	5.040	-0.052[a]	-0.011	0.959
C3	Area	19	4361.957	-1.342[a]	-0.307	0.180
C3	RT	19	17.982	-0.845[a]	-0.193	0.398
C4	SFAR	19	33.548	-0.707[a]	-0.162	0.479
C4	SFAL	19	37.871	-1.558[b]	-0.357	0.119
C4	SFA	19	35.706	-1.191[b]	-0.273	0.234
C4	SFPAR	19	34.594	-1.470[a]	-0.337	0.142
C4	SFPAL	19	38.917	-1.917[b]	-0.439	0.055
C4	SFPA	19	36.747	-0.455[b]	-0.104	0.649
C4	IFAR	19	43.591	-0.805[b]	-0.184	0.421
C4	IFAL	19	41.598	-0.510[b]	-0.117	0.610
C4	IFA	19	42.657	-0.315[b]	-0.072	0.753
C4	IFPAR	19	44.399	-0.283[a]	-0.064	0.777
C4	IFPAL	19	42.572	-0.400[b]	-0.091	0.689
C4	IFPA	19	43.453	-1.025[b]	-0.293	0.306
C4	SVAPAR	19	79.196	-0.628[b]	-0.144	0.530
C4	SVAPAL	19	81.977	-1.307[a]	-0.299	0.191
C4	SVAPA	19	80.204	-0.712[a]	-0.163	0.476
C4	IVAPAR	19	86.390	-1.503[b]	-0.344	0.133
C4	IVAPAL	19	86.121	-0.911[a]	-0.208	0.362
C4	IVAPA	19	86.086	-0.284[a]	-0.065	0.776

[1] Bonferroni Correction: CBA, $p < 0.05$; C1, $p < 0.01$; C2, $p > 0.008$; C3 – L5, $p < 0.004$.
[a] Based on negative ranks.
[b] Based on positive ranks.
[c] The sum negative ranks equals the sum of positive ranks.

Table B-1. Non-significant differences between measurements (cont.).

Level	Variable	N	Mean	z	r	p value[1]
C4	VBPH	19	12.785	-1.369[b]	-0.314	0.171
C4	VBAH	19	11.441	-1.002[b]	-0.229	0.316
C4	SFID	19	34.673	-1.550[a]	-0.355	0.121
C4	IIFD	19	35.386	-1.388[a]	-0.318	0.165
C4	PICP	19	98.572	-0.839[b]	-0.192	0.401
C4	CPBA	19	3.447	-1.014[b]	-0.232	0.311
C4	Area	19	4707.24	0.000	0.000	1.000
C4	RT	19	8.687	-0.523[a]	-0.119	0.601
C5	SFAR	19	38.901	-1.381[a]	-0.316	0.167
C5	SFAL	19	38.544	-0.245[a]	-0.056	0.807
C5	SFA	19	38.783	-1.621[a]	-0.371	0.105
C5	SFPAR	19	39.668	-0.853[a]	-0.195	0.394
C5	SFPAL	19	39.760	-0.350[b]	-0.080	0.726
C5	SFPA	19	39.743	-0.313[a]	-0.071	0.755
C5	IFAR	19	35.946	-1.163[a]	-0.266	0.245
C5	IFAL	19	35.955	-0.052[a]	-0.011	0.959
C5	IFA	19	36.001	-0.825[b]	-0.189	0.409
C5	IFPAR	19	36.513	-1.785[a]	-0.409	0.074
C5	IFPAL	19	37.415	-0.188[b]	-0.043	0.851
C5	IFPA	19	37.124	-0.153[a]	-0.035	0.878
C5	SVAPAR	19	85.270	-1.647[b]	-0.377	0.100
C5	SVAPAL	19	88.390	-0.980[b]	-0.224	0.327
C5	SVAPA	19	86.196	-1.268[b]	-0.290	0.205
C5	IVAPAR	19	85.598	0.000[c]	0.000	1.000
C5	IVAPAL	19	82.728	-0.909[b]	-0.208	0.363
C5	IVAPA	19	84.121	-0.900[b]	-0.206	0.368
C5	VBPH	19	12.461	-0.569[b]	-0.136	0.570
C5	VBAH	19	11.417	-1.067[b]	-0.244	0.286
C5	SFID	19	34.942	-1.127[a]	-0.258	0.260
C5	IIFD	19	36.202	-1.650[a]	-0.378	0.099
C5	PICP	19	95.436	-1.733[b]	-0.397	0.083
C5	CPBA	19	3.435	-1.166[a]	-0.267	0.244
C5	Area	19	4965.788	-1.000[a]	-0.229	0.317
C5	RT	19	7.655	-1.429[a]	-0.327	0.153
C6	SFAR	19	33.708	-0.902[b]	-0.206	0.367
C6	SFAL	19	33.530	-0.786[a]	-0.180	0.432
C6	SFA	19	33.617	-0.541[b]	-0.124	0.589

[1] Bonferroni Correction: CBA, $p < 0.05$; C1, $p < 0.01$; C2, $p < 0.008$; C3 – L5, $p < 0.004$.
[a] Based on negative ranks.
[b] Based on positive ranks.
[c] The sum negative ranks equals the sum of positive ranks.

Table B-1. Non-significant differences between measurements (cont.).

Level	Variable	N	Mean	z	r	p value [1]
C6	SFPAR	19	35.029	-0.825[b]	-0.189	0.410
C6	SFPAL	19	34.576	-0.455[a]	-0.104	0.649
C6	SFPA	19	34.802	-1.478[b]	-0.339	0.139
C6	IFAR	19	28.261	-1.924[a]	-0.441	0.054
C6	IFAL	19	28.726	-1.320[a]	-0.302	0.187
C6	IFA	19	28.493	-1.622[a]	-0.372	0.157
C6	IFPAR	19	29.478	-1.868[a]	-0.428	0.062
C6	IFPAL	19	29.943	-1.295[a]	-0.297	0.195
C6	IFPA	19	29.707	-1.136[a]	-0.260	0.256
C6	SVAPAR	19	83.473	-0.245[a]	-0.056	0.807
C6	SVAPAL	19	85.565	-0.341[b]	-0.078	0.733
C6	SVAPA	19	84.297	-0.142[a]	-0.032	0.887
C6	IVAPAR	19	85.892	-0.628[a]	-0.144	0.530
C6	IVAPAL	19	81.773	-0.937[a]	-0.214	0.349
C6	IVAPA	19	84.061	-0.947[a]	-0.217	0.344
C6	VBPH	19	13.250	-1.613[b]	-0.374	0.103
C6	VBAH	19	11.142	-1.269[b]	-0.291	0.205
C6	SFID	19	36.082	-0.382[a]	-0.087	0.702
C6	IIFD	19	35.376	-1.128[a]	-0.258	0.259
C6	PICP	19	88.918	-1.648[b]	-0.378	0.099
C6	CPBA	19	3.569	-1.100[a]	-0.252	0.271
C6	Area	19	5698.991	0.000[c]	0.000	1.000
C6	RT	19	10.871	-0.101[a]	-0.023	0.920
C7	SFAR	19	25.540	-1.492[a]	-0.342	0.136
C7	SFAL	19	25.040	-1.397[a]	-0.320	0.162
C7	SFA	19	25.549	-1.700[a]	-0.390	0.089
C7	SFPAR	19	26.546	-1.727[a]	-0.396	0.084
C7	SFPAL	19	26.687	-1.328[a]	-0.304	0.184
C7	SFPA	19	26.898	-0.848[a]	-0.194	0.397
C7	IFAR	19	27.619	-0.503[b]	-0.115	0.615
C7	IFAL	19	28.322	-0.455[b]	-0.104	0.649
C7	IFA	19	27.736	-1.365[a]	-0.313	0.172
C7	IFPAR	19	29.970	-0.035[a]	-0.008	0.972
C7	IFPAL	19	29.432	-0.569[b]	-0.130	0.570
C7	IFPA	19	29.648	-0.566[b]	-0.129	0.572
C7	SVAPAR	19	87.700	-0.723[b]	-0.165	0.469

[1] Bonferroni Correction: CBA, $p < 0.05$; C1, $p < 0.01$; C2, $p < 0.008$; C3 – L5, $p < 0.004$.
[a] Based on negative ranks.
[b] Based on positive ranks.
[c] The sum negative ranks equals the sum of positive ranks.

Table B-1. Non-significant differences between measurements (cont.).

Level	Variable	N	Mean	z	r	p value [1]
C7	SVAPAL	19	87.138	-1.381[b]	-0.316	0.167
C7	SVAPA	19	86.761	-0.181[b]	-0.041	0.856
C7	IVAPAR	19	90.380	0.000[c]	0.000	1.000
C7	IVAPAL	19	89.276	-1.538[b]	-0.352	0.124
C7	IVAPA	19	89.748	-0.994[b]	-0.228	0.320
C7	VBPH	19	13.998	-1.067[b]	-0.244	0.286
C7	VBAH	19	12.015	-0.523[a]	-0.119	0.601
C7	SFID	19	35.522	-1.349[a]	-0.309	0.177
C7	IIFD	19	31.816	-0.935[b]	-0.214	0.350
C7	PICP	19	88.185	-0.664[a]	-0.152	0.507
C7	CPBA	19	3.357	-0.275[a]	-0.063	0.784
C7	Area	19	5828.750	0.000[c]	0.000	1.000
C7	RT	19	8.053	-0.592[a]	-0.135	0.554
T1	SFAR	19	27.096	-0.342[a]	-0.078	0.733
T1	SFAL	19	26.000	-1.422[a]	-0.326	0.155
T1	SFA	19	26.163	-0.589[a]	-0.135	0.556
T1	SFPAR	19	27.908	-0.370[a]	-0.084	0.712
T1	SFPAL	19	26.629	-0.595[a]	-0.136	0.552
T1	SFPA	19	27.162	-1.842[a]	-0.422	0.065
T1	IFAR	19	16.198	-0.668[a]	-0.153	0.504
T1	IFAL	19	13.196	-0.768[b]	-0.176	0.443
T1	IFA	19	14.694	-0.309[a]	-0.070	0.758
T1	IFPAR	19	17.400	-1.477[a]	-0.338	0.140
T1	IFPAL	19	14.925	-0.220[b]	-0.050	0.826
T1	IFPA	19	15.896	-1.223[a]	-0.280	0.221
T1	SVAPAR	19	91.196	-0.738[b]	-0.169	0.460
T1	SVAPAL	19	88.911	-0.852[b]	-0.195	0.394
T1	SVAPA	19	90.313	-1.184[b]	-0.271	0.236
T1	IVAPAR	19	105.310	-0.314[b]	-0.072	0.753
T1	IVAPAL	19	104.964	-0.414[a]	-0.094	0.679
T1	IVAPA	19	105.293	-0.545[a]	-0.125	0.586
T1	VBPH	19	14.469	-1.895[b]	-0.434	0.058
T1	VBAH	19	13.810	-0.322[a]	-0.073	0.747
T1	SFID	19	30.895	-1.067[a]	-0.244	0.286
T1	IIFD	19	25.711	-0.414[a]	-0.094	0.679
T1	PICP	19	72.3705	-1.434[b]	-0.328	0.152

[1] Bonferroni Correction: CBA, $p < 0.05$; C1, $p < 0.01$; C2, $p < 0.008$; C3 – L5, $p < 0.004$.
[a] Based on negative ranks.
[b] Based on positive ranks.
[c] The sum negative ranks equals the sum of positive ranks.

Table B-1. Non-significant differences between measurements (cont.).

Level	Variable	N	Mean	z	r	p value [1]
T1	CPBA	19	4.333	-0.369[b]	-0.084	0.712
T1	Area	19	6464.054	0.000[c]	0.000	1.000
T1	RT	19	16.304	-0.564[b]	-0.129	0.573
T2	SFAR	19	24.671	-0.665[b]	-0.152	0.506
T2	SFAL	19	26.036	-0.415[a]	-0.095	0.678
T2	SFA	19	25.222	-0.546[b]	-0.125	0.585
T2	SFPAR	19	25.612	-0.979[b]	-0.224	0.328
T2	SFPAL	19	26.167	-1.423[a]	-0.326	0.155
T2	SFPA	19	26.241	-0.343[b]	-0.078	0.731
T2	IFAR	19	10.733	-1.413[a]	-0.324	0.158
T2	IFAL	19	7.821	-0.879[a]	-0.201	0.379
T2	IFA	19	9.438	-1.735[a]	-0.398	0.083
T2	IFPAR	19	10.442	-1.334[a]	-0.306	0.182
T2	IFPAL	19	9.640	-1.164[b]	-0.267	0.244
T2	IFPA	19	9.808	-1.727[a]	-0.396	0.084
T2	SVAPAR	19	98.534	-1.501[a]	-0.334	0.133
T2	SVAPAL	19	104.170	-1.193[b]	-0.273	0.233
T2	SVAPA	19	102.541	-0.129[a]	-0.029	0.897
T2	IVAPAR	19	112.459	-1.161[b]	-0.266	0.246
T2	IVAPAL	19	114.767	-0.969[a]	-0.222	0.333
T2	IVAPA	19	113.613	-0.371[a]	-0.085	0.711
T2	VBPH	19	16.407	-0.828[b]	-0.189	0.408
T2	VBAH	19	14.947	-0.705[b]	-0.161	0.481
T2	SFID	19	25.968	-1.046[a]	-0.239	0.295
T2	IIFD	19	21.905	-0.141[b]	-0.032	0.888
T2	PICP	19	67.408	-1.503[b]	-0.344	0.133
T2	CPBA	19	3.087	-1.374[a]	-0.315	0.170
T2	Area	19	6366.333	0.000[c]	0.000	1.000
T2	RT	19	10.413	-0.725[a]	-0.166	0.469
T3	SFAR	19	20.682	-1.028[b]	-0.235	0.304
T3	SFAL	19	19.243	-1.483[b]	-0.340	0.138
T3	SFA	19	19.959	-1.349[b]	-0.309	0.177
T3	SFPAR	19	21.740	-0.223[b]	-0.051	0.823
T3	SFPAL	19	20.530	-1.609[b]	-0.369	0.108
T3	SFPA	19	21.132	-1.045[b]	-0.239	0.296
T3	IFAR	19	9.081	-0.388[b]	-0.089	0.698
T3	IFAL	19	8.218	-0.520[b]	-0.119	0.603

[1] Bonferroni Correction: CBA, $p < 0.05$; C1, $p < 0.01$; C2, $p < 0.008$; C3 – L5, $p < 0.004$.
[q] Based on negative ranks.
[b] Based on positive ranks.
[c] The sum negative ranks equals the sum of positive ranks.

Table B-1. Non-significant differences between measurements (cont.).

Level	Variable	N	Mean	z	r	p value [1]
T3	IFA	19	8.653	-1.923[a]	-0.441	0.054
T3	IFPAR	19	9.590	-1.348[a]	-0.309	0.178
T3	IFPAL	19	9.221	-1.363[a]	-0.312	0.173
T3	IFPA	19	9.828	-0.627[a]	-0.143	0.530
T3	SVAPAR	19	102.056	-0.247[a]	-0.056	0.805
T3	SVAPAL	19	103.451	-0.071[a]	-0.016	0.943
T3	SVAPA	19	102.776	-0.349[a]	-0.080	0.727
T3	IVAPAR	19	111.670	-0.235[a]	-0.053	0.814
T3	IVAPAL	19	112.174	-0.722[a]	-0.165	0.470
T3	IVAPA	19	111.963	-0.722[a]	-0.165	0.470
T3	VBPH	19	16.725	-1.470[a]	-0.337	0.142
T3	VBAH	19	15.695	-1.471[b]	-0.337	0.141
T3	SFID	19	22.261	-1.220[a]	-0.279	0.223
T3	IIFD	19	20.387	-1.046[a]	-0.239	0.295
T3	PICP	19	66.699	-1.846[a]	-0.423	0.065
T3	CPBA	19	2.840	-0.256[b]	-0.058	0.798
T3	Area	19	6275.835	-1.000[a]	-0.229	0.317
T3	RT	19	9.324	-0.905[b]	-0.207	0.365
T4	SFAR	19	18.747	-1.837[a]	-0.421	0.066
T4	SFAL	19	19.771	-0.597[b]	-0.136	0.550
T4	SFA	19	19.646	-0.354[a]	-0.081	0.724
T4	SFPAR	19	19.518	-0.713[b]	-0.163	0.476
T4	SFPAL	19	20.763	-0.778[a]	-0.178	0.436
T4	SFPA	19	20.749	-1.220[b]	-0.279	0.222
T4	IFAR	19	9.127	-1.103[b]	-0.253	0.270
T4	IFAL	19	7.212	-0.595[a]	-0.136	0.552
T4	IFA	19	7.281	-0.713[b]	-0.163	0.476
T4	IFPAR	19	8.128	-1.298[b]	-0.297	0.194
T4	IFPAL	19	8.126	-0.825[a]	-0.189	0.410
T4	IFPA	19	8.281	-0.881[b]	-0.202	0.378
T4	SVAPAR	19	102.226	-0.714[b]	-0.163	0.475
T4	SVAPAL	19	102.412	-0.629[b]	-0.144	0.530
T4	SVAPA	19	102.312	-0.471[b]	-0.108	0.638
T4	IVAPAR	19	112.118	-1.647[a]	-0.377	0.099
T4	IVAPAL	19	112.025	-0.199[b]	-0.045	0.842
T4	IVAPA	19	112.365	-0.724[a]	-0.166	0.469

[1] Bonferroni Correction: CBA, $p < 0.05$; C1, $p < 0.01$; C2, $p < 0.008$; C3 – L5, $p < 0.004$.
[a] Based on negative ranks.
[b] Based on positive ranks.
[c] The sum negative ranks equals the sum of positive ranks.

Table B-1. Non-significant differences between measurements (cont.).

Level	Variable	N	Mean	z	r	p value [1]
T4	VBPH	19	17.074	-1.793[a]	-0.411	0.073
T4	VBAH	19	15.666	-1.349[b]	-0.309	0.177
T4	SFID	19	20.870	-1.481[a]	-0.339	0.139
T4	IIFD	19	19.335	-0.531[a]	-0.121	0.596
T4	PICP	19	65.806	-0.035[a]	-0.008	0.972
T4	CPBA	19	3.285	-0.370[b]	-0.084	0.712
T4	Area	19	6307.150	0.000[c]	0.000	1.000
T4	RT	19	9.598	-1.111[a]	-0.254	0.266
T5	SFAR	19	19.914	-0.728[a]	-0.167	0.467
T5	SFAL	19	19.306	-0.284[b]	-0.065	0.776
T5	SFA	19	19.591	-1.806[a]	-0.414	0.071
T5	SFPAR	19	21.300	-1.252[a]	-0.287	0.210
T5	SFPAL	19	20.742	-0.473[a]	-0.108	0.636
T5	SFPA	19	21.018	-0.626[a]	-0.143	0.531
T5	IFAR	19	6.361	-1.886[a]	-0.432	0.056
T5	IFAL	19	6.143	-0.594[b]	-0.136	0.552
T5	IFA	19	6.462	-0.827[a]	-0.229	0.408
T5	IFPAR	19	7.394	-0.848[a]	-0.194	0.396
T5	IFPAL	19	6.857	-0.220[b]	-0.050	0.826
T5	IFPA	19	7.379	-0.466[a]	-0.106	0.641
T5	SVAPAR	19	103.956	-0.996[a]	-0.228	0.319
T5	SVAPAL	19	105.992	-1.350[b]	-0.309	0.177
T5	SVAPA	19	105.141	-1.256[a]	-0.288	0.209
T5	IVAPAR	19	114.278	-1.371[a]	-0.314	0.171
T5	IVAPAL	19	111.556	-0.754[a]	-0.170	0.541
T5	IVAPA	19	113.393	-0.997[a]	-0.228	0.319
T5	VBPH	19	17.232	-0.538[b]	-0.123	0.590
T5	VBAH	19	15.422	-0.967[b]	-0.221	0.334
T5	SFID	19	19.751	-1.691[a]	-0.387	0.091
T5	IIFD	19	19.727	0.000[c]	0.000	1.000
T5	PICP	19	66.989	-1.016[a]	-0.233	0.310
T5	CPBA	19	3.203	-0.659[a]	-0.151	0.510
T5	Area	19	6472.233	-1.000[c]	-0.229	0.317
T5	RT	19	8.431	-0.758[a]	-0.173	0.448
T6	SFAR	19	21.227	-1.656[a]	-0.379	0.098
T6	SFAL	19	21.132	-0.504[a]	-0.115	0.614
T6	SFA	19	21.287	-0.910[a]	-0.208	0.363

[1] Bonferroni Correction: CBA, $p < 0.05$; C1, $p < 0.01$; C2, $p < 0.008$; C3 – L5, $p < 0.004$.
[a] Based on negative ranks.
[b] Based on positive ranks.
[c] The sum negative ranks equals the sum of positive ranks.

Table B-1. Non-significant differences between measurements (cont.).

Level	Variable	N	Mean	z	r	p value [1]
T6	IFAR	19	7.407	-1.400[a]	-0.321	0.161
T6	IFAL	19	7.976	-1.713[a]	-0.392	0.087
T6	IFA	19	7.898	-0.073[a]	-0.016	0.942
T6	IFPAR	19	8.554	-1.762[a]	-0.404	0.078
T6	IFPAL	19	8.772	-0.187[a]	-0.042	0.852
T6	IFPA	19	9.013	-0.862[b]	-0.197	0.389
T6	SVAPAR	19	102.774	-0.936[a]	-0.214	0.349
T6	SVAPAL	19	104.184	-0.377[a]	-0.086	0.706
T6	SVAPA	19	103.434	-1.002[a]	-0.229	0.316
T6	IVAPAR	19	115.451	-0.256[b]	-0.058	0.798
T6	IVAPAL	19	111.836	-1.335[b]	-0.306	0.182
T6	IVAPA	19	113.651	-1.630[b]	-0.373	0.103
T6	VBPH	19	17.265	0.000[c]	0.000	1.000
T6	VBAH	19	15.062	-1.872[b]	-0.429	0.061
T6	SFID	19	19.541	-0.694[a]	-0.159	0.487
T6	IIFD	19	19.707	-1.369[a]	-0.314	0.171
T6	PICP	19	67.112	-0.550[a]	-0.126	0.582
T6	CPBA	19	4.023	-0.220[b]	-0.050	0.826
T6	Area	19	6653.889	0.000[c]	0.000	1.000
T6	RT	19	10.634	-0.284[a]	-0.065	0.776
T7	SFAR	19	19.039	-0.446[a]	-0.102	0.656
T7	SFAL	19	20.475	-0.144[a]	-0.229	0.885
T7	SFA	19	19.621	-1.617[a]	-0.539	0.106
T7	SFPAR	19	20.320	-0.593[a]	-0.136	0.553
T7	SFPAL	19	21.256	-0.602[a]	-0.138	0.547
T7	SFPA	19	20.741	-0.514[a]	-0.117	0.607
T7	IFAR	19	9.538	-1.550[a]	-0.355	0.121
T7	IFAL	19	8.205	-0.724[a]	-0.166	0.469
T7	IFA	19	8.869	-1.186[a]	-0.272	0.236
T7	IFPAR	19	10.600	-1.728[a]	-0.396	0.084
T7	IFPAL	19	9.130	-1.905[a]	-0.437	0.057
T7	IFPA	19	9.854	-0.261[b]	-0.059	0.794
T7	SVAPAR	19	103.716	-0.524[b]	-0.120	0.600
T7	SVAPAL	19	103.815	-0.629[a]	-0.144	0.529
T7	SVAPA	19	103.742	-0.283[a]	-0.064	0.777
T7	IVAPAR	19	112.502	-1.255[a]	-0.058	0.209

[1] Bonferroni Correction: CBA, $p < 0.05$; C1, $p < 0.01$; C2, $p < 0.008$; C3 – L5, $p < 0.004$.
[a] Based on negative ranks.
[b] Based on positive ranks.
[c] The sum negative ranks equals the sum of positive ranks.

Table B-1. Non-significant differences between measurements (cont.).

Level	Variable	N	Mean	z	r	p value [1]
T7	IVAPAL	19	112.474	-0.039[b]	-0.008	0.969
T7	IVAPA	19	112.472	-1.452[a]	-0.333	0.147
T7	VBPH	19	17.655	-0.624[b]	-0.143	0.532
T7	VBAH	19	15.581	-0.283[b]	-0.064	0.777
T7	SFID	19	19.446	-1.892[a]	-0.434	0.059
T7	IIFD	19	19.852	-1.147[a]	-0.263	0.251
T7	PICP	19	67.278	-1.633[b]	-0.324	0.103
T7	CPBA	19	3.783	-1.035[b]	-0.237	0.300
T7	Area	19	6884.342	0.000[c]	0.000	1.000
T7	RT	19	9.187	-0.893[a]	-0.204	0.372
T8	SFAR	19	20.342	-0.169[b]	-0.038	0.866
T8	SFAL	19	20.861	-0.806[a]	-0.184	0.420
T8	SFA	19	20.771	-0.089[b]	-0.020	0.929
T8	SFPAR	19	21.266	-0.179[a]	-0.041	0.858
T8	SFPAL	19	21.763	-0.714[a]	-0.163	0.476
T8	SFPA	19	21.354	-1.016[a]	-0.233	0.310
T8	IFAR	19	8.249	-1.375[b]	-0.315	0.169
T8	IFAL	19	8.853	-1.374[a]	-0.315	0.169
T8	IFA	19	8.515	-1.039[a]	-0.238	0.299
T8	IFPAR	19	9.198	-1.495[a]	-0.342	0.135
T8	IFPAL	19	9.703	-0.040[b]	-0.009	0.968
T8	IFPA	19	9.572	-1.879[a]	-0.431	0.060
T8	SVAPAR	19	103.064	-0.233[a]	-0.053	0.816
T8	SVAPAL	19	102.322	-0.758[b]	-0.173	0.449
T8	SVAPA	19	102.956	-0.698[b]	-0.160	0.485
T8	IVAPAR	19	108.099	-0.909[b]	-0.208	0.363
T8	IVAPAL	19	109.337	-0.210[b]	-0.048	0.834
T8	IVAPA	19	108.974	-1.051[b]	-0.241	0.293
T8	VBPH	19	17.774	-0.704[b]	-0.161	0.481
T8	VBAH	19	16.046	-1.020[b]	-0.234	0.308
T8	SFID	19	19.833	-0.663[a]	-0.152	0.507
T8	IIFD	19	20.255	-1.229[a]	-0.281	0.219
T8	PICP	19	68.852	-0.332[b]	-0.076	0.740
T8	CPBA	19	2.825	-0.314[a]	-0.072	0.753
T8	Area	19	7069.550	0.000[c]	0.000	1.000
T8	RT	19	6.502	-1.268[a]	-0.290	0.205
T9	SFAR	19	19.633	-1.489[a]	-0.341	0.137

[1] Bonferroni Correction: CBA, $p < 0.05$; C1, $p < 0.01$; C2, $p < 0.008$; C3 – L5, $p < 0.004$.
[a] Based on negative ranks.
[b] Based on positive ranks.
[c] The sum negative ranks equals the sum of positive ranks.

Table B-1. Non-significant differences between measurements (cont.).

Level	Variable	N	Mean	z	r	p value [1]
T9	SFAL	19	18.977	-0.787[b]	-0.180	0.431
T9	SFA	19	19.303	-0.814[b]	-0.186	0.415
T9	SFPAR	19	20.377	-0.365[b]	-0.083	0.715
T9	SFPAL	19	19.795	-0.704[b]	-0.161	0.481
T9	SFPA	19	20.083	-0.249[a]	-0.057	0.803
T9	IFAR	19	8.668	-1.569[a]	-0.359	0.117
T9	IFAL	19	8.411	-0.189[a]	-0.043	0.850
T9	IFA	19	8.940	-0.526[a]	-0.120	0.599
T9	IFPAR	19	9.224	-1.386[a]	-0.317	0.166
T9	IFPAL	19	9.150	-0.456[a]	-0.104	0.648
T9	IFPA	19	9.635	-0.668[a]	-0.153	0.504
T9	SVAPAR	19	104.591	-0.398[b]	-0.091	0.691
T9	SVAPAL	19	104.295	-0.699[b]	-0.160	0.485
T9	SVAPA	19	104.415	-0.744[b]	-0.170	0.457
T9	IVAPAR	19	111.598	-0.740[a]	-0.100	0.580
T9	IVAPAL	19	111.586	-0.440[b]	-0.246	0.660
T9	IVAPA	19	111.705	-1.200[b]	-0.275	0.230
T9	VBPH	19	18.294	-1.630[b]	-0.373	0.103
T9	VBAH	19	16.528	-0.403[b]	-0.092	0.687
T9	SFID	19	20.453	-1.198[a]	-0.274	0.231
T9	IIFD	19	21.921	-1.706[a]	-0.391	0.088
T9	PICP	19	69.991	-1.790[b]	-0.410	0.074
T9	CPBA	19	2.750	-0.035[b]	-0.008	0.972
T9	Area	19	7490.841	0.000[c]	0.000	1.000
T9	RT	19	7.969	-0.523[a]	-0.119	0.601
T10	SFAR	19	19.442	-1.572[a]	-0.360	0.116
T10	SFAL	19	17.872	-0.275[a]	-0.063	0.783
T10	SFA	19	18.647	-1.618[b]	-0.371	0.106
T10	SFPAR	19	20.122	-1.784[a]	-0.409	0.074
T10	SFPAL	19	18.589	-0.134[a]	-0.300	0.894
T10	SFPA	19	19.370	-0.936[a]	-0.214	0.349
T10	IFAR	19	8.822	-0.263[a]	-0.060	0.793
T10	IFAL	19	7.730	-1.225[a]	-0.281	0.221
T10	IFA	19	8.195	-0.774[b]	-0.177	0.439
T10	IFPAR	19	9.544	-1.165[a]	-0.267	0.244
T10	IFPAL	19	8.275	-1.225[a]	-0.281	0.221

[1] Bonferroni Correction: CBA, $p < 0.05$; C1, $p < 0.01$; C2, $p < 0.008$; C3 – L5, $p < 0.004$.
[a] Based on negative ranks.
[b] Based on positive ranks.
[c] The sum negative ranks equals the sum of positive ranks.

Table B-1. Non-significant differences between measurements (cont.).

Level	Variable	N	Mean	z	r	p value [1]
T10	IFPA	19	8.862	-1.840[a]	-0.442	0.066
T10	SVAPAR	19	102.856	-1.209[a]	-0.277	0.227
T10	SVAPAL	19	105.922	-0.827[b]	-0.189	0.408
T10	SVAPA	19	104.387	-0.040[b]	-0.009	0.968
T10	IVAPAR	19	109.965	-1.666[b]	-0.382	0.096
T10	IVAPAL	19	110.262	-0.711[a]	-0.163	0.477
T10	IVAPA	19	109.557	-1.476[b]	-0.388	0.140
T10	VBPH	19	19.304	-0.141[b]	-0.032	0.888
T10	VBAH	19	17.361	-0.443[a]	-0.101	0.658
T10	SFID	19	21.888	-0.817[a]	-0.187	0.414
T10	IIFD	19	21.763	-1.208[a]	-0.277	0.227
T10	PICP	19	71.265	-0.622[b]	-0.142	0.534
T10	CPBA	19	3.174	-0.663[a]	-0.152	0.507
T10	Area	19	7767.337	0.000[c]	0.000	1.000
T10	RT	19	5.962	-0.020[a]	-0.004	0.984
T11	SFAR	19	18.650	-1.460[a]	-0.334	0.144
T11	SFAL	19	17.207	-0.936[a]	-0.214	0.349
T11	SFA	19	18.134	-1.758[a]	-0.403	0.079
T11	SFPAR	19	19.620	-0.421[a]	-0.096	0.674
T11	SFPAL	19	18.100	-0.637[a]	-0.146	0.524
T11	SFPA	19	18.844	-1.343[a]	-0.308	0.179
T11	IFAR	19	13.436	-1.219[a]	-0.279	0.223
T11	IFAL	19	11.422	-0.915[a]	-0.209	0.360
T11	IFA	19	13.390	-0.037[b]	-0.008	0.971
T11	IFPAR	19	14.230	-1.247[a]	-0.286	0.212
T11	IFPAL	19	12.272	-1.259[a]	-0.288	0.208
T11	IFPA	19	13.206	-1.665[a]	-0.381	0.096
T11	SVAPAR	19	102.643	-0.170[b]	-0.039	0.865
T11	SVAPAL	19	104.244	-1.065[b]	-0.224	0.287
T11	SVAPA	19	103104	-0.597[b]	-0.136	0.551
T11	IVAPAR	19	98.113	-1.527[b]	-0.350	0.127
T11	IVAPAL	19	99.484	-0.314[b]	-0.072	0.753
T11	IVAPA	19	98.359	-0.676[a]	-0.155	0.499
T11	VBPH	19	20.664	-0.242[b]	-0.055	0.809
T11	VBAH	19	18.638	-0.584[a]	-0.133	0.560
T11	SFID	19	21.719	-1.630[a]	-0.373	0.103

[1] Bonferroni Correction: CBA, $p < 0.05$; C1, $p < 0.01$; C2, $p < 0.008$; C3 – L5, $p < 0.004$.
[a] Based on negative ranks.
[b] Based on positive ranks.
[c] The sum negative ranks equals the sum of positive ranks.

Table B-1. Non-significant differences between measurements (cont.).

Level	Variable	N	Mean	z	r	p value [1]
T11	IIFD	19	23.354	-1.642[a]	-0.376	0.101
T11	PICP	19	72.965	0.000[c]	0.000	1.000
T11	CPBA	19	2.985	-0.592[b]	-0.135	0.554
T11	Area	19	8256.442	-1.000[a]	-0.229	0.317
T11	RT	19	9.137	-0.610[b]	-0.139	0.542
T12	SFAR	19	19.476	-1.217[a]	-0.279	0.223
T12	SFAL	19	20.755	-0.286[a]	-0.065	0.775
T12	SFA	19	20.112	-1.427[a]	-0.327	0.154
T12	SFPAR	19	20.347	-0.051[a]	-0.002	0.959
T12	SFPAL	19	21.078	-1.357[a]	-0.311	0.175
T12	SFPA	19	20.710	-1.859[a]	-0.426	0.063
T12	IFAR	19	17.146	-0.669[a]	-0.153	0.504
T12	IFAL	19	18.063	-0.210[a]	-0.048	0.883
T12	IFA	19	18.196	-0.830[a]	-0.190	0.407
T12	IFPAR	19	17.825	-0.633[a]	-0.145	0.526
T12	IFPAL	19	18.695	-0.153[a]	-0.035	0.878
T12	IFPA	19	18.797	-0.091[a]	-0.020	0.927
T12	SVAPAR	19	92.308	-1.530[b]	-0.351	0.126
T12	SVAPAL	19	98.548	-0.710[b]	-0.162	0.478
T12	SVAPA	19	94.363	-0.369[b]	-0.084	0.712
T12	IVAPAR	19	61.360	-1.649[a]	-0.378	0.099
T12	IVAPAL	19	61.286	-0.414[b]	-0.094	0.679
T12	IVAPA	19	60.237	-0.664[a]	-0.152	0.607
T12	VBPH	19	22.653	-0.383[b]	-0.087	0.702
T12	VBAH	19	19.983	-1.027[b]	-0.235	0.305
T12	SFID	19	23.346	-1.953[a]	-0.448	0.051
T12	IIFD	19	24.013	-1.591[a]	-0.365	0.112
T12	PICP	19	72.728	-0.937[b]	-0.214	0.349
T12	CPBA	19	3.377	-1.570[b]	-0.360	0.116
T12	Area	19	8896.917	0.000[c]	0.000	1.000
T12	RT	19	31.614	-0.087[a]	-0.019	0.931
T13	SFAR	10	17.470	-1.378[a]	-0.316	0.168
T13	SFAL	10	19.498	-1.265[b]	-0.290	0.206
T13	SFA	10	18.482	-1.892[a]	-0.434	0.058
T13	SFPAR	10	18.366	-1.153[b]	-0.264	0.249
T13	SFPAL	10	20.695	-0.460[a]	-0.105	0.646
T13	SFPA	10	19.484	-0.141[a]	-0.032	0.888

[1] Bonferroni Correction: CBA, $p < 0.05$; C1, $p < 0.01$; C2, $p < 0.008$; C3 – L5, $p < 0.004$.
[a] Based on negative ranks.
[b] Based on positive ranks.
[c] The sum negative ranks equals the sum of positive ranks.

Table B-1. Non-significant differences between measurements (cont.).

Level	Variable	N	Mean	z	r	p value [1]
T13	IFAR	10	17.999	-0.511[b]	-0.117	0.610
T13	IFAL	10	20.082	-1.682[a]	-0.385	0.093
T13	IFA	10	19.037	-1.466[a]	-0.336	0.143
T13	IFPAR	10	18.760	-0.493[b]	-0.113	0.622
T13	IFPAL	10	20.844	-1.495[a]	-0.342	0.135
T13	IFPA	10	19.799	-1.150[a]	-0.263	0.250
T13	SVAPAR	10	82.080	-1.125[a]	-0.258	0.260
T13	SVAPAL	10	84.089	-0.770[b]	-0.176	0.441
T13	SVAPA	10	83.921	-0.866[b]	-0.199	0.386
T13	IVAPAR	10	50.729	-0.845[a]	-0.193	0.398
T13	IVAPAL	10	52.097	-0.849[b]	-0.194	0.396
T13	IVAPA	10	51.413	-0.847[b]	-0.194	0.397
T13	VBPH	10	22.448	-1.378[b]	-0.316	0.168
T13	VBAH	10	19.358	-0.204[a]	-0.046	0.838
T13	SFID	10	22.763	-1.734[a]	-0.397	0.083
T13	IIFD	10	24.314	-0.255[a]	-0.058	0.799
T13	PICP	10	72.744	-0.711[b]	-0.163	0.477
T13	CPBA	10	4.510	-1.244[b]	-0.285	0.214
T13	Area	10	9246.522	-1.000[c]	-0.229	0.317
T13	RT	10	31.220	-0.459[b]	-0.105	0.646
L1	SFAR	19	9.831	-0.236[b]	-0.054	0.814
L1	SFAL	19	8.731	-0.446[a]	-0.023	0.656
L1	SFA	19	9.541	-0395[b]	-0.090	0.693
L1	SFPAR	19	10.657	-0.630[a]	-0.144	0.529
L1	SFPAL	19	9.784	-0.491[b]	-0.112	0.623
L1	SFPA	19	10.297	-1.484[a]	-0.340	0.138
L1	IFAR	19	14.661	-1.022[a]	-0.234	0.307
L1	IFAL	19	15.796	-0.830[a]	-0.190	0.407
L1	IFA	19	15.068	-0.718[a]	-0.164	0.473
L1	IFPAR	19	15.334	-0.877[a]	-0.201	0.201
L1	IFPAL	19	16.657	-0.771[a]	-0.176	0.441
L1	IFPA	19	16.081	-0.654[a]	-0.150	0.513
L1	SVAPAR	19	58.996	-1.287[a]	-0.295	0.198
L1	SVAPAL	19	58.152	-0.653[a]	-0.149	0.513
L1	SVAPA	19	57.457	-0.796[a]	-0.182	0.426
L1	IVAPAR	19	37.093	-0.031[b]	-0.007	0.975

[1] Bonferroni Correction: CBA, $p < 0.05$; C1, $p < 0.01$; C2, $p < 0.008$; C3 – L5, $p < 0.004$.
[a] Based on negative ranks.
[b] Based on positive ranks.
[c] The sum negative ranks equals the sum of positive ranks.

Table B-1. Non-significant differences between measurements (cont.).

Level	Variable	N	Mean	z	r	p value [1]
L1	IVAPAL	19	38.113	-1.064[a]	-0.244	0.287
L1	IVAPA	19	37.601	-0.753[a]	-0.172	0.452
L1	VBPH	19	25.693	-0.101[a]	-0.023	0.920
L1	VBAH	19	22.907	-0.362[a]	-0.083	0.718
L1	SFID	19	22.844	-1.655[a]	-0.379	0.098
L1	IIFD	19	24.975	-0.066[a]	-0.015	0.947
L1	PICP	19	80.627	-1.570[b]	-0.360	0.117
L1	CPBA	19	3.796	-0.420[a]	-0.096	0.674
L1	Area	19	10582.456	0.000[c]	0.000	1.000
L1	RT	19	22.671	-0.161[b]	-0.036	0.872
L2	SFAR	19	8.014	-1.153[a]	-0.264	0.249
L2	SFAL	19	8.457	-0.710[b]	-0.162	0.478
L2	SFA	19	8.232	-0.424[b]	-0.097	0.671
L2	SFPAR	19	8.673	-1.547[a]	-0.354	0.122
L2	SFPAL	19	9.140	-1.494[b]	-0.342	0.135
L2	SFPA	19	8.903	-1.053[a]	-0.241	0.292
L2	IFAR	19	14.778	-1.408[a]	-0.323	0.159
L2	IFAL	19	14.774	-1.483[a]	-0.340	0.138
L2	IFA	19	15.361	-0.605[b]	-0.138	0.545
L2	IFPAR	19	15.803	-1.034[a]	-0.237	0.301
L2	IFPAL	19	15.212	-1.574[a]	-0.361	0.116
L2	IFPA	19	16.019	-0.317[a]	-0.072	0.751
L2	SVAPAR	19	51.901	-0.568[b]	-0.130	0.570
L2	SVAPAL	19	54.742	-1.060[a]	-0.243	0.289
L2	SVAPA	19	52.812	-0.331[b]	-0.075	0.740
L2	IVAPAR	19	37.766	-0.654[b]	-0.150	0.513
L2	IVAPAL	19	39.004	-0.199[b]	-0.045	0.842
L2	IVAPA	19	38.382	-0.087[a]	-0.019	0.931
L2	VBPH	19	26.410	-0.087[a]	-0.019	0.931
L2	VBAH	19	23.757	-0.725[b]	-0.166	0.469
L2	SFID	19	22.815	-0.624[a]	-0.143	0.533
L2	IIFD	19	24.959	-1.721[a]	-0.394	0.085
L2	PICP	19	82.912	-1.490[b]	-0.341	0.136
L2	CPBA	19	4.483	-0.511[a]	-0.117	0.609
L2	Area	19	11127.447	0.000[c]	0.000	1.000
L2	RT	19	15.355	-0.141[a]	-0.032	0.888
L3	SFAR	19	5.656	-0.852[b]	-0.195	0.394

[1] Bonferroni Correction: CBA, $p < 0.05$; C1, $p < 0.01$; C2, $p < 0.008$; C3 – L5, $p < 0.004$.
[a] Based on negative ranks.
[b] Based on positive ranks.
[c] The sum negative ranks equals the sum of positive ranks.

Table B-1. Non-significant differences between measurements (cont.).

Level	Variable	N	Mean	z	r	p value [1]
L3	SFAL	19	5.748	-0.852[a]	-0.195	0.394
L3	SFA	19	5.832	-0.624[a]	-0.143	0.533
L3	SFPAR	19	7.168	-0.105[b]	-0.124	0.916
L3	SFPAL	19	7.242	-0.153[b]	-0.035	0.878
L3	SFPA	19	7.094	-0.051[b]	-0.011	0.959
L3	IFAR	19	14.254	-0.422[b]	-0.096	0.673
L3	IFAL	19	13.630	-0.105[a]	-0.024	0.917
L3	IFA	19	13.470	-1.272[a]	-0.291	0.203
L3	IFPAR	19	15.221	-0.946[b]	-0.217	0.344
L3	IFPAL	19	13.885	-1.474[a]	-0.338	0.140
L3	IFPA	19	14.584	-0.141[b]	-0.032	0.888
L3	SVAPAR	19	51.025	-0.070[a]	-0.016	0.944
L3	SVAPAL	19	50.088	-0.942[b]	-0.216	0.346
L3	SVAPA	19	50.449	-0.427[a]	-0.097	0.669
L3	IVAPAR	19	35.823	-0.483[a]	-0.110	0.629
L3	IVAPAL	19	37.106	-0.103[a]	-0.023	0.918
L3	IVAPA	19	36.021	-0.741[a]	-0.169	0.459
L3	VBPH	19	26.103	-0.958[b]	-0.219	0.338
L3	VBAH	19	24.568	-0.664[b]	-0.147	0.520
L3	SFID	19	23.381	-1.369[a]	-0.314	0.171
L3	IIFD	19	26.224	-1.046[a]	-0.239	0.295
L3	PICP	19	86.782	-1.080[b]	-0.247	0.280
L3	CPBA	19	4.033	-0.597[b]	-0.136	0.550
L3	Area	19	11539.257	0.000[c]	0.000	1.000
L3	RT	19	14.643	-0.564[b]	-0.129	0.573
L4	SFAR	19	6.266	0.000[c]	0.000	1.000
L4	SFAL	19	6.302	-0.152[a]	-0.034	0.879
L4	SFA	19	6.203	-0.989[a]	-0.266	0.323
L4	SFPAR	19	6.286	-0.631[b]	-0.144	0.528
L4	SFPAL	19	6.082	-0.422[b]	-0.096	0.673
L4	SFPA	19	6.248	0.000[c]	0.000	1.000
L4	IFAR	19	16.407	-0.844[a]	-0.193	0.398
L4	IFAL	19	15.540	-1.295[b]	-0.297	0.195
L4	IFA	19	16.404	-0.102[b]	-0.023	0.919
L4	IFPAR	19	17.303	-0.281[a]	-0.064	0.778
L4	IFPAL	19	16.036	-0.945[b]	-0.216	0.345

[1] Bonferroni Correction: CBA, $p < 0.05$; C1, $p < 0.01$; C2, $p < 0.008$; C3 – L5, $p < 0.004$.
[a] Based on negative ranks.
[b] Based on positive ranks.
[c] The sum negative ranks equals the sum of positive ranks.

Table B-1. Non-significant differences between measurements (cont.).

Level	Variable	N	Mean	z	r	p value [1]
L4	IFPA	19	16.712	-0.714[a]	-0.163	0.475
L4	SVAPAR	19	53.086	-0.210[a]	-0.048	0.834
L4	SVAPAL	19	53.897	-0.699[b]	-0.160	0.485
L4	SVAPA	19	52.321	-0.751[a]	-0.172	0.453
L4	IVAPAR	19	43.113	-0.533[a]	-0.122	0.594
L4	IVAPAL	19	40.292	-0.825[a]	-0.189	0.410
L4	IVAPA	19	41.700	-0.796[a]	-0.182	0.426
L4	VBPH	19	25.487	-1.111[b]	-0.254	0.267
L4	VBAH	19	25.298	-0.213[c]	-0.048	0.831
L4	SFID	19	23.422	-0.610[a]	-0.139	0.542
L4	IIFD	19	27.591	-0.801[a]	-0.183	0.423
L4	PICP	19	92.025	-0.770[b]	-0.176	0.441
L4	CPBA	19	4.636	-1.381[b]	-0.316	0.167
L4	Area	19	11201.932	0.000[c]	0.000	1.000
L4	RT	19	12.705	-0.450[b]	-0.103	0.653
L5	SFAR	9	5.730	0.000[c]	0.000	1.000
L5	SFAL	9	6.202	-0.447[b]	-0.102	0.655
L5	SFA	9	5.964	-0.816[b]	-0.187	0.414
L5	SFPAR	9	5.161	-0.447[a]	-0.102	0.655
L5	SFPAL	9	6.060	-0.447[b]	-0.102	0.655
L5	SFPA	9	5.608	0.000[c]	0.000	1.000
L5	IFAR	9	17.056	-0.135[b]	-0.030	0.893
L5	IFAL	9	17.208	-0.184[a]	-0.042	0.854
L5	IFA	9	17.133	-0.345[b]	-0.079	0.730
L5	IFPAR	9	17.731	-0.105[b]	-0.024	0.916
L5	IFPAL	9	17.878	-0.944[a]	-0.228	0.345
L5	IFPA	9	17.808	-0.256[b]	-0.058	0.798
L5	SVAPAR	9	60.251	-0.314[b]	-0.072	0.753
L5	SVAPAL	9	60.520	-0.314[b]	-0.072	0.753
L5	SVAPA	9	60.384	-1.690	-0.387	0.091
L5	IVAPAR	9	47.181	-0.365[b]	-0.083	0.715
L5	IVAPAL	9	45.916	0.000[c]	0.000	1.000
L5	IVAPA	9	46.963	-0.944[b]	-0.216	0.345
L5	VBPH	9	22.978	-0.178[a]	-0.040	0.859
L5	VBAH	9	26.435	-1.067[b]	-0.244	0.286
L5	SFID	9	31.260	-1.007[a]	-0.231	0.314

[1] Bonferroni Correction: CBA, $p < 0.05$; C1, $p < 0.01$; C2, $p < 0.008$; C3 – L5, $p < 0.004$.
[a] Based on negative ranks.
[b] Based on positive ranks.
[c] The sum negative ranks equals the sum of positive ranks.

Table B-1. Non-significant differences between measurements (cont.).

Level	Variable	N	Mean	z	r	p value [1]
L5	IIFD	9	43.076	-1.718[a]	-0.394	0.086
L5	PICP	9	96.317	-0.524[b]	-0.542	0.600
L5	CPBA	9	7.550	-1.069[b]	-0.245	0.285
L5	Area	9	12179.163	0.000[c]	0.000	1.000
L5	RT	9	14.316	-0.280[b]	-0.064	0.779
	TCC	19	19.180	-0.141[b]	-0.032	0.888
	TTC	19	43.035	-0.644[b]	-0.147	0.520
	TLC	19	20.233	-1.349[b]	-0.309	0.177
	TCR	19	69.736	-0.458[a]	-0.104	0.647
	RTCR	19	73.471	-0.026[b]	-0.026	0.979
	TTR	19	152.535	-0.443[a]	-0.101	0.658
	RTTR	19	46.385	-1.811[b]	-0.415	0.070
	TLR	19	72.810	-1.127[b]	-0.258	0.260
	RLTR	19	21.733	-0.906[b]	-0.207	0.365

[1] Bonferroni Correction: CBA, $p < 0.05$; C1, $p < 0.01$; C2, $p < 0.008$; C3 – L5, $p < 0.004$.
[a] Based on negative ranks.
[b] Based on positive ranks.
[c] The sum negative ranks equals the sum of positive ranks.

Appendix C: First PCA component results

Table C-1. PCA component matrix[1].

Variable	First Component
C1 SFA	.435
C1 IFA	.545
C1 SVAPA	.746
C1 IVAPA	-.570
C1 Area	-.639
C2 SFA	-.613
C2 IFA	-.496
C2 SVAPA	.326
C2 IVAPA	.944
C2 Area	.242
C2 RT	.861
C3 SFA	.489
C3 SFPA	.521
C3 IFA	-.428
C3 IFPA	-.410
C3 SVAPA	.785
C3 IVAPA	.547
C3 VBPH	.611
C3 VBAH	.618
C3 SFID	.885
C3 IIFD	.924
C3 PICP	-.103
C3 CPBA	.119
C3 Area	.562
C3 RT	-.387
C4 SFA	.112
C4 SFPA	.105
C4 IFA	-.317
C4 IFPA	-.326
C4 SVAPA	.592
C4 IVAPA	.609
C4 VBPH	.711
C4 VBAH	.756
C4 SFID	.921
C4 IIFD	.933
C4 PICP	-.151
C4 CPBA	.090
C4 Area	.586
C4 RT	.097
C5 SFA	.361

[1] Significance level: $p < 0.025$.

Table C-1. PCA component matrix[1] (cont.).

Variable	First Component
C5 SFPA	.383
C5 IFA	-.343
C5 IFPA	-.345
C5 SVAPA	.728
C5 IVAPA	.632
C5 VBPH	.510
C5 VBAH	.642
C5 SFID	.937
C5 IIFD	.944
C5 PICP	-.499
C5 CPBA	-.128
C5 Area	.463
C5 RT	-.178
C6 SFA	.698
C6 SFPA	.735
C6 IFA	-.195
C6 IFPA	-.183
C6 SVAPA	.753
C6 IVAPA	.504
C6 VBPH	.388
C6 VBAH	.468
C6 SFID	.934
C6 IIFD	.915
C6 PICP	-.580
C6 CPBA	-.282
C6 Area	.287
C6 RT	-.018
C7 SFA	.577
C7 SFPA	.589
C7 IFA	.557
C7 IFPA	.564
C7 SVAPA	.124
C7 IVAPA	-.114
C7 VBPH	.877
C7 VBAH	.739
C7 SFID	.684
C7 IIFD	.881
C7 PICP	-.232
C7 CPBA	-.126
C7 Area	.834
C7 RT	-.111

[1] Significance level: $p < 0.025$.

Table C-1. PCA component matrix[1] (cont.).

Variable	First Component
T1 SFA	.146
T1 SFPA	.185
T1 IFA	.418
T1 IFPA	.427
T1 SVAPA	-.030
T1 IVAPA	-.170
T1 VBPH	.892
T1 VBAH	.935
T1 SFID	.883
T1 IIFD	.831
T1 PICP	.456
T1 CPBA	-.341
T1 Area	.843
T1 RT	-.096
T2 SFA	.200
T2 SFPA	.262
T2 IFA	.596
T2 IFPA	.647
T2 SVAPA	-.376
T2 IVAPA	-.041
T2 VBPH	.919
T2 VBAH	.925
T2 SFID	.847
T2IIFD	.717
T2 PICP	.322
T2 CPBA	-.177
T2 Area	.852
T2 RT	.329
T3 SFA	.553
T3 SFPA	.579
T3 IFA	.459
T3 IFPA	.509
T3 SVAPA	-.265
T3 IVAPA	.186
T3 VBPH	.844
T3 VBAH	.901
T3 SFID	.853
T3 IIFD	.877
T3 PICP	.608
T3 CPBA	.085
T3 Area	.693

[1] Significance level: $p < 0.025$.

Table C-1. PCA component matrix[1] (cont.).

Variable	First Component
T3 RT	.382
T4 SFA	.446
T4 SFPA	.463
T4 IFA	.212
T4 IFPA	.289
T4 SVAPA	-.442
T4 IVAPA	.381
T4 VBPH	.820
T4 VBAH	.859
T4SFID	.933
T4 IIFD	.911
T4 PICP	.710
T4 CPBA	-.545
T4 Area	.625
T4 RT	.725
T5 SFA	.421
T5 SFPA	.413
T5 IFA	.058
T5 IFPA	.088
T5 SVAPA	-.240
T5 IVAPA	.427
T5 VBPH	.918
T5 VBAH	.906
T5 SFID	.920
T5 IIFD	.899
T5 PICP	.621
T5 CPBA	-.054
T5 Area	.760
T5 RT	.605
T6 SFA	.236
T6 SFPA	.293
T6 IFA	-.288
T6 IFPA	-.210
T6 SVAPA	-.154
T6 IVAPA	.384
T6 VBPH	.923
T6 VBAH	.872
T6 SFID	.927
T6 IIFD	.915
T6 PICP	.369
T6 CBPA	-.071

[1] Significance level: $p < 0.025$.

Table C-1. PCA component matrix[1] (cont.).

Variable	First Component
T6 Area	.841
T6 RT	.463
T7 SFA	.033
T7 SFPA	.053
T7 IFA	-.302
T7 IFPA	-.269
T7 SVAPA	-.027
T7 IVAPA	-.122
T7 VBPH	.949
T7 VBAH	.922
T7 SFID	.936
T7 IIFD	.933
T7 PICP	.243
T7 CPBA	.230
T7 Area	.878
T7 RT	-.065
T8 SFA	-.510
T8 SFPA	-.510
T8 IFA	-.547
T8 IFPA	-.545
T8 SVAPA	.245
T8 IVAPA	.400
T8 VBPH	.851
T8 VBAH	.862
T8 SFID	.885
T8 IIFD	.875
T8 PICP	.382
T8 CPBA	-.090
T8 Area	.695
T8 RT	.155
T9 SFA	-.665
T9 SFPA	-.666
T9 IFA	-.469
T9 IFPA	-.448
T9 SVAPA	.103
T9 IVAPA	.302
T9 VBPH	.914
T9 VBAH	.922
T9 SFID	.899
T9 IIFD	.870
T9 PICP	.079

[1] Significance level: $p < 0.025$.

Table C-1. PCA component matrix[1] (cont.).

Variable	First Component
T9 CPBA	-.400
T9 Area	.753
T9 RT	.215
T10 SFA	-.694
T10 SFPA	-.690
T10 IFA	-.435
T10 IFPA	-.437
T10 SVAPA	.457
T10 IVAPA	.233
T10 VBPH	.916
T10 VBAH	.937
T10 SFID	.874
T10 IIFD	.777
T10 PICP	.351
T10 CPBA	-.359
T10 Area	.733
T10 RT	-.176
T11 SFA	-.430
T11 SFPA	-.426
T11 IFA	.537
T11 IFPA	.540
T11 SVAPA	.038
T11 IVAPA	-.620
T11 VBPH	.863
T11 VBAH	.820
T11 SFID	.825
T11 IIFD	.659
T11 PICP	.339
T11 CPBA	-.386
T11 Area	.798
T11 RT	.525
T12 SFA	-.608
T12 SFPA	-.597
T12 IFA	.417
T12 IFPA	.429
T12 SVAPA	-.544
T12 IVAPA	-.861
T12 VBPH	.906
T12 VBAH	.917
T12 SFID	.690
T12 IIFD	.452

[1] Significance level: $p < 0.025$.

Table C-1. PCA component matrix[1] (cont.).

Variable	First Component
T12 PICP	.663
T12 CPBA	-.326
T12 Area	.693
T12 RT	.613
T13 SFA	.154
T13 SFPA	.089
T13 IFA	-.039
T13 IFPA	-.081
T13 SVAPA	.145
T13 IVAPA	.399
T13 VBPH	.869
T13 VBAH	.909
T13 SFID	.815
T13 IIFD	.689
T13 PICP	.719
T13 CPBA	-.712
T13 Area	.886
T13 RT	-.290
L1 SFA	-.597
L1 SFPA	-.595
L1 IFA	-.478
L1 IFPA	-.459
L1 SVAPA	-.508
L1 IVAPA	-.618
L1 VBPH	.698
L1 VBAH	.809
L1SFID	.360
L1 IIFD	.263
L1 PICP	.645
L1 CPBA	.172
L1 Area	.588
L1 RT	.341
L2 SFA	-.568
L2 SFPA	-.572
L2 IFA	-.498
L2 IFPA	-.503
L2 SVAPA	-.503
L2 IVAPA	-.628
L2 VBPH	.631
L2 VBAH	.807
L2 SFID	.215

[1] Significance level: $p < 0.025$.

Table C-1. PCA component matrix[1] (cont.).

Variable	First Component
L2 IIFD	.331
L2 PICP	.717
L2 CPBA	-.161
L2 Area	.597
L2 RT	.394
L3 SFA	-.352
L3 SFPA	-.396
L3 IFA	.094
L3 IFPA	.060
L3 SVAPA	-.433
L3 IVAPA	-.256
L3 VBPH	.706
L3 VBAH	.861
L3 SFID	.696
L3 IIFD	.799
L3 PICP	.692
L3 CPBA	.330
L3 Area	.802
L3 RT	-.112
L4 SFA	-.232
L4 SFPA	-.178
L4 IFA	.381
L4 IFPA	.399
L4 SVAPA	.421
L4 IVAPA	.694
L4 VBPH	.519
L4 VBAH	.698
L4 SFID	.840
L4 IIFD	.907
L4 PICP	.540
L4 CPBA	.594
L4 Area	.738
L4 RT	-.605
L5 SFA	.253
L5 SFPA	.228
L5 IFA	-.440
L5 IFPA	-.456
L5 SVAPA	.094
L5 IVAPA	-.184
L5 VBPH	.531
L5 VBAH	.624

[1] Significance level: $p < 0.025$.

Table C-1. PCA component matrix[1] (cont.).

Variable	First Component
L5 SFID	.639
L5 IIFD	.790
L5 PICP	.279
L5 CPBA	.145
L5 Area	.639
L5 RT	.269

[1] Significance level: $p < 0.025$.

Appendix D: Regression coefficient

Regression (Variable/GM) for male and female (*Homo*)

Table D-1. Significant differences between males and females – *Homo*.

Intercept Variable	Unstandardized Coefficients		t	p value [1]
	B	Std. Error		
C1 IFA	78.322	13.264	5.905	0.000
C2 SFA	108.478	5.441	19.939	0.000
C2 IFA	39.379	9.067	4.434	0.000
C2 IVAPA	-25.353	5.713	-4.437	0.000
C2 Area	5322.680	1054.275	5.049	0.000
C2 RT	-30.821	9.498	-3.245	0.003
C3 IFA	38.367	8.794	4.363	0.000
C3 IFPA	38.444	9.171	4.192	0.000
C3 SVAPA	104.946	21.379	4.909	0.000
C3 IVAPA	74.192	12.898	5.752	0.000
C3 VBPH	11.896	2.653	4.484	0.000
C3 VBAH	8.724	2.803	3.112	0.004
C3 SFID	28.536	3.406	8.379	0.000
C3 IIFD	24.665	4.054	6.084	0.000
C3 PICP	104.112	9.840	10.581	0.000
C3 Area	3843.536	900.084	4.270	0.000
C4 SVAPA	113.658	19.515	5.824	0.000
C4 IVAPA	68.579	16.474	4.163	0.000
C4 VBPH	11.816	2.061	5.734	0.000
C4 VBAH	11.752	2.831	4.152	0.000
C4 SFID	34.650	3.953	8.766	0.000
C4 IIFD	35.362	4.345	8.139	0.000
C4 PICP	103.667	9.256	11.200	0.000
C4 Area	3655.620	890.068	4.107	0.000
C4 RT	-52.603	10.221	-5.146	0.000
C5 SVAPA	77.783	16.866	4.612	0.000
C5 IVAPA	102.971	14.208	7.247	0.000
C5 SFID	27.118	4.255	6.374	0.000
C5 IIFD	28.811	3.783	7.439	0.000
C5 PICP	73.929	13.421	5.508	0.000
C5 RT	-29.884	7.171	-4.168	0.000
C6 SVAPA	95.001	5.465	17.384	0.000
C6 IVAPA	131.996	11.515	11.463	0.000
C6 VBPH	7.362	1.734	4.246	0.000
C6 VBAH	8.233	1.853	4.444	0.000

[1] Bonferroni Correction: C1, $p < 0.01$; C2, $p < 0.008$; C3 – L5, $p < 0.004$.

Table D-1. Significant differences between males and females – *Homo* (cont.).

Intercept Variable	Unstandardized Coefficients		t	p value [1]
	B	Std. Error		
C6 SFID	31.116	2.592	12.007	0.000
C6 IIFD	24.252	2.732	8.877	0.000
C6 PICP	66.671	11.572	5.761	0.000
C6 RT	-42.164	7.143	-5.903	0.000
C7 SVAPA	95.443	18.459	5.171	0.000
C7 IVAPA	79.860	21.595	3.698	0.001
C7 VBPH	12.227	3.122	3.916	0.001
C7 VBAH	16.452	2.924	5.627	0.000
C7 PICP	96.455	10.434	9.245	0.000
T1 IFA	-38.007	7.074	-5.373	0.000
T1 IFPA	-38.243	7.476	-5.116	0.000
T1 SVAPA	134.756	11.722	11.496	0.000
T1 IVAPA	118.330	13.182	8.977	0.000
T1 VBPH	21.465	2.167	9.904	0.000
T1 VBAH	19.271	1.600	12.046	0.000
T1 SFID	38.581	3.393	11.370	0.000
T1 IIFD	34.511	3.173	10.877	0.000
T1 PICP	79.845	12.760	6.258	0.000
T1 Area	9028.851	1540.497	5.861	0.000
T2 SVAPA	142.818	9.525	14.994	0.000
T2 IVAPA	119.073	11.752	10.132	0.000
T2 VBPH	21.449	3.060	7.009	0.000
T2 VBAH	16.709	2.900	5.762	0.000
T2 SFID	28.194	3.186	8.848	0.000
T2 IIFD	27.075	4.459	6.071	0.000
T2 PICP	70.791	15.681	4.515	0.000
T2 Area	8818.958	2038.414	4.326	0.000
T3 IFA	-26.251	6.122	-4.288	0.000
T3 IFPA	-22.498	6.732	-3.342	0.002
T3 SVAPA	117.739	7.386	15.942	0.000
T3 IVAPA	95.778	12.261	7.812	0.000
T3 VBPH	23.145	2.909	7.956	0.000
T3 VBAH	20.666	2.689	7.685	0.000
T3 SFID	30.846	3.806	8.105	0.000
T3 IIFD	28.378	4.065	6.981	0.000
T3 PICP	64.713	11.866	5.454	0.000
T3 Area	9544.515	1982.353	4.815	0.000
T4 IFA	-27.338	4.557	-5.999	0.000

[1] Bonferroni Correction: C1, $p < 0.01$; C2, $p < 0.008$; C3 – L5, $p < 0.004$.

Table D-1. Significant differences between males and females – *Homo* (cont.).

Intercept Variable	Unstandardized Coefficients		t	p value [1]
	B	Std. Error		
T4 IFPA	-27.571	4.207	-6.553	0.000
T4 SVAPA	119.050	10.499	11.340	0.000
T4 IVAPA	109.949	11.926	9.219	0.000
T4 VBPH	22.282	3.227	6.905	0.000
T4 VBAH	22.380	2.840	7.879	0.000
T4 SFID	24.842	3.574	6.951	0.000
T4 IIFD	26.644	3.836	6.946	0.000
T4 PICP	56.961	9.019	6.135	0.000
T4 Area	10334.15	2018.250	5.120	0.000
T5 IFA	-13.113	3.351	-3.913	0.000
T5 IFPA	-12.617	3.240	-3.894	0.000
T5 SVAPA	121.770	7.894	15.426	0.000
T5 IVAPA	112.288	6.165	18.214	0.000
T5 VBPH	21.724	1.962	11.071	0.000
T5 VBAH	17.277	2.000	8.636	0.000
T5 SFID	20.461	2.015	10.152	0.000
T5 IIFD	22.715	2.574	8.824	0.000
T5 PICP	58.352	5.215	11.190	0.000
T5 Area	9182.493	1343.274	6.836	0.000
T6 SVAPA	116.501	8.702	13.387	0.000
T6 IVAPA	97.588	8.062	12.105	0.000
T6 VBPH	23.632	2.184	10.820	0.000
T6 VBAH	24.104	2.724	8.847	0.000
T6 SFID	18.569	3.074	6.042	0.000
T6 IIFD	23.692	3.621	6.543	0.000
T6 PICP	70.310	6.713	10.474	0.000
T6 Area	8639.782	1695.386	5.096	0.000
T7 SVAPA	118.589	7.211	16.444	0.000
T7 IVAPA	104.555	6.334	16.507	0.000
T7 VBPH	21.396	2.193	9.756	0.000
T7 VBAH	19.715	2.436	8.093	0.000
T7 SFID	24.383	3.297	7.396	0.000
T7 IIFD	28.183	3.141	8.974	0.000
T7 PICP	73.276	4.717	15.535	0.000
T7 Area	8307.971	1778.085	4.672	0.000
T8 SVAPA	123.825	10.302	12.020	0.000
T8 IVAPA	105.124	8.707	12.073	0.000
T8 VBPH	22.036	2.747	8.021	0.000

[1] Bonferroni Correction: C1, $p < 0.01$; C2, $p < 0.008$; C3 – L5, $p < 0.004$.

Table D-1. Significant differences between males and females – *Homo* (cont.).

Intercept Variable	Unstandardized Coefficients		t	p value [1]
	B	Std. Error		
T8 VBAH	21.133	2.789	7.576	0.000
T8 SFID	26.820	4.611	5.817	0.000
T8 IIFD	22.991	6.317	3.640	0.001
T8 PICP	80.713	9.156	8.815	0.000
T9 SVAPA	116.747	8.618	13.547	0.000
T9 IVAPA	95.460	8.793	10.856	0.000
T9 VBPH	20.110	2.541	7.915	0.000
T9 VBAH	16.037	2.652	6.047	0.000
T9 SFID	19.092	3.698	5.163	0.000
T9 IIFD	22.559	3.991	5.653	0.000
T9 PICP	66.907	6.791	9.852	0.000
T9 Area	6424.787	2002.693	3.208	0.003
T10 SVAPA	113.503	11.348	10.002	0.000
T10 IVAPA	90.211	14.755	6.114	0.000
T10 VBPH	21.094	2.754	7.659	0.000
T10 VBAH	20.608	3.015	6.835	0.000
T10 SFID	26.025	5.753	4.524	0.000
T10 IIFD	27.140	5.599	4.847	0.000
T10 PICP	77.305	6.961	11.105	0.000
T11 IFA	-21.960	5.319	-4.128	0.000
T11 IFPA	-20.146	5.354	-3.763	0.001
T11 SVAPA	121.590	5.875	20.696	0.000
T11 IVAPA	241.725	25.360	9.532	0.000
T11 VBPH	23.581	2.211	10.664	0.000
T11 VBAH	24.581	1.936	12.694	0.000
T11 SFID	20.410	2.856	7.146	0.000
T11 IIFD	23.563	3.081	7.649	0.000
T11 PICP	83.035	3.781	21.961	0.000
T11 Area	8810.292	1524.787	5.778	0.000
T11 RT	-103.667	19.736	-5.253	0.000
T12 VBPH	22.270	2.453	9.080	0.000
T12 VBAH	20.483	2.901	7.061	0.000
T12 SFID	15.050	3.157	4.768	0.000
T12 IIFD	19.411	2.858	6.791	0.000
T12 PICP	76.922	7.080	10.864	0.000
T12 Area	6452.986	1937.015	3.331	0.002
T12 RT	-84.668	22.324	-3.793	0.001

[1] Bonferroni Correction: C1, $p < 0.01$; C2, $p < 0.008$; C3 – L5, $p < 0.004$.

Table D-1. Significant differences between males and females – *Homo* (cont.).

Intercept Variable	Unstandardized Coefficients		t	p value [1]
	B	Std. Error		
L1 SFA	-13.699	3.484	-3.932	0.000
L1 SFPA	-13.821	3.211	-4.305	0.000
L1 IVAPA	29.989	9.639	3.111	0.004
L1 VBPH	29.572	2.040	14.493	0.000
L1 VBAH	25.289	2.557	9.889	0.000
L1 SFID	26.143	2.292	11.405	0.000
L1 IIFD	26.574	2.914	9.118	0.000
L1 PICP	76.342	5.274	14.474	0.000
L1 Area	13480.73	2080.405	6.480	0.000
L2 SFA	-11.143	3.193	-3.489	0.001
L2 SFPA	-11.042	3.458	-3.193	0.003
L2 IVAPA	43.403	9.677	4.485	0.000
L2 VBPH	25.811	2.957	8.730	0.000
L2 VBAH	24.789	3.558	6.966	0.000
L2 SFID	23.241	3.441	6.755	0.000
L2 IIFD	21.435	3.880	5.525	0.000
L2 PICP	93.606	8.528	10.976	0.000
L3 IVAPA	39.481	11.370	3.473	0.002
L3 VBPH	26.192	2.189	11.966	0.000
L3 VBAH	28.886	2.302	12.546	0.000
L3 SFID	24.744	2.791	8.866	0.000
L3 IIFD	25.151	3.691	6.814	0.000
L3 PICP	93.647	3.831	24.445	0.000
L3 Area	10748.29	2422.794	4.436	0.000
L4 SVAPA	39.974	7.921	5.047	0.000
L4 IVAPA	61.813	14.136	4.373	0.000
L4 VBPH	28.839	3.135	9.200	0.000
L4 VBAH	25.543	2.519	10.140	0.000
L4 SFID	21.424	4.217	5.080	0.000
L4 IIFD	30.477	5.909	5.158	0.000
L4 PICP	94.905	6.329	14.996	0.000
L4 Area	8975.753	2792.413	3.214	0.003
L5 SFA	-16.968	3.675	-4.617	0.000
L5 SFPA	-13.223	3.609	-3.664	0.001
L5 SVAPA	54.268	8.779	6.181	0.000
L5 IVAPA	69.554	11.928	5.831	0.000
L5 VBPH	22.049	2.585	7.715	0.000

[1] Bonferroni Correction: C1, $p < 0.01$; C2, $p < 0.008$; C3 – L5, $p < 0.004$.

Table D-1. Significant differences between males and females – *Homo* (cont.).

Intercept Variable	Unstandardized Coefficients		t	p value [1]
	B	Std. Error		
L5 VBAH	25.029	3.213	7.789	0.000
L5 SFID	25.648	5.205	4.928	0.000
L5 IIFD	33.840	7.488	4.519	0.000
L5 PICP	104.302	4.747	21.974	0.000

[1] Bonferroni Correction: C1, $p < 0.01$; C2, $p < 0.008$; C3 – L5, $p < 0.004$.

Regression (Variable/GM) for male and female (*Gorilla*)

Table D-2. Significant differences between males and females – *Gorilla*.

Intercept Variable	Unstandardized Coefficients		t	p value [1]
	B	Std. Error		
C1 SFA	92.035	6.366	14.458	0.000
C1 IFA	83.644	25.913	3.228	0.007
C2 SFA	108.675	20.127	5.399	0.000
C2 RT	-34.483	9.782	-3.525	0.004
C3 SVAPA	63.936	12.865	4.970	0.000
C3 IVAPA	52.655	15.337	3.433	0.004
C3 IIFD	29.155	7.928	3.677	0.003
C3 PICP	98.567	8.766	11.244	0.000
C4 SVAPA	78.496	14.194	5.530	0.000
C4 IVAPA	47.161	11.843	3.982	0.001
C4 SFID	27.028	5.577	4.846	0.000
C4 IIFD	25.530	6.717	3.801	0.002
C4 PICP	95.335	6.629	14.383	0.000
C4 RT	-25.796	7.349	-3.510	0.003
C5 PICP	156.694	21.092	7.429	0.000
C6 IVAPA	70.457	16.439	4.286	0.001
C6 PICP	120.930	14.845	8.146	0.000
C7 SVAPA	55.923	9.423	5.935	0.000
C7 IVAPA	70.884	10.262	6.907	0.000
C7 PICP	104.415	15.903	6.566	0.000
T1 IVAPA	93.551	26.146	3.578	0.003
T1 PICP	58.351	12.971	4.498	0.001
T2 SVAPA	113.314	13.597	8.334	0.000
T2 IVAPA	101.080	13.655	7.402	0.000
T2 IIFD	16.159	4.156	3.888	0.002
T2 PICP	76.853	9.092	8.453	0.000
T3 SVAPA	117.165	7.618	15.380	0.000
T3 IVAPA	107.736	9.543	11.290	0.000
T3 SFID	19.215	4.257	4.514	0.001
T3 PICP	63.175	9.488	6.659	0.000
T4 SVAPA	116.529	6.434	18.110	0.000
T4 IVAPA	93.966	9.300	10.103	0.000
T4 PICP	55.300	13.486	4.101	0.001
T5 SVAPA	118.913	6.909	17.211	0.000
T5 IVAPA	107.382	6.797	15.799	0.000

[1] Bonferroni Correction: C1, $p < 0.01$; C2, $p < 0.008$; C3 – L5, $p < 0.004$.

Table D-2. Significant differences between males and females – *Gorilla* (cont.).

Intercept Variable	Unstandardized Coefficients		t	p value [1]
	B	Std. Error		
T5 SFID	15.564	4.032	3.860	0.002
T5 IIFD	14.366	3.391	4.236	0.001
T5 PICP	71.318	7.305	9.764	0.000
T6 SVAPA	118.025	9.165	12.878	0.000
T6 IVAPA	106.788	6.913	15.447	0.000
T6 SFID	17.389	4.173	4.168	0.001
T6 IIFD	14.275	3.804	3.753	0.002
T6 PICP	69.325	12.288	5.642	0.000
T7 SVAPA	124.224	8.714	14.255	0.000
T7 IVAPA	119.885	9.873	12.143	0.000
T7 SFID	10.569	2.766	3.820	0.002
T7 IIFD	12.886	3.097	4.161	0.001
T7 PICP	75.337	9.758	7.720	0.000
T8 SVAPA	115.117	4.990	23.069	0.000
T8 IVAPA	98.378	5.624	17.493	0.000
T8 SFID	16.099	2.311	6.967	0.000
T8 IIFD	15.451	2.320	6.660	0.000
T8 PICP	85.253	7.049	12.095	0.000
T9 SVAPA	124.808	6.445	19.365	0.000
T9 IVAPA	97.294	10.760	9.043	0.000
T9 SFID	12.534	3.190	3.929	0.002
T9 PICP	73.781	7.977	9.249	0.000
T10 SVAPA	104.735	7.115	14.721	0.000
T10 IVAPA	88.070	11.415	7.715	0.000
T10 PICP	85.087	10.036	8.478	0.000
T11 SVAPA	110.092	7.896	13.942	0.000
T11 IVAPA	97.618	15.079	6.474	0.000
T11 VBPH	20.05	5.347	3.750	0.002
T11 VBAH	18.201	4.557	3.995	0.001
T11 SFID	15.352	4.129	3.719	0.002
T11 IIFD	20.267	5.655	3.584	0.003
T11 PICP	88.754	6.646	13.355	0.000
T12 SVAPA	109.013	11.315	9.635	0.000
T12 IVAPA	129.615	14.163	9.152	0.000
T12 PICP	77.601	5.078	15.280	0.000
T13 SVAPA	75.138	19.640	3.826	0.002
T13 IVAPA	75.138	19.640	3.826	0.002
T13 SFID	14.678	3.285	4.469	0.001

[1] Bonferroni Correction: C1, $p < 0.01$; C2, $p < 0.008$; C3 – L5, $p < 0.004$.

Table D-2. Significant differences between males and females – *Gorilla* (cont.).

Intercept Variable	Unstandardized Coefficients		t	p value [1]
	B	Std. Error		
T13 IIFD	17.486	4.671	3.744	0.002
T13 PICP	87.070	5.692	15.298	0.000
L1 SVAPA	49.660	13.037	3.809	0.002
L1 VBPH	21.484	5.286	4.064	0.001
L1 VBAH	20.810	4.902	4.245	0.001
L1 SFID	13.947	2.993	4.660	0.000
L1 IIFD	16.558	3.842	4.310	0.001
L1 PICP	94.232	4.230	22.276	0.000
L2 VBPH	21.602	5.747	3.759	0.002
T11 VBAH	18.201	4.557	3.995	0.001
L2 VBAH	22.233	5.171	4.300	0.001
L2 IIFD	14.258	3.802	3.750	0.002
L2 PICP	89.002	7.821	11.380	0.000
L3 VBPH	22.156	4.728	4.687	0.000
L3 VBAH	20.859	4.252	4.905	0.000
L3 SFID	11.831	3.491	3.389	0.004
L3 IIFD	14.080	2.688	5.237	0.000
L3 PICP	80.259	5.640	14.231	0.000
L4 PICP	89.074	7.138	12.479	0.000

[1] Bonferroni Correction: C1, $p < 0.01$; C2, $p < 0.008$; C3 – L5, $p < 0.004$.

Regression (Variable/GM) for male and female (*Pan*)

Table D-3. Significant differences between males and females – *Pan*.

Intercept Variable	Unstandardized Coefficients		t	p value [1]
	B	Std. Error		
C1 SFA	89.750	3.611	24.854	0.000
C1 IFA	76.487	10.222	7.483	0.000
C1 IVAPA	-31.224	6.870	-4.545	0.000
C2 SFA	109.965	14.418	7.627	0.000
C2 IVAPA	-16.850	5.084	-3.314	0.006
C3 VBAH	8.812	2.477	3.558	0.004
C3 PICP	121.044	5.249	23.061	0.000
C4 SVAPA	92.593	15.073	6.143	0.000
C4 IVAPA	59.440	11.735	5.065	0.000
C4 VBAH	8.047	2.318	3.471	0.004
C4 IIFD	24.561	6.067	4.048	0.001
C4 PICP	92.877	16.143	5.753	0.000
C5 IFA	47.740	12.661	3.771	0.002
C5 IFPA	49.351	12.798	3.856	0.002
C5 SVAPA	74.517	11.775	6.329	0.000
C5 IVAPA	61.991	11.834	5.238	0.000
C5 VBPH	7.991	2.241	3.566	0.003
C5 SFID	22.177	4.732	4.686	0.000
C1 SFA	89.750	3.611	24.854	0.000
C5 IIFD	22.418	4.415	5.078	0.000
C5 PICP	95.386	13.138	7.260	0.000
C6 IVAPA	73.496	13.845	5.309	0.000
C6 VBPH	7.464	1.451	5.143	0.000
C6 VBAH	7.818	2.040	3.832	0.002
C6 SFID	30.282	7.531	4.021	0.001
C6 IIFD	29.199	7.544	3.871	0.002
C6 PICP	110.249	7.224	15.261	0.000
C7 VBPH	10.420	1.037	10.050	0.000
C7 VBAH	12.812	1.705	7.516	0.000
C7 SFID	23.603	6.143	3.483	0.002
C7 PICP	130.118	32.314	4.027	0.001
C7 RT	-50.623	12.904	-3.923	0.002
T1 IVAPA	138.135	24.349	5.673	0.000
T1 VBAH	13.659	2.771	4.929	0.000
T1 SFID	26.087	6.969	3.743	0.002
T1 PICP	92.608	25.782	3.592	0.003

[1] Bonferroni Correction: C1, $p < 0.01$; C2, $p < 0.008$; C3 – L5, $p < 0.004$.

Table D-3. Significant differences between males and females – *Pan* (cont.).

Intercept Variable	Unstandardized Coefficients		t	p value [1]
	B	Std. Error		
T1 CPBA	-29.483	6.684	-4.411	0.001
T1 Area	5117.368	1459.379	3.507	0.003
T2 SVAPA	138.418	8.776	15.773	0.000
T2 IVAPA	121.067	9.883	12.251	0.000
T2 VBPH	16.066	1.171	13.722	0.000
T2 VBAH	13.885	1.701	8.164	0.000
T2 IIFD	16.520	3.251	5.081	0.000
T2 PICP	54.516	9.834	5.544	0.000
T2 Area	4696.832	988.833	4.750	0.000
T3 IFA	-10.532	2.474	-4.257	0.001
T3 SVAPA	115.847	6.797	17.043	0.000
T3 IVAPA	102.511	8.179	12.533	0.000
T3 VBPH	15.375	1.573	9.772	0.000
T3 VBAH	13.351	1.574	8.481	0.000
T3 SFID	16.618	2.390	6.953	0.000
T3 IIFD	16.552	2.272	7.284	0.000
T3 PICP	60.356	7.837	7.702	0.000
T3 Area	4274.865	878.504	4.866	0.000
T4 SVAPA	113.556	7.584	14.974	0.000
T4 IVAPA	100.360	6.531	15.366	0.000
T4 VBPH	12.322	1.635	7.536	0.000
T4 VBAH	12.189	1.394	8.743	0.000
T4 SFID	15.346	1.933	7.937	0.000
T4 IIFD	17.197	1.055	16.297	0.000
T4 PICP	62.330	3.937	15.832	0.000
T4 Area	3548.471	697.962	5.084	0.000
T5 SVAPA	120.446	11.582	10.399	0.000
T5 IVAPA	76.538	7.766	9.856	0.000
T5 VBPH	10.059	2.500	4.024	0.001
T5 VBAH	9.009	2.567	3.509	0.003
T5 SFID	16.726	3.867	4.325	0.001
T5 IIFD	13.552	3.769	3.596	0.003
T5 PICP	53.686	12.727	4.128	0.001
T5 RT	-35.632	8.555	-4.165	0.001
T6 SVAPA	113.597	5.917	19.199	0.000
T6 IVAPA	97.919	9.015	10.862	0.000
T6 VBPH	13.283	1.802	7.370	0.000

[1] Bonferroni Correction: C1, $p < 0.01$; C2, $p < 0.008$; C3 – L5, $p < 0.004$.

Table D-3. Significant differences between males and females – *Pan* (cont.).

Intercept Variable	Unstandardized Coefficients		t	p value [1]
	B	Std. Error		
T6 VBAH	12.855	1.301	9.879	0.000
T6 SFID	14.623	3.040	4.810	0.000
T6 IIFD	15.184	3.892	3.901	0.002
T6 PICP	67.494	8.914	7.571	0.000
T7 SVAPA	126.508	9.525	13.281	0.000
T7 IVAPA	99.338	7.932	12.524	0.000
T7 VBPH	12.016	1.741	6.900	0.000
T7 VBAH	11.799	2.142	5.509	0.000
T7 SFID	17.003	2.694	6.311	0.000
T7 IIFD	15.968	1.880	8.491	0.000
T7 PICP	62.552	4.422	14.145	0.000
T8 SVAPA	124.208	10.305	12.053	0.000
T8 IVAPA	100.315	9.988	10.044	0.000
T8 VBPH	11.644	1.687	6.904	0.000
T8 VBAH	8.675	1.735	4.999	0.000
T8 SFID	14.645	2.485	5.893	0.000
T8 IIFD	18.073	2.342	7.716	0.000
T8 PICP	59.070	10.007	5.903	0.000
T8 RT	-23.838	6.091	-3.914	0.002
T9 SVAPA	119.792	11.019	10.871	0.000
T9 IVAPA	90.724	8.474	10.706	0.000
T9 VBPH	14.263	1.993	7.157	0.000
T9 VBAH	10.795	2.685	4.021	0.001
T9 SFID	20.321	3.549	5.725	0.000
T9 IIFD	19.287	3.045	6.335	0.000
T9 PICP	68.384	9.583	7.136	0.000
T10 SVAPA	111.775	11.606	9.630	0.000
T10 IVAPA	94.990	8.806	10.787	0.000
T10 VBPH	12.465	1.833	6.802	0.000
T10 VBAH	12.165	2.755	4.415	0.001
T10 SFID	14.605	3.638	4.015	0.001
T10 IIFD	17.621	4.797	3.673	0.003
T10 PICP	78.573	13.415	5.857	0.000
T11 SVAPA	81.648	9.137	8.936	0.000
T11 IVAPA	80.106	11.626	6.890	0.000
T11 VBPH	12.442	2.643	4.707	0.000
T11 VBAH	9.821	2.440	4.024	0.001

[1] Bonferroni Correction: C1, $p < 0.01$; C2, $p < 0.008$; C3 – L5, $p < 0.004$.

Table D-3. Significant differences between males and females – *Pan* (cont.).

Intercept Variable	Unstandardized Coefficients		t	p value [1]
	B	Std. Error		
T11 SFID	17.565	3.991	4.401	0.001
T11 IIFD	20.558	4.781	4.300	0.001
T11 PICP	59.885	11.819	5.067	0.000
T12 IFA	-32.413	6.687	-4.847	0.000
T12 IFPA	-31.335	6.432	-4.872	0.000
T12 SVAPA	107.227	6.604	16.237	0.000
T12 IVAPA	219.458	36.847	5.956	0.000
T12 VBPH	16.162	1.595	10.130	0.000
T12 VBAH	15.124	1.362	11.103	0.000
T12 SFID	15.892	2.448	6.492	0.000
T12 IIFD	14.671	3.821	3.839	0.002
T12 PICP	68.700	7.370	9.322	0.000
T12 Area	4564.571	1209.974	3.772	0.002
T13 SFA	-36.053	8.293	-4.347	0.001
T13 SFPA	-35.007	8.274	-4.231	0.001
T13 VBPH	17.120	2.506	6.833	0.000
T13 VBAH	13.808	3.289	4.198	0.001
T13 PICP	63.988	11.367	5.629	0.000
L1 SVAPA	57.445	5.603	10.253	0.000
L1 VBPH	20.198	2.111	9.568	0.000
L1 VBAH	19.741	1.790	11.030	0.000
L1 SFID	19.157	2.870	6.675	0.000
L1 IIFD	23.456	4.693	4.998	0.000
L1 PICP	83.275	7.416	11.228	0.000
L1 Area	6553.649	1233.036	5.315	0.000
L2 VBPH	16.851	1.828	9.217	0.000
L2 VBAH	18.596	3.599	5.167	0.000
L2 SFID	16.853	3.149	5.352	0.000
L2 IIFD	20.428	3.847	5.310	0.000
L2 PICP	83.127	6.203	13.401	0.000
L2 Area	5787.229	1224.124	4.728	0.000
L3 SFA	-14.528	3.195	-4.547	0.000
L3 SFPA	-19.839	5.109	-3.883	0.002
L3 SVAPA	24.802	6.556	3.783	0.002
L3 VBPH	18.890	1.696	11.137	0.000
L3 VBAH	20.432	1.659	12.317	0.000
L3 SFID	17.014	2.774	6.133	0.000
L3 IIFD	17.189	3.760	4.571	0.000

[1] Bonferroni Correction: C1, $p < 0.01$; C2, $p < 0.008$; C3 – L5, $p < 0.004$.

Table D-3. Significant differences between males and females – *Pan* (cont.).

Intercept Variable	Unstandardized Coefficients		t	p value[1]
	B	Std. Error		
L3 PICP	88.934	5.853	15.195	0.000
L3 Area	5231.684	1185.011	4.415	0.001
L4 SFA	-16.455	4.491	-3.664	0.004
L4 SFPA	-19.556	2.669	-7.326	0.000
L4 SVAPA	55.933	9.354	5.980	0.000
L4 VBPH	19.554	3.638	5.375	0.000
L4 VBAH	18.120	2.891	6.267	0.000
L4 SFID	18.273	4.935	3.703	0.004
L4 PICP	97.281	17.709	5.493	0.000

[1] Bonferroni Correction: C1, $p < 0.01$; C2, $p < 0.008$; C3 – L5, $p < 0.004$.

Regression (Variable/GM) among taxa (*Homo, Pan,* and *Gorilla*)

Table D-4. Significant differences among taxa.

Intercept Variable	Unstandardized Coefficients		t	p value [1]
	B	Std. Error		
C1 SFA	72.544	9.110	7.963	0.000
C1 IFA	91.657	9.262	9.896	0.000
C1 Area	-6930.899	1714.208	-4.043	0.000
C2 SFA	115.329	4.322	26.684	0.000
C2 IFA	50.904	4.730	10.761	0.000
C2 IVAPA	-20.837	2.765	-7.536	0.000
C2 RT	-18.902	4.267	-4.430	0.000
C3 IFA	45.705	7.696	5.959	0.000
C3 IFPA	44.881	7.550	5.945	0.000
C3 VBPH	7.383	2.425	3.044	0.003
C3 VBAH	7.005	2.091	3.350	0.001
C3 PICP	103.977	5.490	18.941	0.000
C4 IFA	32.066	9.054	3.541	0.001
C4 IFPA	32.478	8.688	3.738	0.000
C4 SVAPA	78.900	12.976	6.080	0.000
C4 IVAPA	50.774	11.292	4.497	0.000
C4 SFID	19.336	4.743	4.077	0.000
C4 IIFD	18.579	4.733	3.925	0.000
C4 PICP	101.135	4.933	20.500	0.000
C4 RT	-31.663	5.475	-5.783	0.000
C5 SVAPA	50.417	13.321	3.785	0.000
C5 IVAPA	79.778	13.946	5.720	0.000
C5 PICP	104.280	8.417	12.390	0.000
C5 RT	-16.369	4.951	-3.306	0.002
C6 SVAPA	68.018	15.304	4.444	0.000
C6 IVAPA	108.893	12.440	8.753	0.000
C6 PICP	100.584	9.038	11.129	0.000
C6 RT	-26.327	6.091	-4.322	0.000
C7 SVAPA	58.919	15.558	3.787	0.000
C7 IVAPA	61.791	17.408	3.550	0.001
C7 PICP	99.419	9.224	10.778	0.000
C7 Area	-5688.253	1856.686	-3.064	0.003
T1 IFA	-33.657	4.579	-7.351	0.000
T1 IFPA	-33.979	4.611	-7.370	0.000
T1 SVAPA	128.593	14.829	8.672	0.000
T1 IVAPA	136.056	11.393	11.942	0.000
T1 VBPH	6.981	1.969	3.546	0.001

[1] Bonferroni Correction: C1, $p < 0.01$; C2, $p < 0.008$; C3 – L5, $p < 0.004$.

Table D-4. Significant differences among taxa (cont.).

Intercept Variable	Unstandardized Coefficients		t	p value [1]
	B	Std. Error		
T1 SFID	17.252	3.293	5.240	0.000
T1IIFD	14.991	3.316	4.521	0.000
T1 PICP	60.314	8.720	6.916	0.000
T2 IFA	-10.815	3.184	-3.397	0.001
T2 IFPA	-10.869	3.063	-3.549	0.001
T2 SVAPA	129.348	6.841	18.907	0.000
T2 IVAPA	113.075	6.897	16.394	0.000
T2 SFID	10.950	2.456	4.458	0.000
T2 IIFD	9.671	2.767	3.495	0.001
T2 PICP	53.931	7.149	7.544	0.000
T2 RT	-14.786	4.731	-3.125	0.003
T3 IFA	-7.577	2.209	-3.430	0.001
T3 IFPA	-7.401	2.221	-3.332	0.001
T3 SVAPA	111.864	3.498	31.979	0.000
T3 IVAPA	97.079	4.847	20.028	0.000
T3 VBPH	7.365	1.778	4.143	0.000
T3 SFID	7.883	2.196	3.590	0.001
T3 PICP	43.556	4.668	9.332	0.000
T3 RT	-15.934	4.097	-3.889	0.000
T4 SVAPA	116.460	3.915	29.744	0.000
T4 IVAPA	94.746	4.714	20.098	0.000
T4 VBPH	6.910	1.842	3.751	0.000
T4 IIFD	6.735	2.050	3.286	0.002
T4 PICP	38.330	4.290	8.936	0.000
T4 CPBA	5.562	1.331	4.178	0.000
T4 RT	-21.098	3.546	-5.950	0.000
T5 SVAPA	118.585	4.221	28.093	0.000
T5 VBPH	6.678	1.983	3.367	0.001
T5 VBAH	5.663	1.864	3.038	0.003
T5 SFID	9.609	1.924	4.995	0.000
T5 IIFD	9.161	2.080	4.404	0.000
T5 PICP	50.114	3.731	13.433	0.000
T5 IVAPA	102.709	4.150	24.748	0.000
T5 RT	-13.724	3.532	-3.886	0.000
T6 SVAPA	117.578	4.343	27.071	0.000
T6 IVAPA	101.863	4.868	20.924	0.000
T6 VBAH	8.920	2.504	3.562	0.001
T6 SFID	10.398	2.360	4.407	0.000

[1] Bonferroni Correction: C1, $p < 0.01$; C2, $p < 0.008$; C3 – L5, $p < 0.004$.

Table D-4. Significant differences among taxa (cont.).

Intercept Variable	Unstandardized Coefficients		t	p value [1]
	B	Std. Error		
T6 IIFD	11.374	2.752	4.134	0.000
T6 PICP	61.006	4.428	13.777	0.000
T6 RT	-12.940	4.143	-3.123	0.003
T7 IFA	-12.330	3.798	-3.247	0.002
T7 IFPA	-11.542	3.827	-3.016	0.004
T7 SVAPA	123.952	4.342	28.549	0.000
T7 IVAPA	116.297	4.668	24.914	0.000
T7 VBPH	10.414	2.739	3.802	0.000
T7 VBAH	9.857	2.456	4.013	0.000
T7 SFID	16.118	2.863	5.631	0.000
T7 IIFD	17.826	2.907	6.131	0.000
T7 PICP	66.024	3.350	19.710	0.000
T8 SVAPA	121.076	4.074	29.720	0.000
T8 IVAPA	109.786	4.410	24.895	0.000
T8 VBPH	8.830	2.773	3.184	0.002
T8 VBAH	9.151	2.563	3.570	0.001
T8 SFID	15.044	2.767	5.437	0.000
T8 IIFD	14.780	3.057	4.835	0.000
T8 PICP	67.124	4.738	14.166	0.000
T8 RT	-10.997	3.624	-30.035	0.004
T9 IFA	-13.344	4.119	-3.240	0.002
T9 IFPA	-12.456	4.223	-2.950	0.004
T9 SVAPA	122.206	4.899	24.947	0.000
T9 IVAPA	105.782	6.035	17.529	0.000
T9 SFID	16.242	3.640	4.462	0.000
T9 IIFD	17.098	3.707	4.613	0.000
T9 PICP	63.417	4.404	14.401	0.000
T10 SVAPA	113.737	7.264	15.657	0.000
T10 IVAPA	97.926	9.966	9.826	0.000
T10 VBPH	16.129	5.015	3.216	0.002
T10 VBAH	15.686	5.300	2.960	0.004
T10 SFID	20.136	5.179	3.888	0.000
T10 IIFD	19.477	4.361	4.466	0.000
T10 PICP	76.434	6.754	11.316	0.000
T11 SFA	12.352	3.982	3.102	0.003
T11 SFPA	13.582	4.087	3.323	0.001
T11 IFA	-14.569	3.529	-4.128	0.000
T11 IFPA	-13.497	3.574	-3.776	0.000

[1] Bonferroni Correction: C1, $p < 0.01$; C2, $p < 0.008$; C3 – L5, $p < 0.004$.

Table D-4. Significant differences among taxa (cont.).

Intercept Variable	Unstandardized Coefficients		t	p value [1]
	B	Std. Error		
T11 SVAPA	104.324	5.002	20.856	0.000
T11 IVAPA	193.224	15.602	12.384	0.000
T11 VBPH	10.770	2.987	3.605	0.001
T11 VBAH	11.325	2.758	4.073	0.000
T11 SFID	13.195	2.225	5.929	0.000
T11 IIFD	18.366	2.427	7.568	0.000
T11 PICP	74.473	3.947	18.867	0.000
T11 RT	-78.204	11.213	-6.974	0.000
T12 IFA	-18.045	4.173	-4.324	0.000
T12 IFPA	-17.529	4.239	-4.135	0.000
T12 SVAPA	74.155	16.695	4.442	0.000
T12 IVAPA	151.448	28.984	5.225	0.000
T12 VBPH	12.540	3.493	3.590	0.001
T12 VBAH	11.809	3.596	3.284	0.002
T12 SFID	12.621	2.504	5.041	0.000
T12 IIFD	15.927	2.217	7.184	0.000
T12 PICP	69.242	4.987	13.884	0.000
T12 RT	-78.334	20.565	-3.809	0.000
T13 IIFD	15.401	3.780	4.074	0.000
T13 PICP	76.210	7.853	9.705	0.000
L1 SFA	-15.052	2.779	-5.417	0.000
L1 SFPA	-15.501	2.733	-5.671	0.000
L1 SVAPA	32.097	7.736	4.149	0.000
L1 VBPH	22.766	2.854	7.978	0.000
L1 VBAH	21.128	3.072	6.877	0.000
L1 SFID	18.594	1.972	9.431	0.000
L1 IIFD	22.190	2.024	10.966	0.000
L1 PICP	86.224	4.235	20.358	0.000
L1 Area	7096.356	2226.114	3.188	0.002
L2 SFA	-14.476	2.928	-4.944	0.000
L2 SFPA	-14.445	2.866	-5.039	0.000
L2 VBPH	22.745	2.975	7.645	0.000
L2 VBAH	22.671	3.433	6.604	0.000
L2 SFID	19.091	2.573	7.419	0.000
L2 IIFD	18.086	2.412	7.497	0.000
L2 PICP	87.314	5.825	14.989	0.000
L2 Area	7150.082	2389.543	2.992	0.004

[1] Bonferroni Correction: C1, $p < 0.01$; C2, $p < 0.008$; C3 – L5, $p < 0.004$.

Table D-4. Significant differences among taxa (cont.).

Intercept Variable	Unstandardized Coefficients		t	p value [1]
	B	Std. Error		
L3 SFA	-9.524	2.219	-4.291	0.000
L3 SFPA	-9.723	2.500	-3.890	0.000
L3 SVAPA	21.670	6.780	3.196	0.002
L3 IVAPA	26.128	7.663	3.410	0.001
L3 VBPH	21.954	2.482	8.845	0.000
L3 VBAH	22.841	2.953	7.735	0.000
L3 SFID	17.711	2.099	8.436	0.000
L3 IIFD	19.182	3.041	6.307	0.000
L3 PICP	87.520	5.924	14.773	0.000
L3 Area	7112.633	2248.869	3.163	0.002
L4 SVAPA	31.238	6.486	4.816	0.000
L4 VBPH	21.613	3.019	7.158	0.000
L4 VBAH	17.718	3.014	5.878	0.000
L4 PICP	83.923	5.418	15.490	0.000

[1] Bonferroni Correction: C1, $p < 0.01$; C2, $p < 0.008$; C3 – L5, $p < 0.004$.

Appendix E: Mann-Whitney U-test results

Homo

Table E-1. Significant differences between males and females - *Homo*.

Species: *Homo sapiens* (M/F)							
Level	Variable	Male Mdn	Female Mdn	U	z	r	p value [1]
C1	Area	5671.38	5068.25	20.00	-4.179	-0.716	0.000
C4	Area	4643.25	4099.23	33.00	-3.830	-0.656	0.000
C6	IFPA	28.09	22.43	61.50	-2.847	-0488	0.004
C7	VBAH	13.72	12.73	61.00	-2.865	-0.491	0.004
C7	Area	6283.83	5190.51	20.00	-4.158	-0.713	0.000
T1	VBPH	17.30	15.90	52.00	-3.174	-0.544	0.002
T1	IIFD	29.32	26.68	48.00	-3.313	-0.497	0.001
T1	Area	7138.70	5862.44	17.00	-4.382	-0.791	0.000
T2	IFA	6.65	10.87	39.00	-3.471	-0.595	0.001
T2	IFPA	7.93	13.18	17.00	-3.616	-0.620	0.000
T2	IIFD	26.51	23.72	34.50	-3.778	-0.647	0.000
T2	Area	7252.70	6067.67	23.00	-4.175	-0.716	0.000
T3	VBAH	18.07	17.09	59.50	-2.916	-0.500	0.004
T3	IIFD	24.11	22.04	35.00	-3.761	-0.508	0.000
T3	Area	7192.06	6140.41	19.00	-4.313	-0.739	0.000
T4	Area	7428.69	6320.98	20.00	-4.279	-0.733	0.000
T5	VBPH	20.30	18.97	52.50	-3.158	-0.541	0.002
T5	IIFD	22.99	21.06	48.00	-3.312	-0.568	0.001
T5	Area	7660.48	6480.49	14.00	-4.486	-0.769	0.000
T6	Area	8287.69	6755.50	25.00	-4.106	-0.704	0.000
T7	IIFD	23.79	21.29	28.00	-4.002	-0.686	0.000
T7	Area	8637.82	7093.63	26.00	-4.071	-0.698	0.000
T8	Area	8763.33	7363.71	34.00	-3.795	-0.650	0.000
L1	Area	11976.88	10007.74	31.00	-3.899	-0.668	0.000

[1] Bonferroni Correction: C1, $p < 0.01$; C2, $p < 0.008$; C3 – L5, $p < 0.004$.

Gorilla

Table E-2. Significant differences between males and females - *Gorilla*.

Species: *Gorilla gorilla* (M/F)							
Level	Variable	Male Mdn	Female Mdn	U	z	r	p value [1]
C1	Area	6159.14	4341.21	0.00	-3.240	-0.810	0.001
C2	Area	7248.87	4912.77	0.00	-3.240	-0.810	0.001
C3	VBPH	16.62	11.90	0.00	-3.361	-0.840	0.001
C3	Area	7991.76	4420.11	0.00	-3.361	-0.840	0.001
C4	VBPH	16.90	12.85	0.00	-3.361	-0.840	0.001
C4	VBAH	15.09	10.25	0.00	-3.361	-0.840	0.001
C4	Area	8547.35	5045.94	0.00	-3.361	-0.840	0.001
C5	VBPH	17.78	13.25	0.00	-3.361	-0.840	0.001
C5	VBAH	17.76	10.51	0.00	-3.361	-0.840	0.001
C5	SFID	37.67	31.15	0.00	-3.361	-0.840	0.001
C5	IIFD	40.48	31.54	0.00	-3.361	-0.840	0.001
C5	CPBA	1.81	4.26	0.00	-3.361	-0.840	0.001
C5	Area	9263.01	5552.55	0.00	-3.361	-0.840	0.001
C6	VBPH	18.62	13.56	0.00	-3.361	-0.840	0.001
C6	VBAH	15.21	10.76	0.00	-3.361	-0.840	0.001
C6	SFID	37.95	29.55	0.00	-3.361	-0.840	0.001
C6	IIFD	38.76	31.62	0.00	-3.361	-0.840	0.001
C6	Area	10479.11	6190.11	0.00	-3.361	-0.840	0.001
C7	VBPH	18.31	13.99	2.00	-3.151	-0.787	0.002
C7	VBAH	14.42	10.86	0.00	-3.361	-0.840	0.001
C7	SFID	37.20	29.29	1.00	-3.256	-0.840	0.001
C7	IIFD	37.24	29.94	0.00	-3.361	-0.840	0.001
C7	PICP	81.65	86.93	0.00	-3.361	-0.840	0.001
C7	Area	10227.74	6116.29	0.00	-3.361	-0.840	0.001
T1	VBPH	18.46	14.32	0.00	-3.046	-0.761	0.001
T1	VBAH	16.37	12.48	0.00	-3.361	-0.840	0.002
T1	IIFD	27.70	21.80	0.00	-3.046	-0.761	0.002
T1	Area	10686.73	6316.92	0.00	-3.361	-0.840	0.001
T2	VBPH	20.78	16.37	0.00	-3.361	-0.840	0.001
T2	VBAH	18.18	13.66	0.00	-3.361	-0.840	0.001
T2	Area	10113.69	6133.84	0.00	-3.361	-0.840	0.001
T3	VBPH	20.03	15.60	0.00	-3.361	-0.840	0.001
T3	VBAH	18.38	13.55	0.00	-3.361	-0.840	0.001
T3	Area	9621.82	5614.43	0.00	-3.361	-0.840	0.001
T4	VBPH	19.67	14.97	0.00	-3.361	-0.840	0.001
T4	VBAH	16.89	12.21	0.00	-3.361	-0.840	0.001

[1] Bonferroni Correction: C1, $p < 0.01$; C2, $p < 0.008$; C3 – L5, $p < 0.004$.

Table E-2. Significant differences between males and females - *Gorilla* (cont.).

Species: *Gorilla gorilla* (M/F)							
Level	Variable	Male Mdn	Female Mdn	U	z	r	p value [1]
T4	IIFD	20.32	16.68	2.00	-3.151	-0.787	0.002
T4	SFID	22.03	17.92	0.00	-3.361	-0.840	0.001
T4	Area	9148.76	5659.00	0.00	-3.361	-0.840	0.001
T5	VBPH	19.48	14.38	0.00	-3.361	-0.840	0.001
T5	VBAH	17.68	12.66	0.00	-3.363	-0.840	0.001
T5	Area	8999.50	5692.31	0.00	-3.361	-0.840	0.001
T6	VBPH	19.21	14.53	0.00	-3.361	-0.840	0.001
T6	VBAH	17.80	12.12	0.00	-3.256	-0.814	0.001
T6	Area	9057.39	5616.28	0.00	-3.361	-0.840	0.001
T7	VBPH	19.58	14.97	0.00	-3.361	-0.840	0.001
T7	VBAH	17.49	14.38	0.00	-3.151	-0.787	0.002
T7	Area	9064.06	5780.05	0.00	-3.361	-0.840	0.001
T8	Area	9200.48	5762.53	0.00	-3.361	-0.840	0.001
T9	VBPH	19.56	13.88	0.00	-3.361	-0.840	0.001
T9	VBAH	17.81	13.20	0.00	-3.363	-0.840	0.001
T9	Area	9765.22	6288.44	0.00	-3.361	-0.840	0.001
T10	VBPH	20.49	15.79	0.00	-3.361	-0.840	0.001
T10	VBAH	18.29	14.11	0.00	-3.351	-0.840	0.002
T10	Area	10192.72	6486.28	0.00	-3.361	-0.840	0.001
T11	VBPH	22.08	16.64	0.00	-3.046	-0.761	0.001
T11	IIFD	26.79	21.76	4.00	-2.941	-0.735	0.003
T11	Area	11258.38	6832.91	0.00	-3.361	-0.840	0.001
T12	Area	12474.11	7591.11	0.00	-3.361	-0.840	0.001
T13	VBPH	28.02	21.58	0.00	-3.361	-0.840	0.001
T13	VBAH	24.02	18.64	0.00	-3.046	-0.761	0.002
T13	Area	14022.13	8139.72	0.00	-3.361	-0.840	0.001
L1	Area	15638.08	8733.67	0.00	-3.361	-0.840	0.001
L2	Area	15424.76	9708.53	0.00	-3.361	-0.840	0.001
L3	Area	15687.61	9597.37	0.00	-3.361	-0.840	0.001
L4	Area	14842.88	9054.33	0.00	-3.098	-0.774	0.001

[1] Bonferroni Correction: C1, $p < 0.01$; C2, $p < 0.008$; C3 – L5, $p < 0.004$.

Appendix F: Kruskal-Wallis H test

Table F-1. Significant differences among taxa.

Species: *Homo sapiens* *Pan troglodytes* *Gorilla gorilla*			
Level	Variable	H(2)	p value [1]
C1	SFA	13.969	0.001
C1	IFA	16.276	0.000
C1	SVAPA	21.848	0.000
C1	IVAPA	20.185	0.000
C1	Area	33.902	0.000
C2	SFA	38.137	0.000
C2	IFA	28.423	0.000
C2	SVAPA	30.893	0.000
C2	IVAPA	22.114	0.000
C2	Area	34.004	0.000
C3	IFA	25.849	0.000
C3	IFPA	24.928	0.000
C3	SVAPA	18.872	0.000
C3	IVAPA	18.317	0.000
C4	SFA	11.720	0.003
C4	SFPA	12.680	0.002
C4	IFA	18.826	0.000
C4	IFPA	17.961	0.000
C4	SVAPA	13.408	0.001
C4	IVAPA	13.408	0.000
C4	VBPH	40.136	0.000
C4	VBAH	23.878	0.000
C4	SFID	25.458	0.000
C4	IIFD	23.389	0.000
C4	PICP	14.084	0.001
C4	Area	47.567	0.001
C5	SFA	13.190	0.001
C5	SFPA	13.784	0.001
C5	IFA	17.07	0.000
C5	IFPA	16.610	0.000
C5	SVAPA	25.514	0.000
C5	IVAPA	29.739	0.000
C5	VBPH	31.779	0.000
C5	VBAH	22.055	0.000
C5	SFID	24.847	0.000
C5	PICP	24.222	0.000

[1] Bonferroni Correction: C1, $p < 0.01$; C2, $p < 0.008$; C3 – L5, $p < 0.004$.

Table F-1. Significant differences among taxa (cont.).

Species: *Homo sapiens* *Pan troglodytes* *Gorilla gorilla*			
Level	Variable	H(2)	p value [1]
C5	Area	44.528	0.000
C6	SFA	17.743	0.000
C6	SFPA	21.577	0.000
C6	IFA	17.717	0.000
C6	IFPA	17.864	0.000
C6	SVAPA	35.505	0.000
C6	IVAPA	23.710	0.000
C6	VBPH	29.685	0.000
C6	VBAH	23.326	0.000
C6	SFID	29.609	0.000
C6	IIFD	28.172	0.000
C6	PICP	24.972	0.000
C6	Area	45.247	0.000
C7	SVAPA	29.437	0.000
C7	IVAPA	34.450	0.000
C7	VBPH	29.055	0.000
C7	VBAH	34.504	0.000
C7	SFID	39.600	0.000
C7	IIFD	32.448	0.000
C7	Area	42.432	0.000
T1	SFA	11.890	0.003
T1	SFPA	12.387	0.002
T1	IFA	28.811	0.000
T1	IFPA	27.467	0.000
T1	SVAPA	38.300	0.000
T1	IVAPA	41.703	0.000
T1	VBAH	18.126	0.000
T1	IIFD	17.607	0.000
T1	PICP	24.238	0.000
T1	Area	38.677	0.000
T1	RT	12.728	0.002
T2	SVAPA	30.399	0.000
T2	VBAH	33.776	0.000
T2	IIFD	15.872	0.000
T2	PICP	16.788	0.000
T2	Area	36.432	0.000
T3	SFA	17.778	0.000

[1] Bonferroni Correction: C1, $p < 0.01$; C2, $p < 0.008$; C3 – L5, $p < 0.004$.

Table F-1. Significant differences among taxa (cont.).

Species: *Homo sapiens* *Pan troglodytes* *Gorilla gorilla*			
Level	Variable	H(2)	p value [1]
T3	SFPA	22.293	0.000
T3	SVAPA	30.963	0.000
T3	IVAPA	29.116	0.000
T3	PICP	9.885	0.000
T3	Area	34.011	0.000
T3	RT	6.424	0.040
T4	SFA	13.621	0.001
T4	SFPA	14.771	0.001
T4	SVAPA	33.472	0.000
T4	IVAPA	27.563	0.000
T4	CPBA	27.290	0.000
T4	Area	33.463	0.000
T4	RT	30.732	0.000
T5	SFA	11.947	0.003
T5	SVAPA	26.535	0.000
T5	IVAPA	26.626	0.000
T5	PICP	12.655	0.002
T5	Area	33.055	0.000
T6	IFA	19.425	0.000
T6	IFPA	17.610	0.000
T6	SVAPA	20.872	0.000
T6	IVAPA	20.673	0.000
T6	VBPH	16.103	0.000
T6	SFID	11.488	0.003
T6	IIFD	13.486	0.001
T6	Area	33.059	0.000
T7	IFA	35.811	0.000
T7	IFPA	32.498	0.000
T7	SVAPA	13.184	0.001
T7	IVAPA	19.008	0.000
T7	VBPH	32.906	0.000
T7	VBAH	26.937	0.000
T7	SFID	26.017	0.000
T7	IIFD	25.251	0.000
T7	Area	33.025	0.000
T8	SFA	13.272	0.001

[1] Bonferroni Correction: C1, $p < 0.01$; C2, $p < 0.008$; C3 – L5, $p < 0.004$.

Table F-1. Significant differences among taxa (cont.).

Species: *Homo sapiens* *Pan troglodytes* *Gorilla gorilla*			
Level	Variable	H(2)	p value [1]
T8	SFPA	12.165	0.002
T8	IFA	32.663	0.000
T8	IFPA	26.752	0.001
T8	SVAPA	14.289	0.001
T8	IVAPA	20.360	0.000
T8	VBPH	31.394	0.000
T8	VBAH	31.488	0.000
T8	SFID	22.791	0.000
T8	IIFD	21.513	0.000
T8	Area	33.362	0.000
T9	SFA	22.055	0.000
T9	SFPA	22.362	0.000
T9	IFA	28.003	0.000
T9	IFPA	25.659	0.000
T9	IVAPA	19.024	0.000
T9	VBPH	43.820	0.000
T9	VBAH	45.039	0.000
T9	SFID	36.638	0.000
T9	IIFD	32.337	0.000
T9	CPBA	15.187	0.001
T9	Area	32.087	0.000
T10	SFA	26.340	0.000
T10	SFPA	24.576	0.000
T10	IFPA	29.219	0.000
T10	IVAPA	15.025	0.001
T10	VBPH	35.622	0.000
T10	VBAH	40.246	0.000
T10	SFID	30.338	0.000
T10	IIFD	19.455	0.000
T10	CPBA	16.076	0.000
T10	Area	32.537	0.000
T11	SFA	27.417	0.000
T11	SFPA	28.881	0.000
T11	IFPA	10.967	0.004

[1] Bonferroni Correction: C1, $p < 0.01$; C2, $p < 0.008$; C3 – L5, $p < 0.004$.

Table F-1. Significant differences among taxa (cont.).

Species: *Homo sapiens* *Pan troglodytes* *Gorilla gorilla*			
Level	Variable	H(2)	p value [1]
T11	IVAPA	11.141	0.004
T11	VBPH	21.248	0.000
T11	VBAH	21.522	0.000
T11	CPBA	12.502	0.002
T11	Area	28.196	0.000
T12	SFA	24.920	0.000
T12	SFPA	24.043	0.000
T12	SVAPA	25.138	0.000
T12	IVAPA	45.901	0.000
T12	VBPH	29.514	0.000
T12	VBAH	32.864	0.000
T12	SFID	10.969	0.004
T12	Area	31.992	0.000
T12	RT	33.229	0.000
T13	VBPH	12.102	0.001
T13	VBAH	14.713	0.000
T13	SFID	13.688	0.000
T13	CPBA	13.236	0.000
T13	Area	13.225	0.000
L1	SFA	11.081	0.004
L1	SFPA	12.391	0.002
L1	IFA	14.672	0.001
L1	SVAPA	15.917	0.000
L1	IVAPA	48.714	0.000
L1	VBPH	16.138	0.000
L1	VBAH	20.230	0.000
L1	Area	19.848	0.000
L2	SVAPA	28.254	0.000
L2	IVAPA	42.321	0.000
L2	VBPH	22.007	0.000
L2	VBAH	21.426	0.000
L2	CPBA	13.512	0.001
L2	Area	25.007	0.000
L2	RT	18.149	0.000
L3	IFA	11.736	0.003
L3	SVAPA	15.053	0.001
L3	VBPH	12.713	0.002
L3	VBAH	19.233	0.000

[1] Bonferroni Correction: C1, $p < 0.01$; C2, $p < 0.008$; C3 – L5, $p < 0.004$.

Table F-1. Significant differences among taxa (cont.).

Species: *Homo sapiens* *Pan troglodytes* *Gorilla gorilla*			
Level	Variable	H(2)	p value [1]
L3	IIFD	19.674	0.000
L3	Area	28.965	0.000
L4	IFPA	11.624	0.003
L4	IVAPA	27.360	0.000
L4	VBPH	11.893	0.003
L4	VBAH	15.455	0.000
L4	IIFD	44.476	0.000
L4	CPBA	16.094	0.000
L4	Area	28.259	0.000
L4	RT	21.922	0.000

[1] Bonferroni Correction: C1, $p < 0.01$; C2, $p < 0.008$; C3 – L5, $p < 0.004$.

Appendix G: *Post hoc* Mann-Whitney tests

Table G-1. Significant differences between *Homo* and *Gorilla*.

Species: *Homo sapiens* *Gorilla gorilla*							
Level	Variable	*Homo* Mdn	*Gorilla* Mdn	U	z	r	p value [1]
C1	SVAPA	23.20	28.96	100.00	-3.496	-0.494	0.000
C1	IVAPA	27.64	21.34	66.00	-4.221	-0.596	0.000
C2	SFA	96.64	106.88	641.00	-4.534	-0.641	0.000
C2	IVAPA	35.84	24.61	75.00	-4.097	-0.579	0.000
C3	IFA	37.08	42.41	90.00	-3.579	-0.506	0.000
C3	IFPA	38.14	43.02	96.00	-3.449	-0.487	0.001
C3	IVAPA	95.31	77.52	73.00	-3.948	-0.558	0.000
C3	SFID	35.50	30.51	65.00	-4.306	-0.608	0.000
C3	IIFD	38.27	34.36	121.00	-3.140	-0.444	0.002
C3	Area	4165.94	6118.81	108.00	-3.411	-0.482	0.001
C4	SFPA	37.17	32.57	129.00	-2.974	-0.420	0.003
C4	SVAPA	88.68	73.55	119.00	-3.182	-0.450	0.001
C4	IVAPA	95.50	80.44	77.00	-4.055	-0.573	0.000
C4	VBPH	12.85	15.20	120.00	-3.161	-0.447	0.002
C4	SFID	37.50	32.89	124.00	-3.078	-0.435	0.002
C4	Area	4272.79	6866.15	55.00	-4.513	-0.638	0.000
C5	SFA	41.03	33.52	106.00	-3.369	-0.476	0.001
C5	SFPA	42.30	33.88	99.00	-3.518	-0.497	0.000
C5	IFA	33.45	42.15	107.00	-3.432	-0.485	0.001
C5	IFPA	34.54	43.34	112.00	-3.327	-0.470	0.001
C5	SVAPA	97.50	79.43	112.00	-3.328	-0.470	0.000
C5	IVAPA	97.74	71.45	24.00	-5.117	-0.723	0.000
C5	VBPH	12.59	15.83	117.50	-3.213	-0.454	0.001
C5	SFID	38.48	33.90	91.00	-3.688	-0.521	0.000
C5	IIFD	39.84	34.68	117.00	-3.134	-0.443	0.002
C5	Area	4639.95	7208.26	76.00	-4.077	-0.576	0.000
C6	SFA	36.92	31.45	127.00	-3.016	-0.426	0.003
C6	SFPA	39.04	32.35	116.50	-3.234	-0.457	0.001
C6	IFA	24.62	34.77	78.00	-4.035	-0.570	0.000
C6	IFPA	25.98	35.68	75.50	-4.087	-0.517	0.000
C6	SVAPA	99.74	72.20	16.00	-5.249	-0.742	0.000
C6	IVAPA	93.25	68.68	56.00	-4.374	-0.618	0.000
C6	VBPH	13.08	13.28	114.00	-3.286	-0.467	0.000
C6	SFID	40.08	33.82	80.00	-3.849	-0.544	0.000

[1] Bonferroni Correction: C1, $p < 0.01$; C2, $p < 0.008$; C3 – L5, $p < 0.004$.

Table G-1. Significant differences between *Homo* and *Gorilla* (cont.).

Species: *Homo sapiens* *Gorilla gorilla*							
Level	Variable	*Homo* Mdn	*Gorilla* Mdn	U	z	r	p value [1]
C6	IIFD	39.22	33.53	97.00	-3.477	-0.491	0.001
C6	Area	4898.16	8570.90	52.00	-4.575	-0.647	0.000
C7	SVAPA	97.35	69.33	15.00	-5.231	-0.739	0.000
C7	IVAPA	101.61	69.81	4.00	-5.478	-0.774	0.000
C7	CPBA	2.77	4.44	111.50	-3.252	-0.459	0.000
C7	Area	5490.09	8166.04	53.00	-4.378	-0.619	0.001
T1	SFA	25.28	24.18	123.00	-3.099	-0.438	0.002
T1	SFPA	26.42	24.64	117.00	-3.224	-0.455	0.001
T1	IFA	11.21	22.84	77.00	-4.055	-0.573	0.000
T1	IFPA	12.59	23.92	87.00	-3.847	-0.544	0.000
T1	SVAPA	101.02	67.14	2.00	-5.615	-0.794	0.000
T1	IVAPA	113.33	87.61	15.00	-5.345	-0.755	0.000
T1	IIFD	27.77	24.03	79.00	-4.014	-0.567	0.000
T1	PICP	80.44	70.03	53.00	-4.555	-0.644	0.000
T1	RT	13.55	21.10	90.00	-3.785	-0.535	0.000
T2	IIFD	24.67	19.97	73.00	-3.811	-0.538	0.000
T3	SFA	22.33	16.48	111.00	-3.349	-0.473	0.001
T3	SFPA	23.63	16.86	93.00	-3.723	-0.526	0.000
T3	SVAPA	102.77	99.57	104.00	-3.104	-0.438	0.002
T4	SFA	20.25	15.32	120.00	-3.161	-0.447	0.002
T4	SFPA	21.51	15.98	117.00	-3.224	-0.455	0.001
T4	SVAPA	102.58	100.60	102.00	-3.536	-0.500	0.000
T4	CPBA	2.78	3.94	81.00	-3.099	-0.561	0.000
T4	RT	13.03	4.99	58.00	-4.451	-0.629	0.000
T6	IFA	5.34	9.75	70.00	-4.202	-0.594	0.000
T6	IFPA	6.66	10.43	79.00	-4.014	-0.567	0.000
T6	VBPH	19.78	17.25	123.00	-3.099	-0.438	0.002
T6	SFID	21.86	18.79	127.00	-3.016	-0.426	0.003
T7	IFA	5.41	14.78	17.00	-5.266	-0.774	0.000
T7	IFPA	6.14	15.78	25.000	-5.095	-0.720	0.000
T7	VBPH	20.11	17.71	42.00	-4.733	-0.669	0.000
T7	VBAH	17.63	15.58	63.00	-4.285	-0.605	0.000
T7	SFID	22.22	18.94	46.00	-4.648	-0.657	0.000
T7	IIFD	22.72	19.25	57.00	-4.413	-0.624	0.000
T8	SFA	17.90	23.41	105.00	-3.473	-0.491	0.001
T8	IFA	5.64	16.72	18.00	-5.164	-0.730	0.000
T8	IFPA	6.85	17.57	40.00	-4.825	-0.682	0.000
T8	VBPH	20.73	17.20	50.00	-4.445	-0.628	0.000

[1] Bonferroni Correction: C1, $p < 0.01$; C2, $p < 0.008$; C3 – L5, $p < 0.004$.

Table G-1. Significant differences between *Homo* and *Gorilla* (cont.).

Species: *Homo sapiens* *Gorilla gorilla*							
Level	Variable	*Homo* Mdn	*Gorilla* Mdn	U	z	r	p value [1]
T8	VBAH	18.70	15.13	62.00	-4.176	-0.590	0.000
T8	SFID	22.84	1943	62.00	-4.176	-0.590	0.000
T8	IIFD	23.27	18.97	61.00	-4.198	-0.593	0.000
T9	SFA	15.64	22.72	61.00	-4.388	-0.620	0.000
T9	IFA	5.28	13.08	30.00	-4.881	-0.690	0.000
T9	IFPA	6.52	14.59	38.00	-4.707	-0.665	0.000
T9	IVAPA	114.05	106.12	100.00	-3.362	-0.475	0.001
T9	VBPH	21.53	17.24	13.00	-5.250	-0.700	0.000
T9	VBAH	19.53	15.41	12.00	-5.271	-0.745	0.000
T9	SFID	23.22	18.92	21.00	-5.076	-0.717	0.000
T9	IIFD	24.38	20.88	43.00	-4.599	-0.650	0.000
T10	SFA	15.79	22.42	55.00	-4.513	-0.587	0.000
T10	SFPA	16.57	22.90	63.00	-4.347	-0.614	0.000
T10	IFA	5.32	12.80	25.00	-5.138	-0.726	0.000
T10	IFPA	5.86	13.74	25.00	-4.961	-0.701	0.000
T10	IVAPA	111.76	102.90	87.00	-3.438	-0.486	0.000
T10	VBPH	22.37	17.36	59.00	-4.102	-0.580	0.000
T10	VBAH	21.17	15.20	33.00	-4.719	-0.667	0.000
T10	SFID	24.79	20.42	66.00	-3.936	-0.556	0.000
T10	IIFD	24.15	21.51	107.00	-2.964	-0.419	0.000
T11	SFA	15.82	19.43	82.00	-3.951	-0.558	0.000
T11	SFPA	17.17	20.38	74.00	-4.118	-0.582	0.000
T12	SFA	13.69	21.96	80.00	-3.993	-0.564	0.000
T12	SFPA	14.73	23.17	83.00	-3.931	-0.555	0.000
T12	IVAPA	28.79	93.48	0.00	-5.657	-0.800	0.000
T12	VBPH	25.70	22.41	111.00	-3.348	-0.565	0.000
T12	VBAH	23.66	19.06	84.00	-3.910	-0.552	0.000
T12	RT	48.79	7.24	11.00	-5.428	-0.767	0.000
L1	SFA	6.68	11.56	110.00	-3.193	-0.451	0.000
L1	SFPA	7.39	12.63	100.00	-3.412	-0.482	0.000
L1	SVAPA	51.64	68.95	108.00	-3.237	-0.457	0.000
L1	IVAPA	21.96	55.76	0.00	-5.657	-0.800	0.000
L1	RT	28.30	12.01	68.00	-4.243	-0.600	0.000
L2	SVAPA	46.18	57.82	34.00	-4.950	-0.700	0.000
L2	IVAPA	28.29	51.65	10.00	-5.499	-0.770	0.000
L2	CPBA	4.62	3.21	100.00	-3.577	-0.505	0.000
L3	SFPA	4.26	8.32	115.00	-3.177	-0.449	0.000

[1] Bonferroni Correction: C1, $p < 0.01$; C2, $p < 0.008$; C3 – L5, $p < 0.004$.

Table G-1. Significant differences between *Homo* and *Gorilla* (cont.).

Species: *Homo sapiens* *Gorilla gorilla*							
Level	Variable	*Homo* Mdn	*Gorilla* Mdn	U	z	r	p value [1]
L3	SVAPA	47.92	62.47	101.00	-3.475	-0.491	0.000
L3	IIFD	29.69	23.07	85.00	-3.816	-0.491	0.000
L3	CPBA	4.86	3.52	114.00	-3.198	-0.452	0.000
L4	IVAPA	49.43	31.41	55.00	-4.151	-0.587	0.000
L4	IIFD	34.76	21.18	0.00	-5.398	-0.767	0.000
L4	CPBA	5.34	3.50	90.00	-3.357	-0.474	0.000

[1] Bonferroni Correction: C1, $p < 0.01$; C2, $p < 0.008$; C3 – L5, $p < 0.004$.

Table G-2. Significant differences between *Homo* and *Pan*.

Species: *Homo sapiens* *Pan troglodytes*							
Level	Variable	*Homo* Mdn	*Pan* Mdn	U	z	r	p value [1]
C1	SFA	93.50	92.84	103.00	-3.433	-0.485	0.001
C1	IFA	96.39	102.25	48.00	-4.605	-0.651	0.000
C1	SVAPA	23.20	30.02	75.00	-4.030	-0.569	0.000
C1	Area	5068.25	3032.65	0.00	-5.628	-0.705	0.000
C2	SFA	96.64	101.76	25.00	-4.989	-0.705	0.000
C2	IFA	45.19	47.44	28.00	-4.924	-0.696	0.000
C2	SVAPA	17.80	8.69	32.00	-4.991	-0.705	0.000
C2	IVAPA	35.84	19.34	36.00	-4.908	-0.694	0.000
C2	Area	5437.95	3290.97	2.00	-5.488	-0.776	0.000
C3	IFA	37.08	43.75	46.00	-4.355	-0.651	0.000
C3	IFPA	38.11	44.32	47.00	-4.332	-0.612	0.000
C3	SVAPA	80.30	58.62	61.00	-4.015	-0.567	0.000
C3	SFID	35.50	25.10	0.00	-5.658	-0.800	0.000
C3	IIFD	38.27	28.41	0.00	-5.657	-0.800	0.000
C3	Area	4165.94	2772.97	0.00	-5.657	-0.800	0.000
C4	IFA	37.93	44.39	77.00	-3.861	-0.546	0.000
C4	IFPA	39.17	45.49	74.00	-3.926	-0.555	0.000
C4	VBPH	12.85	10.63	9.50	-5.459	-0.772	0.000
C4	VBPH	12.10	9.56	40.00	-4.825	-0.682	0.000
C4	SFID	37.50	37.50	30.00	-4.881	-0.690	0.000
C4	IIFD	38.46	29.63	35.00	-4.772	-0.674	0.000
C4	IVAPA	95.50	78.44	122.00	-2.885	-0.408	0.004
C4	PICP	99.64	100.73	101.00	-3.341	-0.472	0.001
C4	Area	4272.79	2992.36	0.00	-5.657	-0.800	0.000
C5	IFA	33.45	40.74	111.00	-3.348	-0.473	0.001
C5	IFPA	34.54	41.56	117.00	-3.224	-0.455	0.001
C5	VBPH	12.59	10.54	53.00	-4.555	-0.644	0.000
C5	VBAH	11.56	9.11	68.00	-4.243	-0.600	0.000
C5	SFID	38.48	29.15	53.00	-4.326	-0.611	0.000
C5	IIFD	39.84	30.06	45.00	-4.504	-0.636	0.000
C5	SVAPA	97.50	74.26	117.00	-2.903	-0.410	0.001
C5	PICP	94.09	100.31	35.00	-4.727	-0.668	0.000
C5	Area	4639.95	3176.98	6.00	-5.533	-0.782	0.000
C6	SFA	36.92	28.46	91.00	-3.764	-0.532	0.000
C6	SFPA	39.04	27.76	70.00	-4.201	-0.594	0.000
C6	SVAPA	99.74	74.17	82.00	-3.805	-0.538	0.000
C6	VBPH	13.08	11.07	61.00	-4.389	-0.620	0.000
C6	VBAH	11.80	9.81	63.00	-4.347	-0.614	0.000

[1] Bonferroni Correction: C1, $p < 0.01$; C2, $p < 0.008$; C3 – L5, $p < 0.004$.

Table G-2. Significant differences between *Homo* and *Pan* (cont.).

Species: *Homo sapiens* *Pan troglodytes*							
Level	Variable	*Homo* Mdn	*Pan* Mdn	U	z	r	p value [1]
C6	SFID	40.08	29.05	32.00	-4.899	-0.692	0.000
C6	IIFD	39.22	28.83	35.00	-4.833	-0.683	0.000
C6	PICP	85.56	99.07	38.00	-4.768	-0.674	0.000
C6	Area	4898.16	3863.89	19.00	-5.262	-0.744	0.000
C7	VBPH	14.558	11.77	16.00	-5.185	-0.733	0.000
C7	VBAH	13.29	9.51	0.00	-5.657	-0.800	0.000
C7	SFID	39.03	28.89	0.00	-5.628	-0.795	0.000
C7	IIFD	34.22	27.07	2.00	-5.615	-0.794	0.000
C7	Area	5490.09	3958.32	15.00	-5.097	-0.720	0.000
T1	IFA	11.21	6.60	131.00	-2.932	-0.521	0.000
T1	IVAPA	113.33	111.21	92.00	-3.744	-0.528	0.000
T1	VBAH	15.38	10.66	91.00	-3.764	-0.532	0.000
T1	Area	6464.94	4239.54	0.00	-5.657	-0.800	0.000
T2	SFA	25.36	23.66	125.00	-2.865	-0.405	0.004
T2	SVAPA	104.36	105.74	34.00	-4.855	-0.686	0.000
T2	IVAPA	116.26	112.43	33.00	-4.877	-0.689	0.000
T2	VBAH	16.73	11.77	0.00	-5.57	-0.800	0.000
T2	CPBA	2.65	4.01	66.000	-4.155	-0.587	0.000
T2	Area	6497.76	4161.23	105.00	-3.302	-0.466	0.001
T3	SFA	22.33	18.13	105.00	-3.473	-0.491	0.001
T3	SFPA	23.63	18.62	83.50	-3.920	-0.554	0.000
T3	SVAPA	102.53	106.49	22.00	-5.118	-0.723	0.000
T3	IVAPA	112.99	110.60	17.00	-5.227	-0.739	0.000
T3	PICP	70.71	61.35	112.00	-3.149	-0.445	0.002
T3	Area	6502.55	4224.25	0.00	-5.657	-0.800	0.000
T3	RT	11.20	4.74	119.00	-3.182	-0.450	0.001
T4	SFPA	21.51	18.66	131.00	-2.932	-0.383	0.003
T4	SVAPA	102.58	108.90	9.00	-5.194	-0.734	0.000
T4	IVAPA	114.88	112.01	17.00	-5.013	-0.708	0.000
T4	CPBA	2.78	3.29	43.00	-4.423	-0.625	0.000
T4	Area	6739.12	4257.41	0.00	-5.657	-0.800	0.000
T4	RT	13.03	3.47	41.00	-4.468	-0.631	0.000
T5	SFA	20.12	16.63	127.50	-3.005	-0.424	0.003
T5	SVAPA	103.95	108.15	41.00	-4.804	-0.679	0.000
T5	IVAPA	115.29	111.88	39.00	-4.846	-0.605	0.000
T5	PICP	70.99	62.88	99.00	-3.598	-0.508	0.000
T5	Area	6981.55	4382.77	0.00	-5.657	-0.800	0.000
T6	SVAPA	103.97	106.91	58.00	-4.274	-0.604	0.000

[1] Bonferroni Correction: C1, $p < 0.01$; C2, $p < 0.008$; C3 – L5, $p < 0.004$.

Table G-2. Significant differences between *Homo* and *Pan* (cont.).

Species: *Homo sapiens* *Pan troglodytes*							
Level	Variable	*Homo* Mdn	*Pan* Mdn	U	z	r	p value [1]
T6	IVAPA	114.79	110.85	66.00	-4.100	-0.579	0.000
T6	VBPH	19.78	13.42	99.00	-3.384	-0.478	0.001
T6	Area	7430.68	4433.01	0.00	-5.657	-0.800	0.000
T7	IFA	5.41	7.16	103.00	-3.433	-0.485	0.001
T7	IVAPA	112.37	115.44	118.00	-3.113	-0.440	0.002
T7	VBPH	20.11	14.05	49.00	-4.584	-0.648	0.000
T7	VBAH	17.63	12.58	70.00	-4.136	-0.584	0.000
T7	SFID	22.22	16.63	105.00	-3.390	-0.479	0.001
T7	IIFD	22.72	16.57	96.00	-3.582	-0.506	0.000
T7	Area	7825.04	4571.86	0.00	-5.657	-0.800	0.000
T8	SFPA	19.34	19.38	105.00	-2.988	-0.422	0.003
T8	SVAPA	104.25	106.31	96.00	-3.199	-0.452	0.001
T8	IVAPA	111.38	109.23	77.00	-3.644	-0.515	0.000
T8	VBPH	20.73	14.07	33.00	-4.675	-0.661	0.000
T8	VBAH	18.70	12.66	20.00	-4.979	-0.704	0.000
T8	SFID	22.84	16.61	90.00	-3.339	-0.472	0.001
T8	IIFD	23.27	17.26	103.00	-3.034	-0.467	0.002
T8	Area	8036.41	4740.27	0.00	-5.657	-0.800	0.000
T9	VBPH	21.53	14.63	10.00	-5.449	-0.770	0.000
T9	VBAH	19.53	12.71	5.00	-5.553	-0.785	0.000
T9	SFID	23.22	17.37	46.00	-4.700	-0.664	0.000
T9	IIFD	24.38	18.53	53.00	-4.555	-0.644	0.000
T9	CPBA	2.32	3.75	102.00	-3.536	-0.500	0.000
T9	Area	8304.52	5030.67	0.00	-5.657	-0.800	0.000
T10	SFA	15.79	21.29	92.00	-3.744	-0.529	0.000
T10	SFPA	16.57	21.57	98.00	-3.619	-0.511	0.000
T10	VBPH	22.37	15.25	4.00	-5.406	-0.764	0.000
T10	VBAH	21.17	13.15	2.00	-5.454	-0.771	0.000
T10	SFID	24.79	18.07	26.00	-4.884	-0.690	0.000
T10	IIFD	24.15	19.97	63.00	-4.007	-0.566	0.000
T10	Area	8683.81	5199.40	0.00	-3.744	-0.800	0.000
T11	SFA	15.82	22.07	60.00	-4.409	-0.623	0.000
T11	SFPA	17.17	23.08	55.00	-4.513	-0.638	0.000
T11	IVAPA	98.41	109.97	125.00	-3.057	-0.432	0.002
T11	VBPH	24.16	16.47	49.00	-4.638	-0.655	0.000
T11	VBAH	21.74	14.36	49.00	-4.638	-0.655	0.000

[1] Bonferroni Correction: C1, $p < 0.01$; C2, $p < 0.008$; C3 – L5, $p < 0.004$.

Table G-2. Significant differences between *Homo* and *Pan* (cont.).

Species: *Homo sapiens* *Pan troglodytes*							
Level	Variable	*Homo* Mdn	*Pan* Mdn	U	z	r	p value [1]
T11	CPBA	3.05	3.73	113.00	-3.307	-0.467	0.001
T11	Area	8946.97	55.96.95	17.00	-5.303	-0.749	0.000
T12	SFA	13.69	21.14	75.00	-4.097	-0.579	0.000
T12	SFPA	14.73	21.86	79.00	-4.014	-0.567	0.000
T12	SVAPA	87.88	106.33	47.00	-4.679	-0.661	0.000
T12	IVAPA	28.79	85.66	16.00	-5.324	-0.752	0.000
T12	VBPH	25.70	18.00	30.00	-5.033	-0.711	0.000
T12	VBAH	23.66	15.45	26.00	-5.116	-0.723	0.000
T12	SFID	25.01	20.51	115.00	-3.265	-0.461	0.001
T12	Area	9626.91	6369.61	0.00	-5.657	-0.800	0.000
T12	RT	48.97	19.44	116.00	-3.244	-0.458	0.001
L1	IFA	13.76	13.76	19.16	-3.640	-0.141	0.000
L1	IFPA	14.97	19.65	110.00	-3.369	-0.476	0.001
L1	SVAPA	52.57	60.47	89.00	-3.223	-0.455	0.001
L1	IVAPA	21.96	46.60	6.00	-5.532	-0.782	0.000
L1	VBPH	26.95	21.35	56.00	-4.011	-0.567	0.000
L1	VBAH	25.31	18.29	35.00	-4.512	-0.638	0.000
L1	RT	28.30	12.50	64.00	-4.326	-0.611	0.000
L2	SVAPA	46.18	56.63	113.00	-3.307	-0.467	0.001
L2	IVAPA	28.29	41.01	39.00	-4.846	-0.685	0.000
L2	VBPH	27.12	22.75	78.00	-4.035	-0.570	0.000
L2	VBAH	25.79	18.69	92.00	-4.388	-0.620	0.000
L2	Area	12061.24	8820.39	41.00	-4.804	-0.679	0.000
L3	VBPH	27.69	22.34	104.00	-3.411	-0.482	0.001
L3	VBAH	27.22	19.59	62.00	-4.307	-0.609	0.000
L3	IIFD	29.69	23.33	107.00	-3.347	-0.473	0.001
L3	Area	12787.00	8507.55	15.00	-5.309	-0.750	0.000
L4	IVAPA	49.43	26.08	44.00	-4.210	-0.595	0.000
L4	VBAH	26.93	19.59	85.00	-2.977	-0.421	0.003
L4	IIFD	34.76	21.25	0.00	-5.256	-0.743	0.000
L4	CPBA	5.34	2.96	93.00	-3.045	-0.430	0.002
L4	Area	12396.72	7610.83	2.00	-3.744	-0.736	0.000
L4	RT	8.92	23.73	29.00	-4.567	-0.645	0.000

[1] Bonferroni Correction: C1, $p < 0.01$; C2, $p < 0.008$; C3 – L5, $p < 0.004$.

Table G-3. Significant differences between *Pan* and *Gorilla*.

Species: *Pan troglodytes* *Gorilla gorilla*							
Level	Variable	*Pan* Mdn	*Gorilla* Mdn	U	z	r	p value[1]
C1	IFA	102.25	100.29	30.00	-3.558	-0.628	0.000
C1	Area	3032.65	5283.66	9.00	-4.388	-0.775	0.000
C2	SFA	101.76	106.88	31.00	-3.380	-0.597	0.000
C2	SVAPA	8.69	13.21	15.00	-4.152	-0.733	0.000
C2	IFA	47.44	42.45	43.00	-2.883	-0.407	0.004
C2	Area	3290.97	6177.95	2.00	-4.583	-0.810	0.000
C3	SFID	25.10	30.51	0.00	-4.826	-0.853	0.000
C3	IIFD	28.41	34.36	0.00	-4.824	-0.852	0.000
C3	Area	2772.97	6118.81	1.00	-4.786	-0.846	0.000
C3	RT	19.69	10.47	52.00	-2.864	-0.405	0.004
C4	SFA	33.61	32.31	36.00	-3.320	-0.586	0.001
C4	SFPA	34.77	32.57	38.00	-3.241	-0.572	0.001
C4	VBPH	10.63	15.20	0.00	-4.824	-0.852	0.000
C4	VBAH	9.56	12.49	34.00	-3.543	-0.626	0.000
C4	PICP	100.73	98.70	-3.162	-3.162	-0.447	0.002
C4	Area	2992.36	6866.15	0.00	-4.824	-0.852	0.000
C5	SFA	37.18	33.52	46.00	-2.925	-0.413	0.003
C5	SFPA	38.15	33.88	46.00	-2.925	-0.413	0.003
C5	IVAPA	80.52	71.45	14.00	-4.190	-0.740	0.000
C5	VBPH	10.54	15.83	12.00	-4.372	-0.772	0.000
C5	VBAH	9.11	13.19	31.00	-3.656	-0.646	0.000
C5	PICP	100.31	96.24	22.00	-3.874	-0.684	0.000
C5	Area	3176.98	7208.26	0.00	-4.824	-0.852	0.000
C6	SVAPA	74.17	72.20	48.00	-3.015	-0.426	0.003
C6	IVAPA	80.91	68.68	15.00	-4.259	-0.752	0.000
C6	VBPH	11.07	16.31	19.00	-4.109	-0.726	0.000
C6	VBAH	9.81	13.28	29.00	-3.732	-0.659	0.000
C6	PICP	99.07	92.09	24.00	-3.920	-0.692	0.000
C6	Area	3863.89	8570.90	0.00	-4.824	-0.852	0.000
C7	IFA	24.54	31.93	52.00	-2.865	-0.405	0.004
C7	SVAPA	77.72	69.33	21.00	-3.913	-0.691	0.000
C7	IVAPA	84.94	69.81	1.00	-4.704	-0.831	0.000
C7	VBPH	11.77	15.89	19.00	-3.994	-0.706	0.000
C7	VBAH	9.51	12.63	11.00	-4.410	-0.779	0.000
C7	SFID	28.89	33.52	41.00	-3.279	-0.579	0.001
C7	IIFD	27.07	32.51	21.00	-4.743	-0.838	0.000
C7	Area	3958.32	8166.04	0.00	-3.744	-0.736	0.000

[1] Bonferroni Correction: C1, $p < 0.01$; C2, $p < 0.008$; C3 – L5, $p < 0.004$.

Table G-3. Significant differences between *Pan* and *Gorilla* (cont.).

Species: *Pan troglodytes* *Gorilla gorilla*							
Level	Variable	*Pan* Mdn	*Gorilla* Mdn	U	z	r	p value [1]
T1	SFPA	23.78	24.64	51.00	-2.902	0.513	0.004
T1	IFA	6.60	22.84	7.00	-4.560	-0.806	0.000
T1	IFPA	7.46	23.92	6.00	-4.598	-0.812	0.000
T1	SVAPA	98.04	67.14	0.00	-4.824	-0.852	0.000
T1	IVAPA	111.21	87.61	0.00	-4.824	-0.852	0.000
T1	PICP	67.34	70.03	18.00	-4.146	-0.732	0.000
T1	Area	4239.54	8505.27	0.00	-4.824	-0.852	0.000
T2	IFPA	6.08	11.62	47.00	-2.886	-0.408	0.004
T2	SVAPA	105.74	90.80	10.00	-4.348	-0.768	0.000
T2	IVAPA	112.43	104.90	9.00	-4.388	-0.775	0.000
T2	VBPH	13.29	18.17	20.00	-4.071	-0.719	0.000
T3	SVAPA	106.49	99.57	48.00	-2.846	-0.402	0.004
T3	IVAPA	110.60	103.56	44.00	-3.004	-0.424	0.003
T3	Area	4224.25	6742.41	10.00	-4.348	-0.768	0.000
T4	IVAPA	112.01	104.62	39.00	-3.035	-0.425	0.002
T4	CPBA	2.78	3.29	43.00	-4.423	-0.625	0.000
T4	Area	4257.41	7318.17	14.00	-4.297	-0.759	0.000
T5	IFA	4.31	8.22	31.00	-3.656	-0.646	0.000
T5	IFPA	5.44	8.93	37.00	-3.430	-0.606	0.001
T5	SVAPA	108.15	100.22	24.00	-3.920	-0.692	0.000
T5	IVAPA	111.88	107.18	17.00	-4.183	-0.739	0.000
T5	Area	4382.77	7360.91	16.00	-4.221	-0.746	0.000
T6	SVAPA	106.91	100.81	24.00	-3.795	-0.670	0.000
T6	IVAPA	110.85	107.19	24.00	-3.795	-0.670	0.000
T6	Area	4433.01	7467.68	17.00	-4.183	-0.739	0.000
T7	IFA	7.16	14.78	28.00	-3.769	-0.666	0.000
T7	IFPA	7.63	15.78	30.00	-3.694	-0.653	0.000
T7	SVAPA	104.89	101.50	41.00	-3.279	-0.579	0.001
T7	IVAPA	115.44	107.59	29.00	-3.731	-0.659	0.000
T7	Area	4571.86	7501.76	19.00	-4.108	-0.726	0.000
T8	IFA	6.67	16.72	23.00	-3.834	-0.677	0.000
T8	IFPA	7.26	17.57	19.00	-4.108	-0.726	0.000
T8	SVAPA	106.31	100.51	45.00	-2.965	-0.419	0.003
T8	IVAPA	109.23	105.59	32.00	-3.479	-0.615	0.001
T8	Area	4740.27	7534.26	23.00	-3.957	-0.699	0.000
T9	IFA	7.04	12.66	21.00	-3.913	-0.691	0.000
T9	IFPA	7.92	14.59	24.00	-3.795	-0.670	0.000

[1] Bonferroni Correction: C1, $p < 0.01$; C2, $p < 0.008$; C3 – L5, $p < 0.004$.

Table G-3. Significant differences between *Pan* and *Gorilla* (cont.).

Species: *Pan troglodytes* *Gorilla gorilla*							
Level	Variable	*Pan* Mdn	*Gorilla* Mdn	U	z	r	p value [1]
T9	IVAPA	114.16	106.12	21.00	-3.913	-0.691	0.000
T9	CPBA	3.75	1.93	38.00	-3.374	-0.596	0.001
T9	Area	5030.67	7936.07	27.00	-3.807	-0.672	0.000
T10	IFA	7.46	12.80	27.50	-3.790	-0.669	0.000
T10	IFPA	8.07	13.74	26.00	-3.846	-0.679	0.000
T10	IVAPA	114.35	102.90	41.00	-3.279	-0.579	0.001
T10	CPBA	4.00	1.88	32.00	-3.620	-0.639	0.000
T10	Area	5199.40	8410.54	25.00	-3.822	-0.686	0.000
T11	IFA	9.04	13.35	44.00	-3.166	-0.447	0.002
T11	IFPA	10.01	14.62	38.00	-3.392	-0.599	0.001
T11	CPBA	3.73	2.64	51.00	-2.902	-0.410	0.004
T11	Area	5595.95	8932.16	29.00	-3.731	-0.659	0.000
T12	Area	6369.61	10248.67	22.00	-3.995	-0.706	0.000
T13	VBPH	20.00	24.76	32.00	-3.479	-0.615	0.001
T13	VBAH	16.26	21.64	23.00	-3.836	-0.678	0.000
T13	SFID	20.54	25.14	23.00	-3.700	-0.654	0.000
T13	CPBA	5.84	3.55	28.00	-3.638	-0.643	0.000
T13	Area	7266.66	11146.04	28.00	-3.637	-0.642	0.000
L1	IFA	19.16	14.71	48.00	-3.015	-0.532	0.003
L1	IFPA	19.65	15.40	51.00	-2.902	-0.410	0.004
L1	Area	8164.25	13097.99	30.00	-3.409	-0.602	0.001
L2	VBAH	18.69	24.06	31.00	-3.656	-0.646	0.000
L2	Area	8820.39	12704.58	30.00	-3.694	-0.653	0.000
L3	IFA	14.96	10.08	44.00	-3.167	-0.559	0.002
L3	IFPA	15.86	10.98	52.00	-2.865	-0.405	0.004
L3	Area	8507.55	13337.60	30.00	-3.694	-0.653	0.000
L4	VBPH	21.69	27.82	20.00	-3.292	-0.581	0.001
L4	VBAH	20.77	26.98	15.00	-3.549	-0.627	0.000
L4	Area	7610.83	11247.24	19.00	-3.494	-0.617	0.000

[1] Bonferroni Correction: C1, $p < 0.01$; C2, $p < 0.008$; C3 – L5, $p < 0.004$.

Appendix H: MLR classification and validation results of taxa

Table H-1. Model classification and validation for C1.

C1 Model Classification				
	Predicted			
Observed	*Homo sapiens*	*Pan troglodytes*	*Gorilla gorilla*	Percent Correct
Homo sapiens	31	0	2	93.9%
Pan troglodytes	0	16	0	100.0%
Gorilla gorilla	2	1	12	80.0%
Overall Percentage	51.6%	26.6%	21.9%	92.2%
Model Statistics				
Likelihood Ratio[1]				
Area [χ^2 (2) = 27.206; p = 0.000]				
SVAPA [χ^2 (2) = 37.991; p = 0.000]				
IFA [χ^2 (2) = 21.082; p = 0.000]				
Model Fit[1]				
Final [-2 log likelihood value 31.703; χ^2 (6) = 99.900; p = 0.000]				
Goodness of Fit				
Pearson [χ^2 (120) = 69.401; p = 1.000]				
Deviance [χ^2 (120) = 37.701; p = 1.000]				
Pseudo R^2				
Cox and Snell R^2 = 0.79; Nagelkerke R^2 = 0.90; McFadden R^2 = 0.75				

C1 Validation Classification				
	Predicted			
Observed	*Homo sapiens*	*Pan troglodytes*	*Gorilla gorilla*	Percent Correct
Homo sapiens	1175	7	75	91.5%
Pan troglodytes	12	538		97.8%
Gorilla gorilla	99	35	441	73.7%
Overall Percentage	55.5%	25.0%	23.3%	90.1%
Validation Statistics 50 Tests (Homo n = 26, Pan n = 11, Gorilla n = 11) % Averages				
Model Fitting[2] Final Model: p = 0.000				
		Minimum	Maximum	
Goodness of Fit: Pearson		0.324	1.000	
Deviance		0.589	1.000	
Pseudo R Square: Cox and Snell		0.161	0.836	
Nagelkerke		0.186	0.965	
McFadden		0.088	0.899	
Total Misclassifications		228		

[1] Alpha level: $p < 0.05$.
[2] Bonferroni Correction: $p < 0.01$.

Table H-2. Model classification and validation for C2.

C2 Model Classification				
	Predicted			
Observed	*Homo sapiens*	*Pan troglodytes*	*Gorilla gorilla*	Percent Correct
Homo sapiens	30	0	4	88.2%
Pan troglodytes	1	14	0	93.3%
Gorilla gorilla	4	2	9	60.0%
Overall Percentage	54.7%	25.0%	20.3%	82.8%
Model Statistics				
Likelihood Ratio[1]				
IFA [χ^2 (2) = 6.490; p = 0.035]				
SVAPA [χ^2 (2) = 39.339; p = 0.000]				
RT [χ^2 (2) = 15.891; p = 0.000]				
Model Fit[1]				
Final [-2 log likelihood value 46.078; χ^2 (6) = 83.983; p = 0.000]				
Goodness of Fit				
Pearson [χ^2 (120) = 61.393; $p = 1.000$]				
Deviance [χ^2 (120) = 46.078; p = 1.000]				
Pseudo R^2				
Cox and Snell R^2 = 0.73; Nagelkerke R^2 = 0.84; McFadden R^2 = 0.64				

C2 Validation Classification				
	Predicted			
Observed	*Homo sapiens*	*Pan troglodytes*	*Gorilla gorilla*	Percent Correct
Homo sapiens	1217	5	78	93.5%
Pan troglodytes	51	455	17	86.7%
Gorilla gorilla	161	50	229	58.6%
Overall Percentage	61.6%	21.7%	16.9%	84.4%
Validation Statistics				
50 Tests (Homo n = 26, Pan n = 11, Gorilla n = 11) % Averages				
Model Fitting[2]				
Final Model: p = 0.000				
		Minimum	Maximum	
Goodness of Fit: Pearson		0.517	1.000	
Deviance		1.000	1.000	
Pseudo R Square: Cox and Snell		0.623	0.773	
Nagelkerke		0.723	0.900	
McFadden		0.494	0.758	
Total Misclassification		362		

[1] Alpha level: p < 0.05.
[2] Bonferroni Correction: p < 0.01.

Table H-3. Model classification and validation for C3.

C3 Model Classification				
	Predicted			
Observed	*Homo sapiens*	*Pan troglodytes*	*Gorilla gorilla*	Percent Correct
Homo sapiens	30	0	4	88.2%
Pan troglodytes	0	13	1	92.9%
Gorilla gorilla	4	1	10	66.7%
Overall Percentage	54.0%	22.2%	23.8%	84.1%
Model Statistics				
Likelihood Ratio[1]				
IFA [χ^2 (2) = 36.471; p = 0.000]				
SVAPA [χ^2 (2) = 31.088; p = 0.000]				
IVAPA [χ^2 (2) = 21.595; p = 0.000]				
CPBA [χ^2 (2) = 8.477; p = 0.014]				
Model Fit[1]				
Final [-2 log likelihood value 33.680; χ^2 (8) = 93.427; p = 0.000]				
Goodness of Fit				
Pearson [χ^2 (116) = 37.998; p = 1.000]				
Deviance [χ^2 (116) = 33.680; p = 1.000]				
Pseudo R^2				
Cox and Snell R^2 = 0.77; Nagelkerke R^2 = 0.89; McFadden R^2 = 0.73				

C3 Validation Classification				
	Predicted			
Observed	*Homo sapiens*	*Pan troglodytes*	*Gorilla gorilla*	Percent Correct
Homo sapiens	1168	42	88	88.1%
Pan troglodytes	64	397	28	81.0%
Gorilla gorilla	124	23	367	71.1%
Overall Percentage	58.9%	20.0%	20.9%	83.9%
Validation Statistics 50 Tests (Homo n = 26, Pan n = 11, Gorilla n = 11) % Averages				
Model Fitting[2] Final Model: p = 0.000				
		Minimum	Maximum	
Goodness of Fit: Pearson		0.846	1.000	
Deviance		0.979	1.000	
Pseudo R Square: Cox and Snell		0.460	0.824	
Nagelkerke		0.537	0.953	
McFadden		0.317	0.870	
Total Misclassification		369		

[1] Alpha level: p < 0.05.
[2] Bonferroni Correction: p < 0.01.

Table H-4. Model classification and validation for C4.

C4 Model Classification				
	Predicted			
Observed	*Homo sapiens*	*Pan troglodytes*	*Gorilla gorilla*	Percent Correct
Homo sapiens	33	1	0	97.1%
Pan troglodytes	1	13	1	86.7%
Gorilla gorilla	3	1	12	75.0%
Overall Percentage	56.9%	23.1%	20.0%	89.2%
Model Statistics[1]				
Likelihood Ratio				
IFPA [χ^2 (2) = 20.523; p = 0.000]				
IVAPA [χ^2 (2) = 16.229; p = 0.000]				
VBPH [χ^2 (2) = 33.670; p = 0.000]				
PICP [χ^2 (2) = 26.177; p = 0.000]				
C4 RT [χ^2 (2) = 7.480; p = 0.024]				
Model Fit[1]				
Final [-2 log likelihood value 33.157;: χ^2 (10) = 99.756; p = 0.000]				
Goodness of Fit				
Pearson [χ^2 (118) = 36.147; p = 1.000]				
Deviance [χ^2 (118) = 33.157; p = 1.000]				
Pseudo R^2				
Cox and Snell R^2 = 0.78; Nagelkerke R^2 = 0.90; McFadden R^2 = 0.75				

C4 Validation Classification				
	Predicted			
Observed	*Homo sapiens*	*Pan troglodytes*	*Gorilla gorilla*	Percent Correct
Homo sapiens	1183	91	26	91.0%
Pan troglodytes	84	418	24	79.6%
Gorilla gorilla	102	40	406	74.0%
Overall Percentage	56.7%	23.1%	19.1%	84.6%
Validation Statistics 50 Tests (Homo n = 26, Pan n = 11, Gorilla n = 11) % Averages				
Model Fitting[2] Final Model: p = 0.000				
		Minimum	Maximum	
Goodness of Fit: Pearson		0.175	1.000	
Deviance		0.997	1.000	
Pseudo R Square: Cox and Snell		0.481	0.762	
Nagelkerke		0.555	0.882	
McFadden		0.325	0.720	
Total Misclassification		367		

[1] Alpha level: p < 0.05.
[2] Bonferroni Correction: p < 0.01.

Table H-5. Model classification and validation for C5.

C5 Model Classification				
	Predicted			
Observed	*Homo sapiens*	*Pan troglodytes*	*Gorilla gorilla*	Percent Correct
Homo sapiens	30	1	2	90.9%
Pan troglodytes	3	11	1	73.3%
Gorilla gorilla	2	1	13	81.3%
Overall Percentage	54.7%	20.3%	25.0%	84.4%
Model Statistics				
Likelihood Ratio[1]				
IVAPA [χ^2 (2) = 46.435; p = 0.000]				
IIFD [χ^2 (2) = 31.091; p = 0.000]				
Model Fit[1]				
Final [-2 log likelihood value 57.314; χ^2 (4) = 74.289; p = 0.000]				
Goodness of Fit				
Pearson [χ^2 (122) = 89.728; p = 0.987]				
Deviance [χ^2 (122) = 57.314; p = 1.000]				
Pseudo R^2				
Cox and Snell R^2 = 0.68; Nagelkerke R^2 = 0.78; McFadden R^2 = 0.56				

C5 Validation Classification				
	Predicted			
Observed	*Homo sapiens*	*Pan troglodytes*	*Gorilla gorilla*	Percent Correct
Homo sapiens	1199	12	54	94.7%
Pan troglodytes	345	123	66	6.1%
Gorilla gorilla	100	5	442	80.6%
Overall Percentage	87.5%	2.0%	24.9%	71.5%
Validation Statistics 50 Tests (Homo n = 26, Pan n = 11, Gorilla n = 11) % Averages				
Model Fitting[2] Final Model: p = 0.000				
		Minimum	Maximum	
Goodness of Fit: Pearson		0.575	1.000	
Deviance		0.963	1.000	
Pseudo R Square: Cox and Snell		0.435	0.806	
Nagelkerke		0.501	0.933	
McFadden		0.281	0.821	
Total Misclassification		582		

[1] Alpha level: p < 0.05.
[2] Bonferroni Correction: p < 0.01.

Table H-6. Model classification and validation for C6.

C6 Model Classification				
	Predicted			
Observed	*Homo sapiens*	*Pan troglodytes*	*Gorilla gorilla*	Percent Correct
Homo sapiens	32	0	0	100.0%
Pan troglodytes	1	15	0	93.8%
Gorilla gorilla	1	0	15	93.8%
Overall Percentage	53.1%	23.4%	23.4%	96.9%
Model Statistics				
Likelihood Ratio[1]				
SFID [χ^2 (2) = 13.781; p = 0.000]				
SVAPA [χ^2 (2) = 23.615; p = 0.000]				
IVAPA [χ^2 (2) = 40.689; p = 0.000]				
IIFD [χ^2 (2) = 11.130; p = 0.004]				
Model Fit[1]				
Final [-2 log likelihood value 17.504; χ^2 (8) = 116.031; p = 0.000]				
Goodness of Fit				
Pearson [χ^2 (118) = 26.423; p = 1.000]				
Deviance [χ^2 (118) = 17.054; p = 1.000]				
Pseudo R^2				
Cox and Snell R^2 = 0.83; Nagelkerke R^2 = 0.95; McFadden R^2 = 0.87				

C6 Validation Classification				
	Predicted			
Observed	*Homo sapiens*	*Pan troglodytes*	*Gorilla gorilla*	Percent Correct
Homo sapiens	1198	25	3	97.2%
Pan troglodytes	32	507	13	91.8%
Gorilla gorilla	6	16	526	91.9%
Overall Percentage	53.1%	23.5%	23.3%	95.9%
Validation Statistics 50 Tests (Homo n = 26, Pan n = 11, Gorilla n = 11) % Averages				
Model Fitting[2] Final Model: p = 0.000				
		Minimum	Maximum	
Goodness of Fit: Pearson		0.771	1.000	
Deviance		1.000	1.000	
Pseudo R Square: Cox and Snell		0.686	0.871	
Nagelkerke		0.790	1.000	
McFadden		0.571	1.000	
Total Misclassification		95		

[1] Alpha level: p < 0.05.
[2] Bonferroni Correction: p < 0.01.

Table H-7. Model classification and validation for C7.

C 7 Model Classification				
	Predicted			
Observed	*Homo sapiens*	*Pan troglodytes*	*Gorilla gorilla*	Percent Correct
Homo sapiens	29	2	0	93.5%
Pan troglodytes	2	13	0	86.7%
Gorilla gorilla	1	0	15	93.8%
Overall Percentage	51.6%	24.2%	24.2%	91.9%
Model Statistics				
Likelihood Ratio[1]				
IVAPA [χ^2 (2) = 28.543; p = 0.000]				
Area [χ^2 (2) = 42.466; p = 0.000]				
Model Fit[1]				
Final [-2 log likelihood value 25.240; χ^2 (4) = 103.653; p = 0.000]				
Goodness of Fit				
Pearson [χ^2 (118) = 30.768; p = 1.000]				
Deviance [χ^2 (118) = 25.240; p = 1.000]				
Pseudo R^2				
Cox and Snell R^2 = 0.81; Nagelkerke R^2 = 0.92; McFadden R^2 = 0.84				

C7 Validation Classification				
	Predicted			
Observed	*Homo sapiens*	*Pan troglodytes*	*Gorilla gorilla*	Percent Correct
Homo sapiens	1124	58	8	94.3%
Pan troglodytes	60	461	0	75.9%
Gorilla gorilla	37	0	501	93.4%
Overall Percentage	56.8%	20.0%	23.0%	89.9%
Validation Statistics 50 Tests (Homo n = 26, Pan n = 11, Gorilla n = 11) % Averages				
Model Fitting[2] Final Model: p = 0.000				
		Minimum	Maximum	
Goodness of Fit: Pearson		0.989	1.000	
Deviance		1.000	1.000	
Pseudo R Square: Cox and Snell		0.634	0.871	
Nagelkerke		0.731	1.000	
McFadden		0.496	1.000	
Total Misclassification		163		

[1] Alpha level: p < 0.05.
[2] Bonferroni Correction: p < 0.01.

Table H-8. Model classification and validation for T1.

T1 Model Classification				
	Predicted			
Observed	*Homo sapiens*	*Pan troglodytes*	*Gorilla gorilla*	Percent Correct
Homo sapiens	32	1	1	94.1%
Pan troglodytes	4	12	0	75.0%
Gorilla gorilla	1	0	15	93.8%
Overall Percentage	56.1%	19.7%	24.2%	89.4%
Model Statistics				
Likelihood Ratio[1]				
IFPA [χ^2 (2) = 10.415; p = 0.005]				
SVAPA [χ^2 (2) = 46.137; p = 0.000]				
SFID [χ^2 (2) = 17.302; p = 0.000]				
Model Fit[1]				
Final [-2 log likelihood value 42.008; χ^2 (6) = 93.788; p = 0.000]				
Goodness of Fit				
Pearson [χ^2 (124) = 63.910; p = 1.000]				
Deviance [χ^2 (124) = 42.008; p = 1.000]				
Pseudo R^2				
Cox and Snell R^2 = 0.75; Nagelkerke R^2 = 0.87; McFadden R^2 = 0.69				

T1 Validation Classification				
	Predicted			
Observed	*Homo sapiens*	*Pan troglodytes*	*Gorilla gorilla*	Percent Correct
Homo sapiens	1222	58	24	94.0%
Pan troglodytes	177	373	0	67.5%
Gorilla gorilla	18	0	519	96.6%
Overall Percentage	58.2%	17.7%	23.1%	88.5%
Validation Statistics 50 Tests (Homo n = 26, Pan n = 11, Gorilla n = 11) % Averages				
Model Fitting[2] Final Model: p = 0.000				
		Minimum	Maximum	
Goodness of Fit: Pearson		0.644	1.000	
Deviance		1.000	1.000	
Pseudo R Square: Cox and Snell		0.618	0.811	
Nagelkerke		0.714	0.936	
McFadden		0.486	0.827	
Total Misclassification		277		

[1] Alpha level: p < 0.05.
[2] Bonferroni Correction: p < 0.01.

Table H-9. Model classification and validation for T2.

T2 Model Classification				
	Predicted			
Observed	*Homo sapiens*	*Pan troglodytes*	*Gorilla gorilla*	Percent Correct
Homo sapiens	29	0	3	90.6%
Pan troglodytes	1	14	1	87.5%
Gorilla gorilla	5	3	7	46.7%
Overall Percentage	55.6%	27.0%	17.5%	79.4%
Model Statistics				
Likelihood Ratio[1]				
IVAPA [χ^2 (2) = 52.987; p = 0.000]				
IIFD [χ^2 (2) = 27.392; p = 0.000]				
Model Fit[1]				
Final [-2 log likelihood value 54.569; χ^2 (4) = 75.695; p = 0.000]				
Goodness of Fit				
Pearson [χ^2 (120) = 65.582; p = 1.000]				
Deviance [χ^2 (120) = 54.569; p = 1.000]				
Pseudo R^2				
Cox and Snell R^2 = 0.69; Nagelkerke R^2 = 0.80; McFadden R^2 = 0.58				

T2 Validation Classification				
	Predicted			
Observed	*Homo sapiens*	*Pan troglodytes*	*Gorilla gorilla*	Percent Correct
Homo sapiens	1091	5	87	93.0%
Pan troglodytes	24	458	41	87.8%
Gorilla gorilla	165	67	253	53.3%
Overall Percentage	58.4%	24.1%	17.3%	82.9%
Validation Statistics 50 Tests (Homo n = 26, Pan n = 11, Gorilla n = 11) % Averages				
Model Fitting[2] Final Model: p = 0.000				
		Minimum	Maximum	
Goodness of Fit: Pearson		0.529	1.000	
Deviance		0.966	1.000	
Pseudo R Square: Cox and Snell		0.464	0.805	
Nagelkerke		0.533	0.926	
McFadden		0.305	0.805	
Total Misclassification		389		

[1] Alpha level: p < 0.05.
[2] Bonferroni Correction: p < 0.01.

Table H-10. Model classification and validation for T3.

T3 Model Classification				
	Predicted			
Observed	*Homo sapiens*	*Pan troglodytes*	*Gorilla gorilla*	Percent Correct
Homo sapiens	32	0	0	100.0%
Pan troglodytes	0	15	1	93.8%
Gorilla gorilla	1	1	13	86.7%
Overall Percentage	52.4%	25.4%	22.2%	95.2%
Model Statistics				
Likelihood Ratio[1]				
Area [χ^2 (2) = 34.121; p = 0.000]				
IIFD [χ^2 (2) = 27.463; p = 0.006]				
IVAPA [χ^2 (2) = 23.630; p = 0.000]				
SFPA [χ^2 (2) = 11.644; p = 0.000]				
Model Fit[1]				
Final [-2 log likelihood value 18.219; χ^2 (8) = 112.044; p = 0.000]				
Goodness of Fit				
Pearson [χ^2 (116) = 24.882; p = 1.000]				
Deviance [χ^2 (116) = 18.219; p = 1.000]				
Pseudo R^2				
Cox and Snell R^2 = 0.69; Nagelkerke R^2 = 0.80; McFadden R^2 = 0.58				

T3 Validation Classification				
	Predicted			
Observed	*Homo sapiens*	*Pan troglodytes*	*Gorilla gorilla*	Percent Correct
Homo sapiens	1157	4	41	96.2%
Pan troglodytes	26	518	19	93.7%
Gorilla gorilla	57	54	396	78.7%
Overall Percentage	54.5%	25.1%	20.9%	91.7%
Validation Statistics 50 Tests (Homo n = 26, Pan n = 11, Gorilla n = 11) % Averages				
Model Fitting[2] Final Model: p = 0.000				
		Minimum	Maximum	
Goodness of Fit: Pearson		0.776	1.000	
Deviance		0.999	1.000	
Pseudo R Square: Cox and Snell		0.646	0.871	
Nagelkerke		0.746	1.000	
McFadden		0.516	1.000	
Total Misclassification		201		

[1] Alpha level: p < 0.05.
[2] Bonferroni Correction: p < 0.01.

Table H-11. Model classification and validation for T4.

T4 Model Classification				
	Predicted			
Observed	*Homo sapiens*	*Pan troglodytes*	*Gorilla gorilla*	Percent Correct
Homo sapiens	32	0	2	94.1%
Pan troglodytes	0	13	1	92.9%
Gorilla gorilla	2	1	13	81.3%
Overall Percentage	53.1%	21.9%	25.0%	90.6%
Model Statistics				
Likelihood Ratio[1]				
SVAPA [χ^2 (2) = 36.812; p = 0.000]				
IIFD [χ^2 (2) = 25.782; p = 0.000]				
RT [χ^2 (2) = 10.891; p = 0.004]				
Model Fit[1]				
Final [-2 log likelihood value 41.242; χ^2 (6) = 88.686; p = 0.000]				
Goodness of Fit				
Pearson [χ^2 (120) = 70.429; p = 1.000]				
Deviance [χ^2 (120) = 41.242; p = 1.000]				
Pseudo R^2				
Cox and Snell R^2 = 0.75; Nagelkerke R^2 = 0.86; McFadden R^2 = 0.68				

T4 Validation Classification				
	Predicted			
Observed	*Homo sapiens*	*Pan troglodytes*	*Gorilla gorilla*	Percent Correct
Homo sapiens	1213	0	63	93.3%
Pan troglodytes	0	450	36	92.8%
Gorilla gorilla	96	57	399	72.6%
Overall Percentage	57.1%	25.2%	21.1%	89.3%
Validation Statistics[1\]				
50 Tests (Homo n = 26, Pan n = 11, Gorilla n = 11) % Averages				
Model Fitting[2]				
Final Model: p = 0.000				
		Minimum	Maximum	
Goodness of Fit: Pearson		0.926	1.000	
Deviance		1.000	1.000	
Pseudo R Square: Cox and Snell		0.672	0.843	
Nagelkerke		0.778	0.976	
McFadden		0.559	0.930	
Total Misclassification		252		

[1] Alpha level: p < 0.05.
[2] Bonferroni Correction: p < 0.01.

Table H-12. Model classification and validation for T5.

T5 Model Classification				
	Predicted			
Observed	*Homo sapiens*	*Pan troglodytes*	*Gorilla gorilla*	Percent Correct
Homo sapiens	31	0	3	91.2%
Pan troglodytes	0	15	1	93.8%
Gorilla gorilla	5	4	7	43.8%
Overall Percentage	54.5%	28.8%	16.7%	80.3%
Model Statistics				
Likelihood Ratio[1]				
IFA [χ^2 (2) = 12.669; p = 0.002]				
VBPH [χ^2 (2) = 58.624; p = 0.000]				
SFA [χ^2 (2) = 14.357; p = 0.001].				
Model Fit[1]				
Final [-2 log likelihood value 50.742; χ^2 (6) = 85.054; p = 0.000]				
Goodness of Fit				
Pearson [χ^2 (124) = 64.630; p = 1.000]				
Deviance [χ^2 (124) = 50.742; p = 1.000]				
Pseudo R^2				
Cox and Snell R^2 = 0.72; Nagelkerke R^2 = 0.83; McFadden R^2 = 0.62				

T5 Validation Classification				
	Predicted			
Observed	*Homo sapiens*	*Pan troglodytes*	*Gorilla gorilla*	Percent Correct
Homo sapiens	1007	35	215	80.7%
Pan troglodytes	390	101	57	19.1%
Gorilla gorilla	255	39	186	48.9%
Overall Percentage	49.5%	6.1%	21.8%	58.6%
Validation Statistics 50 Tests (Homo n = 26, Pan n = 11, Gorilla n = 11) % Averages				
Model Fitting[2] Final Model: p = 0.000				
		Minimum	Maximum	
Goodness of Fit: Pearson		0.211	0.955	
Deviance		0.905	0.977	
Pseudo R Square: Cox and Snell		0.141	0.594	
Nagelkerke		0.162	0.685	
McFadden		0.075	0.447	
Total Misclassification		991		

[1] Alpha level: p < 0.05.
[2] Bonferroni Correction: p < 0.01.

Table H-13. Model classification and validation for T6.

T6 Model Classification				
	Predicted			
Observed	*Homo sapiens*	*Pan troglodytes*	*Gorilla gorilla*	Percent Correct
Homo sapiens	33	0	1	97.1%
Pan troglodytes	0	15	0	100.0%
Gorilla gorilla	1	0	15	93.8%
Overall Percentage	52.3%	23.1%	24.6%	96.9%
Model Statistics				
Likelihood Ratio[1]				
Area [χ^2 (2) = 34.018; p = 0.000]				
SFPA [χ^2 (2) = 18.547; p = 0.000]				
VBPH [χ^2 (2) = 37.812; p = 0.000]				
SVAPA [χ^2 (2) = 12.044; p = 0.002]				
PICP [χ^2 (2) = 15.319; p = 0.000]				
IFA [χ^2 (2) = 28.107; p = 0.000]				
Model Fit[1]				
Final [-2 log likelihood value 7.416; χ^2 (12) = 125.497; p = 0.000]				
Goodness of Fit				
Pearson [χ^2 (116) = 8.107; p = 1.000]				
Deviance [χ^2 (116) = 7.416; p = 1.000]				
Pseudo R^2				
Cox and Snell R^2 = 0.85; Nagelkerke R^2 = 0.98; McFadden R^2 = 0.94				

T6 Validation Classification				
	Predicted			
Observed	*Homo sapiens*	*Pan troglodytes*	*Gorilla gorilla*	Percent Correct
Homo sapiens	1193	1	55	95.7%
Pan troglodytes	7	437	38	91.1%
Gorilla gorilla	74	58	407	74.5%
Overall Percentage	56.1%	22.5%	21.5%	90.1%
Validation Statistics 50 Tests (Homo n = 26, Pan n = 11, Gorilla n = 11) % Averages				
Model Fitting[2] Final Model: p = 0.000				
		Minimum	Maximum	
Goodness of Fit: Pearson		0.144	1.000	
Deviance		1.000	1.000	
Pseudo R Square: Cox and Snell		0.698	0.864	
Nagelkerke		0.808	1.000	
McFadden		0.600	1.000	
Total Misclassification		233		

[1] Alpha level: p < 0.05.
[2] Bonferroni Correction: p < 0.01.

Table H-14. Model classification and validation for T7.

T7 Model Classification				
	Predicted			
Observed	*Homo sapiens*	*Pan troglodytes*	*Gorilla gorilla*	Percent Correct
Homo sapiens	33	0	0	100.0%
Pan troglodytes	0	16	0	100.0%
Gorilla gorilla	1	0	15	93.8%
Overall Percentage	52.3%	24.6%	23.1%	98.5%
Model Statistics				
Likelihood Ratio[1]				
Area [χ^2 (2) = 31.445; p = 0.000]				
IFA [χ^2 (2) = 13.668; p = 0.001]				
VBPH [χ^2 (2) = 14.396; p = 0.000]				
PICP [χ^2 (2) = 21.592; p = 0.000]				
Model Fit[1]				
Final [-2 log likelihood value 15.009; χ^2 (8) = 119.446; p = 0.000]				
Goodness of Fit				
Pearson [χ^2 (120) = 83.807; p = 0.995]				
Deviance [χ^2 (120) = 15.009; p = 1.000]				
Pseudo R^2				
Cox and Snell R^2 = 0.84; Nagelkerke R^2 = 0.96; McFadden R^2 = 0.96				

T7 Validation Classification				
	Predicted			
Observed	*Homo sapiens*	*Pan troglodytes*	*Gorilla gorilla*	Percent Correct
Homo sapiens	1217	31	24	95.6%
Pan troglodytes	43	492	17	89.0%
Gorilla gorilla	47	41	460	83.9%
Overall Percentage	65.2%	23.7%	21.1%	91.4%
Validation Statistics 50 Tests (Homo n = 26, Pan n = 11, Gorilla n = 11) % Averages				
Model Fitting[2] Final Model: p = 0.000				
		Minimum	Maximum	
Goodness of Fit: Pearson		0.141	1.000	
Deviance		1.000	1.000	
Pseudo R Square: Cox and Snell		0.668	0.869	
Nagelkerke		0.771	1.000	
McFadden		0.547	1.000	
Total Misclassification		203		

[1] Alpha level: p < 0.05.
[2] Bonferroni Correction: p < 0.01.

Table H-15. Model classification and validation for T8.

T8 Model Classification				
	Predicted			
Observed	*Homo sapiens*	*Pan troglodytes*	*Gorilla gorilla*	Percent Correct
Homo sapiens	31	0	0	100.0%
Pan troglodytes	1	14	0	93.3%
Gorilla gorilla	1	3	12	75.0%
Overall Percentage	53.2%	27.4%	19.4%	91.9%
Model Statistics				
Likelihood Ratio[1]				
Area [χ^2 (2) = 48.199; p = 0.000]				
IFA [χ^2 (2) = 44.197; p = 0.000]				
CPBA [χ^2 (2) = 9.481; p = 0.009]				
Model Fit[1]				
Final [-2 log likelihood value 24.879; χ^2 (6) = 102.613; p = 0.000]				
Goodness of Fit				
Pearson [χ^2 (116) = 67.801; p = 1.000]				
Deviance [χ^2 (116) = 26.280; p = 1.000]				
Pseudo R^2				
Cox and Snell R^2 = 0.80; Nagelkerke R^2 = 0.92; McFadden R^2 = 0.79				

T8 Validation Classification				
	Predicted			
Observed	*Homo sapiens*	*Pan troglodytes*	*Gorilla gorilla*	Percent Correct
Homo sapiens	1135	24	29	95.7%
Pan troglodytes	53	381	70	76.4%
Gorilla gorilla	57	69	489	77.0%
Overall Percentage	54.5%	21.9%	23.0%	86.3%
Validation Statistics 50 Tests (Homo n = 26, Pan n = 11, Gorilla n = 11) % Averages				
Model Fitting: Final Model: p = 0.000				
		Minimum	Maximum	
Goodness of Fit: Pearson		0.135	1..000	
Deviance		0.969	1.000	
Pseudo R Square: Cox and Snell		0.476	0.871	
Nagelkerke		0.546	1.000	
McFadden		0.316	1.000	
Total Misclassification		302		

[1] Alpha level: p < 0.05.
[2] Bonferroni Correction: p < 0.01.

Table H-16. Model classification and validation for T9.

T9 Model Classification				
	Predicted			
Observed	*Homo sapiens*	*Pan troglodytes*	*Gorilla gorilla*	Percent Correct
Homo sapiens	33	0	1	97.1%
Pan troglodytes	0	15	1	93.8%
Gorilla gorilla	2	2	11	73.3%
Overall Percentage	53.8%	26.2%	20.0%	90.8%
Model Statistics				
Likelihood Ratio[1]				
SVAPA [χ^2 (2) = 11.285; p = 0.004]				
IFA [χ^2 (2) = 23.771; p = 0.000]				
VBPH [χ^2 (2) = 63.690; p = 0.000]				
Model Fit[1]				
Final [-2 log likelihood value 24.879; χ^2 (6) = 108.034; p = 0.000]				
Goodness of Fit				
Pearson [χ^2 (122) = 25.497; p = 1.000]				
Deviance [χ^2 (122) = 24.879; p = 1.000]				
Pseudo R^2				
Cox and Snell R^2 = 0.81; Nagelkerke R^2 = 0.93; McFadden R^2 = 0.81				

T9 Validation Classification				
	Predicted			
Observed	*Homo sapiens*	*Pan troglodytes*	*Gorilla gorilla*	Percent Correct
Homo sapiens	1242	20	38	95.5%
Pan troglodytes	32	446	66	80.7%
Gorilla gorilla	74	74	358	72.0%
Overall Percentage	56.9%	22.8%	20.1%	86.8%
Validation Statistics 50 Tests (Homo n = 26, Pan n = 11, Gorilla n = 11) % Averages				
Model Fitting[2] Final Model: p = 0.000				
		Minimum	Maximum	
Goodness of Fit: Pearson		0.816	1.000	
Deviance		0.947	1.000	
Pseudo R Square: Cox and Snell		0.403	0.864	
Nagelkerke		0.467	1.000	
McFadden		0.259	1.000	
Total Misclassification		304		

[1] Alpha level: p < 0.05.
[2] Bonferroni Correction: p < 0.01.

Table H-17. Model classification and validation for T10.

T10 Model Classification				
	Predicted			
Observed	*Homo sapiens*	*Pan troglodytes*	*Gorilla gorilla*	Percent Correct
Homo sapiens	28	1	0	96.6%
Pan troglodytes	0	14	2	87.5%
Gorilla gorilla	0	2	14	87.5%
Overall Percentage	45.9%	27.9%	26.2%	91.8%
Model Statistics				
Likelihood Ratio[1]				
IFPA [χ^2 (2) = 19.168; p = 0.000]				
VBAH [χ^2 (2) = 18.654; p = 0.000]				
VBPH [χ^2 (2) = 13.291; p = 0.001]				
CPBA [χ^2 (2) = 15.811; p = 0.000]				
Model Fit[1]				
Final [-2 log likelihood value 16.175; χ^2 (8) = 112.603; p = 0.000]				
Goodness of Fit				
Pearson [χ^2 (122) = 14.368; p = 1.000]				
Deviance [χ^2 (122) = 16.175; p = 1.000]				
Pseudo R^2				
Cox and Snell R^2 = 0.84; Nagelkerke R^2 = 0.95; McFadden R^2 = 0.87				

T10 Validation Classification				
	Predicted			
Observed	*Homo sapiens*	*Pan troglodytes*	*Gorilla gorilla*	Percent Correct
Homo sapiens	1086	36	4	94.5%
Pan troglodytes	24	406	122	73.4%
Gorilla gorilla	16	93	493	70.7%
Overall Percentage	50.5%	24.05%	25.3%	85.5%
Validation Statistics 50 Tests (Homo n = 26, Pan n = 11, Gorilla n = 11) % Averages				
Model Fitting[2] Final Model: p = 0.000				
		Minimum	Maximum	
Goodness of Fit: Pearson		0.517	1.000	
Deviance		0.871	1.000	
Pseudo R Square: Cox and Snell		0.379	0.875	
Nagelkerke		0.435	1.000	
McFadden		0.231	1.000	
Total Misclassification		295		

[1] Alpha level: p < 0.05.
[2] Bonferroni Correction: p < 0.01.

.

Table H-18. Model classification and validation for T11.

T11 Model Classification				
	Predicted			
Observed	*Homo sapiens*	*Pan troglodytes*	*Gorilla gorilla*	Percent Correct
Homo sapiens	34	0	0	100.0%
Pan troglodytes	0	15	1	93.8%
Gorilla gorilla	0	1	15	93.8%
Overall Percentage	51.5%	24.2%	24.2%	97.0%
Model Statistics				
Likelihood Ratio[1]				
VBPH [χ^2 (2) = 76.977; p = 0.000]				
PICP [χ^2 (2) = 56.808; p = 0.000]				
Area [χ^2 (2) = 64.551; p = 0.000]				
Model Fit[1]				
Final [-2 log likelihood value 10.651; χ^2 (6) = 125.145; p = 0.000]				
Goodness of Fit				
Pearson [χ^2 (124) = 9.533; p = 1.000]				
Deviance [χ^2 (124) = 10.651; p = 1.000]				
Pseudo R^2				
Cox and Snell R^2 = 0.85; Nagelkerke R^2 = 0.97; McFadden R^2 = 0.92				

T11 Validation Classification				
	Predicted			
Observed	*Homo sapiens*	*Pan troglodytes*	*Gorilla gorilla*	Percent Correct
Homo sapiens	1262	16	22	99.0%
Pan troglodytes	17	521	14	94.35%
Gorilla gorilla	48	25	475	86.7%
Overall Percentage	55.3%	23.4%	25.4%	94.0%
Validation Statistics 50 Tests (Homo n = 26, Pan n = 11, Gorilla n = 11) % Averages				
Model Fitting[2] Final Model: p = 0.000				
		Minimum	Maximum	
Goodness of Fit: Pearson		0.250	1.000	
Deviance		0.994	1.000	
Pseudo R Square: Cox and Snell		0.597	0.867	
Nagelkerke		0.689	1.000	
McFadden		0.451	1.000	
Total Misclassification		142		

[1] Alpha level: p < 0.05.
[2] Bonferroni Correction: p < 0.01.

Table H-19. Model classification and validation for T12.

T12 Model Classification				
	Predicted			
Observed	*Homo sapiens*	*Pan troglodytes*	*Gorilla gorilla*	Percent Correct
Homo sapiens	34	0	0	100.0%
Pan troglodytes	1	12	3	75.0%
Gorilla gorilla	0	4	12	75.0%
Overall Percentage	53.0%	24.2%	22.7%	87.9%
Model Statistics				
Likelihood Ratio[1]				
IVAPA [χ^2 (2) = 81.252; p = 0.000]				
SFID [χ^2 (2) = 21.285; p = 0.000]				
Model Fit[1]				
Final [-2 log likelihood value 42.954; χ^2 (4) = 92.843; p = 0.000]				
Goodness of Fit				
Pearson [χ^2 (126) = 57.894; p = 1.000]				
Deviance [χ^2 (126) = 42.954; p = 1.000]				
Pseudo R^2				
Cox and Snell R^2 = 0.75; Nagelkerke R^2 = 0.86; McFadden R^2 = 0.68				

T12 Validation Classification				
	Predicted			
Observed	*Homo sapiens*	*Pan troglodytes*	*Gorilla gorilla*	Percent Correct
Homo sapiens	1287	5	8	98.9%
Pan troglodytes	84	352	116	63.6%
Gorilla gorilla	23	179	395	62.9%
Overall Percentage	59.2%	22.3%	19.5%	82.6%
Validation Statistics 50 Tests (Homo n = 26, Pan n = 11, Gorilla n = 11) % Averages				
Model Fitting[2] Final Model: p = 0.000				
		Minimum	Maximum	
Goodness of Fit: Pearson		0.159	1.000	
Deviance		0.550	1.000	
Pseudo R Square: Cox and Snell		0.137	0.798	
Nagelkerke		0.158	0.921	
McFadden		0.073	0.795	
Total Misclassification		415		

[1] Alpha level: p < 0.05.
[2] Bonferroni Correction: p < 0.01.

Table H-20. Model classification and validation for T13.

T13 Model Classification			
	Predicted		
Observed	*Pan troglodytes*	*Gorilla gorilla*	Percent Correct
Pan troglodytes	13	1	92.9%
Gorilla gorilla	1	15	93.8%
Overall Percentage	46.7%	53.3%	93.3%
Model Statistics			
Likelihood Ratio[1]			
IVAPA [χ^2 (1) = 10.432; p = 0.001]			
VBAH [χ^2 (1) = 24.917; p = 0.000]			
Model Fit[1]			
Final [-2 log likelihood value 10.608; χ^2 (2) = 30.848; p = 0.000]			
Goodness of Fit			
Pearson [χ^2 (27) = 11.932; p = 0.995]			
Deviance [χ^2 (27) = 10.608; p = 0.998]			
Pseudo R^2			
Cox and Snell R^2 = 0.64; Nagelkerke R^2 = 0.85; McFadden R^2 = 0.74			

T13 Validation Classification			
	Predicted		
Observed	*Pan troglodytes*	*Gorilla gorilla*	Percent Correct
Pan troglodytes	387	96	80.0%
Gorilla gorilla	108	440	80.1%
Overall Percentage	47.9%	52.0%	92.3%
Validation Statistics 50 Tests (Homo n = 26, Pan n = 11, Gorilla n = 11) % Averages			
Model Fitting[2] Final Model: p = 0.000			
	Minimum	Maximum	
Goodness of Fit: Pearson	0.468	0.999	
Deviance	0.338	0.995	
Pseudo R Square: Cox and Snell	0.307	0.662	
Nagelkerke	0.412	0.883	
McFadden	0.269	0.784	
Total Misclassification	204		

[1] Alpha level: $p < 0.05$.
[2] Bonferroni Correction: $p < 0.01$.

Table H-21. Model classification and validation for L1.

L1 Model Classification				
	Predicted			
Observed	*Homo sapiens*	*Pan troglodytes*	*Gorilla gorilla*	Percent Correct
Homo sapiens	31	1	0	96.9%
Pan troglodytes	1	11	2	78.6%
Gorilla gorilla	0	3	13	81.3%
Overall Percentage	51.6%	24.2%	24.2%	88.7%
Model Statistics				
Likelihood Ratio[1]				
IVAPA [χ^2 (2) = 68.879; p = 0.000]				
VBAH [χ^2 (2) = 14.477; p = 0.001]				
Model Fit[1]				
Final [-2 log likelihood value 34.419; χ^2 (4) = 92.923; p = 0.000]				
Goodness of Fit				
Pearson [χ^2 (118) = 47.290; p = 1.000]				
Deviance [χ^2 (118) = 34.419; p = 1.000]				
Pseudo R^2				
Cox and Snell R^2 = 0.77; Nagelkerke R^2 = 0.89; McFadden R^2 = 0.73				

L1 Validation Classification				
	Predicted			
Observed	*Homo sapiens*	*Pan troglodytes*	*Gorilla gorilla*	Percent Correct
Homo sapiens	1193	24	16	96.7%
Pan troglodytes	85	165	104	34.7%
Gorilla gorilla	33	102	463	74.8%
Overall Percentage	58.3%	12.9%	28.7%	79.3%
Validation Statistics 50 Tests (Homo n = 26, Pan n = 11, Gorilla n = 11) % Averages				
Model Fitting[2] Final Model: p = 0.000				
		Minimum	Maximum	
Goodness of Fit: Pearson		0.999	1.000	
Deviance		1.000	1.000	
Pseudo R Square: Cox and Snell		0.606	0.804	
Nagelkerke		0.703	0.929	
McFadden		0.469	0.812	
Total Misclassification		364		

[1] Alpha level: p < 0.05.
[2] Bonferroni Correction: p < 0.01.

Table H-22. Model classification and validation for L2.

L2 Model Classification				
	Predicted			
Observed	*Homo sapiens*	*Pan troglodytes*	*Gorilla gorilla*	Percent Correct
Homo sapiens	34	0	0	100.0%
Pan troglodytes	1	15	0	93.8%
Gorilla gorilla	0	1	15	93.8%
Overall Percentage	53.0%	24.2%	22.7%	97.0%
Model Statistics				
Likelihood Ratio[1]				
Area [χ^2 (2) = 48.015; p = 0.000]				
IIFD [χ^2 (2) = 33.616; p = 0.000]				
IVAPA [χ^2 (2) = 71.815; p = 0.000]				
Model Fit[1]				
Final [-2 log likelihood value 10.033; χ^2 (6) = 125.763; p = 0.000]				
Goodness of Fit				
Pearson [χ^2 (124) = 12.459; p = 1.000]				
Deviance [χ^2 (124) = 10.033; p = 1.000]				
Pseudo R^2				
Cox and Snell R^2 = 0.85; Nagelkerke R^2 = 0.97; McFadden R^2 = 0.92				

L2 Validation Classification				
	Predicted			
Observed	*Homo sapiens*	*Pan troglodytes*	*Gorilla gorilla*	Percent Correct
Homo sapiens	1262	4	7	99.0%
Pan troglodytes	22	497	33	90.0%
Gorilla gorilla	6	49	493	89.9%
Overall Percentage	54.8%	22.9%	22.2%	94.8%
Validation Statistics 50 Tests (Homo n = 26, Pan n = 11, Gorilla n = 11) % Averages				
Model Fitting[2] Final Model: p = 0.000				
		Minimum	Maximum	
Goodness of Fit: Pearson		1.000	1.000	
Deviance		1.000	1.000	
Pseudo R Square: Cox and Snell		0.735	0.867	
Nagelkerke		0.848	1.000	
McFadden		0.659	1.000	
Total Misclassification		121		

[1] Alpha level: p < 0.05.
[2] Bonferroni Correction: p < 0.01.

Table H-23. Model classification and validation for L3.

L3 Model Classification				
	Predicted			
Observed	*Homo sapiens*	*Pan troglodytes*	*Gorilla gorilla*	Percent Correct
Homo sapiens	32	0	1	97.0%
Pan troglodytes	1	15	0	93.8%
Gorilla gorilla	1	0	15	93.8%
Overall Percentage	52.3%	23.1%	24.6%	95.4%
Model Statistics				
Likelihood Ratio[1]				
IIFD [χ^2 (2) = 46.508; p = 0.000]				
SVAPA [χ^2 (2) = 10.409; p = 0.005]				
VBPH [χ^2 (2) = 8.492; p = 0.014]				
SFID [χ^2 (2) = 18.120; p = 0.000]				
Area [χ^2 (2) = 23.030; p = 0.000]				
Model Fit[1]				
Final [-2 log likelihood value 18.915; χ^2 (10) = 115.541; p = 0.000]				
Goodness of Fit				
Pearson [χ^2 (118) = 78.093; p = 0.998]				
Deviance [χ^2 (118) = 18.915; p = 1.000]				
Pseudo R^2				
Cox and Snell R^2 = 0.83; Nagelkerke R^2 = 0.95; McFadden R^2 = 0.85				

L3 Validation Classification				
	Predicted			
Observed	*Homo sapiens*	*Pan troglodytes*	*Gorilla gorilla*	Percent Correct
Homo sapiens	1188	15	62	93.9%
Pan troglodytes	34	496	22	89.8%
Gorilla gorilla	124	74	350	63.7%
Overall Percentage	56.9%	24.5%	18.3%	86.0%
Validation Statistics 50 Tests (Homo n = 26, Pan n = 11, Gorilla n = 11) % Averages				
Model Fitting[2] Final Model: p = 0.000				
		Minimum	Maximum	
Goodness of Fit: Pearson		0.342	1.000	
Deviance		0.991	1.000	
Pseudo R Square: Cox and Snell		0.455	0.869	
Nagelkerke		0.524	1.000	
McFadden		0.229	1.000	
Total Misclassification		331		

[1] Alpha level: p < 0.05.
[2] Bonferroni Correction: p < 0.01.

Table H-24. Model classification and validation for L4.

L4 Model Classification				
	Predicted			
Observed	*Homo sapiens*	*Pan troglodytes*	*Gorilla gorilla*	Percent Correct
Homo sapiens	32	0	2	94.1%
Pan troglodytes	0	11	1	91.7%
Gorilla gorilla	3	2	9	64.3%
Overall Percentage	58.3%	21.7%	20.0%	86.7%
Model Statistics				
Likelihood Ratio[1]				
IFPA [χ^2 (2) = 15.695; p = 0.000]				
IVAPA [χ^2 (2) = 10.716; p = 0.005]				
Area [χ^2 (2) = 39.306; p = 0.000]				
RT [χ^2 (2) = 7.526; p = 0.023]				
Model Fit[1]				
Final [-2 log likelihood value 35.597; χ^2 (8) = 81.400; p = 0.000]				
Goodness of Fit				
Pearson [χ^2 (110) = 48.600; p = 0.998]				
Deviance [χ^2 (110) = 36.597; p = 1.000]				
Pseudo R^2				
Cox and Snell R^2 = 0.74; Nagelkerke R^2 = 0.86; McFadden R^2 = 0.69				

L4 Validation Classification				
	Predicted			
Observed	*Homo sapiens*	*Pan troglodytes*	*Gorilla gorilla*	Percent Correct
Homo sapiens	1142	31	63	92.7%
Pan troglodytes	79	376	17	88.1%
Gorilla gorilla	206	57	208	43.5%
Overall Percentage	65.9%	21.0%	13.0%	95.9%

Validation Statistics 50 Tests (Homo n = 26, Pan n = 11, Gorilla n = 11) % Averages		
Model Fitting[2]		
Final Model: p = 0.000		
	Minimum	Maximum
Goodness of Fit: Pearson	0.214	1.000
Deviance	0.995	1.000
Pseudo R Square: Cox and Snell	0.402	0.753
Nagelkerke	0.474	0.883
McFadden	0.272	0.729
Total Misclassification	453	

[1] Alpha level: p < 0.05.
[2] Bonferroni Correction: p < 0.01.

Appendix I: Spearman's rho correlation results

Table I-1. Spearman's rho, significant correlation for *Homo*.

Level	Variable	*Homo*					
		Variable	r_s	p value [1]	Variable	r_s	p value [2]
C1	SFA	Area	0.525	0.002			
C2	IFA				IVAPA RT	-0.392 -0.433	0.022 0.011
C2	SVAPA	RT	-0.502	0.002			
C2	IVAPA	RT	0.808	0.000	IFA	-0.392	0.022
C2	RT	SVAPA IVAPA	0.502 0.818	0.002 0.000	IFA	-0.433	0.011
C3	SFA	SFPA	0.983	0.000	SVAPA	0.435	0.010
C3	SFPA	SFA	0.983	0.000	SVAPA	0.412	0.015
C3	IFA	IFPA IVAPA RT	0.962 -0.593 -0.436	0.000 0.000 0.010			
C3	IFPA	IFA IVAPA	0.962 -0.516	0.000 0.002	RT	-0.425	0.012
C3	SVAPA				SFA SFPA RT	0.435 0.412 -0.738	0.010 0.015 0.015
C3	IVAPA	IFA IFPA RT	-0.593 0.516 0.440	0.000 0.002 0.009			
C3	VBPH	VBAH IIFD Area	0.687 0.522 0.619	0.000 0.002 0.000	SFID	0.416	0.014
C3	CVAH	VBPH IIFD Area	0.687 0.502 0.592	0.000 0.003 0.000			
C3	SFID	IIFD Area	0.752 0.654	0.000 0.000	VBPH	0.416	0.014
C3	IIFD	VBPH VBAH SFID	0.522 0.502 0.752	0.000 0.002 0.000	CPBA	0.377	0.028
C3	PICP				Area	-0.359	0.037
C3	CPBA				IIFD	0.377	0.028
C3	Area	VBPH VBAH IIFD	0.619 0.592 0.767	0.000 0.000 0.000	PICP	-0.359	0.037

[1] Alpha level: $p < 0.01$; [2] Alpha level: $p < 0.05$.

Table I-1. Spearman's rho, significant correlation for *Homo* (cont.).

Level	Variable	*Homo*					
		Variable	r_s	p value [1]	Variable	r_s	p value [2]
C3	RT	IFA	-0.436	0.010	IFPA	-0.425	0.012
		SVAPA	-0.738	0.000			
		IVAPA	0.440	0.009			
C4	SFA	SFPA	0.968	0.000			
C4	SFPA	SFA	0.968	0.000			
C4	IFA	IFPA	0.983	0.000	Area	-0.360	0.036
C4	IFPA	IFA	0.983	0.000	Area	-0.382	0.026
C4	SVAPA	SFID	0.422	0.009	IIFD	0.359	0.037
		Area	0.452	0.007			
		RT	-0.449	0.008			
C4	IVAPA				RT	0.346	0.045
C4	VBPH	VBAH	0.743	0.000			
		SFID	0.665	0.000			
		IIFD	0.529	0.001			
		Area	0.787	0.000			
C4	VBAH	VBPH	0.743	0.000			
		SFID	0.468	0.005			
		IIFD	0.489	0.003			
		Area	0.620	0.000			
C4	SFID	SVAPA	0.442	0.009			
		VBPH	0.665	0.000			
		VBAH	0.468	0.005			
		Area	0.577	0.000			
C4	IIFD	VBPH	0.529	0.001	SVAPA	0.359	0.037
		VBAH	0.489	0.003			
		SFID	0.729	0.000			
		Area	0.606	0.000			
C4	Area	SVAPA	0.452	0.007	IFA	-0.360	0.036
		VBPH	0.787	0.000	IFPA	-0.382	0.026
		VBAH	0.620	0.000			
		SFID	0.577	0.000			
		IIFD	0.606	0.000			
C4	RT	SVAPA	-0.449	0.008	IVAPA	0.346	0.045
C5	SFA	SFPA	0.995	0.000			
C5	SFPA	SFA	0.995	0.000			
C5	IFA	IFPA	0.986	0.000	IVAPA	-0.405	0.017
		RT	0.528	0.001	VBPH	0.376	0.028
C5	IFPA	IFA	0.986	0.000	IVAPA	-0.422	0.013
		RT	0.520	0.002	VBPH	0.366	0.033
C5	SVAPA	SFID	0.531		IIFD	0.408	0.017

[1] Alpha level: $p < 0.01$; [2] Alpha level: $p < 0.05$.

Table I-1. Spearman's rho, significant correlation for *Homo* (cont.).

Level	Variable	*Homo*					
		Variable	r_s	p value [1]	Variable	r_s	p value [2]
C5	IVAPA				IFA	-0.405	0.017
					IFPA	-0.422	0.013
					RT	-0.409	0.016
C5	VBPH	VBAH	0.612	0.000	IFA	0.376	0.028
		SFID	0.536	0.001	IFPA	0.366	0.033
C5	VBAH	VBPH	0.612	0.000	IIFD	0.390	
		SFID	0.544	0.001			
		Area	0.549	0.001			
C5	SFID	SVAPA	0.531	0.001			
		VBPH	0.536	0.001			
		VBAH	0.544	0.001			
		IIFD	0.772	0.000			
		Area	0.648	0.000			
C5	IIFD	VBPH	0.510	0.002	SVAPA	0.408	0.017
		SFID	0.772	0.000	VBAH	0.390	0.022
		Area	0.596	0.000			
C5	Area	VBPH	0.765	0.000			
		VBAH	0.549	0.001			
		SFID	0.648	0.000			
		IIFD	0.596	0.000			
C5	RT	IFA	0.528	0.001	IVAPA	-0.409	0.016
		IFPA	0.520	0.002			
C6	SFA	SFPA	0.993	0.000	SFID	0.357	0.038
		IFA	0.440	0.009	IIFD	0.355	0.039
		IFPA	0.440	0.009			
C6	SFPA	SFPA	0.993	0.000	IFA	0.428	0.012
					IFPA	0.435	0.010
					SFID	0.345	0.046
					IIFD	0.345	0.045
C6	IFA	SFA	0.440	0.009	SFPA	0.428	0.012
		IFPA	0.991	0.000	SFID	0.383	0.025
		IVAPA	-0.571	0.000	Area	0.354	0.040
		IIFD	0.545	0.001			
		PICP	0.489	0.003			
C6	IFPA	SFA	0.440	0.009	SFPA	0.435	0.010
		IFA	0.991	0.000	RT	0.376	0.016
		IVAPA	-0.565	0.001			
		SFID	0.439	0.009			
		IIFD	0.572	0.000			
		PICP	0.477	0.004			

[1]Alpha level: $p < 0.01$; [2]Alpha level: $p < 0.05$.

Table I-1. Spearman's rho, significant correlation for *Homo* (cont.).

Level	Variable	*Homo*					
		Variable	r_s	p value [1]	Variable	r_s	p value [2]
C6	SVAPA	IIFD	0.518	0.002	SFID	0.387	0.029
C6	IVAPA	IFA	-0.571	0.000			
		IFPA	-0.565	0.001			
		RT	-0.494	0.003			
C6	VBPH	VBAH	0.569	0.000	RT	0.347	0.044
		SFID	0.496	0.003			
		IIFD	0.499	0.003			
		Area	0.753	0.000			
C6	VBAH	VBPH	0.569	0.000			
		Area	0.531	0.001			
C6	SFID	IFPA	0.439	0.009	SFA	0.357	0.038
		VBPH	0.496	0.003	SFPA	0.345	0.046
		IIFD	0.533	0.001	IFA	0.383	0.025
		Area	0.572	0.000	SVAPA	0.387	0.029
C6	IIFD	IFPA	0.572	0.001	SFA	0.355	0.039
		SVAPA	0.518	0.002	SFPA	0.345	0.045
		VBPH	0.499	0.003	IFA	0.545	0.018
		SFID	0.553	0.001	Area	0.403	0.018
					RT	0.389	0.023
C6	PICP	IFA	0.489	0.003			
		IFPA	0.477	0.004			
C6	Area	VBPH	0.753	0.000	IFA	0.354	0.040
		VBAH	0.531	0.001	IFPA	0.411	0.016
		SFID	0.572	0.000	IIFD	0.403	0.018
C6	RT	IVAPA	-0.494	0.003	IFA	0.377	0.028
					IFPA	0.376	0.028
					VBPH	0.344	0.044
					SVAPA	0.389	0.023
C7	SFA	SFPA	0.991	0.000	SVAPA	0.436	0.011
		SFID	0.515	0.002	IIFD	0.422	0.013
C7	SFPA	SFA	0.991	0.000	SVAPA	0.436	0.011
		SFID	0.524	0.002	IIFD	0.422	0.014
C7	IFA	IFPA	0.993	0.000	IVAPA	-0.343	0.047
C7	IFPA	IFA	0.993	0.000	IVAPA	-0.367	0.033
C7	SVAPA	CPBA	-0.460	0.008	SFA	0.436	0.011
					SFPA	0.436	0.011
C7	VBPH	VBAH	0.792	0.000	SFID	0.363	0.038
		IIFD	0.481	0.004			
		Area	0.687	0.000			

[1]Alpha level: $p < 0.01$; [2]Alpha level: $p < 0.05$.

Table I-1. Spearman's rho, significant correlation for *Homo* (cont.).

Level	Variable	*Homo*					
		Variable	r_s	p value [1]	Variable	r_s	p value [2]
C7	VBAH	VBPH	0.792	0.000			
		Area	0.586	0.000			
C7	SFID	SFA	0.515	0.002	VBPH	0.363	0.038
		SFPA	0.524	0.002			
		IIFD	0.618	0.000			
		Area	0.450	0.004			
C7	IIFD	VBPH	0.481	0.004	SFA	0.426	0.013
		Area	0.620	0.000	SFPA	0.422	0.014
		SFID	0.618	0.000	IVAPA	-0.384	0.025
C7	CPBA	SVAPA	-0.460	0.008	RT	0.399	0.024
C7	Area	VBPH	0.687	0.008			
		VBAH	0.586	0.000			
		SFID	0.450	0.009			
		IIFD	0.620	0.000			
C7	RT				CPBA	0.399	0.024
T1	SFA	SFPA	0.984	0.000			
T1	SFPA	SFA	0.984	0.000			
T1	IFA	IFPA	0.959	0.000	SVAPA	-0.343	0.047
					VBPH	-0.343	0.047
					VBAH	-0.393	0.022
T1	IFPA	IFA	0.959	0.000	SVAPA	-0.365	0.034
					IVAPA	-0.390	0.023
					VBPH	-0.394	0.021
					VBAH	-0.403	0.018
T1	SVAPA	RT	-0.565	0.001	IFA	-0.343	0.047
					IFPA	-0.365	0.034
					VBPH	0.425	0.012
					VBAH	0.413	0.015
T1	IVAPA	RT	0.540	0.000	IFPA	-0.390	0.023
T1	VBPH	Area	0.776	0.000	IFA	-0.343	0.047
		IIFD	0.339	0.000	IFPA	-0.394	0.021
					SVAPA	0.425	0.012
					VBAH	0.772	0.050
T1	VBAH	VBPH	0.772	0.000	IFA	-0.393	0.022
		Area	0.613	0.000	IFPA	-0.403	0.018
					SVAPA	0.413	0.015
T1	SFID	Area	0.481	0.000			
		IIFD	0.583	0.000			

[1]Alpha level: $p < 0.01$; [2]Alpha level: $p < 0.05$.

Table I-1. Spearman's rho, significant correlation for *Homo* (cont.).

Level	Variable	*Homo*					
		Variable	r_s	p value [1]	Variable	r_s	p value [2]
T1	IIFD	SFID	0.583	0.000	VBPH	0.339	0.050
		Area	0.633	0.000	RT	-0.435	0.010
T1	CPBA				Area	-0.410	0.016
T1	Area	VBPH	0.766	0.000	CPBA	-0.410	0.016
		VBAH	0.613	0.000			
		SFID	0.481	0.004			
		IIFD	0.633	0.000			
T1	RT	SVAPA	-0.565	0.001	IIFD	-0.435	0.010
		IVAPA	0.540	0.001			
T2	SFA	SFPA	0.971	0.000			
T2	SFPA	SFA	0.971	0.000			
T2	IFA	IFPA	0.976	0.000	VBPH	-0.432	0.012
		Area	-0.475	0.005	VBAH	-0.405	0.019
					IIFD	-0.356	0.042
T2	IFPA	IFA	0.976	0.000	VBAH	-0.454	0.032
		VBPH	-0.454	0.008			
		Area	-0.483	0.004			
T2	SVAPA				IVAPA	0.395	0.021
					CBPA	-0.394	0.038
T2	IVAPA				SVAPA	0.395	0.021
					CPBA	-0.358	0.032
T2	VBPH	IFPA	-0.454	0.008	IFA	-0.432	0.012
		VBAH	0.660	0.000			
		Area	0.685	0.000			
T2	VBAH	VBPH	0.660	0.000	IFA	-0.405	0.019
		Area	0.639	0.000	IFPA	-0.437	0.011
T2	SFID				IIFD	0.378	0.028
T2	IIFD	Area	0.585	0.000	IFA	-0.356	0.042
					SFID	0.378	0.028
T2	PICP				Area	-0.346	0.045
T2	CPBA				SVAPA	-0.394	0.021
					IVAPA	-0.358	0.028
T2	Area	IFA	-0.475	0.005	PICP	-0.346	0.045
		IFPA	-0.483	0.004			
		VBPH	0.685	0.000			
		VBAH	0.639	0.000			
		IIFD	0.585	0.000			
T2	RT	SVAPA	-0.623	0.000			
T3	SFA	SFPA	0.937	0.000	IFA	0.356	0.039
		SFID	-0.457	0.007	IIFD	-0.347	0.044

[1]Alpha level: $p < 0.01$; [2]Alpha level: $p < 0.05$.

Table I-1. Spearman's rho, significant correlation for *Homo* (cont.).

Level	Variable	*Homo*					
		Variable	r_s	p value [1]	Variable	r_s	p value [2]
T3	SFPA	SFA	0.937	0.000	SFID	-0.378	0.027
					IIFD	-0.353	0.041
T3	IFA	IFPA	0.979	0.000	SFA	0.356	0.039
					VBPH	-0.389	0.023
T3	IFPA	IFA	0.979	0.000	VBPH	-0.382	0.039
T3	SVAPA	Area	0.472	0.006	SFID	0.359	0.044
		RT	-0.570	0.001			
T3	IVAPA	VBAH	-0.480	0.004	Area	-0.341	0.048
		RT	0.653	0.000			
T3	VBPH	VBAH	0.642	0.000	IFA	-0.389	0.023
		Area	0.641	0.000	IFPA	-0.382	0.026
T3	VBAH	IVAPA	-0.480	0.004			
		VBPH	0.642	0.000			
		Area	0.712	0.000			
		RT	-0.464	0.006			
T3	SFID	SFA	-0.457	0.007	SFA	-0.457	0.027
		IIFD	0.721	0.000	SFPA	-0.378	0.044
					SVAPA	0.359	0.029
					Area	0.374	0.029
T3	IIFD	SFID	0.721	0.000	SFA	-0.347	0.044
		Area	0.652	0.000	SFPA	-0.353	0.041
					VBAH	0.374	0.029
					RT	-0.411	0.016
T3	Area	SVAPA	0.472	0.006	IVAPA	-0.341	0.048
		VBPH	0.641	0.000	SFID	0.374	0.029
		VBAH	0.712	0.000			
		IIFD	0.652	0.000			
		RT	-0.619	0.000			
T4	SFA	SFPA	0.950	0.000			
		IVAPA	0.471	0.005			
		VBAH	-0.641	0.000			
T4	SFPA	SFA	0.950	0.000	VBPH	-0.341	0.048
		IVAPA	0.596	0.000	RT	0.369	0.032
		VBAH	-0.677	0.000			
T4	IFA	IFPA	0.973	0.000	Area	-0.342	0.048
T4	IFPA	IFA	0.973	0.000			
T4	SVAPA	RT	-0.482	0.004	IVAPA	0.379	0.027
					PICP	-0.343	0.047

[1]Alpha level: $p < 0.01$; [2]Alpha level: $p < 0.05$.

Table I-1. Spearman's rho, significant correlation for *Homo* (cont.).

Level	Variable	*Homo*					
		Variable	r_s	p value [1]	Variable	r_s	p value [2]
T4	IVAPA	SFA	0.471	0.005	SVAPA	0.379	0.027
		SFPA	0.379	0.000			
		RT	-0.477	0.004			
T4	VBPH	VBAH	0.677	0.000	SFPA	-0.341	0.048
		Area	0.607	0.001			
		RT	-0.533	0.000			
T4	VBAH	SFA	-0.641	0.000	Area	0.417	0.014
		SFPA	-0.677	0.000			
		IVAPA	-0.571	0.000			
		VBPH	0.677	0.000			
		RT	-0.515	0.002			
T4	SFID	IIFD	0.724	0.000	Area	0.405	0.017
		CPBA	-0.477	0.000			
T4	IIFD	Area	0.648	0.000			
T4	PICP	Area	-0.575	0.000	SVAPA	-0.343	0.047
					IIFD	-0.354	0.040
T4	CPBA	SFID	-0.477	0.004			
T4	Area	VBPH	0.607	0.000	IFA	-0.342	0.048
		IIFD	0.648	0.000	SFID	0.405	0.014
		PICP	-0.575	0.000			
		RT	-0.532	0.001			
T4	RT	SVAPA	-0.482	0.004	SFPA	0.369	0.048
		IVAPA	0.477	0.004			
		VBPH	-0.553	0.001			
		VBAH	-0.515	0.002			
		Area	-0.532	0.001			
T5	SFA	SFPA	0.964	0.000			
		VBAH	-0.440	0.009			
T5	SFPA	SFA	0.964	0.000			
		VBAH	-0.499	0.003			
T5	IFA	IFPA	0.958	0.000	IIFD	-0.347	0.034
		PICP	0.440	0.009	Area	-0.435	0.042
T5	IFPA	IFA	0.958	0.000	PICP	0.376	0.028
					Area	-0.395	0.021
T5	SVAPA	CPBA	0.476	0.000	IVAPA	0.421	0.013
		RT	-0.673	0.000			
T5	IVAPA				SVAPA	0.421	0.013

[1]Alpha level: $p < 0.01$; [2]Alpha level: $p < 0.05$.

Table I-1. Spearman's rho, significant correlation for *Homo* (cont.).

Level	Variable	*Homo*					
		Variable	r_s	p value [1]	Variable	r_s	p value [2]
T5	VBPH	VBAH	0.809	0.000			
		Area	0.713	0.000			
T5	VBAH	SFA	-0.440	0.009	SVAPA	-0.376	0.038
		SFPA	-0.499	0.003	Area	0.421	0.013
		VBPH	0.809	0.000			
T5	SFID	IIFD	0.746	0.000	Area	0.409	0.016
T5	IIFD	SFID	0.746	0.000	IFA	-0.347	0.044
		PICP	-0.503	0.000			
		Area	0.687	0.000			
T5	PICP	IFA	0.440	0.009	IFPA	0.376	0.028
		IIFD	-0.503	0.002	Area	-0.422	0.013
T5	CPBA	SVAPA	0.476	0.004			
		RT	-0.499	0.003			
T5	Area	VBPH	0.713	0.000	IFA	-0.435	0.010
		IIFD	0.678	0.000	IFPA	-0.395	0.021
					VBAH	0.421	0.013
					SFID	0.409	0.016
					PICP	-0.422	0.013
					RT	-0.358	0.038
T5	RT	SVAPA	-0.673	0.000	Area	-0.358	0.038
		CPBA	-0.499	0.003			
T6	SFA	SFPA	0.975	0.000	IFA	0.409	0.016
		VBAH	-0.624	0.000	IFPA	0.348	0.044
		CPBA	0.542	0.001	SVAPA	0.367	0.033
					IVAPA	0.351	0.042
					VBPH	-0.405	0.017
T6	SFPA	SFA	0.975	0.000	IFA	0.361	0.036
		VBAH	-0.568	0.000	IFPA	0.399	0.050
		CPBA	0.513	0.002	IVAPA	0.354	0.040
					VBPH	-0.386	0.024
T6	IFA	IFPA	0.959	0.000	SFA	0.409	0.016
					SFPA	0.361	0.036
					IIFD	-0.364	0.034
					CPBA	0.369	0.032
T6	IFPA	IFA	0.959	0.000	SFA	0.348	0.044
					SFPA	0.339	0.050
					IFA	-0.383	0.026
					CPBA	0.361	0.036
T6	SVAPA	RT	-0.556	0.001	SFA	0.367	0.033

[1]Alpha level: $p < 0.01$; [2]Alpha level: $p < 0.05$.

Table I-1. Spearman's rho, significant correlation for *Homo* (cont.).

Level	Variable	*Homo*					
		Variable	r_s	p value [1]	Variable	r_s	p value [2]
T6	IVAPA	RT	0.625	0.000	SFA	0.351	0.042
					SFPA	0.354	0.040
					VBPH	-0.384	0.025
					VBAH	-0.431	0.011
T6	VBPH	VBAH	0.67	0.000	SFA	-0.405	0.017
		IIFD	0.446	0.005	SFPA	-0.386	0.024
		Area	0.594	0.000	IVAPA	-0.384	0.025
					CPBA	-0.423	0.013
T6	VBAH	SFA	-0.624	0.000	IVAPA	-0.431	0.011
		SFPA	-0.568	0.000	Area	0.343	0.047
		VBPH	0.671	0.000			
		CPBA	-0.535	0.001			
T6	SFID	IIFD	0.778	0.000			
		Area	0.585	0.000			
T6	IIFD	VBPH	0.446	0.005	IFA	-0.364	0.034
		SFID	0.778	0.000	IFPA	-0.383	0.026
		Area	0.755	0.000			
T6	PICP				Area	-0.358	0.037
T6	CPBA	SFA	0.542	0.001	IFA	0.369	0.032
		SFPA	0.513	0.002	IFPA	0.361	0.036
		VBAH	-0.535	0.001	VBPH	-0.423	0.013
T6	Area	VBPH	0.594	0.000	VBAH	0.343	0.048
		SFID	0.585	0.000	PICP	-0.358	0.049
		IIFD	0.755	0.000			
T6	RT	SVAPA	-0.556	0.001			
		IVAPA	0.625	0.000			
T7	SFA	SFPA	0.982	0.000	VBPH	-0.434	0.010
		VBAH	-0.499	0.003			
T7	SFPA	SFA	0.982	0.000	VBPH	-0.416	0.014
		VBAH	-0.500	0.003			
T7	IFA	IFPA	0.937	0.000	IIFD	-0.402	0.018
T7	IFPA	IFA	0.937	0.000	IIFD	-0.415	0.015
T7	SVAPA	RT	-0.626	0.000	VBPH	-0.387	0.024
T7	IVAPA	RT	0.478	0.004			
T7	VBPH	VBPH	0.793	0.000	SFA	-0.434	0.010
		IIFD	0.452	0.007	SFPA	-0.416	0.014
		Area	0.496	0.003	SVAPA	-0.387	0.024

[1]Alpha level: $p < 0.01$; [2]Alpha level: $p < 0.05$.

Table I-1. Spearman's rho, significant correlation for *Homo* (cont.).

Level	Variable	*Homo*					
		Variable	r_s	p value [1]	Variable	r_s	p value [2]
T7	VBAH	SFA	-0.499	0.003	SFID	0.375	0.029
		SFPA	-0.500	0.003	IIFD	0.496	0.003
		VBPH	0.793	0.000			
		Area	0.452	0.011			
T7	SFID	IIFD	0.792	0.000	VBPH	0.375	0.029
		Area	0.674	0.000	VBAH	0.422	0.013
T7	IIFD	VBPH	0.452	0.007	IFA	-0.402	0.018
		SFID	0.792	0.000	IFPA	-0.415	0.015
		Area	0.788	0.000	VBAH	0.432	0.011
					RT	-0.361	0.036
T7	CPBA				VBAH	-0.360	0.037
T7	Area	VBPH	0.496	0.003	VBAH	-0.371	0.031
		SFID	0.674	0.000			
		IIFD	0.788	0.000			
T7	RT	SVAPA	-0.626	0.000	IIFD	0.674	0.036
		IVAPA	0.478	0.004			
T8	SFA	SFPA	0.965	0.000			
T8	SFPA	SFA	0.965	0.000			
T8	IFA	IFPA	0.963	0.000	VBPH	-0.390	0.039
					CPBA	-0.389	0.038
T8	IFPA	IFA	0.963	0.000	SFID	-0.355	0.039
		VBPH	-0.472	0.005	Area	-0.357	0.038
T8	SVAPA	RT	-0.665	0.000			
T8	IVAPA				RT	0.376	0.029
T8	VBPH	IFPA	-0.472	0.005	IFA	-0.39	0.025
		VBAH	0.569	0.001	Area	0.388	0.024
T8	VBAH	VBPH	0.596	0.001			
T8	SFID	IIFD	0.814	0.000	IFPA	-0.355	0.039
		Area	0.607	0.000			
T8	IIFD	SFID	0.814	0.000			
		Area	0.828	0.000			
T8	PICP				CPBA	-0.377	0.033
T8	CPBA				IFA	-0.389	0.030
					PICP	-0.377	0.033
T8	Area	SFID	0.607	0.000	IFPA	-0.357	0.038
		IIFD	0.828	0.000	VBPH	0.388	0.024
T8	RT	SVAPA	0.376	0.000	IVAPA	-0.665	0.029
T9	SFA	SFPA	0.973	0.000	VBPH	-0.341	0.048
					VBAH	-0.402	0.019

[1]Alpha level: $p < 0.01$; [2]Alpha level: $p < 0.05$.

Table I-1. Spearman's rho, significant correlation for *Homo* (cont.).

Level	Variable	*Homo*					
		Variable	r_s	p value [1]	Variable	r_s	p value [2]
T9	SFPA	SFA	0.973	0.000	VBPH	-0.374	0.029
					VBAH	-0.380	0.016
T9	IFA	IFPA	0.962	0.000	PICP	0.389	0.029
T9	IFPA	IFA	0.962	0.000			
		PICP	0.439	0.009			
T9	SVAPA				IVAPA	0.392	0.022
					VBPH	-0.389	0.023
					RT	-0.394	0.021
T9	IVAPA	RT	0.621	0.000	SVAPA	0.392	0.022
T9	VBPH	VBAH	0.629	0.000	SFA	-0.341	0.048
					SFPA	-0.374	0.029
					SVAPA	-0.389	0.023
T9	VBAH	VBPH	0.629	0.000	SFA	-0.402	0.019
					SFPA	-0.380	0.026
					RT	0.374	0.029
T9	SFID	IIFD	0.773	0.000			
		Area	0.689	0.000			
T9	IIFD	SFID	0.733	0.000			
		Area	0.695				
T9	PICP	IFPA	0.439	0.009	IFA	0.389	0.023
T9	Area	SFID	0.689	0.000			
		IIFD	0.695	0.000			
T9	RT	IVAPA	0.621	0.000	SVAPA	-0.394	0.021
					VBAH	0.374	0.029
T10	SFA	SFPA	0.991	0.000			
T10	SFPA	SFA	0.991	0.000			
T10	IFA	IFPA			IIFD	-0.403	0.018
T10	IFPA	IFA	0.733	0.000			
T10	SVAPA				IVAPA	0.373	0.030
T10	IVAPA	RT	0.708	0.000			
T10	VBPH	VBAH	0.795	0.000			
		Area	0.624	0.000			
T10	VBAH	VBPH	0.795	0.000	Area	0.430	0.030
T10	SFID	IIFD	0.676	0.000			
		Area	0.561	0.001			
T10	IIFD	SFID	0.676	0.000	IFA	-0.403	0.018
		PICP	-0.494	0.003			
		Area	0.709	0.000			

[1]Alpha level: $p < 0.01$; [2]Alpha level: $p < 0.05$.

Table I-1. Spearman's rho, significant correlation for *Homo* (cont.).

Level	Variable	*Homo*					
		Variable	r_s	p value [1]	Variable	r_s	p value [2]
T10	PICP	IIFD	-0.494	0.003			
		Area	-0.647				
T10	Area	VBPH	0.624	0.000	VBAH	0.430	0.011
		SFID	0.561	0.001			
		IIFD	0.709	0.000			
T10	RT	IVAPA	0.708	0.000			
T11	SFA	SFPA	0.989	0.000	SFID	0.351	0.042
					IIFD	0.371	0.031
T11	SFPA	SFA	0.989	0.000	SFID	0.373	0.030
					IIFD	0.393	0.021
					Area	0.352	0.041
T11	IFA	IFPA	0.900	0.000			
		SVAPA	-0.552	0.001			
		IVAPA	-0.745	0.000			
		RT	0.568	0.000			
T11	IFPA	IFA	0.900	0.000	PICP	-0.346	0.045
		SVAPA	-0.507	0.002			
		IVAPA	-0.724	0.000			
		RT	0.549	0.000			
T11	SVAPA	IFA	-0.532	0.001	Area	0.433	0.010
		IFPA	-0.507	0.002			
		IVAPA	0.587	0.000			
		CPBA	-0.445	0.008			
		RT	-0.499	0.003			
T11	IVAPA	IFA	-0.745	0.000			
		IFPA	-0.724	0.000			
		SVAPA	0.587	0.000			
T11	IVAPA	PICP	0.442	0.009			
		RT	-0.791	0.000			
T11	VBPH	VBAH	0.644	0.000			
		Area	0.510	0.002			
T11	VBAH	VBPH	0.664	0.000			
T11	SFID	IIFD	0.539	0.001	SFA	0.351	0.042
		Area	0.578	0.000	SFPA	0.373	0.030
T11	IIFD	SFID	0.539	0.001	SFA	0.371	0.031
		Area	0.649	0.000	SFPA	0.393	0.021
T11	PICP	IVAPA	0.442	0.009	IFPA	-0.346	0.045
					RT	-0.435	0.010
T11	CPBA	SVAPA	-0.455	0.008			

[1]Alpha level: $p < 0.01$; [2]Alpha level: $p < 0.05$.

Table I-1. Spearman's rho, significant correlation for *Homo* (cont.).

Level	Variable	*Homo*					
		Variable	r_s	p value [1]	Variable	r_s	p value [2]
T11	Area	VBPH	0.510	0.002	SFPA	0.352	0.041
		SFID	0.578	0.000	SVAPA	0.433	0.010
		IIFD	0.649	0.000			
T11	RT	IFA	0.568	0.000	PICP	-0.435	0.010
		IFPA	0.549	0.001			
		SVAPA	-0.499	0.003			
		IVAPA	-0.791	0.000			
T12	SFA	SFPA	0.991	0.000	SFID	0.414	0.015
		SVAPA	0.515	0.002	IIFD	0.371	0.031
					RT	0.402	0.018
T12	SFPA	SFA	0.991	0.000	SFID	0.415	0.015
		SVAPA	0.514	0.002	IIFD	0.392	0.022
					RT	0.415	0.015
T12	IFA	IFPA	0.994	0.000	IVAPA	-0.413	0.015
T12	IFPA	IFA	0.994	0.000	IVAPA	-0.409	0.016
T12	SVAPA	SFA	0.515	0.002	IVAPA	0.345	0.022
		SFPA	0.514	0.002	SFID	0.420	0.015
		IIFD	0.508	0.000			
		RT	0.753	0.000			
T12	IVAPA				IFA	-0.413	0.015
					IFPA	-0.409	0.016
					SVAPA	0.354	0.040
					CPBA	-0.372	0.030
T12	VBPH	VBAH	0.519	0.002			
		Area	0.555	0.001			
T12	VBAH	VBPH	0.519	0.002	RT	0.400	0.019
T12	SFID	Area	0.489	0.000	SFA	0.414	0.015
					SFPA	0.415	0.015
					SVAPA	0.420	0.013
					IIFD	0.627	0.012
T12	IIFD	SVAPA	0.508	0.002	SFA	0.371	0.031
		SFID	0.627		SFPA	0.392	0.022
T12	CPBA				IVAPA	-0.372	0.030
T12	Area	VBPH	0.555	0.001			
		SFID	0.489	0.003			
T12	RT	SVAPA	0.753	0.000	SFA	0.402	0.018
					SFPA	0.415	0.015
					VBPH	0.400	0.019
L1	SFPA	SFA	0.987	0.000	CPBA	-0.373	0.037

[1]Alpha level: $p < 0.01$; [2]Alpha level: $p < 0.05$.

Table I-1. Spearman's rho, significant correlation for *Homo* (cont.).

Level	Variable	*Homo*					
		Variable	r_s	p value [1]	Variable	r_s	p value [2]
L1	IFA	IFPA	0.951	0.000	VBPH CPBA	-0.351 0.422	0.042 0.013
L1	IFPA	IFA	0.951	0.000	VBPH CPBA	-0.380 0.344	0.027 0.046
L1	SVAPA	RT	0.728	0.000	SFID	-0.413	0.019
L1	IVAPA	RT	-0.438	0.010	VBPH	0.365	0.034
L1	VBPH	VBAH Area	0.556 0.471	0.001 0.005	IFA IFPA IVAPA CPBA	-0.351 -0.380 0.365 -0353	0.042 0.027 0.034 0.041
L1	VBAH	VBPH	0.556	0.001	PICP	0.352	0.041
L1	SFID	IIFD	0.724	0.000	SVAPA	-0.413	0.019
L1	IIFD	SFID	0.724	0.000			
L1	PICP				VBAH	0.352	0.041
L1	CPBA				SFA SFPA IFA IFPA VBPH	-0.358 -0.373 0.422 0.344 -0.353	0.037 0.030 0.013 0.046 0.041
L1	Area	VBPH	0.471	0.005			
L1	RT	SVAPA IVAPA	0.728 -0.438	0.000 0.010			
L2	SFA	SFPA	0.988	0.000	SFID	0.348	0.044
L2	SFPA	SFA	0.988	0.000	SFID	-0.381	0.026
L2	IFA	IFPA SFID IIFD	0.900 0.518 0.488	0.000 0.002 0.003	VBPH	-0371	0.031
L2	IFPA	IFA SFID IIFD	0.900 0.503 0.460	0.000 0.002 0.006			
L2	SVAPA	RT	0.847	0.000	SFID	-0.380	0.027
L2	VBAH	VBPH	0.740	0.001	Area	0.357	0.031
L2	IVAPA	RT	-0.544	0.001			
L2	VBPH	VBAH Area	0.740 0.530	0.000 0.001	IFA IFPA	-0.371 -0.391	0.031 0.022
L2	SFID	IFA IFPA	0.518 0.503	0.002 0.002	SFA SFPA SVAPA	-0.348 -0.381 -0.380	0.044 0.026 0.027

[1]Alpha level: $p < 0.01$; [2]Alpha level: $p < 0.05$.

Table I-1. Spearman's rho, significant correlation for *Homo* (cont.).

Level	Variable	*Homo*					
		Variable	r_s	p value [1]	Variable	r_s	p value [2]
L2	IIFD	IFPA SFID	0.460 0.778	0.003			
L2	Area	VBAH	0.357	0.000	VBPH	0.530	0.038
L2	RT	SVAPA IVAPA	0.847 -0.544	0.000 0.001	SFID	-0.356	0.039
L3	SFA	SFPA	0.956	0.000	CPBA	-0.345	0.046
L3	SFPA	SFA	0.956	0.000	CPBA	-0.399	0.020
L3	IFA	IFPA	0.984	0.000			
L3	IFPA	IFA	0.984	0.000			
L3	SVAPA	RT	0.556	0.001			
L3	IVAPA	RT	-0.538	0.001			
L3	VBPH	VBAH Area	0.748 0.647	0.000 0.000			
L3	VBAH	VBPH Area	0.748 0.496	0.000 0.003			
L3	SFID	IIFD	0.845	0.000			
L3	IIFD	SFID	0.845	0.000			
L3	CPBA				SFA SFPA	-0.345 -0.399	0.046 0.020
L3	Area	VBPH VBAH	0.647 0.496	0.000 0.003			
L3	RT	SVAPA IVAPA	0.556 -0.538	0.001 0.001			
L4	SFA	SFPA	0.899	0.000			
L4	SFPA	SFA	0.899	0.000			
L4	IFA	IFPA VBPH	0.900 -0.480	0.000 0.004			
L4	IFPA	IFA VBPH	0.900 -0.496	0.000 0.003	IVAPA	-0.349	0.043
L4	IVAPA	RT	-0.512	0.002	IFA IFPA IIFD	-0.352 -0.349 0.359	0.041 0.043 0.037
L4	SFID	IIFD	0.570	0.000			
L4	VBPH	IFA IFPA VBAH Area	-0.480 -0.496 0.692 0.443	0.004 0.003 0.000 0.009			
L4	VBAH	VBPH	0.692	0.000			

[1]Alpha level: $p < 0.01$; [2]Alpha level: $p < 0.05$.

Table I-1. Spearman's rho, significant correlation for *Homo* (cont.).

Level	Variable	*Homo*					
		Variable	r_s	p value [1]	Variable	r_s	p value [2]
L4	IIFD				IVAPA SFID CPBA Area	0.359 0.570 0.411 0.355	0.037 0.011 0.016 0.040
L4	CPBA				IIFD	0.411	0.016
L4	Area	VBPH	0.443	0.009	IIFD	0.355	0.040
L4	RT	IVAPA	-0.512	0.002			
L5	SFA	SFPA PICP	0.908 -0.440	 0.009			
L5	SFPA	SFA	0.908	0.000	PICP	-0.355	0.040
L5	IFA	IFPA	0.872	0.000			
L5	IFPA	IFA	0.872	0.000	IVAPA	-0.370	0.031
L5	SVAPA				RT	0.342	0.048
L5	IVAPA	RT	-0.709	0.000	IFPA	-0.370	0.031
L5	VBPH	VBAH	0.500	0.003			
L5	VBAH	VBPH	0.500	0.003	CPBA	0.359	0.037
L5	SFID	IIFD Area	0.589 0.508	0.000 0.000			
L5	IIFD	SFID Area	0.589 0.508	0.000 0.002			
L5	PICP	SFA	-0.440	0.009	SFPA	-0.355	0.040
L5	CPBA				VBAH	0.359	0.037
L5	Area	IIFD	0.508	0.002			
L5	RT	IVAPA	-0.709	0.000	SVAPA	0.342	0.048

[1] Alpha level: $p < 0.01$; [2] Alpha level: $p < 0.05$.

Table I-2. Spearman's rho, significant correlation for *Gorilla*.

Level	Variable	*Gorilla*					
		Variable	r_s	p value[1]	Variable	r_s	p value[2]
C1	SFA				SVAPA	0.579	0.019
C1	SVAPA				SFA	0.579	0.019
					Area	-0.539	0.038
C1	Area				SVAPA	-0.539	0.038
C2	IFA	Area	0.755	0.001	IVAPA	-0.524	0.037
C2	IVAPA	RT	0.795	0.000	IFA	-.524	0.037
					Area	-0.586	0.032
C2	Area	IFA	0.755	0.001	IVAPA	-0.586	0.022
C2	RT	IVAPA	0.795	0.000			
C3	SFA	SFPA	0.938	0.000			
C3	SFPA	SFA	0.938	0.000	RT	-0.515	0.041
C3	IFA	IFPA	0.985	0.000	SFID	0.550	0.027
C3	IFPA	IFA	0.985	0.000	SFID	0.506	0.045
C3	IVAPA	RT	0.718	0.002			
C3	VBPH	VBAH	0.634	0.008			
		SFID	0.774	0.000			
		IIFD	0.785	0.000			
		Area	0.844	0.000			
C3	VBAH	VBPH	0.634	0.008			
		IIFD	0.849	0.000			
		Area	0.776	0.000			
C3	SFID	VBPH	0.744	0.000	IFA	0.550	0.027
		IIFD	0.729	0.001	IFPA	0.506	0.045
		Area	0.635	0.008	RT	-0.500	0.049
C3	IIFD	VBPH	0.785	0.000	RT	-0.574	0.020
C3	IIFD	VBAH	0.849	0.000			
		SFID	0.729	0.000			
		Area	0.900	0.001			
C3	Area	VBPH	0.844	0.000			
		VBAH	0.766	0.000			
		SFID	0.635	0.008			
		IIFD	0.900	0.000			
C3	RT	IVAPA	0.718	0.002	SFPA	-0.515	0.041
					SFID	-0.500	0.049
					IIFD	-0.574	0.020
C4	SFA	SFPA	0.976	0.000			
C4	SFPA	SFA	0.976	0.000			
C4	IFA	SFA	0.741	0.000	PICP	-0.535	0.033
		SFPA	0.741	0.000			
		IFPA	0.994	0.001			

[1] Alpha level: $p < 0.01$; [2] Alpha level: $p < 0.05$.

Table I-2. Spearman's rho, significant correlation for *Gorilla* (cont.).

Level	Variable	*Gorilla*					
		Variable	r_s	p value[1]	Variable	r_s	p value[2]
C4	IFPA	SFA	0.771	0.000	PICP	-0.541	0.030
		SFPA	0.745	0.002			
		IFA	0.904	0.000			
C4	IVAPA	CPBA	0.712	0.002	RT	0.521	0.039
C4	VBPH	VBAH	0.847	0.000			
		SFID	0.759	0.001			
		IIFD	0.770	0.000			
		Area	0.885	0.000			
C4	VBAH	VBPH	0.847	0.000			
		SFID	0.715	0.002			
		IIFD	0.779	0.000			
		Area	0.768	0.001			
C4	SFID	VBPH	0.759	0.001			
		VBAH	0.715	0.002			
C4	SFID	IIFD	0.926	0.001			
		Area	0.803	0.002			
C4	IIFD	VBPH	0.776	0.000			
		VBAH	0.779	0.000			
		SFID	0.926	0.000			
		Area	0.788	0.000			
C4	PICP				SFA	-0.550	0.030
					SFPA	-0.535	0.027
					IFA	-0.535	0.033
					IFPA	-0.541	0.032
C4	CPBA	IVAPA	0.712	0.002			
C4	Area	VBPH	0.885	0.000			
		VBAH	0.768	0.001			
		SFID	0.803	0.000			
		IIFD	0.788	0.000			
C4	RT				IVAPA	0.521	0.039
C5	SFA	SFPA	0.991	0.000			
		IFA	0.785	0.000			
		IFPA	0.768	0.001			
		PICP	-0.668	0.005			
C5	SFPA	SFA	0.991	0.000			
		IFA	0.768	0.001			
		IFPA	0.750	0.001			
		PICP	-0.665	0.005			

[1] Alpha level: $p < 0.01$; [2] Alpha level: $p < 0.05$.

Table I-2. Spearman's rho, significant correlation for *Gorilla* (cont.).

Level	Variable	*Gorilla*					
		Variable	r_s	p value[1]	Variable	r_s	p value[2]
C5	IFA	SFA	0.785	0.000			
		SFPA	0.768	0.001			
		IFPA	0.997	0.000			
		PICP	-0.818	0.000			
C5	IFPA	SFA	0.768	0.001			
C5	IFPA	SFPA	0.750	0.001			
		IFA	0.997	0.000			
		PICP	-0.803	0.000			
C5	IVAPA				RT	-0.597	0.015
C5	VBPH	VBAH	0.926	0.000	RT	-0.579	0.019
		SFID	0.726	0.001			
		IIFD	0.744	0.001			
		CPBA	-0.747	0.001			
		Area	0.926	0.000			
C5	VBAH	VBPH	0.926	0.000	RT	-0.591	0.016
		SFID	0.703	0.002			
		IIFD	0.759	0.001			
		CPBA	-0.803	0.000			
		Area	0.855	0.000			
C5	SFID	VBPH	0.726	0.001	RT	-0.526	0.036
		VBAH	0.703	0.002			
		IIFD	0.974	0.000			
		CPBA	-0.753	0.001			
		Area	0.829	0.000			
C5	IIFD	VBPH	0.744	0.001	RT	-0.532	0.034
		VBAH	0.974	0.001			
		CPBA	-0.771	0.000			
		Area	0.862	0.000			
C5	PICP	SFA	-0.668	0.005			
		SFPA	-0.665	0.005			
		IFA	-0.818	0.000			
		IFPA	-0.803	0.000			
C5	CPBA	VBPH	-0.747	0.001			
		VBAH	-0.803	0.000			
		SFID	-0.753	0.001			
		IIFD	-0.771	0.000			
		Area	-0.794	0.000			

[1] Alpha level: $p < 0.01$; [2] Alpha level: $p < 0.05$.

Table I-2. Spearman's rho, significant correlation for *Gorilla* (cont.).

Level	Variable	*Gorilla*					
		Variable	r_s	p value[1]	Variable	r_s	p value[2]
C5	Area	VBAH	0.885	0.000			
		IIFD	0.862	0.000			
		CPBA	-0.794	0.000			
		VBPH	0.926	0.000			
		SFID	0.829	0.000			
C5	RT				IVAPA	-0.597	0.015
					VBPH	-0.579	0.019
					VBAH	-0.591	0.016
					SFID	-0.526	0.036
					IIFD	-0.532	0.034
C6	SFA	SFPA	0.941	0.000	IFA	0.587	0.017
					IFPA	0.599	0.014
C6	SFPA	SFA	0.941	0.000	IFA	.596	0.015
		IFPA	0.625	0.010			
C6	IFA	IFPA	0.991	0.000	SFA	0.587	0.017
					SFPA	0.596	0.015
					PICP	-0.615	0.011
C6	IFPA	SFPA	0.625	0.010	SFA	0.599	0.014
		IFA	0.991	0.000	PICP	-0.565	0.023
C6	VBPH	VBAH	0.827	0.000			
		SFID	0.690	0.003			
		IIFD	0.788	0.000			
		Area	0.900	0.000			
C6	VBAH	VBPH	0.827	0.000			
		SFID	0.627	0.009			
		IIFD	0.759	0.000			
		Area	0.787	0.000			
C6	SFID	VBPH	0.690	0.003	CPBA	-0.503	0.023
		IIFD	0.866	0.009			
		Area	0.767	0.000			
C6	IIFD	VBPH	0.788	0.000	CPBA	-0.544	0.029
C6	IIFD	VBAH	0.759	0.001			
		SFID	0.866	0.000			
		Area	0.841	0.000			
C6	PICP				IFA	-0.651	0.011
					IFPA	-0.565	0.023
C6	CPBA				SFID	-0.503	0.047
					IIFD	-0.544	0.029

[1] Alpha level: $p < 0.01$; [2] Alpha level: $p < 0.05$.

Table I-2. Spearman's rho, significant correlation for *Gorilla* (cont.).

Level	Variable	*Gorilla*					
		Variable	r_s	p value[1]	Variable	r_s	p value[2]
C6	Area	VBPH	0.900	0.000			
		VBAH	0.787	0.000			
		SFID	0.767	0.001			
		IIFD	0.841	0.000			
C7	SFA	SFPA	0.994	0.000	SVAPA	0.550	0.027
		IFA	0.697	0.000	VBPH	0.556	0.025
		IFPA	0.694	0.003	VBAH	0.521	0.039
					PICP	-0.532	0.034
C7	SFPA	SFA	0.994	0.000	SVAPA	0.524	0.037
		IFA	0.688	0.003	BNPH	0.568	0.037
		IFPA	0.682	0.004	VBAH	0.524	0.043
					IIFD	0.512	0.043
					PICP	-0.579	0.019
C7	IFA	SFA	0.697	0.003			
		SFPA	0.688	0.003			
		IFPA	0.997	0.000			
C7	IFPA	SFA	0.694	0.003	CBPA	-0.509	0.044
		SFPA	0.682	0.004			
		IFA	0.997	0.000			
C7	SVAPA				SFA	0.550	0.027
					SFPA	0.524	0.037
C7	VBPH	VBAH	0.826	0.000	SFA	0.556	0.025
		SFID	0.850	0.000	SFPA	0.568	0.022
		IIFD	0.897	0.000			
		Area	0.903	0.000			
C7	VBAH	VBPH	0.826	0.000	SFA	0.521	0.039
		SFID	0.774	0.000	SFPA	0.524	0.037
		IIFD	0.844	0.000			
		Area	0.779	0.000			
C7	SFID	VBPH	0.850	0.000			
		VBAH	0.744	0.000			
		IIFD	0.844	0.000			
		Area	0.806	0.000			
C7	IIFD	VBPH	0.897	0.000	SFPA	0.512	0.043
		VBAH	0.844	0.000			
		SFID	0.844	0.000			
		Area	0.815	0.000			
C7	PICP				SFA	-0.532	0.034
					SFPA	-0.579	0.019

[1] Alpha level: $p < 0.01$; [2] Alpha level: $p < 0.05$.

Table I-2. Spearman's rho, significant correlation for *Gorilla* (cont.).

Level	Variable	*Gorilla*					
		Variable	r_s	p value[1]	Variable	r_s	p value[2]
C7	Area	VBPH	0.903	0.000			
		VBAH	0.779	0.000			
		SFID	0.806	0.000			
		IIFD	0.815	0.000			
T1	SFA	SFPA	0.956	0.000			
		RT	-0.634	0.008			
T1	SFPA	SFA	0.956	0.000			
		RT	-0.665	0.008			
T1	IFA	IFPA	0.997	0.000			
T1	IFPA	IFA	0.997	0.000			
T1	SVAPA				IVAPA	0.574	0.020
T1	IVAPA				SVAPA	0.574	0.020
T1	VBPH	VBAH	0.800	0.000			
		SFID	0.671	0.004			
		IIFD	0.771	0.000			
		Area	0.844	0.000			
T1	VBAH	VBPH	0.800	0.000			
		SFID	0.829	0.000			
		IIFD	0.741	0.001			
		Area	0.803	0.000			
T1	SFID	VBPH	0.671	0.004			
		VBAH	0.829	0.000			
		IIFD	0.671	0.004			
		Area	0.662	0.005			
T1	IIFD	VBPH	0.771	0.000			
		VBAH	0.741	0.001			
		SFID	0.671	0.004			
		Area	0.776	0.000			
T1	Area	VBPH	0.844	0.000			
		VBAH	0.803	0.000			
		SFID	0.662	0.005			
		IIFD	0.776	0.000			
T1	RT	SFA	-0.634	0.008			
		SFPA	-0.665	0.005			
T2	SFA	PICP	-0.706	0.002	IFA	0.571	0.020
		SFPA	0.982	0.000	IFPA	0.535	0.017
					CPBA	0.563	0.029
T2	SFPA	SFA	0.982	0.000	IFA	0.503	0.047
		PICP	-0.682	0.004	IFPA	0.535	0.033
					CPBA	0.563	0.023

[1] Alpha level: $p < 0.01$; [2] Alpha level: $p < 0.05$.

Table I-2. Spearman's rho, significant correlation for *Gorilla* (cont.).

Level	Variable	*Gorilla*					
		Variable	r_s	p value[1]	Variable	r_s	p value[2]
T2	IFA	IFPA	0.985	0.000	SFA SFPA	0.571 0.503	0.021 0.047
T2	IFPA	IFA	0.985	0.000	SFA	0.588	0.017
T2	IFPA				SFPA	0.535	0.017
T2	SVAPA				CPBA	-0.571	0.033
T2	IVAPA	RT	0.656	0.006	VBAH	-0.524	0.021
T2	VBPH	VBAH IIFD SFID Area	0.979 0.679 0.838 0.971	0.000 0.004 0.000 0.000			
T2	VBAH	VBPH SFID IIFD Area	0.979 0.856 0.691 0.950	0.000 0.000 0.003 0.000	IVAPA	-0.524	0.023
T2	SFID	VBPH VBAH IIFD Area	0.838 0.856 0.741 0.829	0.000 0.000 0.000 0.000			
T2	IIFD	VBPH VBAH Area	0.679 0.691 0.664	0.004 0.003 0.007			
T2	PICP	SFA SFPA	-0.706 -0.682	0.002 0.0040	IFA	-0.515	0.041
T2	CPBA				SFA SFPA SVAPA RT	0.546 0.563 -0.571 0.527	0.029 0.023 0.021 0.036
T2	Area	VBPH VBAH SFID IIFD	0.971 0.950 0.829 0.664	0.000 0.000 0.007 0.006			
T2	RT	IVAPA	0.656	0.006	CPBA	0.527	0.036
T3	SFA	SFPA PICP CPBA	0.994 -0.641 0.770	0.000 0.007 0.000			
T3	SFPA	SFA PICP CPBA	0.994 -0.629 0.794	0.000 0.009 0.000			
T3	IFA	IFPA	0.991	0.000			

[1] Alpha level: $p < 0.01$; [2] Alpha level: $p < 0.05$.

Table I-2. Spearman's rho, significant correlation for *Gorilla* (cont.).

Level	Variable	*Gorilla*					
		Variable	r_s	p value[1]	Variable	r_s	p value[2]
T3	IFPA	IFA	0.991	0.000			
T3	IVAPA				VBPH	-0.591	0.016
					RT	0.590	0.016
T3	VBPH	VBAH	0.971	0.000	IVAPA	-0.591	0.024
		SFID	0.656	0.006			
		IIFD	0.768	0.001			
		Area	0.929	0.000			
T3	VBAH	VBPH	0.971	0.000			
		SFID	0.646	0.009			
		IIFD	0.775	0.001			
		Area	0.918	0.000			
T3	SFID	VBPH	0.656	0.006			
		VBAH	0.646	0.009			
		IIFD	0.874	0.000			
		Area	0.636	0.000			
T3	IIFD	VBPH	0.768	0.001			
		VBAH	0.775	0.001			
		SFID	0.874	0.000			
		Area	0.764	0.001			
T3	PICP	SFA	-0.641	0.007	CPBA	-0.513	0.042
		SFPA	-0.629	0.009			
T3	CPBA	SFA	0.770	0.000	PICP	-0.513	0.042
		SFPA	0.794	0.000			
T3	Area	VBPH	0.929	0.000	SFID	0.636	0.046
		VBAH	0.918	0.000			
		IIFD	0.764	0.000			
T3	RT				IVAPA	0.590	0.016
T4	SFA	SFPA	0.976	0.000	PICP	-0515	0.041
T4	SFPA	SFA	0.976	0.000			
T4	IFA	IFPA	0.889	0.000			
T4	IFPA	IFA	0.889	0.000			
T4	SVAPA				SFID	-0.506	0.046
					RT	-0.572	0.020
T4	IVAPA	RT	0.698	0.003	VBPH	-0.500	0.049
					PICP	0.515	0.041
T4	VBPH	VBAH	0.912	0.000			
		SFID	0.826	0.000			
		IIFD	0.794	0.000			
		Area	0.921	0.000			

[1] Alpha level: $p < 0.01$; [2] Alpha level: $p < 0.05$.

Table I-2. Spearman's rho, significant correlation for *Gorilla* (cont.).

Level	Variable	*Gorilla*					
		Variable	r_s	p value[1]	Variable	r_s	p value[2]
T4	VBAH	VBPH	0.912	0.000			
		SFID	0.821	0.000			
		IIFD	0.791	0.000			
		Area	0.794	0.000			
T4	SFID	VBPH	0.826	0.000	SVAPA	-0.506	0.046
		VBAH	0.821	0.000			
		IIFD	0.935	0.000			
		Area	0.850	0.000			
T4	IIFD	VBPH	0.794	0.000			
		VBAH	0.791	0.000			
		SFID	0.935	0.000			
		Area	0.856	0.000			
T4	PICP				SFA	-0.515	0.049
					IVAPA	0.515	0.041
					Area	-0.538	0.031
T4	Area	VBPH	0.921	0.000	PICP	-0.538	0.031
		VBAH	0.794	0.000			
		SFID	0.850	0.000			
		IIFD	0.856	0.000			
T4	RT	IVAPA	0.698	0.003	SVAPA	-0.572	0.020
T5	SFA	SFPA	0.982	0.000	VBAH	-0.586	0.017
					SFID	-0.503	0.047
					CPBA	0.572	0.020
T5	SFPA	SFA	0.982	0.000	VBAH	-0.587	0.017
					IIFD	-0.512	0.043
					CPBA	0.524	0.037
T5	IFA	IFPA	0.943	0.000			
T5	IFPA	IFA	0.943	0.000			
T5	SVAPA	IVAPA	0.650	0.006	VBPH	-0.588	0.017
		RT	-0.676	0.004	IIFD	-0.550	0.027
					Area	-0.582	0.018
T5	IVAPA	SVAPA	0.650	0.006	IIFD	-0.568	0.022
					Area	-0.506	0.046
T5	VBPH	VBAH	0.893	0.000	SVAPA	-0.588	0.017
		SFID	0.850	0.000			
		IIFD	0.706	0.000			
		Area	0.900	0.000			

[1] Alpha level: $p < 0.01$; [2] Alpha level: $p < 0.05$.

Table I-2. Spearman's rho, significant correlation for *Gorilla* (cont.).

Level	Variable	*Gorilla*					
		Variable	r_s	p value[1]	Variable	r_s	p value[2]
T5	VBAH	VBPH	0.893	0.000	SFA	-0.586	0.017
		SFID	0.812	0.000			
		IIFD	0.717	0.000			
		Area	0.773	0.000			
T5	SFID	VBPH	0.850	0.000	SFA	-0.503	0.047
		VBAH	0.812	0.000			
		IIFD	0.868	0.000			
		Area	0.797	0.000			
T5	IIFD	VBPH	0.706	0.002	SFPA	-0.512	0.043
		VBAH	0.717	0.002	SVAPA	-0.550	0.027
		SFID	0.868	0.000	IVAPA	-0.586	0.022
		Area	0.697	0.003			
T5	CPBA				SFA	0.572	0.020
					SFPA	0.524	0.037
T5	Area	VBPH	0.900	0.000	SVAPA	-0.582	0.014
		VBAH	0.773	0.000	IVAPA	-0.506	0.025
		SFID	0.797	0.000			
		IIFD	0.697	0.003			
T5	RT	SVAPA	-0.676	0.004			
T6	SFA	SFPA	0.964	0.000			
		CPBA	0.790	0.000			
T6	SFPA	SFA	0.964	0.000			
		CPBA	0.732	0.001			
T6	IFA	IFPA	0.979	0.000			
T6	IFPA	IFA	0.979	0.000			
T6	SVAPA				VBPH	-0.570	0.021
T6	IVAPA				IIFD	-0.557	0.025
					RT	0.583	0.018
T6	VBPH	VBAH	0.900	0.000	SVAPA	-0.570	0.021
		IIFD	0.679	0.000	SFID	0.565	0.023
		Area	0.906	0.000			
T6	VBAH	VBPH	0.900	0.000			
T6	VBAH	SFID	0.682	0.004			
		IIFD	0.789	0.000			
		Area	0.809	0.000			
T6	SFID	VBAH	0.682	0.004	VBPH	0.565	0.023
		IIFD	0.798	0.000			
		Area	0.682	0.000			

[1] Alpha level: $p < 0.01$; [2] Alpha level: $p < 0.05$.

Table I-2. Spearman's rho, significant correlation for *Gorilla* (cont.).

Level	Variable	*Gorilla*					
		Variable	r_s	p value[1]	Variable	r_s	p value[2]
T6	IIFD	VBPH	0.679	0.004	IVAPA	-0.557	0.025
		VBAH	0.789	0.000			
		SFID	0.798	0.000			
		Area	0.736	0.001			
T6	CPBA	SFA	0.790	0.000			
		SFPA	0.732	0.000			
T6	Area	VBPH	0.906	0.000			
		VBAH	0.809	0.000			
		SFID	0.682	0.004			
		IIFD	0.736	0.001			
T6	RT				IVAPA	0.583	0.018
T7	SFA	SFPA	0.997	0.000			
T7	SFPA	SFA	0.997	0.000	IFA	0.532	0.034
					IFPA	0.529	0.035
T7	IFA	IFPA	0.968	0.000	SFA	0.509	0.044
					SFPA	0.532	0.034
T7	IFPA	IFA	0.968	0.000	SFPA	0.529	0.035
					Area	0.500	0.049
T7	SVAPA	RT	-0.720	0.002	CPBA	-0.526	0.036
T7	VBPH	VBAH	0.924				
		SFID	0.650	0.006			
		Area	0.941				
T7	VBAH	VBPH	0.924	0.000			
		SFID	0.632	0.009			
		Area	0.818	0.000			
T7	SFID	VBPH	0.650	0.006			
		VBAH	0.632	0.009			
		Area	0.674	0.004			
T7	CPBA				SVAPA	-0.526	0.036
					Area	0.582	0.018
T7	Area	VBPH	0.941	0.000	IFPA	0.500	0.049
		VBAH	0.818	0.000	CPBA	0.582	0.018
		SFID	0.674	0.004			
T7	RT	SVAPA	-0.720	0.002			
T8	SFA	SFPA	0.988	0.000	IFA	0.544	0.029
					IFPA	0.547	0.028
T8	SFPA	SFA	0.988	0.000	IFA	0.535	0.029
					IFPA	0.524	0.028

[1] Alpha level: $p < 0.01$; [2] Alpha level: $p < 0.05$.

Table I-2. Spearman's rho, significant correlation for *Gorilla* (cont.).

Level	Variable	*Gorilla*					
		Variable	r_s	p value[1]	Variable	r_s	p value[2]
T8	IFA	IFPA	0.979	0.000	SFA SFPA Area	0.544 0.535 0.579	0.029 0.033 0.019
T8	IFPA	IFA	0.979	0.000	SFA SFPA Area	0.547 0.524 0.588	0.028 0.037 0.017
T8	SVAPA	PICP	0.524	0.002	VBPH RT	-0.539 -0.573	0.031 0.020
T8	IVAPA				RT	0.542	0.030
T8	VBPH	VBAH SFID IIFD Area	0.897 0.712 0.691 0.950	0.000 0.002 0.003 0.000	SVAPA	-0.539	0.031
T8	VBAH	VBPH SFID Area	0.897 0.656 0.865	0.000 0.006 0.000			
T8	SFID	VBPH VBAH IIFD Area	0.712 0.656 0.885 0.676	0.002 0.006 0.000 0.004			
T8	IIFD	VBPH SFID Area	0.691 0.885 0.638	0.003 0.000 0.008	CPBA	0.612	0.012
T8	PICP	SVAPA	0.706	0.002			
T8	CPBA				IIFD	0.612	0.012
T8	Area	VBPH VBAH SFID IIFD	0.950 0.865 0.676 0.638	0.000 0.000 0.004 0.008	IFA	0.579	0.019
T8	RT				SVAPA IVAPA	-0.573 0.542	0.020 0.030
T9	SFA	SFPA	0.970	0.000			
T9	SFPA	SFA	0.970	0.000			
T9	IFA	IFPA	0.986	0.000			
T9	IFPA	IFA	0.986	0.000			
T9	SVAPA	VBPH RT	-0.699 -0.637	0.003 0.008	VBAH Area	-0.533 -0.519	0.033 0.039
T9	VBPH	SVAPA VBAH SFID	-0.699 0.846 0.653	0.000 0.000 0.000			

[1] Alpha level: $p < 0.01$; [2] Alpha level: $p < 0.05$.

Table I-2. Spearman's rho, significant correlation for *Gorilla* (cont.).

Level	Variable	*Gorilla*					
		Variable	r_s	p value[1]	Variable	r_s	p value[2]
T9	VBPH	IIFD	0.656	0.003			
		Area	0.903	0.000			
T9	VBAH	VBPH	0.846	0.006	SVAPA	-0.533	0.033
		IIFD	0.665	0.006	SFID	0.536	0.031
		Area	0.758	0.001			
T9	SFID	VBPH	0.653	0.000	VBAH	0.538	0.031
		IIFD	0.820	0.006			
		Area	0.680	0.001			
T9	IIFD	VBPH	0.656	0.006			
		VBAH	0.655	0.000			
		SFID	0.820	0.004			
		Area	0.800	0.006			
T9	Area	VBPH	0.903	0.006	SVAPA	-0.519	0.039
		VBAH	0.758	0.001			
		SFID	0.680	0.004			
		IIFD	0.800				
T9	RT	SVAPA	-0.637	0.008			
T10	SFA	SFPA	0.997	0.000			
T10	SFPA	SFA	0.997	0.000			
T10	IFA	IFPA	0.994	0.000	VBAH	0.566	0.022
		IIFD	0.646	0.000	SFID	0.522	0.038
					Area	0.510	0.043
					RT	-0.555	0.026
T10	IFPA	IFA	0.994	0.000	VBAH	0.575	0.020
		IIFD	0.626	0.000	SFID	0.501	0.048
					Area	0.522	0.038
					RT	-0.531	0.034
T10	IVAPA				RT	0.620	0.010
T10	VBPH	VBAH	0.891	0.000			
T10	VBPH	SFID	0.782	0.000			
		IIFD	0.627	0.009			
		Area	0.968	0.000			
T10	VBAH	VBPH	0.891	0.000	IFA	0.566	0.022
		SFID	0.885	0.000	IFPA	0.575	0.020
		IIFD	0.736	0.001	CPBA	-0.589	0.016
		Area	0.885	0.000	RT	-0.529	0.035
T10	SFID	VBPH	0.782	0.000	IFA	0.522	0.038
		VBAH	0.885	0.000	IFPA	0.501	0.048
		IIFD	0.902	0.000	CPBA	-0.593	0.015
		Area	0.794	0.000			

[1] Alpha level: $p < 0.01$; [2] Alpha level: $p < 0.05$.

Table I-2. Spearman's rho, significant correlation for *Gorilla* (cont.).

Level	Variable	*Gorilla*					
		Variable	r_s	p value[1]	Variable	r_s	p value[2]
T10	IIFD	IFA	0.646	0.007			
		IFPA	0.626	0.010			
		VBPH	0.627	0.009			
		VBAH	0.736	0.001			
		SFID	0.902	0.000			
		CPBA	-0.629	0.009			
		Area	0.670	0.000			
T10	CPBA	IIFD	-0.629	0.009	VBAH	-0.589	0.016
					SFID	-0.593	0.015
T10	Area	VBPH	0.968	0.000	IFA	0.510	0.043
		VBAH	0.885	0.000	IFPA	0.522	0.038
		SFID	0.794	0.000	RT	-0.541	0.030
		IIFD	0.670	0.005			
T10	RT				IFA	-0.555	0.026
					IFPA	-0.531	0.034
					IVAPA	0.620	0.010
					VBAH	-0.529	0.035
					Area	-0.541	0.030
T11	SFA	SFPA	0.997	0.000	CPBA	0.562	0.024
T11	SFPA	SFA	0.997	0.000	CPBA	0.556	0.025
T11	IFA	IFPA	0.985	0.000			
		SVAPA	-0.790	0.000			
		PICP	-0.626	0.009			
T11	IFPA	IFA	0.985	0.000	Area	0.512	0.043
		SVAPA	-0.781	0.000			
		PICP	-0.641	0.007			
T11	SVAPA	IFA	-0.790	0.000			
		IFPA	-0.781	0.000			
T11	IVAPA				Area	-0.535	
T11	VBPH	Area	0.900	0.000	VBAH	0.594	0.033
					SFID	0.621	0.015
					IIFD	0.603	0.010
					RT	-0.529	0.013
T11	VBAH				VBPH	0.594	0.035
					Area	0.518	0.015
T11	SFID	IIFD	0.665	0.005	VBPH	0.621	0.010
		Area	0.709	0.002			
T11	IIFD	SFID	0.665	0.005	VBPH	0.603	0.013
		Area	0.715	0.002			

[1] Alpha level: $p < 0.01$; [2] Alpha level: $p < 0.05$.

Table I-2. Spearman's rho, significant correlation for *Gorilla* (cont.).

Level	Variable	*Gorilla*					
		Variable	r_s	p value[1]	Variable	r_s	p value[2]
T11	PICP	IFA	-0.626	0.009			
		IFPA	-0.641	0.007			
T11	CPBA				SFA	0.562	0.024
					SFPA	0.556	0.025
T11	Area	VBPH	0.900		IFPA	0.512	0.043
		SFID	0.709	0.002	IVAPA	-0.535	0.033
		IIFD	0.715	0.002	VBAH	0.518	0.040
T11	RT				VBPH	-0.529	0.035
T12	SFA	SFPA	0.991	0.000	PICP	-0.614	0.011
T12	SFPA	SFA	0.991	0.000	PICP	-0.602	0.014
T12	IFA	IFPA	0.991	0.000	RT	0.550	0.027
T12	IFPA	IFA	0.910	0.000	RT	0.574	0.020
T12	SVAPA				IVAPA	0.503	0.047
					VBPH	-0.499	0.049
					VBAH	-0.521	0.039
					Area	-0.531	0.034
T12	IVAPA	RT	-0.675	0.004	SVAPA	0.503	0.047
T12	VBPH	VBAH	0.891	0.000	SVAPA	-0.499	0.049
		SFID	0.668	0.005			
		IIFD	0.668	0.005			
		Area	0.935	0.000			
T12	VBAH	VBPH	0.891	0.000	SVAPA	-0.521	0.039
		IIFD	0.647	0.007	SFID	0.606	0.013
		Area	0.818	0.000			
T12	SFID	VBPH	0.668	0.005	VBAH	0.606	0.013
		IIFD	0.703	0.002	CPBA	0.524	0.037
		Area	0.756	0.001			
T12	IIFD	VBPH	0.668	0.005	Area	0.618	0.011
		VBAH	0.647	0.007			
		SFID	0.703	0.002			
T12	PICP				SFA	-0.614	0.011
					SFPA	-0.602	0.014
T12	CPBA				SFID	0.524	0.037
T12	Area	VBPH	0.935	0.000	SVAPA	-0.531	0.034
		VBAH	0.818	0.000	IIFD	0.618	0.011
		SFID	0.756	0.001			
T12	RT	IVAPA	-0.675	0.000	IFA	0.550	0.027
					IFPA	0.574	0.020

[1] Alpha level: $p < 0.01$; [2] Alpha level: $p < 0.05$.

Table I-2. Spearman's rho, significant correlation for *Gorilla* (cont.).

Level	Variable	*Gorilla*					
		Variable	r_s	p value[1]	Variable	r_s	p value[2]
T13	SFA	SFPA	0.979	0.000			
		IFA	0.756	0.001			
		IFPA	0.747	0.000			
T13	SFPA	SFA	0.979	0.000			
		IFA	0.762	0.001			
		IFPA	0.765	0.001			
T13	IFA	SFA	0.756	0.001			
		SFPA	0.765	0.001			
		IFPA	0.991	0.000			
T13	IFPA	SFA	0.747	0.001			
		SFPA	0.765	0.001			
		IFA	0.991	0.000			
T13	IVAPA	RT	-0.843	0.000			
T13	VBPH	VBAH	0.924	0.000			
		Area	0.926	0.000			
T13	VBAH	VBPH	0.924	0.000			
		Area	0.794	0.000			
T13	SFID				IIFD	0.532	0.034
T13	IIFD				SFID	0.532	0.034
T13	PICP	CPBA	-0.679	0.004			
T13	CPBA	PICP	-0.679	0.004			
T13	Area	VBPH	0.926	0.000			
		VBAH	0.794	0.000			
T13	RT	IVAPA	-0.843	0.000			
L1	SFA	SFPA	0.982	0.000	SVAPA	0.508	0.045
L1	SFA	PICP	-0.641	0.007	SFID	0.594	0.015
L1	SFPA	SFA	0.982	0.000	SVAPA	0.525	0.037
		PICP	-0.700	0.003	SFID	0.585	0.017
					RT	0.538	0.031
L1	IFA	IFPA	0.982	0.000	PICP	-0.538	0.031
L1	IFPA	IFA	0.982	0.000			
		PICP	-0.664	0.007			
L1	SVAPA				SFA	0.508	0.045
					SFPA	0.525	0.037
					IVAPA	0.505	0.046
					RT	0.521	0.039
L1	IVAPA	SFID	0.638	0.008	SVAPA	0.505	0.046
L1	VBPH	VBAH	0.900	0.000			
		IIFD	0.706	0.002			
		Area	0.929	0.000			

[1] Alpha level: $p < 0.01$; [2] Alpha level: $p < 0.05$.

Table I-2. Spearman's rho, significant correlation for *Gorilla* (cont.).

Level	Variable	*Gorilla*					
		Variable	r_s	p value[1]	Variable	r_s	p value[2]
L1	VBAH	VBPH	0.900	0.000			
		IIFD	0.676	0.004			
		Area	0.803	0.000			
L1	SFID	IVAPA	0.683	0.008	SFA	0.594	0.015
		IIFD	0.671	0.004	SFPA	0.585	0.017
L1	IIFD	VBPH	0.706	0.002			
		VBAH	0.706	0.004			
		SFID	0.671	0.004			
		Area	0.862	0.000			
L1	PICP	SFA	-0.641	0.007	IFA	-0.538	0.031
		SFPA	-0.700	0.003			
		IFPA	-0.644	0.007			
L1	Area	VBPH	0.929	0.000			
		VBAH	0.803	0.000			
L1	Area	IIFD	0.862	0.000			
L1	RT				SFPA	0.538	0.031
					SVAPA	0.521	0.039
L2	SFA	SFPA	0.955	0.000	IVAPA	0.579	0.019
		SVAPA	0.782	0.000			
L2	SFPA	SFA	0.955	0.000	IVAPA	0.568	0.022
		SVAPA	0.744	0.001			
L2	IFA	IFPA	0.996	0.000	IIFD	0.620	0.010
		SFID	0.627	0.009	RT	-0.529	0.035
L2	IFPA	IFA	0.996	0.000	RT	-0.503	0.015
		SFID	0.650	0.006			
		IIFD	0.652	0.006			
L2	SVAPA	SFA	0.782	0.000			
		SFPA	0.744	0.001			
		IVAPA	0.858	0.000			
L2	IVAPA	SVAPA	0.858	0.000	SFA	0.579	0.019
					SFPA	0.568	0.022
					SFID	0.550	0.027
L2	VBPH	VBAH	0.894	0.000	IIFD	0.603	0.013
		Area	0.900	0.000			
L2	VBAH	VBPH	0.894	0.000	IIFD	0.593	0.015
		Area	0.900	0.000			
L2	SFID	IFA	0.627	0.009	IVAPA	0.550	0.027
		IFPA	0.650	0.006	PICP	-0.597	0.015
		IIFD	0.674	0.004	RT	-0.596	0.015

[1] Alpha level: $p < 0.01$; [2] Alpha level: $p < 0.05$.

Table I-2. Spearman's rho, significant correlation for *Gorilla* (cont.).

Level	Variable	*Gorilla*					
		Variable	r_s	p value[1]	Variable	r_s	p value[2]
L2	IIFD	IFPA	0.652	0.006	IFA	0.620	0.010
		SFID	0.674	0.004	VBPH	0.603	0.013
		Area	0.655	0.006	VBAH	0.593	0.015
L2	PICP				SFID	-0.597	0.015
L2	Area	VBPH	0.900	0.000			
		VBAH	0.824	0.000			
		IIFD	0.655	0.006			
L2	RT				IFA	-0.529	0.035
					SFID	-0.596	0.047
L3	SFA	SFPA	0.988	0.000	IFA	0.596	0.015
					IFPA	0.595	0.015
					SVAPA	0.597	0.015
					IVAPA	0.606	0.013
L3	SFPA	SFA	0.988	0.000	IFA	0.611	0.012
		IVAPA	0.626	0.009	IFPA	0.614	0.011
					SVAPA	0.576	0.019
L3	IFA	IFPA	0.998	0.000	SFA	0.596	0.015
					SFPA	0.611	0.012
L3	IFPA	IFA	0.998	0.000	SFA	0.595	0.015
					SFPA	0.614	0.011
L3	SVAPA	IVAPA	0.721	0.002	SFA	0.597	0.015
		SFPA	0.576	0.009			
L3	IVAPA	SVAPA	0.721	0.002	SFA	0.606	0.015
					SFPA	0.626	0.019
L3	VBPH	VBAH	0.829	0.000	SFID	0.582	0.018
		IIFD	0.629	0.009	PICP	-0.529	0.035
		Area	0.944	0.000			
L3	VBAH	VBPH	0.829	0.009	IIFD	0.615	0.011
		Area	0.788	0.000			
L3	SFID	IIFD	0.791	0.000	VBPH	0.582	0.018
					Area	0.524	0.037
L3	IIFD	VBPH	0.629	0.009	VBAH	0.615	0.011
		SFID	0.791	0.000	Area	0.565	0.023
L3	PICP				VBPH	-0.529	0.035
					Area	-0.526	0.036
L3	Area	VBPH	0.944	0.000	SFID	0.524	0.037
		VBAH	0.778	0.000	IIFD	0.565	0.023
					PICP	-0.526	0.036

[1] Alpha level: $p < 0.01$; [2] Alpha level: $p < 0.05$.

Table I-2. Spearman's rho, significant correlation for *Gorilla* (cont.).

Level	Variable	*Gorilla*					
		Variable	r_s	p value[1]	Variable	r_s	p value[2]
L4	SFA	SFPA	0.930	0.000			
L4	SFPA	SFA	0.930	0.000			
L4	IFA	IFPA CPBA	0.900 0.855	0.000 0.001			
L4	IFPA	IFA CPBA	0.900 0.799	0.000 0.000			
L4	VBPH	VBAH Area	0.930 0.866	0.000 0.000			
L4	VBAH	VBPH Area	0.930 0.895	0.000 0.000			
L4	CPBA	IFA IFPA	0.855 0.799	0.000 0.001			
L4	Area	VBPH VBAH	0.866 0.895	0.000 0.000			

[1] Alpha level: $p < 0.01$; [2] Alpha level: $p < 0.05$.

Table I-3. Spearman's rho, significant correlation for *Pan.*

Level	Variable	*Pan*					
		Variable	r_s	p value[1]	Variable	r_s	p value[2]
C1	SFA				SVAPA	0.531	0.034
C1	SVAPA				SFA IVAPA	0.531 0.536	0.034 0.032
C1	IVAPA				SVAPA	0.536	0.032
C2	IFA				RT	-0.288	0.043
C2	IVAPA	RT	0.879				
C2	RT	IVAPA	0.879		IFA	-0.512	0.043
C3	SFA	SFPA	0.944		IVAPA	0.588	0.017
C3	SFPA	SFA	0.944		IVAPA	0.562	0.024
C3	IFA	IFPA	0.968				
C3	IFPA	IFA	0.968				
C3	SVAPA				VBPH RT	0.533 -0.562	0.050 0.037
C3	IVAPA				SFA SFPA IIFD	0.588 0.562 0.509	0.017 0.024 0.044
C3	VBPH	Area	0.768		SVAPA	0.533	0.050
C3	VBAH	Area	0.638	0.008			
C3	SFID	IIFD	0.823				
C3	IIFD	SFID PICP	0.823 -0.661	 0.005	IVAPA	0.509	0.024
C3	PICP	IIFD	-0.661	0.005	RT	-0.517	0.044
C3	Area	VBPH	0.768	0.001			
C3	Area	VBAH	0.638	0.008			
C3	RT				SVAPA RT	-0.562 -0.517	0.037 0.040
C4	SFA	SFPA	0.976	0.000			
C4	SFPA	SFA	0.976	0.000			
C4	IFA	IFPA	0.996	0.000	SVAPA SFID	-0.522 -0.506	0.038 0.045
C4	IFPA	IFA	0.996	0.000	SVAPA	-0.536	0.032
C4	SVAPA				IFA IFPA IIFD	-0.522 -0.536 0.546	0.038 0.032 0.029
C4	VBPH				VBAH Area	0.614 0.529	0.045 0.035
C4	VBAH				VBPH	0.614	0.011
C4	SFID	Area IIFD	0.626 0.838	0.009 0.000	IFA	-0.506	0.045

[1] Alpha level: $p < 0.01$; [2] Alpha level: $p < 0.05$.

Table I-3. Spearman's rho, significant correlation for *Pan* (cont.).

Level	Variable	*Pan*					
		Variable	r_s	p value[1]	Variable	r_s	p value[2]
C4	IIFD	SFID Area	0.838 0.609	0.009 0.000	SVAPA	0.546	0.012
C4	CPBA				RT	0.553	0.026
C4	Area	SFID	0.626	0.000	VBPH IIFD	0.529 0.609	0.035 0.012
C4	RT				SVAPA CPBA	-0.508 0.533	0.045 0.026
C5	SFA	SFPA	0.982	0.000	IFA	0.541	0.035
C5	SFPA	SFA	0.982	0.000	IFA	0.535	0.033
C5	SFPA				IFPA	0.550	0.027
C5	IFA	IFPA	0.994	0.000	SFA SFPA RT	0.529 0.535 -0.521	0.030 0.027 0.020
C5	IFPA	IFA	0.944	0.000	SFA SFPA RT	0.541 0.550 -0.574	0.027 0.020 0.010
C5	SVAPA				RT	-0.638	0.012
C5	VBPH	Area	0.738	0.000			
C5	SFID	IIFD	0.844	0.000			
C5	IIFD	SFID	0.844	0.000	CPBA	0.559	0.024
C5	CPBA				IIFD	0.599	0.024
C5	Area	VBPH	0.738	0.001			
C5	RT				IFA IFPA SVAPA	-0.521 -0.574 -0.638	0.039 0.020 0.010
C6	SFA	SFPA	0.944	0.000			
C6	SFPA	SFA	0.944	0.000			
C6	IFA	IFPA	0.982	0.000	SFID	-0.456	0.029
C6	IFPA	IFA	0.982	0.000	SFID	-0.551	0.027
C6	SVAPA				RT	-0.556	0.025
C6	VBPH	RT	0.633	0.008	PICP Area	-0.563 0.563	0.023 0.023
C6	SFID	IIFD	0.781	0.000	IFA	-0.546	0.029
C6	SFID				IFPA CPBA	-0.546 -0.527	0.029 0.036
C6	IIFD	SFID	0.781	0.000			
C6	PICP				VBPH RT	-0.563 -0.502	0.023 0.047

[1] Alpha level: $p < 0.01$; [2] Alpha level: $p < 0.05$.

Table I-3. Spearman's rho, significant correlation for *Pan* (cont.).

Level	Variable	*Pan*					
		Variable	r_s	p value[1]	Variable	r_s	p value[2]
C6	CPBA				IVAPA	-0.497	0.050
					SFID	-0.527	0.036
C6	Area				VBPH	0.563	0.023
C6	RT	VBPH	0.633	0.008	SVAPA	-0.556	0.025
					PICP	-0.502	0.047
C7	SFA	SFPA	0.950	0.000	IFPA	0.590	0.016
		VBPH	-0.662	0.005	SVAPA	0.515	0.041
C7	SFPA	SFA	0.950	0.000	IFPA	0.618	0.011
		VBPH	-0.741	0.001			
C7	IFA	IFPA	0.616	0.005	SVAPA	0.584	0.017
		RT	-0.670	0.005			
C7	IFPA				SFA	0.590	0.016
					SFPA	0.618	0.011
					IFA	0.616	0.011
C7	SVAPA	SFID	0.718	0.002	SFA	0.515	0.041
					IFA	0.584	0.017
C7	IVAPA				Area	0.512	0.043
C7	VBPH	Area	0.799	0.000	IIFD	0.523	0.045
					CPBA	0.616	0.014
C7	VBAH	SFA	-0.662	0.005			
		SFPA	-0.741	0.001			
C7	SFID	SVAPA	0.718	0.002			
C7	IIFD	Area	0.674	0.004	VBPH	0.523	0.045
C7	IIFD				CPBA	0.585	0.017
C7	CPBA	Area	0.616	0.002	VBPH	0.616	0.014
					IIFD	0.585	0.017
C7	Area	VBPH	0.799	0.000	IVAPA	0.512	0.043
		IIFD	0.674	0.004			
		CPBA	0.7112	0.002			
C7	RT	IFA	-0.670	0.005			
T1	SFA	SFPA	0.991	0.000	VBPH	0.546	0.029
		SVAPA	0.703	0.002			
		PICP	-0.697	0.003			
		RT	-0.683	0.004			
T1	SFPA	SFA	0.991	0.000	VBPH	0.597	0.015
		SVAPA	0.721	0.000			
		PICP	-0.697	0.003			

[1] Alpha level: $p < 0.01$; [2] Alpha level: $p < 0.05$.

Table I-3. Spearman's rho, significant correlation for *Pan* (cont.).

Level	Variable	*Pan*					
		Variable	r_s	p value[1]	Variable	r_s	p value[2]
T1	SFPA	RT	-0.667	0.004			
T1	IFA	IFPA	0.903	0.000	SVAPA	-0.499	0.049
		Area	-0.698	0.003			
T1	IFPA	IFA	0.903	0.000	IVAPA	-0.581	0.018
					Area	-0.521	0.039
T1	SVAPA	SFA	0.703	0.002	IFA	-0.499	0.049
		SFPA	0.721	0.002	VBPH	0.565	0.023
		RT	-0.784	0.000			
T1	IVAPA	IIFD	-0.668	0.005	IFPA	-0.581	0.018
T1	VBPH				SFA	0.546	0.029
					SFPA	0.597	0.015
T1	VBPH				SVAPA	0.565	0.023
					PICP	-0.543	0.030
T1	SFID	IIFD	0.700	0.003			
T1	IIFD	IVAPA	-0.668	0.005			
		SFID	0.700	0.003			
T1	PICP	SFA	-0.697	0.003	VBPH	-0.543	0.030
		SFPA	-0.697	0.003	Area	-0.535	0.033
T1	Area	IFA	-0.698	0.003	IFPA	-0.521	0.039
					PICP	-0.535	0.033
T1	RT	SFA	-0.683	0.004			
		SFPA	-0.677	0.004			
		SVAPA	-0.784	0.000			
T2	SFA	SFPA	0.974	0.000	VBAH	-0.543	0.030
T2	SFPA	SFA	0.974	0.000	VBAH	-0.586	0.017
T2	IFA	IFPA	0.904	0.000	IIFD	-0.586	0.013
T2	IFPA	IFA	0.904	0.000	IIFD	-0.555	0.026
T2	SVAPA	SFID	-0.717	0.002			
		RT	-0.805				
T2	VBPH	RT	-0.682	0.004			
T2	VBAH				SFA	-0.543	0.030
					SFPA	-0.586	0.017
					Area	0.508	0.045
T2	SFID	SVAPA	-0.717	0.002			
		IIFD	0.774	0.000			
		RT	0.732	0.000			
T2	IIFD	SFID	0.744	0.000	IFA	-0.605	0.013

[1] Alpha level: $p < 0.01$; [2] Alpha level: $p < 0.05$.

Table I-3. Spearman's rho, significant correlation for *Pan* (cont.).

Level	Variable	*Pan*					
		Variable	r_s	p value[1]	Variable	r_s	p value[2]
T2	IIFD				IFPA	-0.555	0.026
					Area	0.558	0.025
T2	PICP				RT	0.500	0.049
T2	Area				VBPH	0.508	0.045
					IIFD	0.558	0.025
T2	RT	SVAPA	-0.805	0.000	PICP	0.500	0.049
		VBPH	-0.682	0.004			
		SFID	0.732	0.000			
T3	SFA	SFPA	0.982	0.000			
T3	SFPA	SFA	0.982	0.000			
T3	IFA	IFPA	0.941	0.000	RT	0.512	0.043
T3	IFPA	IFA	0.941	0.000			
T3	SVAPA				RT	-0.564	0.023
T3	IVAPA				RT	0.530	0.035
T3	VBPH	VBAH	0.821	0.000			
		Area	0.625	0.001			
T3	VBAH	VBPH	0.821	0.000			
		Area	0.724	0.002			
T3	SFID	IIFD	0.690	0.003	Area	0.594	0.015
T3	IIFD	SFID	0.690	0.003			
		Area	0.686	0.003			
T3	Area	VBPH	0.625	0.001	SFID	0.594	0.015
		VBAH	0.725	0.002			
		IIFD	0.686	0.003			
T3	RT				IFA	0.512	0.043
T3	RT				SVAPA	-0.564	0.023
					IVAPA	0.530	0.035
T4	SFA	SFPA	0.918	0.000			
T4	SFPA	SFA	0.918	0.000			
T4	IFA	IFPA	0.964	0.000			
T4	IFPA	IFA	0.964	0.000			
T4	SVAPA	IVAPA	0.676	0.004			
T4	IVAPA	SVAPA	0.676	0.004			
T4	VBPH	Area	0.770	0.000	VBAH	0.532	0.034
T4	VBAH				VBPH	0.532	0.034
					Area	0.597	0.015
T4	SFID				IIFD	0.526	0.044
					Area	0.564	0.023
T4	IIFD	Area	0.518	0.000	SFID	0.526	0.044
					Area	0.518	0.048

[1] Alpha level: $p < 0.01$; [2] Alpha level: $p < 0.05$.

Table I-3. Spearman's rho, significant correlation for *Pan* (cont.).

Level	Variable	*Pan*					
		Variable	r_s	p value[1]	Variable	r_s	p value[2]
T4	Area	VBPH	0.770	0.000	VBAH SFID IIFD	0.597 0.564 0.518	0.015 0.023 0.048
T5	SFA	SFPA	0.964	0.000	IVAPA	0.556	0.025
T5	SFPA	SFA	0.964	0.000			
T5	IFA	IFPA	0.938	0.000	SFID IIFD	-0.500 -0.563	0.049 0.023
T5	IFPA	IFA	0.938	0.000			
T5	IVAPA				SFA	0.556	0.028
T5	VBPH	VBAH Area	0.749 0.664	0.001 0.005			
T5	VBAH	VBPH	0.749	0.001	IVAPA SFID IIFD Area	0.547 0.503 0.573 0.526	0.028 0.047 0.020 0.036
T5	SFID	IIFD	0.869	0.000	IFA VBAH Area	-0.500 0.503 0.535	0.049 0.047 0.033
T5	IIFD	SFID	0.869	0.000	IFA VBAH	-0.563 0.573	0.023 0.020
T5	Area	VBPH	0.664	0.005	VBAH SFID	0.526 0.535	0.036 0.033
T5	RT	IVAPA	0.779	0.000			
T6	SFA	SFPA	0.988	0.000	SVAPA RT	-0.558 0.535	0.025 0.014
T6	SFPA	SFA	0.988	0.000	SVAPA RT	-0.528 0.535	0.035 0.033
T6	IFA	IFPA	0.955	0.000			
T6	IFPA	IFA	0.955	0.000			
T6	SVAPA				SFA SFPA	-0.558 -0.528	0.025 0.035
T6	IVAPA	RT	0.766	0.000			
T6	VBPH				VBAH Area	0.560 0.594	0.030 0.015
T6	VBAH				VBPH CPBA	0.560 -0.521	0.030 0.047
T6	VBAH				Area	0.599	0.018
T6	SFID	IIFD	0.838	0.000	PICP	-0.574	0.020
T6	SFID				Area	0.550	0.027

[1] Alpha level: $p < 0.01$; [2] Alpha level: $p < 0.05$.

Table I-3. Spearman's rho, significant correlation for *Pan* (cont.).

Level	Variable	*Pan*					
		Variable	r_s	p value[1]	Variable	r_s	p value[2]
T6	IIFD	Area SFID	0.676 0.838	0.000 0.000			
T6	PICP				SFID	-0.574	0.020
T6	CPBA				VBAH	-0.521	0.047
T6	Area	IIFD	0.767	0.001	VBPH VBAH SFID	0.594 0.599 0.550	0.015 0.018 0.027
T6	RT	IVAPA	0.766	0.000	SFA SFPA	0.600 0.535	0.014 0.033
T7	SFA	SFPA CPBA	0.968 0.889	0.000 0.000	IVAPA RT	0.532 0.519	0.034 0.039
T7	SFPA	SFA CPBA	0.968 0.824	0.000 0.000	RT	0.522	0.038
T7	IFA	IFPA	0.944	0.000	PICP	0.552	0.027
T7	IFPA	IFA	0.944	0.000			
T7	SVAPA	RT	-0.765	0.001			
T7	IVAPA				SFA RT	0.532 0.519	0.034 0.039
T7	VBPH	IIFD Area	0.635 0.726	0.000 0.008			
T7	VBAH	VBPH IIFD	0.784 0.683	0.000 0.004	SFID	0.603	0.013
T7	VBAH	Area	0.636	0.008			
T7	SFID	IIFD	0.898	0.000	VBAH	0.603	0.013
T7	IIFD	VBPH	0.635	0.008	Area	0.529	0.035
T7	IIFD	VBAH SFID	0.683 0.898	0.004			
T7	PICP				IFA	0.552	0.027
T7	CPBA	SFA SFPA	0.889 0.824	0.000 0.000			
T7	Area	VBPH VBAH	0.726 0.636	0.001 0.008	IIFD	0.529	0.039
T7	RT	SVAPA	-0.765	0.000	SFA SFPA IVAPA	0.519 0.522 0.519	0.038 0.038 0.039
T8	SFA	SFPA	0.987	0.000			
T8	SFPA	SFA	0.987	0.000			
T8	IFA	IFPA	0.965	0.000			
T8	IFPA	IFA	0.965	0.000			

[1] Alpha level: $p < 0.01$; [2] Alpha level: $p < 0.05$.

Table I-3. Spearman's rho, significant correlation for *Pan* (cont.).

Level	Variable	*Pan*					
		Variable	r_s	p value[1]	Variable	r_s	p value[2]
T8	SVAPA				IVAPA	0.521	0.039
					VBPH	-0.509	0.044
					VBAH	-0.500	0.049
					RT	-0.579	0.015
T8	IVAPA				SVAPA	0.521	0.039
T8	VBPH	VBAH	0.635	0.008	SVAPA	-0.509	0.044
		Area	0.638	0.008	RT	0.576	0.019
T8	VBAH	VBPH	0.635	0.008	SVAPA	-0.500	0.044
T8	VBAH				SFID	0.591	0.049
					Area	0.541	0.016
					RT	0.606	0.016
T8	SFID	IIFD	0.843	0.000	VBAH	0.591	0.015
					Area	0.599	0.024
T8	IIFD	SFID	0.843	0.000			
T8	Area	VBPH	0.638	0.008	VBAH	0.541	0.030
					SFID	0.559	0.024
					RT	0.606	0.013
T8	RT				SVAPA	-0.579	0.019
					VBPH	0.576	0.019
					VBAH	0.606	0.013
					Area	0.606	0.013
T9	SFA	SFPA	0.940	0.000			
T9	SFPA	SFA	0.940	0.000			
T9	IFA	IFPA	0.991	0.000			
T9	IFPA	IFA	0.991	0.000			
T9	SVAPA	RT	-0.747	0.001			
T9	IVAPA				RT	0.585	0.017
T9	VBPH	VBAH	0.806	0.000	CPBA	-0.535	0.033
		Area	0.632	0.009			0.034
T9	VBAH	VBPH	0.806	0.000	CPBA	-0.532	0.033
		Area	0.635	0.008			
T9	SFID	IIFD	0.784	0.000			
T9	IIFD	SFID	0.784	0.000	Area	0.534	0.033
T9	CPBA				VBPH	0.353	0.033
					VBAH	-0.532	0.034
T9	Area	VBPH	0.632	0.009	IIFD	0.534	0.033
		VBAH	0.635	0.008	RT	0.529	0.035
T9	RT	SVAPA	-0.747	0.001	IVAPA	-0.747	0.017
T9	RT				Area	0.529	0.035

[1] Alpha level: $p < 0.01$; [2] Alpha level: $p < 0.05$.

Table I-3. Spearman's rho, significant correlation for *Pan* (cont.).

Level	Variable	*Pan*					
		Variable	r_s	p value[1]	Variable	r_s	p value[2]
T10	SFA	SFPA CPBA	0.952 0.715	0.000 0.002			
T10	SFPA	SFA CPBA	0.952 0.667	0.000 0.005			
T10	IFA	IFPA IVAPA	0.939 -0.647	0.000 0.007			
T10	IFPA	IFA	0.939	0.000	IVAPA	-0.563	0.023
T10	SVAPA				RT	-0.518	0.040
T10	IVAPA	IFA RT	-0.647 0.676	0.007 0.004	IFPA	-0.563	0.023
T10	VBPH	VBAH	0.644	0.007	Area	0.522	0.038
T10	VBAH	VBPH SFID Area	0.664 0.664 0.684	0.007 0.005 0.006	CPBA	-0.543	0.030
T10	SFID	VBAH IIFD Area	0.664 0.712 0.656	0.005 0.002 0.006			
T10	IIFD	SFID	0.712	0.002			
T10	CPBA	SFA SFPA	0.715 0.667	0.002 0.005	VBAH	-0.543	0.030
T10	Area	VBAH SFID	0.658 0.656	0.006 0.006	VBPH RT	0.522 0.526	0.038 0.036
T10	RT	IVAPA	0.676	0.004	SVAPA Area	0.518 0.526	0.040 0.036
T11	SFA	SFPA	0.982	0.000			
T11	SFPA	SFA	0.982	0.000	IFPA	0.505	0.046
T11	IFA	IFPA	0.958	0.000			
T11	IFPA	IFA	0.958	0.000	SFPA	0.505	0.046
T11	IVAPA				RT	0.555	0.026
T11	VBPH				VBAH Area	0.557 0.596	0.025 0.015
T11	VBAH	Area	0.653	0.006	VBPH	0.557	0.025
T11	SFID	IIFD	0.662	0.005			
T11	IIFD	SFID	0.662	0.005	CPBA Area	-0.558 0.568	0.025 0.022
T11	CPBA				IIFD	-0.558	0.025
T11	Area	VBAH	0.653	0.006	VBPH IIFD	0.596 0.568	0.015 0.022

[1] Alpha level: $p < 0.01$; [2] Alpha level: $p < 0.05$.

Table I-3. Spearman's rho, significant correlation for *Pan* (cont.).

Level	Variable	*Pan*					
		Variable	r_s	p value[1]	Variable	r_s	p value[2]
T11	RT				IVAPA	0.555	0.026
T12	SFA	SFPA	0.938	0.000			
T12	SFPA	SFA	0.938	0.000			
T12	IFA	IFPA	0.976	0.000			
		IVAPA	-0.832	0.000			
		RT	0.753	0.001			
T12	IFPA	IFA	0.976	0.000	SFID	0.537	
		IVAPA	-0.847	0.000			
		RT	0.694	0.000			
T12	IVAPA	IFA	-0.832	0.000			
		IFPA	-0.847	0.000			
		RT	-0.788	0.000			
T12	VBPH	VBAH	0.697	0.003	PICP	0.586	0.017
T12	VBAH	VBPH	0.697	0.003	IIFD	0.697	0.025
		CPBA	-0.664	0.005			
		Area	0.773	0.000			
T12	SFID	IIFD	0.737	0.001	IFPA	0.537	0.032
		CPBA	-0.650	0.006	Area	0.593	0.015
T12	IIFD	SFID	0.737	0.001	VBAH	0.558	0.015
		CPBA	0.664	0.005			
T12	PICP				VBPH	0.586	0.017
T12	CPBA	VBAH	-0.664	0.005			
		SFID	-0.650	0.006			
		IIFD	-0.665	0.005			
		Area	-0.921	0.000			
T12	Area	VBAH	0.773	0.000	SFID	0.593	0.015
		IIFD	0.664	0.007			
		CPBA	-0.921	0.000			
T12	RT	IFA	0.753	0.001			
		IFPA	0.694	0.003			
		IVAPA	-0.788	0.000			
T13	SFA	SFPA	0.989	0.000	IVAPA	-0.548	0.043
T13	SFPA	SFA	0.989	0.000	SVAPA	0.575	0.035
					IVAPA	0.561	0.045
T13		SVAPA	-0.736	0.002			
T13	IFPA	IFA	0.993	0.000	Area	0.571	0.026
		SVAPA	-0.721	0.002			
T13	SVAPA	IFA	-0.736	0.002	SFA	0.593	0.020
		IFPA	-0.210	0.002	SFPA	0.575	0.025

[1] Alpha level: $p < 0.01$; [2] Alpha level: $p < 0.05$.

Table I-3. Spearman's rho, significant correlation for *Pan* (cont.).

Level	Variable	*Pan*					
		Variable	r_s	p value[1]	Variable	r_s	p value[2]
T13	SVAPA			0.000	IVAPA	0.616	0.019
T13	IVAPA			0.000	SFA SFPA SVAPA	0.548 0.561 0.616	0.043 0.037 0.019
T13	VBPH	VBAH Area	0.805 0.681	0.000 0.005	IIFD	0.556	0.031
T13	VBAH	VBPH	0.805	0.000			
T13	SFID				IIFD	0.564	0.028
T13	IIFD	Area	0.732	0.002	VBPH SFID	0.556 0.564	0.031
T13	PICP				Area	0.536	0.040
T13	Area	VBPH IIFD	0.681 0.732	0.005 0.002	IFA IFPA PICP	0.546 0.571 0.536	0.035 0.026 0.040
L1	SFA	SFPA	0.985	0.000			
L1	SFPA	SFA	0.985	0.000			
L1	IFA	IFPA	0.918	0.000			
L1	IFPA	IFA	0.918	0.000			
L1	SVAPA	IVAPA	0.752	0.002			
L1	IVAPA	SVAPA	0.752	0.002	SFID PICP	0.531 -0597	0.034 0.015
L1	VBPH	Area	0.785	0.008	IIFD	0.618	0.011
L1	SFID	IIFD	0.640	0.008	IVAPA Area	0.531 0.600	0.034 0.014
L1	IIFD	SFID Area	0.640 0.792	0.008	VBPH	0.618	0.011
L1	PICP				IVAPA	-0.597	0.015
L1	Area	VBPH IIFD	0.785 0.792	0.000 0.000	SFID	0.600	0.014
L2	SFA	SFPA IVAPA VBPH	0.985 0.679 0.624	0.000 0.004 0.001	CPBA Area	0.538 0.526	0.031 0.036
L2	SFPA	SFA IVAPA VBPH	0.985 0.665 0.671	0.000 0.005 0.004	CPBA Area	0.538 0.550	0.031 0.027
L2	IFA	IFPA	0.998	0.000			
L2	IFPA	IFA	0.998	0.000			
L2	SVAPA				IVAPA	0.506	0.046

[1] Alpha level: $p < 0.01$; [2] Alpha level: $p < 0.05$.

Table I-3. Spearman's rho, significant correlation for *Pan* (cont.).

Level	Variable	*Pan*					
		Variable	r_s	p value[1]	Variable	r_s	p value[2]
L2	IVAPA	SFA	0.679	0.004	SVAPA	0.506	0.046
		SFPA	0.665	0.005	VBPH	0.524	0.037
L2	VBPH	SFA	0.624	0.001	IVAPA	0.524	0.037
		SFPA	0.671	0.004			
		Area	0.644	0.007			
L2	VBAH	IIFD	0.626	0.009	PICP	0.555	0.026
L2	SFID	IIFD	0.656	0.006			
L2	SFID	Area	0.748	0.001			
L2	IIFD	VBAH	0.626	0.009			
		SFID	0.656	0.006			
		Area	0.776	0.000			
L2	PICP				VBAH	0.555	
L2	CPBA				SFA	0.538	0.026
					SFPA	0.538	0.031
L2	Area	VBPH	0.664	0.007	SFPA	0.550	0.031
		SFID	0.748	0.001			
		IIFD	0.776	0.000			
L3	SFA	SFPA	0.967	0.000	VBPH	0.514	0.042
		SVAPA	0.673	0.004	Area	0.558	0.025
		IVAPA	0.665	0.005			
L3	SFPA	SFA	0.967	0.000	SVAPA	0.600	0.014
					IVAPA	0.545	0.029
					Area	0.524	0.037
L3	IFA	IFPA	0.943	0.000			
L3	IFPA	IFA	0.943	0.000			
L3	SVAPA	SFA	0.673	0.004	SFPA	0.600	0.014
		IVAPA	0.662	0.005			
L3	IVAPA	SFA	0.665	0.005	SFPA	0.545	0.029
		SVAPA	0.662	0.005	IIFD	0.517	0.040
		VBPH	0.660	0.005	Area	0.567	0.022
		PICP	-0.641	0.007			
		RT	-0.740	0.001			
L3	VBPH	IVAPA	0.660	0.005	SFA	0.514	0.042
					IIFD	0.540	0.031
L3	SFID	IIFD	0.809	0.000			
L3	SFID	Area	0.632	0.009			
L3	IIFD	SFID	0.809	0.000	IVAPA	0.517	0.040
		Area	0.759	0.001	VBPH	0.540	0.031

[1] Alpha level: $p < 0.01$; [2] Alpha level: $p < 0.05$.

Table I-3. Spearman's rho, significant correlation for *Pan* (cont.).

Level	Variable	*Pan*					
		Variable	r_s	p value[1]	Variable	r_s	p value[2]
L3	PICP	IVAPA	-0.641	0.007	CPBA	-0.597	0.015
					RT	0.508	0.045
L3	CPBA				PICP	-0.597	0.015
L3	Area	SFID	0.632	0.009	SFA	0.558	0.025
		IIFD	0.759	0.001	SFPA	0.524	0.037
					IVAPA	0.567	0.022
					RT	-0.550	0.027
L3	RT	IVAPA	-0.740	0.001	PICP	0.508	0.045
					Area	-0.550	0.017
L4	SFA	SFPA	0.885	0.000			
L4	SFPA	SFA	0.885	0.000			
L4	IFA	IFPA	0.958	0.000			
L4	IFPA	IFA	0.985	0.000			
L4	SVAPA				IVAPA	0.657	0.015
					VBPH	0.608	0.028
					PICP	-0.575	0.040
L4	IVAPA	RT	-0.718	0.006	SVAPA	0.657	0.015
					IIFD	0.559	0.031
L4	VBPH				SVAPA	0.608	0.028
L4	SFID	IIFD	0.929	0.000	CPBA	-0.669	0.012
		Area	0.791	0.001			
L4	IIFD	SFID	0.929	0.000	IVAPA	0.599	0.031
		Area	0.725	0.005	CPBA	-0.674	0.012
L4	IIFD				RT	-0.575	0.040
L4	PICP				SVAPA	-0.575	0.040
L4	CPBA				IIFD	-0.674	0.012
L4	Area	SFID	0.791	0.001			
		IIFD	0.725	0.005			
L4	RT	IVAPA	-0.718	0.006	IIFD	-0.575	0.040

[1] Alpha level: $p < 0.01$; [2] Alpha level: $p < 0.05$.

Appendix J: MLR classification and validation results

Table J-1. Model classification and validation for taxa (CBA).

Cranial Base Angle Model Classification				
	Predicted			
Observed	*Homo sapiens*	*Pan troglodytes*	*Gorilla gorilla*	Percent Correct
Homo sapiens	33	1	0	97.1%
Pan troglodytes	2	11	3	68.8%
Gorilla gorilla	0	3	13	81.3%
Overall Percentage	53.0%	22.7%	24.2%	86.4%
Model Statistics				
Likelihood Ratio[1]				
CBA [χ^2 (2) = 97.109; p = 0.000]				
Model Fit[1]				
Final [-2 log likelihood value 38.687; χ^2 (2) = 97.109; p = 0.000]				
Goodness of Fit				
Pearson [χ^2 (128) = 39.505; p = 1.000]				
Deviance [χ^2 (128) = 38.687; p = 1.000]				
Pseudo R^2				
Cox and Snell R^2 = 0.77; Nagelkerke R^2 = 0.88; McFadden R^2 = 0.71				

Cranial Base Angle Validation Classification				
	Predicted			
Observed	*Homo sapiens*	*Pan troglodytes*	*Gorilla gorilla*	Percent Correct
Homo sapiens	1251	49	0	96.2%
Pan troglodytes	92	362	98	65.5%
Gorilla gorilla	0	98	450	82.1%
Overall Percentage	55.9%	21.1%	22.8%	85.9%
Validation Statistics 50 Tests (Homo n = 26, Pan n = 11, Gorilla n = 11) % Averages				
Model Fitting[2] Final Model: p = 0.000				
		Minimum	Maximum	
Goodness of Fit: Pearson		1.000	1.000	
Deviance		1.000	1.000	
Pseudo R Square: Cox and Snell		0.737	0.797	
Nagelkerke		0.850	0.920	
McFadden		0.663	0.792	
Total Misclassification		337		

[1] Alpha level: p < 0.05.
[2] Bonferroni Correction: p < 0.01.

Table J-2. Model classification and validation for taxa (TTC and TLC).

Curvature Model Classification				
	Predicted			
Observed	*Homo sapiens*	*Pan troglodytes*	*Gorilla gorilla*	Percent Correct
Homo sapiens	32	2	0	94.1%
Pan troglodytes	2	8	6	50.0%
Gorilla gorilla	0	3	13	81.3%
Overall Percentage	51.5%	19.7%	28.8%	80.3%
Model Statistics				
Likelihood Ratio[1]				
TLC [χ^2 (2) = 48.134; p = 0.000]				
TTC [χ^2 (2) = 19.352; p = 0.000]				
Model Fit[1]				
Final [-2 log likelihood value 48.241; χ^2 (4) = 87.555; p = 0.000]				
Goodness of Fit				
Pearson [χ^2 (126) = 47.790; p = 1.000]				
Deviance [χ^2 (126) = 48.241; p = 1.000]				
Pseudo R^2				
Cox and Snell R^2 = 0.73; Nagelkerke R^2 = 0.84; McFadden R^2 = 0.64				

Curvature Validation Classification				
	Predicted			
Observed	*Homo sapiens*	*Pan troglodytes*	*Gorilla gorilla*	Percent Correct
Homo sapiens	1268	65	3	94.7%
Pan troglodytes	76	292	186	52.5%
Gorilla gorilla	0	97	451	82.2%
Overall Percentage	54.5%	18.8%	26.6%	82.2%
Validation Statistics 50 Tests (Homo n = 26, Pan n = 11, Gorilla n = 11) % Averages				
Model Fitting[2] Final Model: p = 0.000				
		Minimum	Maximum	
Goodness of Fit: Pearson		1.000	1.000	
Deviance		1.000	1.000	
Pseudo R Square: Cox and Snell		0.662	0.792	
Nagelkerke		0.763	0.914	
McFadden		0.538	0.780	
Total Misclassification		427		

[1] Alpha level: p < 0.05.
[2] Bonferroni Correction: p < 0.01.

Appendix K: MLR classification and validation for positional-locomotory complex

Table K-1. Model classification and validation (CBA).

CBA Model Classification				
	Predicted			
Observed	Bipedal	Knuckle walk G	Knuckle walk P	Percent Correct
Bipedal	33	0	1	97.1%
Knuckle walk G	0	13	3	81.3%
Knuckle walk P	2	3	11	68.8%
Overall Percentage	53.0%	24.2%	22.7%	86.4%
Model Statistics				
Likelihood Ratio[1]				
CBA [χ^2 (2) = 97.109; p = 0.000]				
Model Fit[1]				
Final [-2 log likelihood value 38.687; χ^2 (2) = 97.109; p = 0.000]				
Goodness of Fit				
Pearson [χ^2 (128) = 39.505; p = 1.000]				
Deviance [χ^2 (128) = 38.687; p = 1.000]				
Pseudo R^2				
Cox and Snell R^2 = 0.77; Nagelkerke R^2 = 0.88; McFadden R^2 = 0.71				

CBA Validation Classification				
	Predicted			
Observed	Bipedal	Knuckle walk G	Knuckle walk P	Percent Correct
Bipedal	1202	0	46	95.7%
Knuckle walk G	0	443	85	84.1%
Knuckle walk P	85	93	350	65.5%
Overall Percentage	65.7%	22.8%	29.0%	87.3%

Validation Statistics 50 Tests (Homo n = 26, Pan n = 11, Gorilla n = 11) % Averages		
Model Fitting[2]		
Final Model: p = 0.000		
	Minimum	Maximum
Goodness of Fit: Pearson	1.000	1.000
Deviance	1.000	1.000
Pseudo R Square: Cox and Snell	0.737	0.797
Nagelkerke	0.850	0.920
McFadden	0.663	0.792
Total Misclassification	309	

[1] Alpha level: p < 0.05.

[2] Bonferroni Correction: p < 0.01.

Table K-2. Model classification and validation (TTC and TLC).

TTC and TLC Model Classification				
	Predicted			
Observed	Bipedal	Knuckle walk G	Knuckle walk P	Percent Correct
Bipedal	32	0	2	94.1%
Knuckle walk G	0	13	3	81.3%
Knuckle walk P	2	6	8	50.0%
Overall Percentage	51.5%	28.8%	19.7%	80.3%
Model Statistics				
Likelihood Ratio[1]				
TLC [χ^2 (2) = 48.134; p = 0.000]				
TTC [χ^2 (2) = 19.352; p = 0.000]				
Model Fit[1]				
Final [-2 log likelihood value 48.241; χ^2 (4) = 87.555; p = 0.000]				
Goodness of Fit				
Pearson [χ^2 (126) = 47.790; p = 1.000]				
Deviance [χ^2 (126) = 48.241; p = 1.000]				
Pseudo R^2				
Cox and Snell R^2 = 0.73; Nagelkerke R^2 = 0.84; McFadden R^2 = 0.64				

TTC and TLC Validation Classification				
	Predicted			
Observed	Bipedal	Knuckle walk G	Knuckle walk P	Percent Correct
Bipedal	1232	3	65	94.7%
Knuckle walk G	0	451	97	82.2%
Knuckle walk P	76	186	290	52.5%
Overall Percentage	53.4%	26.2%	22.9%	82.2%
Validation Statistics 50 Tests (Homo n = 26, Pan n = 11, Gorilla n = 11) % Averages				
Model Fitting[2] Final Model: p = 0.000				
		Minimum	Maximum	
Goodness of Fit: Pearson		1.000	1.000	
Deviance		1.000	1.000	
Pseudo R Square: Cox and Snell		0.662	0.792	
Nagelkerke		0.713	0.914	
McFadden		0.538	0.780	
Total Misclassification		427		

[1] Alpha level: $p < 0.05$.
[2] Bonferroni Correction: $p < 0.01$.

Post hoc tests

Table K-3. Model classification and verification for cervical CPBA.

Cervical CPBA Classification				
	Predicted			
Observed	Bipedal	Knuckle walk G	Knuckle walk P	Percent Correct
Bipedal	25	3	2	83.3%
Knuckle walk G	3	12	0	80.0%
Knuckle walk P	6	3	4	30.8%
Overall Percentage	58.6%	31.0%	10.3%	70.7%
Model Statistics				
Likelihood Ratio[1]				
C7CPBA [χ^2 (2) = 22.751; p = 0.000]				
C3 CPBA [χ^2 (2) = 12.170; p = 0.002]				
Model Fit[1]				
Final [-2 log likelihood value 88.488; χ^2 (4) = 30.521; p = 0.000]				
Goodness of Fit				
Pearson [χ^2 (110) = 109.966; p = 0.483]				
Deviance [χ^2 (110) = 88.488; p = 0.935]				
Pseudo R^2				
Cox and Snell R^2 = 0.40; Nagelkerke R^2 = 0.46; McFadden R^2 = 0.25				

Cervical CPBA Validation Classification				
	Predicted			
Observed	Bipedal	Knuckle walk G	Knuckle walk P	Percent Correct
Bipedal	1069	110	8	88.2%
Knuckle walk G	263	274	11	49.9%
Knuckle walk P	320	165	25	4.9%
Overall Percentage	86.7%	24.4%	1.9%	60.9%

Validation Statistics 50 Tests (Homo n = 26, Pan n = 11, Gorilla n = 11) % Averages		
Model Fitting[2]		
Final Model: p = 0.000		
	Minimum	Maximum
Goodness of Fit: Pearson	0.150	0.660
Deviance	0.511	0.858
Pseudo R Square: Cox and Snell	0.129	0.411
Nagelkerke	0.148	0.478
McFadden	0.068	0.270
Total Misclassification	877	

[1] Alpha level: $p < 0.05$.
[2] Bonferroni Correction: $p < 0.01$.

Table K-4. Model classification and validation for thoracic CPBA.

Thoracic CPBA Model Classification				
	Predicted			
Observed	Bipedal	Knuckle walk G	Knuckle walk P	Percent Correct
Bipedal	21	3	0	87.5%
Knuckle walk G	2	12	1	80.0%
Knuckle walk P	1	0	11	91.7%
Overall Percentage	47.1%	29.4%	23.5%	86.3%
Model Statistics				
Likelihood Ratio[1]				
T2 CPBA [χ^2 (2) = 19.830; p = 0.000]				
T4 CPBA [χ^2 (2) = 8.022; p = 0.018]				
T7 CPBA [χ^2 (2) = 12.689; p = 0.002]				
T10 CPBA [χ^2 (2) = 21.315; p = 0.000]				
Model Fit[1]				
Final [-2 log likelihood value 38.716; χ^2 (8) = 68.905; p = 0.000]				
Goodness of Fit				
Pearson [χ^2 (92) = 60.582; p = 0.995]				
Deviance [χ^2 (92) = 38.716; p = 1.000]				
Pseudo R^2				
Cox and Snell R^2 = 0.74; Nagelkerke R^2 = 0.84; McFadden R^2 = 0.64				

Thoracic CPBA Validation Classification				
	Predicted			
Observed	Bipedal	Knuckle walk G	Knuckle walk P	Percent Correct
Bipedal	895	69	12	90.0%
Knuckle walk G	152	268	46	62.4%
Knuckle walk P	47	27	349	78.4%
Overall Percentage	55.9%	22.9%	21.1%	94.1%

Validation Statistics 50 Tests (Homo n = 26, Pan n = 11, Gorilla n = 11) % Averages		
Model Fitting[2]		
Final Model: p = 0.000		
	Minimum	Maximum
Goodness of Fit: Pearson	0.753	1.000
Deviance	0.615	1.000
Pseudo R Square: Cox and Snell	0.451	0.873
Nagelkerke	0.608	1.000
McFadden	0.443	1.000
Total Misclassification	353	

[1] Alpha level: p < 0.05.
[2] Bonferroni Correction: p < 0.01.

Table K-5. Model classification and validation for lumbar CPBA.

Lumbar CPBA Classification				
	Predicted			
Observed	Bipedal	Knuckle walk G	Knuckle walk P	Percent Correct
Bipedal	28	3	0	90.3%
Knuckle walk G	4	10	0	71.4%
Knuckle walk P	8	1	1	10.0%
Overall Percentage	72.7%	25.5%	1.8%	70.9%
Model Statistics				
Likelihood Ratio[1]				
L2 CPBA [χ^2 (2) = 6.857; p = 0.032]				
L3 CPBA [χ^2 (2) = 18.337; p = 0.00]				
Model Fit[1]				
Final [-2 log likelihood value 80.549; χ^2 (4) = 27.406; p = 0.000]				
Goodness of Fit				
Pearson [χ^2 (104) = 139.689; p = 0.611]				
Deviance [χ^2 (104) = 80.549; p = 0.957]				
Pseudo R^2				
Cox and Snell R^2 = 0.39; Nagelkerke R^2 = 0.45; McFadden R^2 = 0.25				

Lumbar CPBA Validation Classification				
	Predicted			
Observed	Bipedal	Knuckle walk G	Knuckle walk P	Percent Correct
Bipedal	1129	122	8	88.1%
Knuckle walk G	27	269	1	49.7%
Knuckle walk P	463	48	24	5.28%
Overall Percentage	79.6%	18.9%	1.4%	61.4%
Validation Statistics 50 Tests (Homo n = 26, Pan n = 11, Gorilla n = 11) % Averages				
Model Fitting[2] Final Model: p = 0.000				
		Minimum	Maximum	
Goodness of Fit: Pearson		0.104	0.976	
Deviance		0.382	0.964	
Pseudo R Square: Cox and Snell		0.121	0.505	
Nagelkerke		0.139	0.590	
McFadden		0.063	0.363	
Total Misclassification		669		

[1] Alpha level: $p < 0.05$.
[2] Bonferroni Correction: $p < 0.01$.

Appendix L: MLR classification results for hominins

A.L. 288-1

Table L-1. A. L. 288-1 (AH) model classification (T6).

A.L. 288-1 AH (T6) Model Classification					
	Predicted				
Observed	*Homo sapiens*	*Pan troglodytes*	*Gorilla gorilla*	*A. afarensis* AL 288-1	Percent Correct
Homo sapiens	30	1	3	0	88.2%
Pan troglodytes	1	13	1	0	86.7%
Gorilla gorilla	5	1	10	0	62.5%
A. afarensis AL 288-1	1	0	0	0	0.0%
Overall Percentage	56.1%	22.7%	21.2%	0.0%	80.3%
Model Statistics					
Likelihood Ratio[1]					
IFA [χ^2 (3) = 47.215; p = 0.000]					
IVAPA [χ^2 (3) = 49.291; p = 0.000]					
Model Fit[1]					
Final [-2 log likelihood value 66.237; χ^2 (6) = 77.237; p = 0.000]					
Goodness of Fit					
Pearson [χ^2 (189) = 105.233; p = 1.000]					
Deviance [χ^2 (189) = 66.237; p = 1.000]					
Pseudo R^2					
Cox and Snell R^2 = 0.84; Nagelkerke R^2 = 0.95; McFadden R^2 = 0.86					

[1] Alpha level: $p < 0.05$.

A.L. 288-1 AK (L2 or L3?)

Table L-2. A. L. 288-1 (AK) model classification (L2).

A.L. 288-1 AK (L2) Model Classification					
	Predicted				
Observed	*Homo sapiens*	*Pan troglodytes*	*Gorilla gorilla*	*A. afarensis* AL 288-1	Percent Correct
Homo sapiens	31	2	1	0	91.2%
Pan troglodytes	4	8	4	0	50.0%
Gorilla gorilla	0	6	10	0	62.5%
A. afarensis AL 288-1	0	1	0	0	0.0%
Overall Percentage	52.2%	25.4%	22.4%	0.0%	73.1%
Model Statistics					
Likelihood Ratio[1]					
IVAPA [χ^2 (3) = 64.850; p = 0.000]					
Model Fit[1]					
Final [-2 log likelihood value 81.340; χ^2 (3) = 64.850; p = 0.000]					
Goodness of Fit					
Pearson [χ^2 (195) = 123.135; p = 1.000]					
Deviance [χ^2 (195) = 81.340; p = 1.000]					
Pseudo R^2					
Cox and Snell R^2 = 0.62; Nagelkerke R^2 = 0.69; McFadden R^2 = 0.44					

[1] Alpha level: $p < 0.05$.

Table L-3. A. L. 288-1 (AK) model classification (L3).

A.L. 288-1 AK (L3) Model Classification					
	Predicted				
Observed	*Homo sapiens*	*Pan troglodytes*	*Gorilla gorilla*	*A. afarensis* AL 288-1	Percent Correct
Homo sapiens	32	0	1	0	97.0%
Pan troglodytes	12	0	4	0	0.0%
Gorilla gorilla	4	0	12	0	75.0%
A. afarensis AL 288-1	1	0	0	0	0.0%
Overall Percentage	74.2%	0.0%	25.8%	0.0%	66.7%
Model Statistics					
Likelihood Ratio[1]					
PICP [χ^2 (3) = 128.048; p = 0.000]					
IFA [χ^2 (3) = 34.527; p = 0.000]					
Model Fit[1]					
Final [-2 log likelihood value 101.276; χ^2 (6) = 43.544; p = 0.000]					
Goodness of Fit					
Pearson [χ^2 (189) = 105.541; p = 1.000]					
Deviance [χ^2 (189) = 101.276; p = 1.000]					
Pseudo R^2					
Cox and Snell R^2 = 0.48; Nagelkerke R^2 = 0.54; McFadden R^2 = 0.30					

[1] Alpha level: $p < 0.05$.

A.L. 333 x – 12

Table L-4. A.L. 333 (x-12) model classification (T10).

A.L. 333 x-12 (T10) Model Classification					
	Predicted				
Observed	*Homo sapiens*	*Pan troglodytes*	*Gorilla gorilla*	*A. afarensis* AL 333 X -12	Percent Correct
Homo sapiens	26	4	0	0	86.7%
Pan troglodytes	4	9	3	0	56.3%
Gorilla gorilla	1	2	13	0	81.3%
A. afarensis AL 333 X -12	0	0	1	0	0.0%
Overall Percentage	49.2%	23.8%	27.0%	0.0%	76.2%
Model Statistics					
Likelihood Ratio[1]					
IFPA [χ^2 (3) = 38.737; p = 0.000]					
SFA [χ^2 (3) = 18.530; p = 0.000]					
Model Fit[1]					
Final [-2 log likelihood value 71.357; χ^2 (6) = 69.160; p = 0.000]					
Goodness of Fit					
Pearson [χ^2 (180) = 149.275; p = 0.954]					
Deviance [χ^2 (180) = 71.357; p = 1.000]					
Pseudo R^2					
Cox and Snell R^2 = 0.66; Nagelkerke R^2 = 0.74; McFadden R^2 = 0.49					

[1] Alpha level: p < 0.05.

A.L. 333 106 (C5 or C6?)

Table L-5. A. L. 333 (106) model *c*lassification (C5).

A.L. 333 106 (C5) Model Classification					
		Predicted			
Observed	*Homo sapiens*	*Pan troglodytes*	*Gorilla gorilla*	*A. afarensis* AL 333 106	Percent Correct
Homo sapiens	33	0	1	0	97.1%
Pan troglodytes	0	14	1	0	93.3%
Gorilla gorilla	0	2	14	0	87.5%
A. afarensis AL 333 106	0	1	0	0	0.0%
Overall Percentage	50.0%	25.8%	24.2%	0.0%	92.4%
Model Statistics					
Likelihood Ratio[1]					
VBPH [χ^2 (3) = 26.363; p = 0.000]					
SFA [χ^2 (3) = 20.602; p = 0.000]					
IIFD [χ^2 (3) = 60.137; p = 0.000]					
Model Fit[1]					
Final [-2 log likelihood value 28.703; χ^2 (9) = 114.574; p = 0.000]					
Goodness of Fit					
Pearson [χ^2 (186) = 55.008; p = 1.000]					
Deviance [χ^2 (186) = 28.703; p = 1.000]					
Pseudo R^2					
Cox and Snell R^2 = 0.82; Nagelkerke R^2 = 0.93; McFadden R^2 = 0.80					

[1] Alpha level: p < 0.05.

Table L-6. A. L. 333 (106) model classification (C6).

A.L. 333 106 (C6) Classification					
	Predicted				
Observed	*Homo sapiens*	*Pan troglodytes*	*Gorilla gorilla*	*A. afarensis* AL 333 106	Percent Correct
Homo sapiens	26	4	2	0	81.3%
Pan troglodytes	4	12	0	0	75.0%
Gorilla gorilla	1	2	13	0	81.3%
A. afarensis AL 333 106	0	1	0	0	0.0%
Overall Percentage	47.7%	29.2%	23.1%	0.0%	78.5%
Model Statistics					
Likelihood Ratio[1]					
VBPH [χ^2 (3) = 24.643; p = 0.000]					
IVAPA [χ^2 (3) = 21.879; p = 0.000]					
Model Fit[1]					
Final [-2 log likelihood value 75.270; χ^2 (6) = 68.148; p = 0.000]					
Goodness of Fit					
Pearson [χ^2 (186) = 109.689; p = 1.000]					
Deviance [χ^2 (186) = 75.270; p = 1.000]					
Pseudo R^2					
Cox and Snell R^2 = 0.65; Nagelkerke R^2 = 0.73; McFadden R^2 = 0.47					

[1] Alpha level: $p < 0.05$.